ISSN 0021-9673

VOL. 148 NO. 1 JANUARY 21, 1978

5th Int. Symp., Chromatography in the Chemical Industry, Bratislava, April 26–28, 1977

JOURNAL OF CHROMATOGRAPHY

INTERNATIONAL JOURNAL ON CHROMATOGRAPHY, ELECTROPHORESIS AND RELATED METHOD

ELSEVIER SCIENTIFIC PUBLISHING COMPANY
AMSTERDAM

PUBLICATION SCHEDULE FOR 1978

Journal of Chromatography (incorporating *Chromatographic Reviews*) and *Journal of Chromatography, Biomedical Applications*

MONTH	J	F	M	A	M	J	J	A	S	O	N	D
Journal of Chromatography	147 148/1	148/2 149	150/1 150/2	151/1 151/2 151/3	152/1 152/2	153/1 153/2	154/1 154/2	155/1 155/2 156/1	156/2 157	158 160/1	160/2* 161	
Biomedical Applications	145/1		145/2		145/3		146/1		146/2		146/3	
Chromatographic Reviews		159/1				159/2				159/3		

* Cumulative indexes Vols. 141–160.

Scope. The *Journal of Chromatography* publishes papers on all aspects of chromatography, electrophoresis and related methods. Contributions consist mainly of research papers dealing with chromatographic theory, instrumental development and their applications. The section *Biomedical Applications*, which is under separate editorship, deals with the following aspects: developments in and applications of chromatographic and electrophoretic techniques related to clinical diagnosis (including the publication of normal values); screening and profiling procedures with special reference to metabolic disorders; results from basic medical research with direct consequences in clinical practice; combinations of chromatographic and electrophoretic methods with other physicochemical techniques such as mass spectrometry. In *Chromatographic Reviews*, reviews on all aspects of chromatography, electrophoresis and related methods are published.

Submission of Papers. Papers in English, French and German may be submitted, if possible in three copies. Manuscripts should be submitted to:
The Editor of *Journal of Chromatography*, P.O. Box 681, Amsterdam, The Netherlands
or to:
The Editor of *Journal of Chromatography, Biomedical Applications*, P.O. Box 681, Amsterdam, The Netherlands.
Reviews are invited or proposed by letter to the Editors and will appear in *Chromatographic Reviews* or *Biomedical Applications*. An outline of the proposed review should first be forwarded to the Editors for preliminary discussion prior to preparation.

Subscription Orders. Subscription orders should be sent to: Elsevier Scientific Publishing Company, P.O. Box 211, Amsterdam, The Netherlands. The *Journal of Chromatography, Biomedical Applications* can be subscribed to separately.

Publication. The *Journal of Chromatography* (including *Biomedical Applications* and *Chromatographic Reviews*) has 17 volumes in 1978. The subscription price for 1978 (Vols. 145–161) is Dfl. 2006.00 plus Dfl. 255.00 (postage) (total *ca.* US$ 925.00). The subscription price for the *Biomedical Applications* section only (Vols. 145 and 146) is Dfl. 244.00 plus Dfl. 30.00 (postage) (total *ca.* US$ 112.00). Journals are automatically sent by air mail to the U.S.A. and Canada at no extra costs, and to Japan, Australia and New Zealand with a small additional postal charge. Back volumes of the *Journal of Chromatography* (Vols. 1 through 144) are available at Dfl. 105.00 (plus postage). Claims for issues not received should be made within three months of publication of the issue. If not, they cannot be honoured free of charge.

For further information, see page 3 of cover.

Printed in The Netherlands

VOL. 148, NO. 1 JOURNAL OF CHROMATOGRAPHY JANUARY 21, 1978

CONTENTS

Fifth International Symposium: Progress and Applications of Chromatography in the Chemical Industry, Bratislava (Czechoslovakia), April 26–28, 1977

(Continued overleaf)

Contents (continued)

RS solvents for UV and IR spectrophotometry

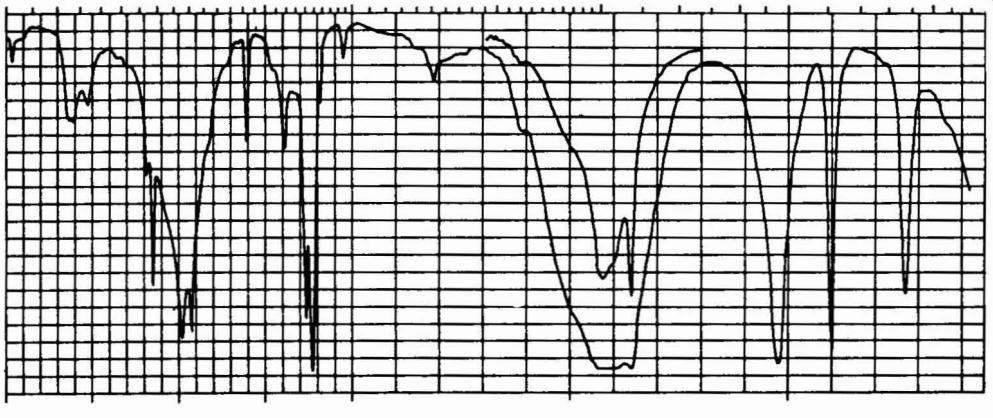

Acetone UV and IR
Acetonitrile UV and IR
Benzene UV and IR
Carbonium sulfide UV and IR
Carbonium tetrachloride UV and IR
Chloroform UV and IR
Cyclohexane UV and IR
N-N-Dimethylformamide UV and IR
Dichloroethane IR
Dimethylsulfoxide UV
Dioxane UV
Ethyl acetate IR
Ethyl alcohol UV 95° and abs.
Ethyl ether UV
n-Heptane UV
n-Hexane UV
Isoctane UV and IR
Isopropyl alcohol UV
Methylene chloride UV and IR
Methyl Alcohol UV
n-Pentane UV
Potassium bromide IR
Tetrachloroethylene IR
Tetrahydrofuran UV and IR
Toluene IR
Trichloroetilene IR

MONTEDISON GROUP
CARLO ERBA

CHEMICALS DIVISION
P.O. Box 3996/20159 Milano/Via Imbonati 24 (Italy)
Telex Erba Mi 36314/Tel. 6995

ref.no. 224

ChromatoFlo™

Liquid Chromatography Components and Accessories

SAVE YOU TIME AND MONEY! HERE'S HOW:

Interchangeable components and accessories within the same column I.D. allow you to

- buy fewer columns
- expand your system as required
- replace broken parts

EXAMPLES

- removable water jackets
- removable packing and solvent reservoirs
- column extenders for fastening one or more columns together
- adjustable plungers for variable bed volume

IN ADDITION

- columns feature all borosilicate glass construction with machined and threaded polypropylene collars, endplates, etc. for positive and easy leak-free assembly time after time

FOR INFORMATION ON OUR COMPLETE LINE of ChromatoFlo products including high pressure jacketed glass columns, UV monitors, HPLC columns, miniature tubing systems, etc., write:

PIERCE
CHEMICAL COMPANY
Box 117, Rockford, Illinois 61105

ref no 158

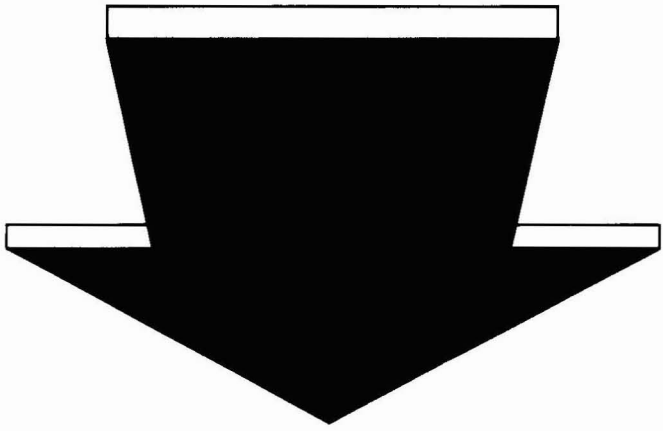

DEAE-Sepharose® CL-6B
CM-Sepharose® CL-6B

Macroporous, bead-formed ion exchangers based on the new high-stability, cross-linked agarose matrix, Sepharose CL

- High resolution and capacity for high molecular weight proteins and other biopolymers
- Exceptionally stable bed volume. Excellent flow rates
- Can be used in polar organic solvents and in solutions of non-ionic detergents
- Can be sterilized repeatedly by autoclaving
- Rapid equilibration. No precycling

Pharmacia Fine Chemicals AB
Box 175
S-751 04 Uppsala 1
Sweden

Pharmacia Fine Chemicals

ref. no. 240

The New LKB Fraction Collector

There is no mistake! The NEW LKB 2120 Vario Perpex II Pump really is a fraction collector.

A new fraction collecting method

Each movement of the pump's stepping motor produces a signal which can be collected in the new LKB RediRac fraction collector. Each signal means a certain volume of liquid displaced by the pump head. By simply dialling in on the preset counter of RediRac you can select precisely the fraction volume you want; you collect *precise-volume* fractions, irrespective of changes in surface tension or applied flow rate.

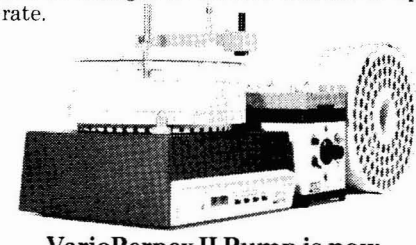

VarioPerpex II Pump is now better than ever

In addition to the new fraction collecting feature, we have added to the popular VarioPerpex Pump a button for immediately obtaining the maximum flow rate. With its wide range of variable flow rates this makes VarioPerpex II Pump more than ever the best you can buy.

The unique roller system

All LKB Perpex Pumps use the same unique system, in which 6 freely-rotating rollers move around an inner driven one. This design gives you minimum pulsation flow, since the increase in pressure on the tubing occurs gradually.

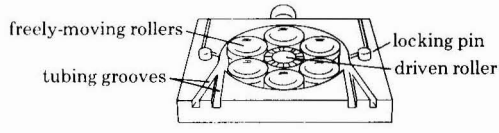

The drag on the tubing is so low that you do not need clips or special tubing. You can use a variety of tubing types and sizes – silicon rubber, Tygon, Viton – just pick the most suitable for you.

LKB family of Perpex Pumps

LKB 10200 Perpex Pump is a single-channel pump, with up to 10 optional gearboxes available to give flow rates of 0.013–800 ml/h.

LKB 2115 MultiPerpex Pump is a variable-speed pump; its four channels and 3 different gearboxes give flow rates of 5–5,000 ml/h per channel.

LKB 2120 VarioPerpex II Pump provides variable flow rates over the range 0.6–400 ml/h, with an optional gearbox giving 0.2–104 ml/h.

LKB

LKB-Produkter AB,
S-161 25 Bromma, Sweden Tel: 08/980040

perfect dosage

✻ the complete dose is contained in the needle of the 7000 Series Microliter Syringes (1 µl, 2 µl and 5 µl) rather than in the glass barrel.

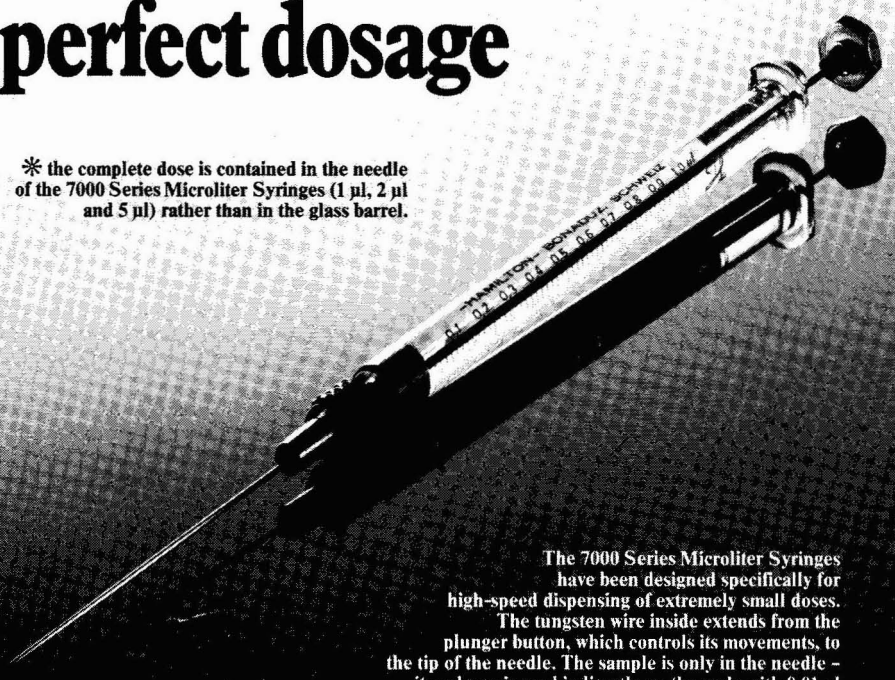

The 7000 Series Microliter Syringes have been designed specifically for high-speed dispensing of extremely small doses. The tungsten wire inside extends from the plunger button, which controls its movements, to the tip of the needle. The sample is only in the needle – its volume is read indirectly on the scale with 0.01 µl divisions. These Microliter Syringes work without the slightest dead volume. They are absolutely hermetic and are suitable also for injecting against high pressures (up to 400 bar).

Fifteen years of experience in the design of the 7000 Series Microliter Syringes and their application has produced a number of additional special features and advanced characteristics. Full details are available on request.

For further information please contact
Hamilton Company, P. O. Box 10030, Reno, Nevada 89510, USA, or
Hamilton Bonaduz AG, CH-7402 Bonaduz, Switzerland.

HAMILTON

Four immuno techniques with one LKB Multiphor

Human serum analysed with LKB Multiphor and
Multiphor Electrophoresis and Immunoelectrophoresis Kits.

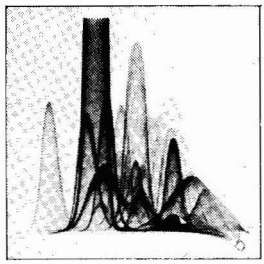

Crossed immunoelectrophoresis

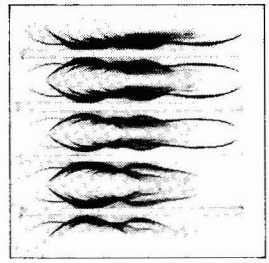

Immunoelectrophoresis according to Grabar & Williams

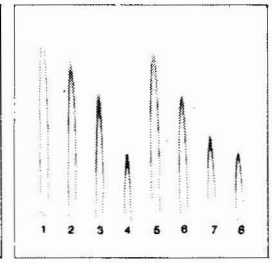

"Laurell" rockets

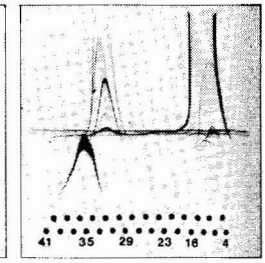

Fused rocket immunoelectrophoresis with intermediate gel.

And that's not all!

The LKB Multiphor Immunoelectrophoresis Kit contains gel punchers and templates for all the up-to-date techniques: single and double diffusion; immunoelectrophoresis according to Grabar & Williams; crossed and tandem crossed immunoelectrophoresis; "Laurell" and fused rockets; and intermediate gel techniques.

With LKB Multiphor it is also possible to combine immuno techniques with electrofocusing and electrophoresis (see LKB Application Note 269).

For both research and clinical use

The researcher will find immunoelectrophoresis useful in protein purification; e.g. the fused rocket technique for determining the number of components in a column chromatography peak. The clinician is able to perform both qualitative and quantitative assays of protein samples.

A new LKB Application Note (No. 249) gives full details of principles, procedures and applications of all these immuno techniques.

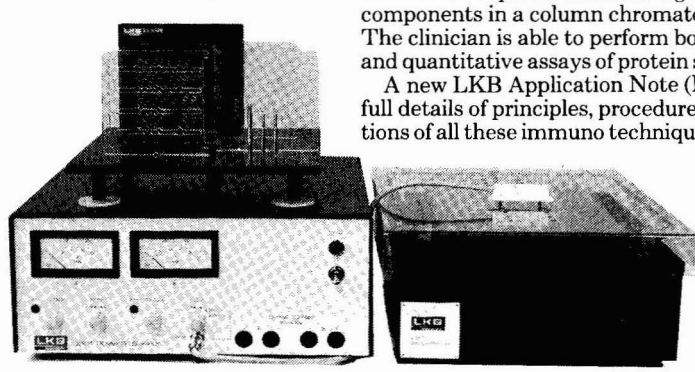

LKB 2121 Power Supply

Specially designed for immunoelectrophoresis: two *independent* outputs, constant voltage from 10 to 300 V, stable to ± 0.2%, voltage probe connection for determination of V/cm, and safety interlock switches.

LKB 2117 Multiphor

1-litre buffer tanks, plug-in electrodes, anticondensation lid, high-efficiency glass cooling plate, and a safety lid to protect the user from high voltage.

Please contact us for more information about LKB equipment for immunoelectrophoresis: LKB 2117-301 Multiphor, 2117-201 Multiphor Electrophoresis Kit, 2117-401 Multiphor Immunoelectrophoresis Kit, and 2121 Power Supply.

LKB

LKB-Produkter AB,
S-16125 Bromma, Sweden. Tel. 08/980040

JOURNAL OF CHROMATOGRAPHY

VOL. 148 (1978)

JOURNAL *of* CHROMATOGRAPHY

INTERNATIONAL JOURNAL ON CHROMATOGRAPHY, ELECTROPHORESIS AND RELATED METHODS

ELSEVIER SCIENTIFIC PUBLISHING COMPANY
AMSTERDAM

Printed in The Netherlands

SPECIAL ISSUE

FIFTH INTERNATIONAL SYMPOSIUM

PROGRESS AND APPLICATIONS OF CHROMATOGRAPHY IN THE CHEMICAL INDUSTRY

Bratislava (Czechoslovakia), April 26–28, 1977

Edited by

K. MACEK (Prague)

J. JANÁK (Brno)

J. NOVÁK (Brno)

CONTENTS

FIFTH INTERNATIONAL SYMPOSIUM: PROGRESS AND APPLICATIONS OF CHROMATOGRAPHY IN THE CHEMICAL INDUSTRY, BRATISLAVA (CZECHOSLOVAKIA), APRIL 26–28, 1977

Journal of Chromatography, 148 (1978) 1

CHROM. 10,618

PREFACE

The Fifth International Symposium on "Progress and Applications of Chromatography in the Chemical Industry" was held from April 26th to 28th, 1977, in Bratislava, Czechoslovakia. It was organized by the Analytical Section of the Czechoslovak Scientific and Technical Society, Slovnaft, Bratislava, the Chromatographic Sections of the Czechoslovak Chemical Society, the Chemical Faculty of the Slovak Technical University, Bratislava, the Chemical Institute of Comenius University, Bratislava, and the Institute of Analytical Chemistry of the Czechoslovak Academy of Sciences, Brno.

Based on experience gained from previous symposia, the programme was more specialized. The main interest was focused towards the application of chromatographic methods in the chemical indistry. Closely connected with this topic were the sections Advances in Chromatographic Techniques and Chromatography in Environmental Protection.

Individual sections of the meeting were introduced by plenary lectures which, however, are not published here:

G. Guiochon: Couplage en ligne des différentes méthodes de chromatographie entre elles ou avec des méthodes spectrometriques.

J. F. K. Huber: Fortschritte in der Hochdruck-Flüssigkeitschromatographie.

M. Lederer: Progress in flat-bed chromatography and electrophoresis.

V. G. Berezkin: Capillary columns and packed materials —perspectives of their applications.

M. S. Vigdergauz: The rational choice of sorbents for gas chromatography.

About 40% of papers read during the meeting or presented in the Poster Sessions were selected for this special volume. The requirements were strict and papers had to meet the criteria for normal publication in the *Journal of Chromatography*. A few papers that were not directly connected with the main theme of the Symposium or that reached the Editor too late for inclusion here will appear in later issues of the *Journal of Chromatography*.

KAREL MACEK

Journal of Chromatography, 148 (1978) 3–10

CHROM. 10,396

IMPORTANCE AND USE OF INCLUSION COMPOUND FORMATION IN GAS–SOLID CHROMATOGRAPHY

E. SMOLKOVÁ, L. FELTL and J. VŠETEČKA

Department of Analytical Chemistry, Faculty of Science, Charles University, 12840 Prague 2, Albertov 2030 (Czechoslovakia)

SUMMARY

Gas chromatography can supply useful information on the course of clathration, and the formation of inclusion compounds can be utilized in the chromatographic separation of substances. In addition to the interactions common in gas–solid and gas–liquid chromatographic systems, specific properties of inclusion compounds play a role and can sometimes be used with advantage for analytical purposes. Systems containing wide-pore silica (Silochrom S-80) or Chromosorb W coated with urea or thiourea as hosts were investigated. The measurements were carried out by using sorbates selected on the basis of their clathrating ability. The temperature dependence of V_g was determined over the temperature range 40–140° on a monomolecular layer of urea on silica. Comparison of the retention data on pure silica and Chromosorb W and on these substances coated with urea or thiourea indicated that the formation of inclusion compounds contributes to the retention of sorbates that are capable of clathration. Although this process is less pronounced in the gaseous phase than in the liquid phase, it is still advantageous for certain types of substances that can be analysed very rapidly, in short columns and at lower temperatures than on common chromatographic packings.

INTRODUCTION

The principal use of inclusion compounds on laboratory and industrial scales is in the separation of substances with different molecular structures. Separations based on the formation of inclusion compounds are usually carried out in liquid systems and their study has been described in many papers (*e.g.*, refs. 1–3). The formation of inclusion compounds is also utilized in modern analytical separation methods, especially in liquid[4–6] and gas chromatography[7–10]. Gas chromatography is a method that permits modelling of the experimental conditions over a wide range and hence enables detailed studies of the formation and properties of clathrates to be carried out. From gas chromatographic data, conclusions can then be drawn about the physico-chemical properties of inclusion compounds and about the possibilities of using them analytically as selective stationary phases.

In view of the importance of inclusion compounds in petrochemistry, we recently studied especially urea adducts with C_8–C_{16} *n*-alkanes[11,12], using more than 30 alkanes with various structures as sorbates. The main factors affecting clathration were followed, *viz.*, the chain length of the guest *n*-alkane molecules, the vapour pressure of the guest molecules and temperature. These studies confirmed that the stability of the adduct increases with increasing chain length. If the adducts are employed as stationary phases, their partial dissociation can be used for the formation of further adducts with the sorbates studied, which can be employed analytically.

The temperature dependences indicated that the urea adducts with *n*-alkanes are decomposed below the melting point of urea and that the decomposition temperature increases with increasing chain length of the *n*-alkanes.

The relatively stable urea adduct with *n*-hexadecane[13] was used for a deeper study of these dependences, not only for *n*-alkanes and branched alkanes, but also for other compounds that can behave as guests, namely olefins, ketones and *n*-alkanols. Depending on the temperature, either the clathrate itself can be used in the gas–solid chromatographic (GSC) system, transition phenomena (*i.e.*, decomposition of the clathrate) can be studied, or its decomposition products (*n*-hexadecane) can be employed as liquid stationary phases in the gas–liquid chromatographic (GLC) system.

In connection with these studies and with published work in which the host was used as a stationary phase for analytical purposes[10,14,15], we have further studied interactions that take place in the GSC system involving a common adsorbent or support coated with the clathrating component. The aim of these experiments was to establish the extent to which the specific properties of inclusion compounds contribute to interactions common in GSC and to ascertain their possible analytical uses.

EXPERIMENTAL

Silochrom S-80 wide-pore silica (particle size 0.16–0.25 mm) (Reakhim, U.S.S.R.) and Chromosorb W (60–80 mesh) coated with 10–20% urea or thiourea to ensure complete coverage of the surface were used.

The sorbates were selected to represent various types of compounds (aliphatic and aromatic hydrocarbons, halogen derivatives, alcohols, ethers and ketones) from the point of view of their various activities in the formation of inclusion compounds. All of the substances used were commercial preparations of analytical-reagent grade.

The measurements were carried out on a Chrom 4 chromatograph (Laboratorní přístroje, Prague, Czechoslovakia) with flame-ionization detection, using stainless-steel columns of length 85 cm and I.D. 6 mm. Nitrogen was used as the carrier gas.

RESULTS AND DISCUSSION

The experiments were based on the properties of sorbents obtained by depositing a monomolecular layer of a strongly adsorbed substance on a strongly adsorbing surface, in this instance wide-pore silica. Then adsorption on a solid sorbent was replaced by adsorption on a monolayer, the volatility of which was substantially decreased by adsorption forces. In this way, the specific properties of the substance

adsorbed on the monolayer can be utilized, while the main advantage of GSC, *viz.* the rapid partition kinetics, permitting rapid analyses, is preserved.

The Silochrom S-80 was coated with a monomolecular layer of urea and the retentions of a wide range of substances of various structural types were measured at 40–140°. Measurements on the original Silochrom S-80 were carried out in parallel. The results of these measurements are summarized in Tables I and II.

A comparison of the data obtained on Silochrom S-80 with those obtained on Silochrom S-80 coated with a monolayer of urea shows that the specific retention volumes are lower on the urea-coated adsorbent, which is caused, for most polar substances, by blocking of the surface hydroxyl groups of silica. This decrease is not strongly affected by a decrease in the surface area, as the retentions of non-specifically interacting substances, *i.e.*, of substances that do not form hydrogen bonds or clathrates, are virtually identical on the two adsorbents.

However, the assumed greater thermal stability of urea adsorbed as a monolayer has not been confirmed. Changes in the properties of the column due to decomposition of urea occur even below the melting point of urea, which is probably caused

TABLE I

SPECIFIC RETENTION VOLUMES ON SILOCHROM C-80 FOR VARIOUS TYPES OF SORBATE

Column: Silochrom S-80 silica gel, particle size 0.16–0.25 mm, length 85 cm, I.D. 6 mm, weight of the packing 9.60 g.

Sorbate	*Column temperature (°C)*					
	40	*60*	*80*	*100*	*120*	*140*
n-Pentane	14.30	7.38	4.02	2.59	1.50	0.94
n-Hexane	37.88	16.87	8.63	4.89	2.71	1.57
n-Heptane	99.09	39.54	18.42	9.49	5.12	2.83
n-Octane	260.65	91.73	38.56	18.13	8.73	4.72
Benzene	138.23	55.88	25.32	11.22	5.72	3.46
Toluene	—	159.21	62.73	27.34	12.34	6.61
Nitromethane	—	264.11	96.68	38.85	15.35	7.87
Dichloromethane	152.28	60.10	25.89	12.37	6.32	2.83
Chloroform	53.95	22.14	10.93	5.47	3.31	2.20
Carbon tetrachloride	38.88	18.45	9.21	5.47	3.31	2.20
1,1-Dichloroethane	71.50	30.05	13.81	7.19	3.91	2.20
1,2-Dichloroethane	145.75	58.52	25.32	12.37	6.32	3.46
1,1,1-Trichloroethane	72.50	31.10	14.96	7.77	4.51	2.83
1,1,2-Trichloroethane	—	117.56	48.34	21.58	9.93	5.35
1,1,1,2-Tetrachloroethane	—	148.14	58.12	26.18	11.74	6.61
1,1,2,2-Tetrachloroethane	—	—	112.22	46.32	18.96	9.76
Vinyl chloride	—	4.22	2.30	1.44	0.90	0.31
1,1-Dichloroethylene	15.80	8.43	4.60	2.59	1.50	0.94
Trichloroethylene	60.46	29.52	12.66	6.62	3.91	2.20
Perchloroethylene	—	42.70	19.57	10.07	5.12	2.83
1,2-Dibromomethane	—	135.48	54.10	24.46	11.14	5.98
Fluorobenzene	144.75	57.46	25.90	12.37	6.32	3.46
Chlorobenzene	—	—	54.67	24.46	11.14	5.98
Bromobenzene	—	—	87.48	37.69	16.56	9.13
Diethyl ether	—	—	—	151.07	51.47	21.09
Acetone	—	—	—	233.94	70.14	36.20

TABLE II

SPECIFIC RETENTION VOLUMES ON A MONOMOLECULAR LAYER OF UREA ON SILOCHROM S-80 FOR VARIOUS TYPES OF SORBATE

Column: Silochrom S-80 silica gel + 12.3% urea, particle size 0.16–0.25 mm, length 85 cm, I.D. 6 mm, weight of the packing 8.80 g.

Sorbate	*Column temperature (°C)*					
	40	*60*	*80*	*100*	*120*	*140*
n-Pentane	11.83	6.99	3.66	1.88	2.17	1.50
n-Hexane	33.30	18.05	8.53	4.39	3.61	2.25
n-Heptane	93.84	42.50	19.50	9.42	6.51	3.75
n-Octane	242.99	103.05	42.04	18.83	11.57	6.00
Benzene	76.23	34.93	16.45	8.79	5.06	3.75
Toluene	239.69	96.64	40.83	18.83	10.12	6.75
Nitromethane	—	132.74	54.84	25.11	12.29	7.50
Dichloromethane	91.09	43.08	20.11	10.67	5.78	3.75
Chloroform	44.30	22.70	11.58	6.28	3.61	2.25
Carbon tetrachloride	36.05	18.63	9.75	5.02	3.61	2.25
1,1-Dichloroethane	50.36	25.03	11.58	6.28	3.61	3.00
1,2-Dichloroethane	90.56	43.08	20.11	10.67	5.78	3.75
1,1,1-Trichloroethane	60.27	30.27	14.62	7.53	5.06	3.00
1,1,2-Trichloroethane	—	114.11	48.72	23.23	10.85	6.75
1,1,1,2-Tetrachloroethane	—	156.61	65.81	30.76	14.46	8.25
1,1,2,2-Tetrachloroethane	—	—	151.12	64.04	23.86	12.00
Vinyl chloride	-	2.91	1.83	1.25	0.72	0.72
1,1-Dichloroethylene	11.83	6.40	3.66	2.51	0.72	0.72
Trichloroethylene	55.86	26.78	13.40	6.28	4.34	3.00
Perchloroethylene	—	44.24	21.33	10.67	7.23	4.50
1,2-Dibromomethane	-	100.72	44.48	21.97	10.85	6.75
Fluorobenzene	84.48	43.08	17.06	10.67	5.78	3.75
Chlorobenzene	—	—	50.57	23.23	12.29	6.75
Bromobenzene	—	—	82.26	30.13	18.08	11.25
Diethyl ether	-	—	90.18	29.51	23.14	21.00
Acetone	-	—	187.68	67.80	45.55	31.30

by catalysis by silica acidic sites. Ammonia was detected in the carrier gas at 120° and for this reason the retention data obtained at 120° and 140° deviated from a linear dependence of log V_g *versus* $1/T$.

It follows from the temperature dependences of the specific retention volumes of substances capable of clathration, *i.e.*, *n*-alkanes and chlorinated hydrocarbons, and of inactive substances, *e.g.*, benzene, toluene and cyclohexane, that these two groups of sorbates behave differently. While the decrease in V_g for inactive substances (Fig. 1) is caused by their inability to interact with the hydroxyl groups over the whole temperature range, hydrocarbons (Fig. 2) and chlorinated hydrocarbons (Fig. 3) exhibit higher V_g values on urea-coated silica than on uncoated silica. This phenomenon can only be explained by assuming that the total energy of interaction determined by non-specific forces is increased by a contribution from a specific interaction due to the formation of the inclusion compounds with urea. This contribution increases with increasing numbers of carbon atoms in *n*-alkane molecules and of chlorine atoms in chloroethanes and chloroethylenes, as illustrated by the dependences in Figs. 1 and 2 and the data in Tables I and II. These conclusions also con-

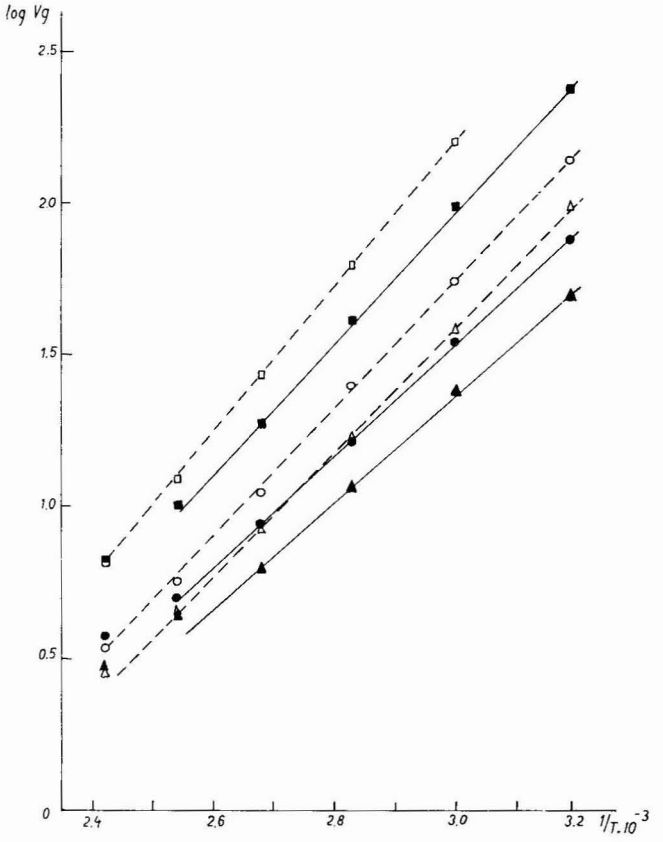

Fig. 1. Temperature dependences of V_g for non-clathrating sorbates on Silochrom S-80 and on a monomolecular layer of urea on Silochrom S-80. ○, Benzene; □, toluene; △, cyclohexene.

firm the results of previous experiments, in which the effect of the carbon chain length on the formation and stability of the adducts was shown. Chlorinated hydrocarbons, in agreement with the behaviour in the liquid phase, also change their elution order compared with the V_g values on silica only from tetrahalogeno derivatives onwards.

Similar experiments were carried out with urea deposited on a common chromatographic support, Chromosorb W. Further, thiourea was selected as a type of host that is capable of forming inclusion compounds with substances of different structural types. Reference experiments were carried out on the two columns.

A contribution from clathration to the overall retention of active sorbates, which can be used analytically, was also verified in these systems. An example is the separation of cyclohexane and *n*-hexane on urea deposited on Chromosorb W at 40° (Fig. 4), where the substances are eluted in the opposite order to that of their boiling points; this behaviour cannot be assigned to other interactions. Another example is analysis of light petroleum under identical conditions on columns with urea and thiourea deposited on Chromosorb W (Fig. 5). Whereas the separation is poor on the urea column, the individual components can readily be differentiated on the

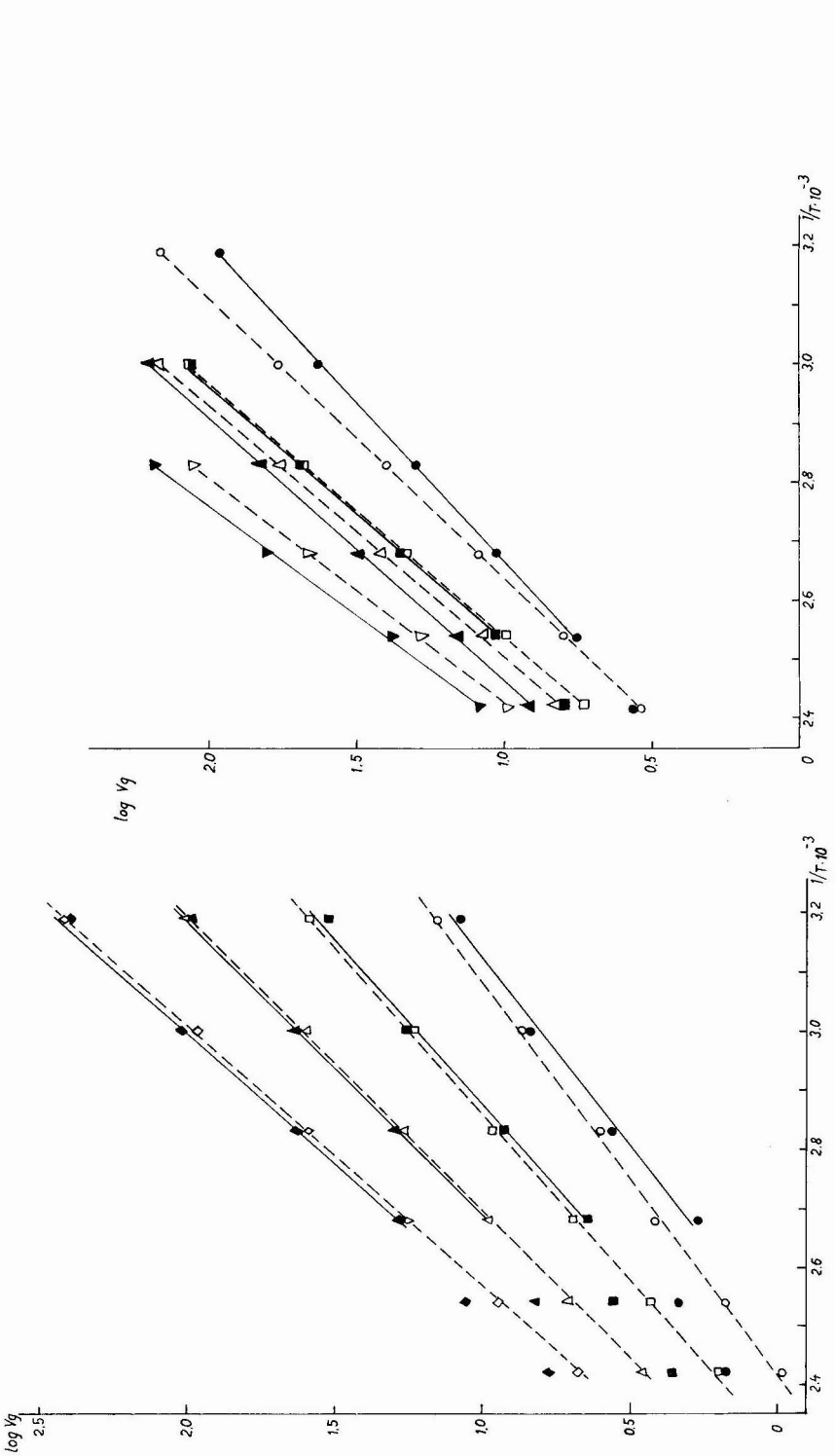

Fig. 2. Temperature dependences of V_g for *n*-alkanes on Silochrom S-80 and on a monomolecular layer of urea on Silochrom S-80. ○, *n*-Pentane; □, *n*-hexane; △, *n*-heptane; ◇, *n*-octane.

Fig. 3. Temperature dependences of V_g for chlorinated ethanes on Silochrom S-80 and on a monomolecular layer of urea on Silochrom S-80. ○, 1,2-Dichloro-; □, 1.1.2-trichloro-; △, 1,1,1,2-tetrachloro-; ▽, 1,1,2,2-tetrachloroethane.

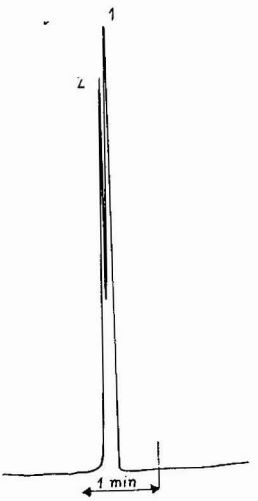

Fig. 4. Separation of cyclohexane and *n*-hexane on urea deposited on Chromosorb W.

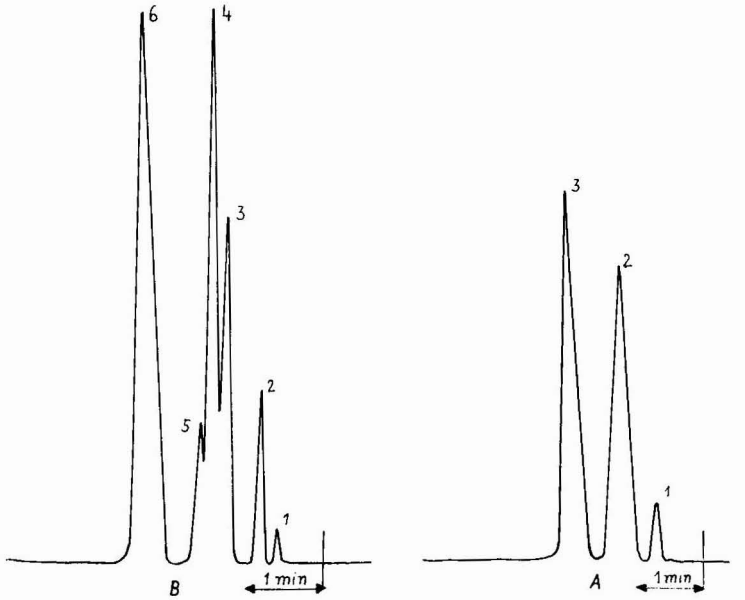

Fig. 5. Chromatograms of light petroleum on (A) urea and (B) thiourea deposited on Chromosorb W.

thiourea-coated column because of the formation of clathrates with the branched alkanes that constitute light petroleum.

In many other analytically useful systems the retention of individual substances cannot be unambiguously ascribed to the formation of inclusion compounds. It can rather be assumed that the separation mechanism is affected by the medium polarity of urea or thiourea. Orientative experiments indicated that these substances might be used with advantage as adsorbents, because of the rapidity of the analyses and the high peak symmetry obtained.

The results obtained confirmed that gas chromatography can detect even interactions as weak as the formation of inclusion compounds from the gaseous phase and that these compounds can sometimes be useful for selective separations.

REFERENCES

1 F. Cramer, *Einschlussverbindungen*, Springer Verlag, Berlin, 1954.
2 W. Schlenk, *Justus Liebigs Ann. Chem.*, 565 (1949) 204.
3 F. Brown, Jr., *Sci. Amer.*, 207 (1962) 82.
4 J. Cassou and G. Sumrell, *J. Biol. Chem.*, 205 (1953) 435.
5 J. Lipkowski, K. Leśniak, A. Bylina, D. Sybilska and K. Duszczyk, *J. Chromatogr.*, 91 (1974) 297.
6 S. Brzozowski, *Rocz. Chem.*, 47 (1973) 612.
7 A. Bhattacharjee and A. N. Basu, *J. Chromatogr.*, 71 (1972) 534.
8 A. C. Bhattacharyya and A. Bhattacharjee, *J. Chromatogr.*, 41 (1969) 446.
9 A. C. Bhattacharyya and A. Bhattacharjee, *Anal. Chem.*, 41 (1969) 2055.
10 J. C. Mailen, T. M. Reed and J. A. Young, *Anal. Chem.*, 36 (1964) 1883.
11 K. Mařík and E. Smolková, *Chromatographia*, 6 (1973) 420.
12 K. Mařík and E. Smolková, *J. Chromatogr.*, 91 (1974) 303.
13 E. Smolková, *9th. International Symposium, Advances in Chromatography, Houston, 1974.*
14 A. O. S. Maczek and C. G. S. Phillips, in R. P. W. Scott (Editor), *Gas Chromatography*, Butterworths, London, 1960, pp. 284–288.
15 A. O. S. Maczek and C. G. S. Phillips, *J. Chromatogr.*, 29 (1967) 7.

Journal of Chromatography, 148 (1978) 11–15

CHROM. 10,397

CALCULATION OF THE RETENTION INDICES OF C_5–C_9 CYCLOALKANES ON SQUALANE

N. DIMOV

Chemical Pharmaceutical Research Institute, Analytical Department, Sofia 1156 (Bulgaria)

and

D. PAPAZOVA

Economic Complex "Neftochim", Institute of Petroleum, Burgas (Bulgaria)

SUMMARY

The relationship between molecular structure, vapour pressure and molecular volume of 30 C_5–C_9 cycloalkanes and their gas chromatographic retention on squalane were investigated. An equation for the accurate and simple calculation of their theoretical retention indices is proposed. The equation permits the calculation of the vapour pressures of these hydrocarbons at different temperatures.

INTRODUCTION

Gas chromatography is suitable for studying the relationship between retention parameters and solute properties, and we have previously carried out investigations on the behaviour of isoalkanes[1], benzene homologues and alkenes[2] on squalane.

In this paper, the relationship between gas chromatographic data and the molecular structure of naphthenes is discussed. This topic has been considered previously by other workers, but in a different manner. Schomburg and co-workers considered the behaviour of saturated and unsaturated alkyl-substituted cyclopentanes and methylcyclopentanes[3] and of other alkyl-branched and unsaturated cyclic hydrocarbons[4] on squalane based on the homomorphic factor. Loewenguth and Tourres[5] and Rijks and Cramers[6] published precise experimental data on the retention of cycloalkanes on squalane.

In this work we considered the relationship between vapour pressure, molecular volume and structure of hydrocarbons and the retention of C_5–C_9 cycloalkanes, a more detailed consideration of which was given in previous publications[1,7,8]. The investigation was carried out not only in order to predict the separation on the basis of the theoretical retention indices, but also with the purpose of calculating the vapour pressure of the cycloalkanes at different temperatures and their boiling points.

CALCULATION

The study was based on the theoretical assumption presented earlier[1] and the retention of cycloalkanes was considered in the same manner. The influence of the

different structural elements of naphthenes on their retention on squalane was studied. Several combinations of significant structural elements were examined in order to derive an equation that would lead to simple calculations. We succeeded in combining all of the elements in an equation of the type

$$SN = a_0 + R(b_1x_1 + b_2x_2) \quad (1)$$

where SN is the structural number, R is a qualitative characteristic with a value of zero when there is no substituent attached to the ring and a value of unity, when there are substituents, independent of their number. All of the elements related to the structures of the substituents are represented by a factor x_1, and those related to their positions by a factor x_2:

$$x_1 = n_{ring} + n_R + n_{CH_3} - n_L \quad (2)$$

$$x_2 = n_v + 2tr_{i,i}^{1,2;\ 1,4} + cis_{i,i,i}^{1,2} - tr_{i,j}^{1,2} \quad (3)$$

where

n_{ring} = number of carbon atoms in the ring;
n_R = number of substituents R;
n_{CH_3} = number of the methyl groups attached to the straight chain of a substituent;
n_L = length of the straight chain of a substituent;
n_v = number of vacant positions in the ring;
$tr_{i,i}^{1,2;\ 1,4}$ = number of 1,2- and 1,4-*trans*-dimethylcycloalkanes;
$cis_{i,i,i}^{1,2}$ = number of 1,2-*cis*-trimethylnaphthenes;
$tr_{i,j}^{1,2}$ = number of 1,2-*trans*-dialkylcycloalkanes with different substituents.

A matrix* from 30 cycloalkanes was constructed. The retention indices for calculations of SN according to eqn. 1 were taken from the literature[5,6]. The physicochemical properties of the cycloalkanes studied were calculated from their vapour pressures[9,10] and specific gravities[9,11]. After solving the matrix, the following values of the coefficients were obtained: $a_0 = -0.4867$, $b_1 = 1.3330$ and $b_2 = 1.0474$.

RESULTS AND DISCUSSION

The results illustrating the relationship between the retentions and structures of C_5–C_9 cycloalkanes are given in Table I. The values show that cyclopentane and cyclohexane have SN values of about zero, indicating that unsubstituted cycloalkanes are retained less strongly than their alkyl-substituted derivatives. The SN values of the other compounds calculated in the range 50–100° show that, like those of the isoalkanes, they are almost independent of temperature.

On increasing the length of the substituent, the difference in the entropy of solution of cycloalkanes seems to decrease, as follows from the values of A_1 which are connected with the entropy of cycloparaffins relative to *n*-paraffins. Branching of the substituent improved the retention, as was the case with the isoalkanes. The *trans*-isomers of 1,2-disubstituted naphthenes are more difficult to dissolve in the stationary phase used than *cis*-isomers, which was observed previously with olefins.

* A sum of data prepared for regression analysis.

TABLE I

DIFFERENCES Δ_1 BETWEEN *I* (RETENTION INDEX) AND *PCI* (PHYSICO-CHEMICAL INDEX) AND Δ_2 BETWEEN *I* AND I^{theor} (SUM OF *PCI* AND *SN*) FOR C_5–C_9 CYCLOALKANES

Hydrocarbon	Δ_1	Δ_2*
Cyclopentane	− 0.3	0.2
Methylcyclopentane	4.8	1.4
Ethylcyclopentane	4.4	0.4
n-Propylcyclopentane	3.1	0.4
Isopropylcyclopentane	7.4	1.2
Cyclohexane	0.2	0.7
Methylcyclohexane	7.9	0.4
Ethylcyclohexane	6.5	0.3
n-Propylcyclohexane	4.6	0.2
Isopropylcyclohexane	7.1	0.4
n-Butylcyclohexane	3.2	0.3
Isobutylcyclohexane	6.0	0.2
1,1-Dimethylcyclopentane	6.4	3.6
1-Methyl-1-ethylcyclopentane	9.7	0.7
1,1-Dimethylcyclohexane	13.6	0.8
1-*trans*-2-Dimethylcyclohexane	13.6	0.2
1-*cis*-2-Dimethylcyclohexane	11.9	0.2
1-*trans*-4-Dimethylcyclohexane	13.4	1.7
1-*cis*-4-Dimethylcyclohexane	10.2	0.6
1-*trans*-3-Dimethylcyclohexane	8.9	1.7
1-*cis*-3-Dimethylcyclohexane	9.3	1.3
1-Methyl-*cis*-2-ethylcyclopentane	7.6	0.4
1-Methyl-*trans*-2-ethylcyclopentane	6.2	0.7
1,1,1-Trimethylcyclopentane	8.9	0.6
1,1,1-Trimethylcyclohexane	12.4	1.8
1,1,2-Trimethylcyclopentane	11.4	2.1
1-*trans*-2-*cis*-4-Trimethylcyclopentane	8.4	2.0
1-*cis*-2-*trans*-4-Trimethylcyclopentane	10.2	1.2
1-*trans*-2-*cis*-3-Trimethylcyclopentane	11.9	0.5
1-*cis*-2-*cis*-3-Trimethylcyclopentane	13.8	0.3

* Variance of Δ_2: $s^2 = 0.97$.

Statistical analysis showed $F^{exp}_{(29,30)} = 1.57$ and $F^{0.05}_{tabular} = 1.87$. The value of 1.57 for the Fischer criterion ($F_{(f_1 f_2, 1-\alpha)}$; ref. 12) represents the relationship between variances for the 29 cycloalkanes in Table I (excluding 1,1-dimethylcyclopentane) and for the 30 cycloalkanes for which I^{exp} values have been published by different workers[4–6].

The accuracy achieved was examined by calculating the vapour pressures of different cycloalkanes and their temperature dependence and by calculating their boiling points. The principle can be demonstrated by considering *n*-propylcyclopentane. To calculate p^0, the following equation was used:

$$\log p_i^0 = \log \frac{p_z^0 \cdot V_{mol,z}}{V_{mol,i}} - \left(\frac{I^{theor} - SN}{100} - z \right) \log \frac{p_z^0 \cdot V_{mol,z}}{p_{z+1}^0 \cdot V_{mol,z+1}} \qquad (4)$$

where p_i^0 = vapour pressure of *i*th cycloparaffin; p_z^0 and p_{z+1}^0 = vapour pressures of *n*-paraffins with *z* and *z* + 1 carbon atoms, respectively; $V_{mol,i}$, $V_{mol,z}$ and $V_{mol,z+1}$

are the corresponding molecular volumes; I^{theor} = calculated theoretical index; and SN = calculated structural number.

Using literature values and our experimental data, we calculated p^0 for *n*-propylcyclopentane at several temperatures (Table II).

TABLE II

VAPOUR PRESSURE (p^0) OF *n*-PROPYLCYCLOPENTANE CALCULATED AT DIFFERENT TEMPERATURES

Temperature (°C)	I^{exp} *value*	*Reference*	$p^0_{calc.}$ *(mmHg)*
60	832.3	6	68.9
70	834.7	This work	103.0
80	836.3	6	151.8
90	838.5	This work	216.9
100	840.2	6	304.2

Values of the constants A, B and C of the Antoine equation were calculated from $p_{calc.}$ (Table II) and the following equation was obtained:

$$\log p^0_{n\text{-Prcp}} = 6.8328 - \frac{1348.9}{t + 210.14} \tag{5}$$

The vapour pressures over the range 20–200° were calculated and are compared in Table III with those given in the literature. The data show that the value of the constants A, B and C remain valid not only in the range 60–100°, which represents the limit of the available I values, but could be used in an extended range from 20 to 200° with satisfactory accuracy.

TABLE III

VAPOUR PRESSURE ($p°$) OF *n*-PROPYLCYCLOPENTANE AT DIFFERENT TEMPERATURES

Temperature (°C)	$p°$ *(mmHg)*		
	Literature value	*Calculated from A, B and C*	*Difference (mmHg)*
20	9.2	9.4	−0.2
40	27.3	27.5	−0.2
50	44.0	44.4	−0.4
80	151.9	151.8	−0.1
100	304.2	304.2	0.0
120	560.6	558.4	+2.2
180	2414	2373	+41 (1.7%)
200	3575	3498	+77 (2.2%)

The boiling points (t_b) of *n*-propylcyclopentane and other cycloalkanes could be calculated according to the equation

$$t_b = \frac{B}{A + \log 760} - C \tag{6}$$

The calculated and actual boiling points of different cycloalkanes are compared in Table IV.

TABLE IV

COMPARISON OF CALCULATED AND ACTUAL BOILING POINTS OF DIFFERENT CYCLOALKANES

Hydrocarbon	*Boiling point (°C)*		*Difference (°C)*
	Calculated	*Actual*	
Cyclopentane	49.0	49.26	0.26
1,1-Dimethylcyclopentane	87.66	87.84	0.18
1-*cis*-3-Dimethylcyclopentane	91.41	90.77	−0.64
1-Methyl-*trans*-2-ethylcyclopentane	121.36	121.20	−0.16
1-Methyl-1-ethylcyclopentane	119.84	121.52	1.68
Isopropylcyclopentane	126.62	126.40	−0.22
n-Propylcyclopentane	130.69	130.95	0.26
1-Methyl-*cis*-2-ethylcyclopentane	128.37	128.05	−0.32
1-Methyl-*trans*-2-ethylcyclopentane	146.2	146.3	0.1
sec-Butylcyclopentane	153.86	154.4	0.54
n-Butylcyclopentane	157.47	156.6	−0.9

The results obtained indicate the possibilities of utilizing I values both for identification purposes and for the calculation of p^0 at particular temperatures. The latter has the advantage of permitting the investigation of compounds in a mixture, because the value of I could easily be determined at different temperatures and is not influenced by the presence of other hydrocarbons.

REFERENCES

1 N. Dimov, *J. Chromatogr.*, 119 (1976) 109.
2 Unpublished results.
3 G. Dielman, D. Schwegers and G. Schomburg, *Chromatographia*, 7 (1974) 215.
4 G. Schomburg, *J. Chromatogr.*, 23 (1966) 18.
5 J. C. Loewenguth and D. A. Tourres, *Z. Anal. Chem.*, 236 (1968) 170.
6 J. A. Rijks and C. A. Cramers, *Chromatographia*, 7 (1974) 99.
7 N. Dimov and D. Shopov, *J. Chromatogr.*, 44 (1969) 170.
8 N. Dimov and D. Shopov, *C.R. Acad. Bulg. Sci.*, 22 (1969) 285.
9 A. Tatevski (Editor), *Fisiko-khimicheskie Svoistva Individualnykh Uglevodorodov*, Izdatelstvo Lenina, Moscow, 1960.
10 *Selected Values of Properties of Hydrocarbons*, A.P.I. Research Project 44, Texas University, College Station, Texas, 1966.
11 B. P. Nicolski (Editor), *Spravochnik Khimika*, Vol. II, GOSCHIMIZDAT, Moscow, 1963.
12 R. A. Fisher, *Statistical Methods and Scientific Interference*, Oliver & Boyd, Edinburgh, 1956.

Journal of Chromatography, 148 (1978) 17–29

CHROM. 10,412

PRE-CALCULATION OF RETENTION INDICES OF AROMATIC COMPOUNDS BY COMPUTER ON THE BASIS OF THEIR MOLECULAR STRUCTURES AND THERMODYNAMICS IN TEMPERATURE-PROGRAMMED GAS CHROMATOGRAPHY

I. FISCH, I. OLÁCSI, M. RICHTER, A. P. SINKA, E. C. TAKÁCS and J. M. TAKÁCS
OGIL, Research Laboratory for the Oil and Gas Industry, Budapest (Hungary)
J. VÖRÖS
OKGT, Hungarian Oil and Gas Trust, Budapest (Hungary)
and
G. TARJÁN
REANAL, Fine Chemicals Factory, Budapest (Hungary)

SUMMARY

Theoretical and practical problems involved in the pre-calculation of retention indices for benzene derivatives are considered in terms of similar problems with alkanes. The determination of increment values on the basis of thermodynamic data (bond energy and bond distance), the determination of increment codes by means of a computer and the pre-calculation of retention indices in classical gas–liquid and temperature-programmed gas chromatography are discussed.

INTRODUCTION

Gas–liquid chromatography (GLC) is widely applied in the petrochemicals industry. As a consequence of the increasing demand for aromatic compounds, their production has increased considerably in recent years. The composition of the end-products of refineries can be analysed by GLC methods, with special particular emphasis on the C_{9+} aromatic compounds.

The basis of the method is that the stationary phase, polyethylene glycol adipate (PEGA), produces large differences in the retentions of aromatic and non-aromatic compounds, especially when temperature programming is applied. The gas chromatographic peaks were identified by means of retention indices[1] and standard materials based on the work of Chang and Karr[2].

The parameters that are suitable for application to experimental data obtained in different laboratories are the specific retention volume, the net retention volume, the relative retention and the retention index. Of these, we considered further the retention index, as proposed by Kováts[3], as this is the only retention parameter in GLC in which the two mostly fundamental properties, namely the net retention vol-

ume and the relative volatility (relative retention expressed in terms of reduced retention times) combined.

There have been three main turning points in the development of this field: (a) the comprehensive paper by Ettre[4], (b) the influence of the lectures and discussions delivered at the 5th International Conference on Column Chromatography in Lausanne (1969), and (c) the production of a chemically homogeneous apolar stationary phase[5], that ensured the availability of a standard stationary phase over a relatively large temperature range. Benzene derivatives have been studied by Janák and co-workers[6,7], Schomburg[8,9], Hively and Hinton[10], Schulz and Reitemeyer[11], Bonastre *et al.*[12], Hatch[13], Krupčik *et al.*[14], Karasek and co-workers[15,16], Louis[17,18], Robinson and Odell[19], Wallaert[20], Dimov and Schopov[21], Cook and Raushel[22], Soják and Hrivnák[23], Fuchs[24], Vernon[25], Mitra *et al.*[26], Engewald *et al.*[27], Švob *et al.*[28], Hartigan and Purcell[29], West and Hall[30], Soják and Rijks[31], Ryba[32,33] and Engewald and Wennrich[34].

In considering the various theoretical and practical problems of the retention index system[35–38] and similar questions with alkanes[39], our attention was turned to benzene derivatives[40]. Relying on data from the literature mentioned above and our work on alkanes, extended studies were made with benzene derivatives. In this paper, the results obtained with methyl-, ethyl- and isopropylbenzenes are presented.

THEORETICAL

As we pointed out previously[39], applying the additive property of retention indices, we can write

$$I = I_a + I_b + I_i \tag{1}$$

where

I = retention index under isothermal conditions, in index units (i.u.);
I_a = atomic index contribution (i.u.);
I_b = bond index contribution (i.u.);
I_i = interaction index contribution (i.u.).

The atomic index contribution was established by definition:

$$I_a = \frac{\text{molecular weight}}{10} \tag{2}$$

The bond index contribution is given by the sum of individual bond increment values.

For an accurate description of the increments, the following code system was introduced for the methyl-, ethyl- and isopropylbenzenes:

(1) C–C bonds are denoted by C.

(2) C–H bonds are denoted by H.

(3) C, H and every independent piece of information are followed by a comma.

(4) After the comma following C, the orders of the two carbon atoms between which the bond has been formed are given in order of decreasing values. The designation of the order of carbon atoms is as follows:

in the ring: order of carbon atom and A;

in a substituted chain: only order of carbon atom;

between the ring and the chain: combination of the two symbols.

For example:

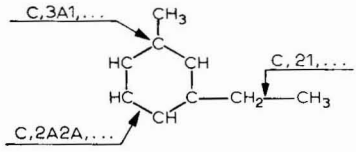

(5) Following the orders of the carbon atoms between which the bond is formed, the orders of the neighbouring carbon atoms (primary environment) are given in increasing order. For example, in the example given in paragraph (4), the code of the carbon–carbon bond between the methyl group and the ring is as follows:

C,3A1,02A2A,000.

(6) The basic code of a carbon-carbon bond:

C,00,000,000.

(7) If all of the places in the basic code are not taken by order values, then the 0 values must remain in the untaken places of the basic code.

(8) An increment code is terminated by a full point.

(9) If two carbon atoms of the same order are bound to each other, then the code of the neighbour of the higher order will be given first.

(10) The basic code of a carbon–hydrogen bond:

H,0,000,000,000,000.

(11) After the comma following H, the order of the carbon atom to which the hydrogen atom is bound is given.

(12) Following the order of the carbon atom bound to the hydrogen atom, the orders of the carbon atoms next to the carbon atom to which the hydrogen in question is bound (primary environment) are given.

(13) After coding of the primary environment, the orders of the carbon atoms bound directly to carbon atoms bound to the former are given (secondary environment), in increasing order. For example, the code of the carbon–hydrogen bond in the molecule of *m*-xylene is as follows:

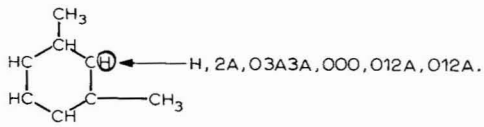

The known fundamental thermodynamic data (bond energies, bond distances, etc.) of the molecule being examined should be combined with the increments or with similar gas chromatographic data such as bond index contributions. Following this, the mean value of the index unit/bond energy unit factor can be calculated by means of corresponding data for 3, 5 and 11 compounds. Then, from the thermodynamic data and the molecular structure, the increment values are determined by means of a computer. In connection with the determination of increment values, it should be noted that while there are many comprehensive works on thermodynamics, *e.g.*, by

Bartell[41–43], Herzberg and Sticheff[44,45] and others[46,47], there are few data available for individual compounds and their derivatives.

From the above considerations, benzene, toluene, *m*-xylene and 1,3,5-trimethylbenzene were selected as examples, as their thermodynamic data were available. For the determination of the increment values, the simplest compound, benzene, is considered.

As the carbon–carbon π-bonds are represented by A, there are two bond types in the benzene molecule:

(a) C,2A2A,002A,002A.

(b) H,2A,02A2A,000,002A,002A.

There are six bonds of each type in the molecule. The atomization energy, taken from the literature, is 1319.4 kcal/mole and is distributed between the two different bond types as follows: each C–C bond, 122.60 kcal/mole, and each C–H bond, 97.30 kcal/mole. Hence, the distribution of the bond index contribution of the molecule is as follows: increment value of each C–C bond, 14.39 i.u., and that of each C–H bond, 11.42 i.u. If there are more than two bond types in the molecule, the value of the index unit/energy unit factor has to be determined by division, by means of the atomization energy and bond index contribution.

When the latter factor and the energy values of the increments are known, then by multiplication the increment values (index units) can be obtained. In Table I, the increment values used in the calculations are presented.

TABLE I

BOND INCREMENT VALUES APPLIED IN CALCULATIONS WITH 1,3,5-TRIMETHYLBENZENE

Increment code	*Bond increment value (i.u.)*
H,1,003A,000,000,02A2A	11.03
H,2A,03A3A,000,012A,012A	9.74
C,3A1,02A2A,000	9.49
C,3A2A,012A,003A	12.28

Assuming that interactions developed on squalane as a stationary phase do not contain individual interaction factors (this is only approximately true, of course) the ΔI values, published in McReynold's paper[48], give the individual interaction index contributions. These data give the possibility of making several other comparisons. A continuous curve can be obtained that represents the interaction contributions *versus* the retention polarity of stationary phases [49], as is shown in Fig. 1.

As the bond and interaction index contributions are determined on the same thermodynamic bases and in the same way, their values can be summed, in certain circumstances. The dependence of the increment (bond + interactions) values for ethylbenzene on different stationary phases is shown in Table II, and the dependence of the increment values for *n*-propylbenzene on column temperature on a standard apolar stationary phase according to Riedo *et al.*[5] is presented in Table III.

The regular increase (95.90 i.u.) in the retention indices for the homologous series of *n*-alkylbenzenes after *n*-hexylbenzene on extending the alkyl chain length by

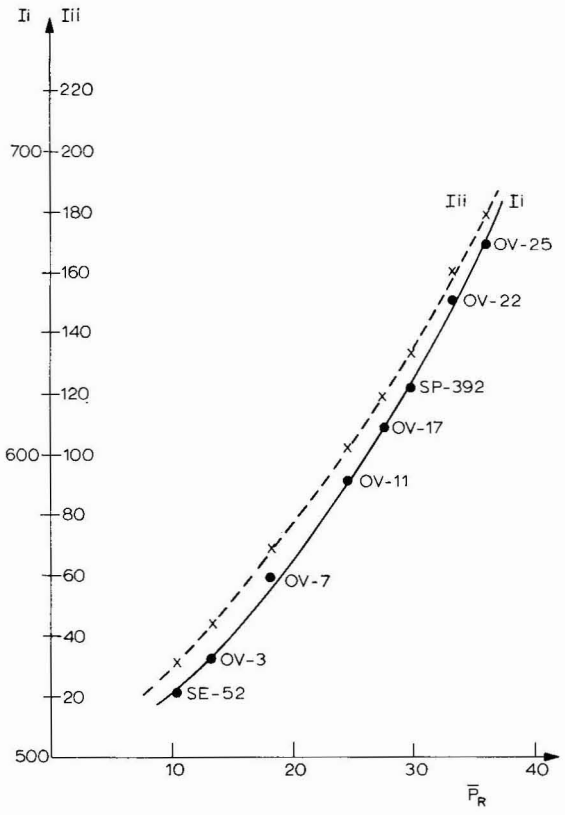

Fig. 1. Interaction contributions *versus* retention polarity of different stationary phases.

TABLE II

DEPENDENCE OF THE INCREMENT VALUES FOR ETHYLBENZENE ON THE TYPE OF STATIONARY PHASE AT 120 °C

Increment code	*Stationary phase*				
	Standard apolar[5]	*APL*	*PEG 20M*	*DEGA*	*DEGS*
C,21,003A,000	39.33	39.37	51.45	54.79	62.50
C,3A2,02A2A,001	40.09	40.13	52.45	55.85	63.71
C,3A2A,02A2,002A	54.87	54.93	71.78	76.44	87.19
C,2A2A,003A,002A	55.45	55.51	72.54	77.25	88.11
C,2A2A,002A,002A	62.42	62.49	81.66	86.96	99.19
H,2A,02A2A,000,003A,002A	46.38	46.43	60.68	64.61	73.70
H,2A,02A3A,000,002A,02A2	41.39	41.44	54.15	57.66	65.77
H,2,013A,000,000,02A2A	37.05	37.09	48.47	51.61	58.88
H,1,002,000,000,003A	45.92	45.97	60.08	63.97	72.97
H,2A,02A2A,000,002A,002A	49.54	49.59	64.81	69.01	78.72

TABLE III

DEPENDENCE OF THE INCREMENT VALUES FOR *n*-PROPYLBENZENE OF COLUMN TEMPERATURE ON STANDARD APOLAR STATIONARY PHASE[5]

Increment code	*Column temperature (°C)*		
	70.0	*130.0*	*190.0*
C,21,002,000	31.55	32.29	33.04
C,22,003A,001	34.26	35.07	35.88
C,3A2,02A2A,002	40.34	41.30	42.25
C,3A2A,02A2,002A	53.86	55.14	56.41
C,2A2A,003A,002A	54.43	55.71	57.00
C,2A2A,002A,002A	61.27	62.72	64.17
H,2A,02A2A,000,003A,002A	45.53	46.60	47.68
H,2A,02A3A,000,002A,02A2	40.63	41.59	42.55
H,2,012,000,000,003A	39.26	40.19	41.12
H,2A,02A2A,000,002A,002A	48.63	49.78	50.93
H,2,012,000,000,003A	37.83	38.73	39.62
H,1,002,000,000,002	36.86	37.73	38.60

TABLE IV

DEPENDENCE OF THE INTERACTION FACTOR ON HEATING RATE IN TPGC APPLYING PPG (UCON LB-550X) AS THE STATIONARY PHASE, AFTER SCHULZ AND REITEMEYER'S[11] MEASUREMENTS

Heating rate (°C/min)	*Interaction factor*
0.5	4.408
1.0	4.422
1.5	4.426
2.0	4.440

one carbon atom on a standard apolar stationary phase at 190° C should be noted.

In the following, the pre-calculation of retention indices for benzene derivatives in temperature-programmed gas chromatography (TPGC) is considered[50]. In recent years, many researchers have dealt with various problems connected with this

TABLE V

INFLUENCE OF THE AMOUNT OF STATIONARY PHASE ON THE INTERACTION FACTOR ON PEG 20M STATIONARY PHASE ON CHROMOSORB P (60–80 MESH) AT 140 °C, AFTER MEASUREMENTS OF BONASTRE *et al.*[12]

Compound	*Stationary phase (%, w/w)*					
	2.5	*5.0*	*10.0*	*15.0*	*20.0*	*30.0*
Benzene	5,202	5.552	5.768	5.860	5.964	6.014
Toluene	4.936	5.210	5.431	5.510	5.583	5.646
Ethylbenzene	4.791	5.082	5.247	5.336	5.393	5.464
n-Propylbenzene	4.682	4.930	5.070	5.156	5.211	5.275
n-Butylbenzene	4.614	4.815	4.946	5.023	5.089	5.147

system. Van den Dool and Kratz's work[51] and also the book by Harris and Habgood[52] are particularly important in TPGC.
In TPGC[54,55]

$$I\,(\mathrm{TPGC}) = I_M \cdot \pi\,(\mathrm{TPGC}) \tag{3}$$

$$\pi\,(\mathrm{T}) = A + \frac{B}{T + C} \tag{4}$$

$$\pi\,(\mathrm{TPGC}) = \frac{\int_{T_0}^{T_R} \pi\,\mathrm{d}T}{T_R - T_0} = A + \frac{B \ln\left(\frac{T_R + C}{T_0 + C}\right)}{T_R - T_0} \tag{5}$$

where

T_R = retention temperature (°K);
T_0 = initial temperature (°K) (TPGC);
A, B and C = constants.

The dependence of the interaction factor on heating rate (°C/min) in TPGC, applying polypropylene glycol (Ucon LB-550X) as the stationary phase, based on the work of Schulz and Reitemeyer[11], is presented in Table IV.

The influence of the amount of PEG 20M stationary phase (%,w/w) on the interaction factor on Chromosorb P (60–80 mesh) at 140°C, based on measurements by Bonastre *et al.*[12], is shown in Table V.

Determination of the codes and calculation of the increment values were effected by means of a computer[53]. The computer program for benzene derivatives is shown in Fig. 2.

The coding and pre-calculation of the retention index of ethylbenzene made by means of a computer is illustrated as an example in Fig. 3.

EXPERIMENTAL

The measurements were performed by means of Perkin-Elmer 900, Erba Science 2300, GI-452, Perkin-Elmer F11 instruments. In each instance flame-ionization detectors were used, together with nitrogen or helium as the carrier gas.

Calculations were performed by means of a Hewlett-Packard 9830A computer fitted with a Hewlett-Packard 9866A printer. Programs were written in BASIC computer language.

Pre-calculations of retention indices made by computer for alkylbenzene derivatives on a standard apolar stationary phase at 100 °C are presented in Table VI.

CONCLUSION

In the pre-calculation of retention data by means of increments the initial problems have been overcome and a method with good practical applicability has been developed. The determination of increment codes by computer should make possible the wider application of the pre-calculation of retention data.

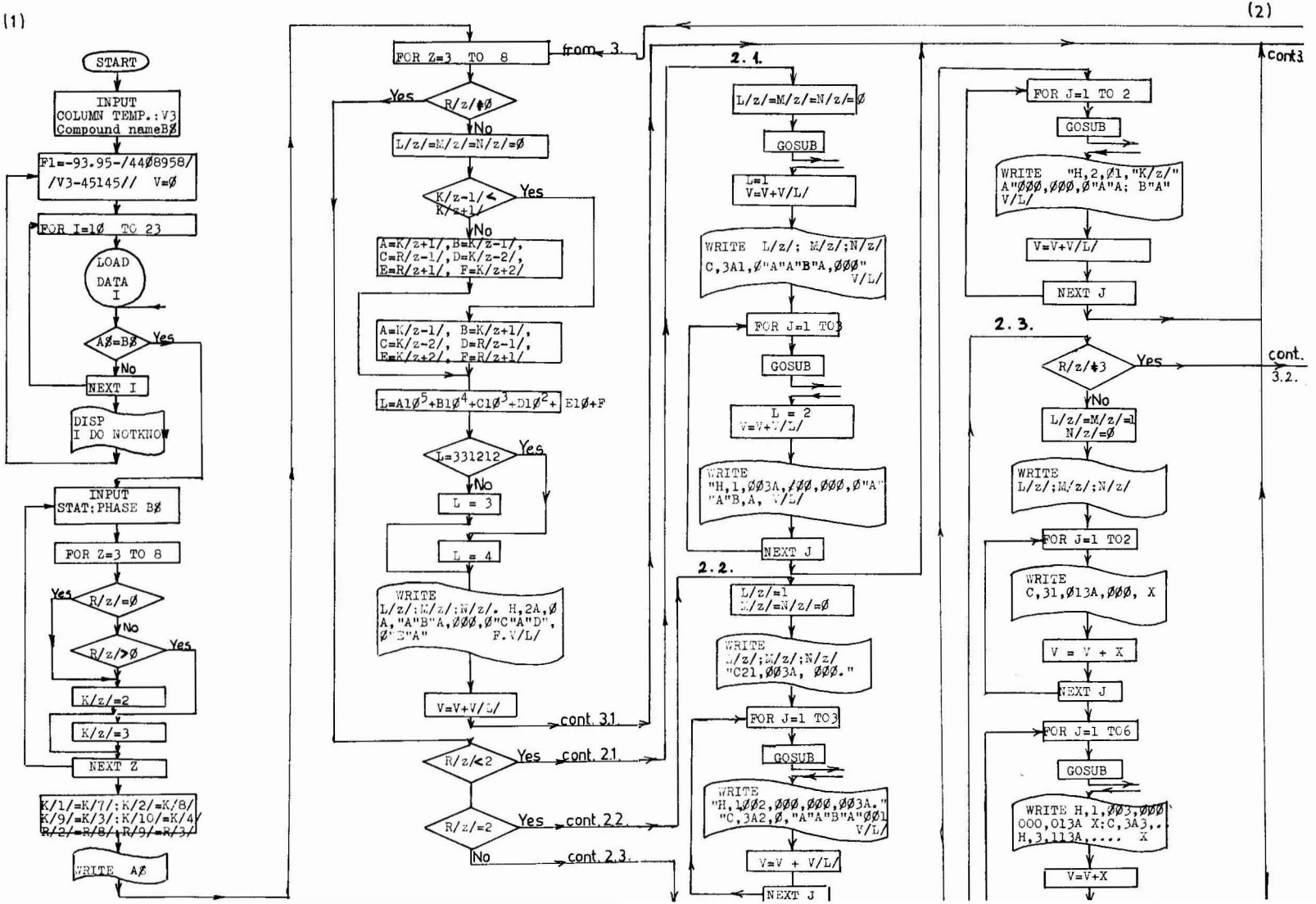
(1)
START
INPUT COLUMN TEMP.:V3 Compound nameBØ
F1=-93.95-/44Ø8958/ /V3-45145// V=Ø
FOR I=1Ø TO 23
LOAD DATA I
AØ=BØ
Yes
No
NEXT I
DISP I DO NOTKNOW
INPUT STAT:PHASE BØ
FOR Z=3 TO 8
R/z/=Ø
R/z/>Ø
K/z/=2
K/z/=3
NEXT Z
K/1/=K/7/;K/2/=K/8/ K/9/=K/3/;K/10/=K/4/ R/2/=R/8/;R/9/=R/3/
WRITE AØ
FOR Z=3 TO 8
from 3.
R/z/ØØ
L/z/=M/z/=N/z/=Ø
K/z-1/< K/z+1/
A=K/z+1/,B=K/z-1/, C=R/z-1/,D=K/z-2/, E=R/z+1/, F=K/z+2/
A=K/z-1/, B=K/z+1/, C=K/z-2/, D=R/z-1/, E=K/z+2/, F=R/z+1/
L=A1Ø^5+B1Ø^4+C1Ø^3+D1Ø^2+ E1Ø+F
L=331212
L = 3
L = 4
WRITE L/z/;M/z/;N/z/. H,2A,Ø A,"A"B"A,ØØØ,Ø"C"A"D", Ø"E"A F.V/L/
V=V+V/L/
cont. 3.1.
R/z/<2
Yes
cont. 2.1.
R/z/=2
cont. 2.2.
No
cont. 2.3.
2. 1.
L/z/=M/z/=N/z/=Ø
GOSUB
L=1 V=V+V/L/
WRITE L/z/; M/z/;N/z/ C,3A1,Ø"A"A"B"A,ØØØ" V/L/
FOR J=1 TO3
L = 2 V=V+V/L/
WRITE "H,1,ØØ3A,ØØØ,ØØØ,Ø"A" "A"B,A, V/L/
NEXT J
2. 2.
L/z/=1 M/z/=N/z/=Ø
WRITE M/z/;M/z/;N/z/ "C21,ØØ3A, ØØØ."
FOR J=1 TO3
WRITE "H,1ØØ2,ØØØ,ØØØ,ØØ3A." "C,3A2,Ø,"A"A"B"A"ØØ1 V/L/
V=V + V/L/
NEXT J
(2)
cont3
FOR J=1 TO 2
WRITE "H,2,Ø1,"K/z/" A"ØØØ,ØØØ,Ø"A"A; B"A" V/L/
V=V+V/L/
NEXT J
2. 3.
R/z/Ø3
Yes
cont. 3.2.
No
L/z/=M/z/=1 N/z/=Ø
WRITE L/z/;M/z/;N/z/
FOR J=1 TO2
WRITE C,31,Ø13A,ØØØ, X
V = V + X
NEXT J
FOR J=1 TO6
GOSUB
WRITE H,1,ØØ3,ØØØ 000,013A X;C,3A3,. H,3,113A,.... X
V=V+X

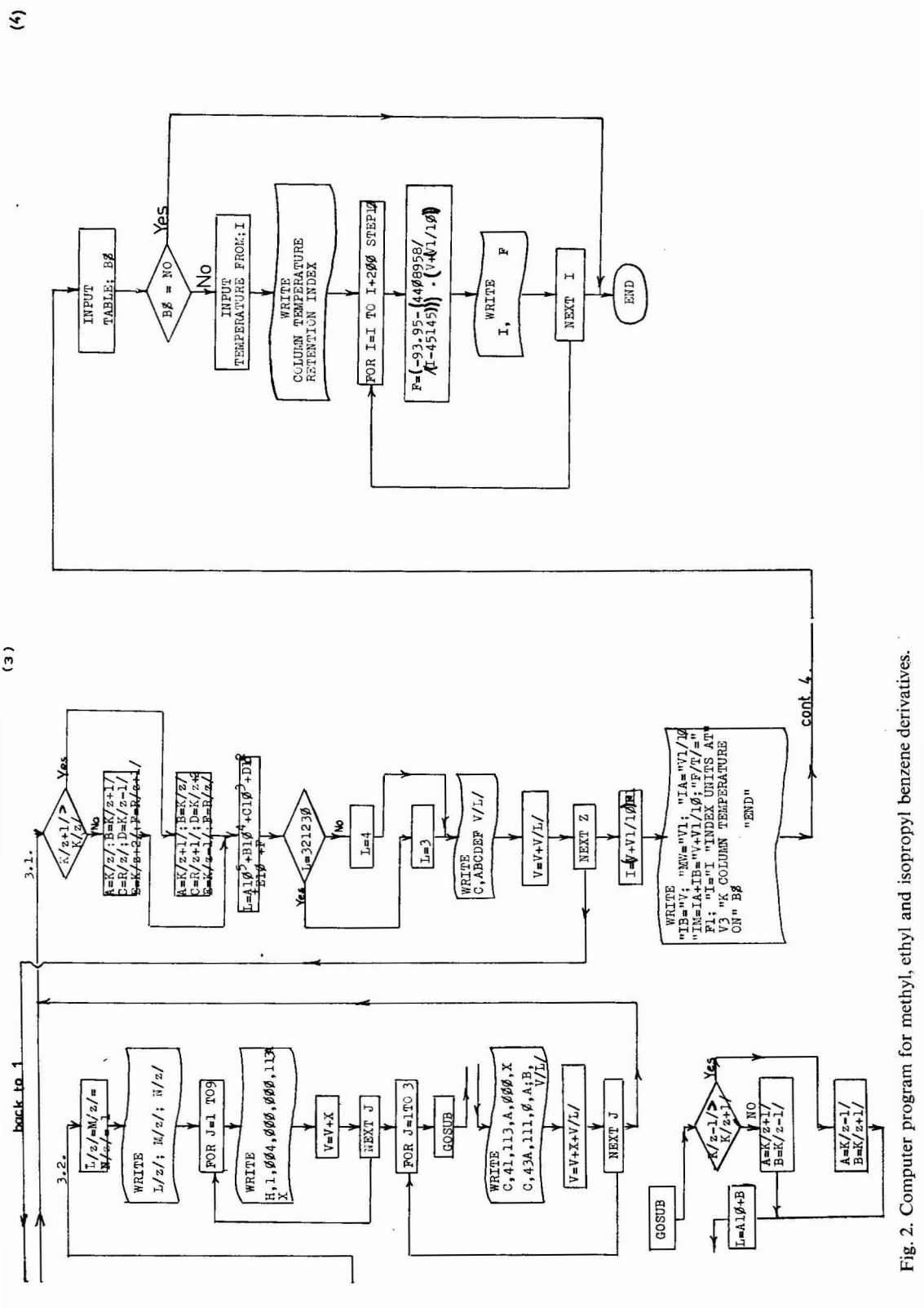

Fig. 2. Computer program for methyl, ethyl and isopropyl benzene derivatives.

```
                    ETHYLBENZENE
L3 = 1    M3 = 0     N3 = 0
C,21,003A,000.                          39.33
H,1,002,C00,000,003A.                   45.92
H,1,002,000,000,003A.                   45.92
H,1,002,000,000,003A.                   45.92
C,3A2,02A2A,001.                        40.09
H,2,013A,000,000,02A2A.                 37.05
H,2,013A,000,000,02A2A.                 37.05
C,3A2A,02A2,002A.                       54.87
L4 = 0    M4 = 0     N4 = 0
H,2A,02A3A,000,002A,02A2.               41.39
C,2A2A,003A,002A.                       55.45
L5 = 0    M5 = 0     N5 = 0
H,2A,02A2A,C00,003A,002A.               46.38
C,2A2A,002A,002A.                       62.42
L6 = 0    M6 = 0     N6 = 0
H,2A,02A2A,000,002A,002A.               49.54
C,2A2A,002A,002A.                       62.42
L7 = 0    M7 = 0     N7 = 0
H,2A,02A2A,000,003A,002A.               46.38
C,2A2A,003A,002A.                       55.45
L8 = 0    M8 = 0     N8 = 0
H,2A,02A3A,000,002A,02A2.               41.39
C,3A2A,02A2,002A.                       54.87
                                  ----------
                          IB + II=  861.84


                    MW = 106
                    IA = 10.60
  STANDARD APOLAR STATIONARY PHASE ACCORDING TC KOVATS
                  AND CC-WORKERS
          I = IA + IB + II = 872.4 IU.
          AT 393.16 K COLUMN TEMPERATURE
               ETHYLBENZENE END
```

Fig. 3. Pre-calculation of retention index for ethylbenzene by increments using a computer.

TABLE VI

PRE-CALCULATION OF RETENTION INDICES OF ALKYLBENZENES ON STANDARD APOLAR STATIONARY PHASE AT 100.0 °C ACCORDING TO RIEDO *et al.*[5]

Compound	*Retention index (i.u.)*	*Compound*	*Retention index (i.u.)*
Benzene	663	1,2,3,5-Tetramethylbenzene	1134
Toluene	774	1,3-Diisopropylbenzene	1141
Ethylbenzene	866	1-Ethyl-4-*n*-propylbenzene	1147
1,4-Dimethylbenzene	881	*n*-Pentylbenzene	1154
1,3-Dimethylbenzene	881	1-Methyl-4-*n*-butylbenzene	1160
1,2-Dimethylbenzene	902	1,2,3,4-Tetramethylbenzene	1160
Isopropylbenzene	925	1,3-Dimethyl-5-*tert.*-butylbenzene	1172
n-Propylbenzene	955	1,4-Diisopropylbenzene	1176
1-Methyl-3-ethylbenzene	967	1-Isopropyl-4-*n*-propylbenzene	1204
1-Methyl-4-ethylbenzene	972	1,2-Di-*n*-propylbenzene	1213
1-Methyl-2-ethylbenzene	984	1,3-Di-*n*-propylbenzene	1218
1,3,5-Trimethylbenzene	987	1,3,5-Triethylbenzene	1220
tert.-Butylbenzene	990	1-Ethyl-2-*n*-butylbenzene	1234
1,2,4-Trimethylbenzene	1005	1,4-Di-*n*-propylbenzene	1235
sec.-Butylbenzene	1009	1-Ethyl-4-*n*-butylbenzene	1250
Isobutylbenzene	1010	*n*-Hexylbenzene	1254
1-Methyl-3-isopropylbenzene	1029	1-Methyl-4-*n*-pentylbenzene	1259
1-Methyl-4-isopropylbenzene	1031	1-Methyl-2-*n*-pentylbenzene	1262
1,2,3-Trimethylbenzene	1032	1,4-Di-*tert.*-butylbenzene	1305
1-Methyl-2-isopropylbenzene	1038	1-*tert.*-Butyl-4-isobutylbenzene	1315
1,3-Diethylbenzene	1046	1-*tert.*-Butyl-4-*sec.*-butylbenzene	1315
1-Methyl-3-*n*-propylbenzene	1055	1,3,5-Triisopropylbenzene	1317
n-Butylbenzene	1056	1,4-Di-*sec.*-butylbenzene	1329
1,2-Diethylbenzene	1058	1-*sec.*-Butyl-4-isobutylbenzene	1330
1-Methyl-4-*n*-propylbenzene	1060	1,4-Diisobutylbenzene	1332
1,4-Diethylbenzene	1060	1-*n*-Propyl-4-*n*-butylbenzene	1335
1-Methyl-2-*n*-propylbenzene	1065	1-Ethyl-4-*n*-pentylbenzene	1347
1,3-Dimethyl-5-ethylbenzene	1068	1-Methyl-4-*n*-hexylbenzene	1358
1,4-Dimethyl-3-ethylbenzene	1080	1-*tert.*-Butyl-4-*n*-butylbenzene	1370
1,4-Dimethyl-2-ethylbenzene	1082	1-*sec.*-Butyl-4-*n*-butylbenzene	1384
1-Methyl-3-*tert.*-butylbenzene	1085	1-Iso-butyl-4-*n*-butylbenzene	1385
1,3-Dimethyl-4-ethylbenzene	1086	1-*n*-Propyl-4-*n*-heptylbenzene	1406
tert.-Pentylbenzene	1091	1,2,4,5-Tetraisopropylbenzene	1432
1,2-Dimethyl-4-ethylbenzene	1093	1,4-Di-*n*-butylbenzene	1437
1,3-Dimethyl-2-ethylbenzene	1094	Hexamethylbenzene	1441
sec.-Pentylbenzene	1098	1-*n*-Propyl-4-*n*-pentylbenzene	1445
1-Methyl-4-*tert.*-butylbenzene	1098	1-Ethyl-4-*n*-hexylbenzene	1447
1,2-Dimethyl-3-ethylbenzene	1110	1-Methyl-4-*n*-heptylbenzene	1461
1,2,4,5-Tetramethylbenzene	1128		

ACKNOWLEDGEMENTS

The authors express their thanks to Mr. Dániel Rácz for supporting the research work and to Mrs. I. Völgyi, Mrs. I. Vér and Mr. R. Kozma for technical assistance.

REFERENCES

1 E. Vermes, L. Ackermann, I. Szebényi and J. Takács, Reprints of IVth *Chromatographic Conference, Györ, 1974*, p. 305.
2 Ta Chuang Lo Chang and C. Karr, *Anal. Chim. Acta*, 24 (1961) 434.
3 E. Sz. Kováts, *Helv. Chim. Acta*, 41 (1958) 1915.
4 L. S. Ettre, *Anal. Chem.*, 34 (1964) 31A.
5 F. Riedo, D. Fritz, G. Tarján and E. Sz. Kováts, *J. Chromatogr.*, 126 (1976) 63.
6 L. Soják, P. Majer, J. Krupčik and J. Janák, *J. Chromatogr.*, 65 (1972) 143.
7 B. B. Agrawal, K. Tesařík and J. Janák, *J. Chromatogr.*, 65 (1972) 207.
8 G. Schomburg, *J. Chromatogr.*, 23 (1966) 18.
9 G. Schomburg, *Chromatographia*, 4 (1971) 286.
10 R. A. Hively and R. E. Hinton, *J. Gas Chromatogr.*, 6 (1968) 203.
11 H. Schulz and H. O. Reitemeyer, *Chromatographia*, 1 (1968) 1.
12 J. Bonastre, Ph. Grenier and P. Cazenave, *Bull. Soc. Chim. Fr.*, (1968) 1266.
13 R. Hatch, *J. Gas Chromatogr.*, 6 (1968) 611.
14 J. Krupčik, O. Liška and L. Soják, *J. Chromatogr.*, 51 (1970) 119.
15 F. W. Karasek, *J. Chromatogr. Sci.*, 8 (1970) 282.
16 F. W. Karasek, A. I. Grimard and B. L. Deelstra, *J. Chromatogr. Sci.*, 10 (1972) 725.
17 R. Louis, *Erdöl Kohle*, 24 (1971) 88.
18 R. Louis, *Erdöl Kohle*, 25 (1972) 582.
19 P. G. Robinson and A. L. Odell, *J. Chromatogr.*, 57 (1971) 1.
20 B. Wallaert, *Bull. Soc. Chim. Fr.*, (1971) 1107.
21 N. Dimov and D. Schopov, *J. Chromatogr.*, 63 (1971) 223.
22 L. E. Cook and F. M. Raushel, *J. Chromatogr.*, 65 (1972) 556.
23 L. Soják and J. Hrivnák, *J. Chromatogr. Sci.*, 10 (1972) 701.
24 P. Fuchs, *J, Chromatogr.*, 65 (1972) 219.
25 F. Vernon, *J. Chromatogr.*, 87 (1973) 29.
26 G. D. Mitra, G. Mohan and A. Sinha, *J. Chromatogr.*, 91 (1974) 633.
27 W. Engewald, K. Epsch, J. Graefe and Th. Welsch, *J. Chromatogr.*, 91 (1974) 623.
28 V. Švob, D. Deur-Šiftar and C. A. Cramers, *J. Chromatogr.*, 91 (1974) 659.
29 M. J. Hartigen and J. E. Purcell, *Chromatogr. Newsl.*, 3 (1974) 1.
30 Sh. D. West and R. C. Hall, *J. Chromatogr. Sci.*, 13 (1975) 5.
31 L. Soják and J. A. Rijks, *J. Chromatogr.*, 119 (1976) 505.
32 M. Ryba, *J. Chromatogr.*, 123 (1976) 317.
33 M. Ryba, *J. Chromatogr.*, 123 (1976) 327.
34 W. Engewald and L. Wennrich, *Chromatographia*, 9 (1976) 540.
35 J. M. Takács. *J. Chromatogr. Sci.*, 11 (1973) 210.
36 J. M. Takács, *J. Chromatogr. Sci.*, 12 (1974) 421.
37 T. S. Lombosi, E. R. Lombosi, I. Bernát, Zs. Sz. Bernát, E. C. Takács and J. M. Takács, *J. Chromatogr.*, 119 (1976) 307.
38 E. C. Takács, J. Vörös and J. M. Takács, *J. Chromatogr.*, in press.
39 J. Takács, C. Szita and G. Tarján, *J. Chromatogr.*, 56 (1971) 1.
40 E. Bojti, M. Mihók, I. Borbély, J. Bárkai and J. M. Takács, *J. Chromatogr.*, 119 (1976) 321.
41 L. S. Bartell, *Tetrahedron.* 17 (1962) 177.
42 L. S. Bartell, *J. Chem. Phys.*, 32 (1960) 827.
43 L. S. Bartell, *J. Chem. Educ.*, 45 (1968) 754.
44 G. Herzberg and B. P. Sticheff, *Nature (London)*, 175 (1955) 79.
45 B. P. Sticheff, *Tetrahedron*, 17 (1962) 135.
46 D. R. Stull, E. F. Westrum, Jr., and G. C. Sinke, *The Chemical Thermodynamics of Organic Compounds*, Wiley, New York, 1969.
47 J. D. Cox and G. Pilcher, *Thermochemistry of Organic and Organometallic Compounds*, Academic Press, New York, 1970.
48 W. O. McReynolds, *J. Chromatogr. Sci.*, 8 (1970) 685.
49 G. Tarján, Á. Kiss, G. Kocsis, S. Mészáros and J. M. Takács, *J. Chromatogr.*, 119 (1976) 327.
50 P. Majlát, Z. Erdös and J. Takács, *J. Chromatogr.*, 91 (1974) 89.
51 H. van den Dool and P. D. Kratz, *J. Chromatogr.*, 11 (1963) 463.

52 W. E. Harris and H. W. Habgood, *Programmed Temperature Gas Chromatography*, Wiley, New York, 1966.
53 I. Fisch, J. Vörös, G. Tarján, B. Tóth, F. Hoffer, E. C. Takács and J. M. Takács, *Magy. Kém. Foly.*, in press.
54 T. Tóth and J. Takács, *Magy. Kém. Foly.*, 77 (1971) 252.
55 I. Fisch, I. Olácsi, M. Richter and J. M. Takács, *1st Danube Symposium on Chromatography, Szeged, 1975.*

Journal of Chromatography, 148 (1978) 31–36

CHROM. 10,398

CONCENTRATION EFFECT IN GEL PERMEATION CHROMATOGRAPHY

II. VISCOSITY PHENOMENA IN THE INTERSTITIAL VOLUME

J. JANČA and S. POKORNÝ

Institute of Macromolecular Chemistry, Czechoslovak Academy of Sciences, 162 06 Prague 6 (Czechoslovakia)

SUMMARY

The effect of the viscosity of the injected polymer solution in gel permeation chromatography was investigated using samples of polystyrene standards with molecular weights above the exclusion limit of the column packing used. It was confirmed that a linear relationship existed between the specific viscosity of the injected polymer solution and the elution volume in the range of the flow-rates in which there was no essential effect of non-Newtonian flow. At higher flow-rates of the solvent, non-Newtonian behaviour of the polymer solution in the chromatographic column was observed.

INTRODUCTION

In Part I of this series[1], the dependence of the elution volume on the concentration of the injected polymer solution in gel permeation chromatography (GPC) on porous glass was studied, under conditions such that the size of the accessible pores did not change with changing thermodynamic properties of the solvent. Equations were derived that quantitatively described the processes responsible for this concentration dependence. It was assumed that the viscosity effect in the interstitial volume also contributed to the overall concentration effect. This assumption was expressed quantitatively as follows:

$$V_v = \frac{k'}{L} \cdot \int_0^L \eta_{spec} \cdot du \tag{1}$$

V_v is the elution volume increment proportional to the difference in the viscosities of the polymer solution along the column, η_{spec} is the specific viscosity of the polymer solution varying during the movement of the chromatographic zone through the column, L is the column length, k' is a proportionality constant and u is the axial coordinate of the chromatographic column. The work described here is an attempt to verify experimentally the general validity of the above assumption.

EXPERIMENTAL

Gel permeation chromatography

GPC measurements were performed with a purpose-built apparatus. A linear feeder of the type usual in the continuous feeding of liquids into chemical reactors was used as the solvent pump. The linear rate of movement of the piston, and thus also the flow-rate of the solvent, were constant with an accuracy greater than 0.05% (accuracy of the experimental method) at all flow-rates used. The measurement of the elution volume was derived from the movement of mechanical parts of the linear feeder and was therefore independent of the flow-rate. The volume of one count was 0.2091 ml in all instances.

The samples were injected using a six-port injection valve (Waters Assoc., Milford, Mass., U.S.A.) and a loop, the total volume injected being 80 μl. The separation column was 30 cm long, 8 mm I.D., and the standard end fitting of the column (Waters) had concentric radial grooves providing a uniform flow distribution throughout the cross-section at the beginning of the column. The stainless-steel fritted discs were replaced with simple stainless-steel sieves of aperture diameter 40 μm. The column was placed in a jacket thermostated, together with the refractometer, at $25 \pm 0.01°$. The R-403 differential refractometer (Waters) was adjusted by reducing the inner diameter of the inlet capillary to 0.25 mm, so that the overall dead volume was reduced as much as possible (to *ca.* 60 μl). The reference cell of the refractometer was connected in the hydraulic circuit between the pump and the injection valve, which was attached to the head of the column with a capillary of I.D. 1 mm and length 5 cm. The silica gel column packing (Porasil B, Waters) was sieved to a particle size of 63–71 μm. A visual microscopical check of the sieving confirmed that there were no irregular or dust particles in the silica gel after sieving. The column was packed in the dry state by the gradual addition of silica gel and tapping. Tetrahydrofuran (THF), distilled from copper(I) chloride, was used as a solvent.

Polystyrene samples

Polystyrene (PS) standards (Waters) with a narrow molecular weight distribution ($\bar{M}_w/\bar{M}_n < 1.1$) were used. The designation of the PS standards and the molecular parameters are given in Table I. All calculations were carried out using the Mark–Houwink equation:

$$[\eta] = 1.17 \cdot 10^{-2} M^{0.717} \tag{2}$$

valid for linear PS in THF at 25°, and the Huggins constant $k_H = 0.362$; the relevant literature references were given in Part I[1].

RESULTS AND DISCUSSION

In reproducing experiments described in Part I[1], but using a column of a higher efficiency as characterized by the height equivalent to a theoretical plate (HETP), we obtained a different shape of the gel permeation chromatograms. It was obvious that some important phenomena could be suppressed owing to a greater dispersion of the chromatographic zone. It was our aim to reduce the total dispersion

of the chromatographic zone as much as possible, which was achieved by careful sieving of the packing, high-quality packing, adjustment of the end fitings of the column and choosing a smaller length of the column.

The calibration graph presented in Fig. 1 was obtained by measurements on PS standards, the concentration of the injected solutions being 0.05% (w/v). Fig. 1 shows that the PS standards with a molecular weight higher than 50 000 lie above the exclusion limit of the packing used and consequently their molecules migrate in the interstitial volume only.

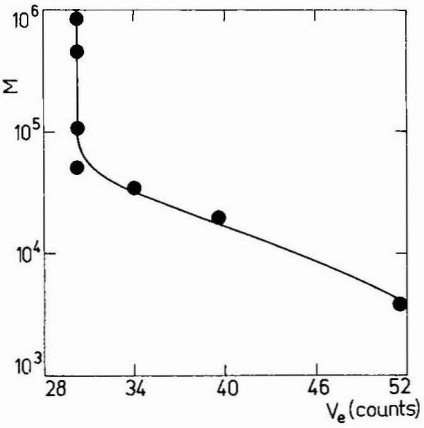

Fig. 1. Calibration graph for the chromatographic column used.

Further investigations were carried out solely with the standards PS 1–PS 3, the molecular weights of which lay above the exclusion limit. The concentrations of these standards were chosen so as to make the η_{spec} values of solutions of different standards always the same, within the limits of experimental error. The η_{spec} values and the corresponding concentrations calculated for the individual standards PS 1–PS 3 using the Huggins equation, the Mark–Houwink equation and the constant k_H are given in Table I. We prepared solutions of the standards PS 1–PS 3 having the highest concentrations given in Table I, lower concentrations being were obtained by diluting the solutions.

TABLE I

MOLECULAR WEIGHTS OF PS STANDARDS AND CONCENTRATIONS AT GIVEN η_{spec} VALUES

Standard	*Molecular weight* $\bar{M}_w \cdot 10^{-3}$	*Concentration of PS standards (%, w/v) at nine* η_{spec} *values*								
		7.286	*2.650*	*1.077*	*0.476*	*0.223*	*0.107*	*0.053*	*0.026*	*0.013*
PS 1	2610	0.71	0.355	0.1775	0.0888	0.0444	0.0222	0.0111		
PS 2	867		0.783	0.3915	0.1958	0.0979	0.0489	0.0245	0.0122	
PS 3	470		1.214	0.607	0.3035	0.1518	0.0759	0.0379	0.0190	0.0095
PS 4	110									
PS 5	51									
PS 6	35									
PS 7	20.8									
PS 8	3.6									

Chromatograms of the standard PS 1 at different injected concentrations and the same sensitivity of the refractometer at a flow-rate of 0.334 ml/min are shown in Fig. 2. Chromatogram 1 was obtained with an injected solution of the standard PS 1 having the lowest η_{spec} (0.053); chromatogram 7 was recorded with an injected solution with the highest η_{spec} (7.286). Chromatograms 1–4, taken at low η_{spec} values, are very similar in character. Chromatograms 5–7, at higher η_{spec} values, possess a more complicated structure; in all instances there is a distinct increase in the width of the chromatograms, and the elution volumes are shifted to higher values. Similar observations were made by Moore[2], who attributed them to viscous fingering[3].

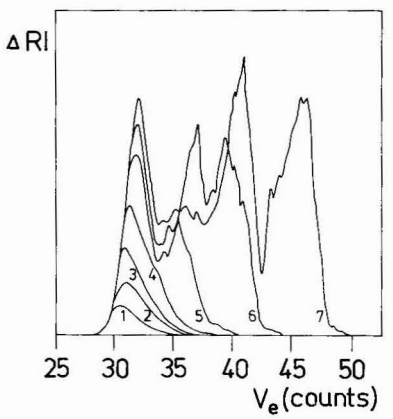

Fig. 2. Chromatograms of standard PS 1 at a flow-rate of 0.334 ml/min. Specific viscosity of injected solution: η_{spec} = 0.053 (chromatogram 1), 0.107 (2), 0.223 (3), 0.476 (4), 1.077 (5), 2.650 (6), 7.286 (7).

We tried to determine the relationship between the average elution volume and the width of the chromatographic zone at various η_{spec} values. Average elution volumes (V_{av}) were calculated from the chromatograms using the expression

$$V_{av} = \frac{\Sigma V_i \cdot h_i}{\Sigma h_i} \tag{3}$$

where h_i are the heights of the chromatograms from the baseline in the elution volumes V_i. The band width of the elution curves was characterized by the variance, var (V), according to

$$\text{var}\,(V) = \frac{\Sigma(h_i \cdot [V_i - V_{av}]^2)}{\Sigma h_i} \tag{4}$$

where var (V) = σ^2 and σ is the standard deviation. In Fig. 3, σ values are plotted against V_{av} for the individual chromatograms in Fig. 2. As can be seen in Fig. 3, there is a linear relationship between σ and V_{av}. This linear relationship was also observed at other flow-rates (0.038 and 3.0 ml/min).

If the assumption expressed by eqn. 1 is correct, then experiments should show that the elution volumes are the same for different PS standards whose injected solutions have the same η_{spec} values. The experimental results shown in Fig. 4 confirm the correctness of the above assumption. With injected solutions of the standards

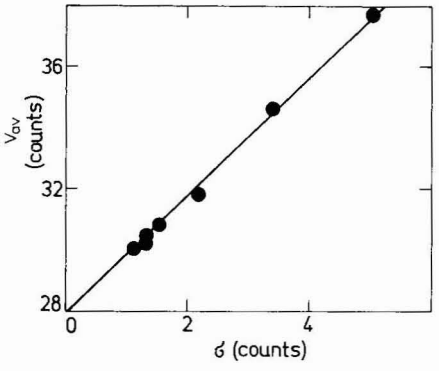

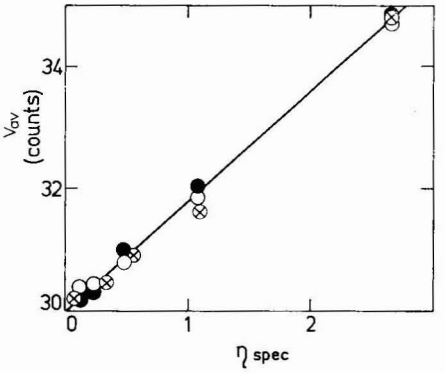

Fig. 3. Dependence of the elution volume (V_{av}) on the width of the chromatogram (σ) (measured at a flow-rate of 0.334 ml/min).

Fig. 4. Dependence of the elution volume (V_{av}) on the specific viscosity (η_{spec}) of solutions of various polystyrene standards: ●, PS 1; ○, PS 2; ⊗, PS 3; flow rate, 0.334 ml/min.

PS 1–PS 3 having the same η_{spec} values, we not only obtained the same V_{av} values, within the limits of experimental error, but the chromatograms for the standards PS 2 and PS 3 were also the same as those of the standard PS 1 in Fig. 2. The linear dependence of V_{av} on η_{spec} within the investigated range of η_{spec} values was also confirmed by the experiment. The results in Fig. 4 were measured at a flow-rate of 0.334 ml/min, but the measurement was also performed at a flow-rate of 0.038 ml/min with similar results.

On extending the range of η_{spec} values of the injected solutions up to 7.286, a deviation from the linearity of the relationship between V_{av} and η_{spec} was observed, which was greater at a flow-rate of 0.334 ml/min than at 0.038 ml/min, as shown in Fig. 5. At a flow-rate of 3 ml/min, the deviation from linearity was even more pronounced; moreover, it began at lower η_{spec} values (Fig. 5). These deviations from linearity may be explained by the non-Newtonian behaviour of more viscous solutions

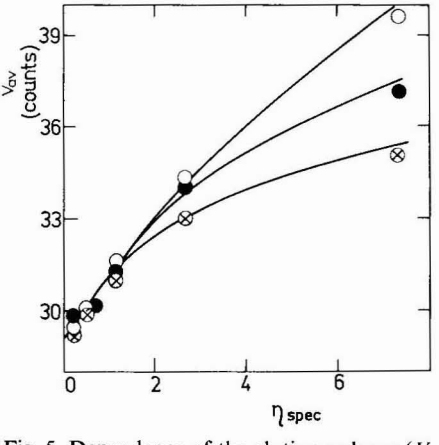

Fig. 5. Dependence of the elution volume (V_{av}) on the specific viscosity (η_{spec}) at various flow-rates: ○, 0.038; ●, 0.334; ⊗, 3.0 ml/min.

of the injected PS standards. The viscosity of concentrated solutions depends on tangential stress[4], which is related to the trans-channel velocity gradient[5]. The decrease in the effect of concentration on the GPC results at high flow-rates (10–35 ml/min) observed by Little *et al.*[6,7] can probably be explained in this way.

The results reported here have confirmed with fairly good accuracy the preceding theoretical reasoning concerning the effect of the viscosity of the polymer solution in GPC column separation. Some other aspects of the viscosity effect and general concentration effects are currently being studied.

ACKNOWLEDGEMENTS

The authors are indebted to Mrs. H. Horká and Mrs. P. Neureutterová for technical assistance.

REFERENCES

1 J. Janča, *J. Chromatogr.*, 134 (1977) 263.
2 J. C. Moore, *Separ. Sci.*, 5 (1970) 723.
3 R. E. Collins, *Flow of Fluids Through Porous Materials*, Reinhold, New York, 1961, pp. 196–200.
4 W. Holzmüller and K. Altenburg, *Physik der Kunststoffe*, Akademie Verlag, Berlin, 1961; Czech translation, SNTL, Prague, 1966, p. 200.
5 J. C. Giddings, *Dynamics of Chromatography*, Marcel Dekker, New York, 1965, p. 42.
6 J. N. Little, J. L. Waters, K. J. Bombaugh and W. J. Pauplis, *J. Polym. Sci., Part A-2*, 7 (1969) 1775.
7 J. N. Little, J. L. Waters, K. J. Bombaugh and W. J. Pauplis, *J. Chromatogr. Sci.*, 9 (1971) 341.

Journal of Chromatography, 148 (1978) 37–41

CHROM. 10,466

GAS–LIQUID CHROMATOGRAPHY ON MICRO-PACKED COLUMNS WITH CHEMICALLY BONDED STATIONARY PHASES

J. GAWDZIK, Z. SUPRYNOWICZ and J. WÓJCIK

Department of Physical Chemistry, Institute of Chemistry, M. Curie-Skłodowska University, Nowotki 12, 20031 Lublin (Poland)

SUMMARY

Column packings with chemically bonded stationary phases of the "brush" type on controlled-porosity glass beads were prepared. The following organosilicon monomers with different functional groups were used: octadecyltrichlorosilane, phenyltrichlorosilane, 2-cyanoethylmethyldichlorosilane and 3-aminopropyltriethoxysilane. Micro-packed columns of length 5 m and I.D. 0.8 mm were prepared.

The efficiency and selectivity of micro-packed and packed columns of I.D. 4 mm were compared. The mean efficiency of micro-packed columns was 2500 theoretical plates per metre for a partition ratio $k' \geqslant 3$.

INTRODUCTION

The development of the synthesis of chemically bonded stationary phases enabled modern column packings to be obtained, which are employed mainly in liquid chromatography in view of their solvolytic stability. These sorbents have been increasing in importance, especially in reversed-phase chromatography. The high thermal stability of brush-type packings and their specific retention mechanism, with modified adsorption prevailing[1–4], indicate that they can also be applied successfully in gas chromatography. However, it is still difficult to predict the properties of a given liquid phase bonded to a given solid support, and it is necessary to investigate these problems more closely and to synthesize a larger number of packings with various properties. Selective adsorption, modified by the chemical bonding of various functional groups and organic radicals, has a stronger effect and is more widely applied in gas than in liquid chromatography. Further, if difficult separations must be performed in a short time, high efficiencies and selectivities of the columns are required.

These advantages are offered by capillary columns, but their capacities (sample sizes) are very low and often insufficient, and their lifetimes and thermal stability are generally poor. In trace analysis in particular it is difficult to maintain the necessary sensitivity of the detector (limit of detection) and the poor reproducibility of the separation results necessitates the frequent use of standard mixtures, which are often composed of extremely rare compounds. Some of these disadvantages can be partially eliminated by the use of PLOT (SCOT) columns, which have higher capacities and

are more stable; although they are difficult to prepare and have irreprodı properties, they may become a very good separation tool if the technical diffic can be solved.

The reproducibility of the results (retention data) on micro-packed colun satisfactory and much larger sample sizes do not lead to detection problems, the separation efficiencies are relatively high[5,6]. The application of sorbents chemically bonded stationary phases for the preparation of micro-packed col may lead to new possibilities in selective and rapid separations, especially at ele temperatures.

EXPERIMENTAL

Glass beads of controlled porosity prepared in this Laboratory[7–9] were as the support for the chemical bonding of liquid phases. The surface of these l is highly pure and the content of metal ions determined with an electron microprob by X-ray fluorescence spectrometry[10] was found to be very low. To remove exc adsorption properties, due presumably to the presence of micro-pores, the porous l were submitted to an additional thermal treatment[8,11]. Monomeric layers of the l type (Si–O–Si) of various polarities were bound to the beads thus prepared[8] Organosilicon monomers with various functional groups [octadecyltrichloros (ODS), phenyltrichlorosilane (Ph), 2-cyanoethylmethyldichlorosilane (CN) ar aminopropyltriethoxysilane (NH_2)] were used in the synthesis. Part of the mat thus prepared was additionally silanized with a 5% solution of hexamethyldisila in toluene[13]. Derivatographic investigations[8] have shown a high thermal stabili the packings, even above 350°. Elemental analysis of the packings permitte determination of the percentage of chemically bonded liquid phases before and silanization, presented in Table I[6] as the percentage of carbon. The surface co trations of radicals in the CN and NH_2 phases corresponded to the average v obtained for the packings investigated by Majors and Hopper[8,12]. Measuremer the energetic heterogeneity (distribution of adsorptive energy) indicated the dominance of the adsorption mechanism of retention on the packings

TABLE I

RESULTS OF ELEMENTAL ANALYSIS

s = silanized, ns = not silanized.

Stationary phase	*Amount of carbon (%, w/w)*	*Surface concentration of radicals (radicals per 100 Å²)*	
		Main radical	*$-Si(CH_3)_3$*
ODS-ns	1.48	0.58	—
ODS-s	1.87	0.58	0.91
Ph-ns	1.81	2.11	—
Ph-s	1.95	2.11	0.32
CN-ns	1.51	2.65	—
CN-s	1.81	2.65	0.70
NH_2-ns	1.84	4.30	—
NH_2-s	1.96	4.30	0.28

chemically bonded liquid phases synthesized during the investigations[8,13]. The silanized and non-silanized sorbents were used to prepare chromatographic columns of both the classical and micro-packed type which were conditioned for 12 h at 200° before use in chromatographic experiments.

The packing of classical columns was assisted by electromechanical vibration with a simultaneous flow of nitrogen, using an apparatus for column packing constructed in this Laboratory[14]. The columns were 1 m long and 3 mm I.D. The experiments were carried out on a Model G.Ch.F.18.3.4. gas chromatograph manufactured by Giede (Berlin, G.D.R.), equipped with a thermal conductivity detector.

Micro-packed columns, (5 m × 0.8 mm I.D.) were made of glass (Sovirel, France) and filled by electromechanical vibration using an apparatus constructed in this Laboratory[15]. The experiments were carried out on a Polish Model 503 chromatograph equipped with a home-made splitter and a microcatharometer (3-μl cell volume).

RESULTS AND DISCUSSION

The average efficiency of a 5-m micro-packed column was 12,500 theoretical plates for solutes with $k' \geqslant 3$. In Fig. 1, HETP is plotted against flow-rate of the carrier gas for classical and micro-packed columns filled with chemically bonded liquid phases. For micro-packed columns the HETP values were less than half of those obtained for classical columns. Further, the range of average flow-rates of carrier gas corresponding to minor changes in HETP was much wider for the micro-

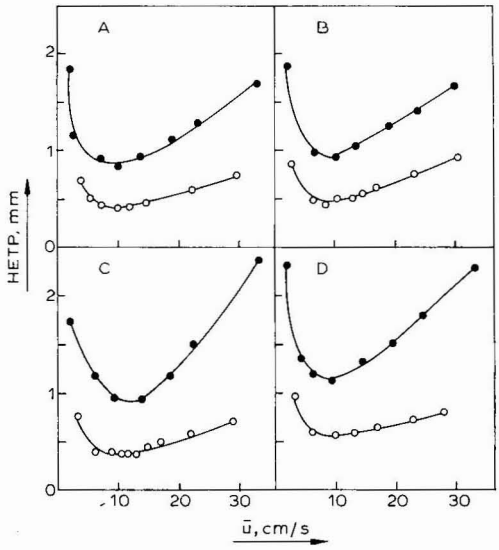

Fig. 1. Plot of HETP *versus* $\bar{u}$ for column packings with chemically bonded stationary phases: A, ODS-s (s = silanized) for *n*-heptane, $k_1' = 3.09$, $k_2' = 4.68$; B, Ph-s for *n*-nonane, $k_1' = 4.35$, $k_2' = 4.66$; C, CN-s for *n*-octane, $k_1' = 4.16$, $k_2' = 4.92$; D, NH_2-s for *n*-heptane, $k_1' = 5.49$, $k_2' = 5.62$. ●, k_1', classical packed column, 4 mm I.D.; ○, k_2', micro-packed column, 0.8 mm I.D. Column temperature, 100°; inlet temperature, 200°; carrier gas, hydrogen.

packed columns. All packings investigated had similar efficiencies, with the exception of the NH_2 type for which had poorer efficiences.

Owing to tailing of the peaks of the more polar substances in the McReynolds' mixture butanol–pyridine–2-methylpentanol, a simpler mixture was used to test the columns. The retention data are given in Table II. Comparison of the chromatograms showed that the ODS and CN packings have the best properties; the peak of nitropropane was asymmetrical for the Ph packing and on the NH_2 packing the solute was completely retained in the column.

TABLE II

PARTITION NUMBERS (k'), RELATIVE RETENTIONS ($r_{1,2}$) (RELATIVE TO *n*-HEPTANE) AND ELUTION OF SQUALANE ON MICRO-PACKED COLUMNS WITH CHEMICALLY BONDED STATIONARY PHASES

Solute	*ODS*			*Ph*			*CN*			*NH_2*		
	Peak No.	k'	$r_{1,2}$	*Peak No.*	k'	$r_{1,2}$	*Peak No.*	k'	$r_{1,2}$	*Peak No.*	k'	$r_{1,2}$
n-Pentane	1	0.82	0.30	1	0.41	0.38	1	0.58	0.34	1	1.15	0.29
n-Hexane	3	1.52	0.55	2	0.66	0.61	2	0.98	0.58	2	2.23	0.57
n-Heptane	5	2.74	1.00	4	1.08	1.00	4	1.69	1.00	4	3.92	1.00
n-Octane	8	4.92	1.80	7	1.74	1.61	5	2.88	1.70	5	8.00	2.04
n-Nonane	9	8.73	3.19	9	2.77	2.56	8	4.85	2.87	7	15.23	3.89
Nitropropane	4	1.92	0.70	8	1.88	1.74	9	7.71	4.56	—	—	—
Benzene	2	1.30	0.47	3	0.74	0.69	3	1.40	0.83	3	3.46	0.88
1-Iodobutane	6	3.64	1.33	5	1.53	1.42	7	3.65	2.16	8	17.77	4.53
1-Octene	7	4.43	1.62	6	1.70	1.57	6	2.96	1.75	6	8.46	2.16

The retentions (relative to *n*-heptane) of benzene, nitropropane and 1-iodobutane increased on the packings in the following order: ODS < Ph < CN < NH_2, whereas for 1-octene the sequence was Ph < ODS < CN < NH_2. In general, ODS is the less polar and NH_2 the most polar of the packings investigated. Benzene was

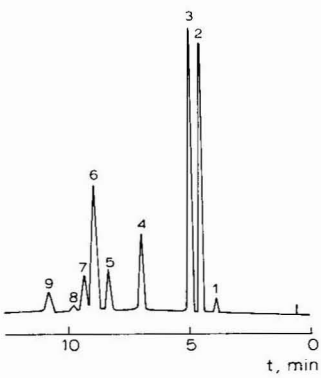

Fig. 2. Separation of light petroleum (b.p. 40–60°) on an ODS-s micro-packed column. Peaks: 1 = 2-methylbutane; 2 = *n*-pentane; 3 = cyclopentane; 4 = 2,2-dimethylbutane; 5 = 2,3-dimethylbutane; 6 = 2-methyl-pentane; 7 = 3-methylpentane; 8 = methylcyclopentane; 9 = *n*-hexane. Column temperature, 35°; inlet temperature, 200°; detector temperature, 100°; carrier gas (hydrogen) flow-rate, 4.6 ml/min; sample volume, 0.04 μl; splitting ratio, 1:5.

eluted ahead of *n*-hexane on the ODS packing after *n*-hexane and on the other packings. The CN packing is more selective towards more polar compounds, especially in the separation of esters. On the other hand, the ODS column is selective towards isomers of light hydrocarbons (Fig. 2), their elution being different from that obtained for a typical partition capillary column with an adhesionally held layer of a non-polar liquid phase (squalane).

The packings with chemically bonded phases gave also interesting results in classical columns; for instance, the CN packing is suitable for the rapid analysis of the less volatile aromatic hydrocarbons (separation of six hydrocarbons in 2 min, Fig. 3A) and the Ph packing for the separation at the relatively low temperature of 120° of a mixture of C_5–C_{16} *n*-alkanes within 6 min (without temperature programming, Fig. 3B).

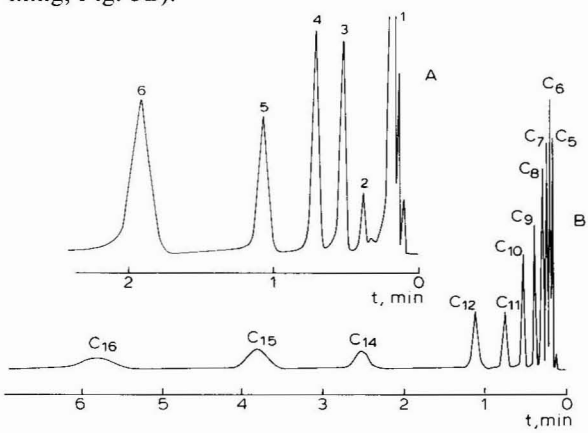

Fig. 3. Chromatograms of rapid separation on packings with chemically bonded stationary phases. A, aromatic hydrocarbons on CN-s: 1 = toluene; 2 = naphthalene; 3 = 2-methylnaphthalene; 4 = 1,3-dimethylnaphthalene; 5 = fluorene; 6 = phenanthrene. Column temperature, 185°; sample volume, 0.5 µl. B. C_5–C_{16} *n*-alkanes on Ph-s. Column temperature, 120°. Packed columns, 1 m × 3 mm I.D.; carrier gas (hydrogen) flow-rate, 50 ml/min; catharometer, 200 mA; sample volume, 0.5 µl.

REFERENCES

1 M. Uihlein and I. Halász, *J. Chromatogr.*, 80 (1973) 15.
2 E. Grushka and J. Kikta, *Anal. Chem.*, 46 (1974) 1370.
3 M. Uihlein and I. Halász, *J. Chromatogr.* 80 (1973) 1.
4 J. J. Pesek and J. E. Daniels, *J. Chromatogr. Sci.*, 14 (1976) 288.
5 C. A. Cramers, J. Rijks and P. Boček, *J. Chromatogr.*, 65 (1972) 29.
6 V. G. Berezkin, L. A. Shkolina and A. T. Svyatoshenko, *J. Chromatogr.*, 99 (1974) 111.
7 A. Waksmundzki, Z. Suprynowicz, J. Gawdzik and A. Dawidowicz, *Chem. Anal. (Warsaw)*, 19 (1974) 1033.
8 J. Gawdzik, *Ph.D. Thesis*, M. C. S. University, Lublin, Poland, 1976.
9 J. Gawdzik, Z. Suprynowicz and M. Jaroniec, *J. Chromatogr.*, 121 (1976) 185.
10 Z. Suprynowicz, E. Tracz and J. Gawdzik, to be published.
11 J. Gawdzik, Z. Suprynowicz and M. Jaroniec, *Chromatographia*, 10 (1977) 191.
12 R. E. Majors and M. J. Hopper, *J. Chromatogr. Sci.*, 12 (1974) 767.
13 J. Gawdzik, Z. Suprynowicz and M. Jaroniec, *J. Chromatogr.*, 131 (1977) 7.
14 Z. Suprynowicz, A. Waksmundzki, A. Gorgol and J. Wójcik, M.C.S. University, Lublin, Poland, unpublished results.
15 Z. Suprynowicz and J. Wójcik, unpublished results.

Journal of Chromatography, 148 (1978) 43–51

CHROM. 10,414

TAILORING POROUS POLYMER GAS CHROMATOGRAPHIC PACKINGS

R. KOMERS, H. KOPECKÁ and M. KRAUS

Institute of Chemical Process Fundamentals, Czechoslovak Academy of Sciences, 165 02 Prague 6-Suchdol (Czechoslovakia)

SUMMARY

The synthesis, thermal stabilities, B.E.T. surface areas and maxima of the pore radii distributions of some porous polymers were studied. The specific retention volumes of selected compounds were measured and McReynolds constants were calculated, providing a classification of polymers for gas chromatographic purposes. The effects of the chemical nature, surface area and porous structure of the polymers on the retentions of solutes with different polarities were determined. Examples of the practical analytical utilization of these stationary phases are presented.

INTRODUCTION

Since Hollis[1] and Hollis and Hayes[2,3] reported the development of porous polymers as stationary phases for gas chromatography (GC), a number of such products have become commercially available and are now widely employed as column packing materials. However, it should be possible to prepare further porous polymers that possess particular properties that are suitable for the separation of different types of compounds. A suitable choice of the functional groups that can be incorporated into the polymer skeleton by the addition of certain monomers, and careful control of the surface area and the porosity during the synthesis of these polymers, make it possible to obtain tailor-made materials for particular applications.

The purpose of this study was to show that the chemical nature, pore size and pore volume exert a considerable influence on the performance of gas chromatographic columns and can be optimized.

The efficiency of a chromatographic separation depends on the retention time of the substances involved and the width of the peaks. In the Kubín and Kučera theory of gas–solid chromatography (GSC)[4–6], these two parameters are defined as the first absolute moment, μ_1, and the second central moment, μ_2, of the chromatographic curve. If the conditions that can be independently selected (particle diameter and flow-rate of the carrier gas) are ignored and if the adsorption is assumed to take place in the linear region of the isotherms, the first and second moments are functions

of the quantities that characterize the chemical nature and texture of a solid packing as follows[7]:

$$\mu_1 = f_1(K_A) \tag{1}$$

$$\mu_2 = f_2(K_A, k_{ads}, \beta, D_{int}^{-1}) \tag{2}$$

where K_A denotes the adsorption equilibrium constant, k_{ads} the adsorption rate constant, β the internal porosity of the particles and D_{int} the effective diffusion coefficient of the separated substances in the pores of the solid.

For the purpose of tailoring a polymeric packing, the relationships between K_A, k_{ads}, β or D_{int} and structural and textural variables have to be considered. The distance of the peak from the start on a chromatogram increases with increase in the adsorption equilibrium constant, K_A, which depends on the strength of the interaction of the solute with the solid phase. This interaction may vary from a weak Van der Waals attraction to chemical bonding caused by hydrogen bonds, a charge-transfer complex or metal complex formation. Polymeric packings offer the possibility of affecting the strength of the interaction by attaching suitable functional groups to the macromolecular skeleton. Even finer modifications of adsorptivity of a given functional group by electronic effects due to different bridges inserted between the group and the polymer chain can be imagined. The choice of the functional groups can be based on both experience with various stationary phases used in gas–liquid chromatography (GLC), characterized by the vague term of polarity, and the more fundamental classification of substances according to their ability to form a hydrogen bond[8] or to act as coordinating solvents[9]. The chemical nature of the porous polymer will be most effective for the separation if it possesses a highly orientated (homogeneous) surface that offers only a single type of group for interaction with the solute. Then, the differences in the K_A values for solutes with different chemical structures will be large. If more than one type of group is available on the surface, the selectivity of the separation of chemically different solutes may be diminished. However, in homologous series of organic compounds when steric effects are absent, K_A should increase with increasing molecular weight, irrespectively of the quality of the surface.

Strong adsorption invariably increases the peak width, as is apparent from eqn. 2 (where K_A is involved) and as is confirmed by experience. Thus, improved separations of different classes of compounds achieved as a result of large differences in retention times are offset by poorer separations of members of the same class due to broadening of the peaks. The effects of the chemical nature of the solute on the k_{ads} value are difficult to predict. However, its effect on peak width is small[7]. The same applies to β, which can be varied only in a narrow range.

Thus, the principal means of independently influencing the peak width already in the synthesis of polymeric packings consists in the regulation of its pore system. In narrow pores, Knudsen diffusion prevails (collisions of molecules with the walls are more frequent than collisions between molecules), and its rate increases linearly with increasing pore diameter. In broad pores, the rate of diffusion is independent of the pore diameter and the effective diffusion coefficient is proportoinal to the bulk diffusion coefficient. Fig. 1 shows an example of the dependence of D_{int} on the average pore diameter calculated for conditions suitable for the chromatography of *n*-hexane with

hydrogen as carrier gas on a porous solid[10,11]. It shows that an increase in the pore diameter by three orders of magnitude increases the diffusion coefficient by more than two orders of magnitude. Therefore, polymers with large pores should give a better performance as chromatographic packing. This has been confirmed experimentally[12].

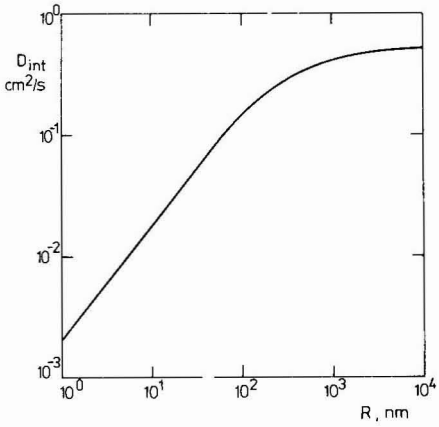

Fig. 1. Dependence of the effective diffusion coefficient, D_{int}, on average pore diameter calculated by means of the equation $1/D_{int} = 1/D_{KB} + 1/D_{AB}$ and taking the bulk diffusion coefficient $D_{AB} = 0.5148$ cm²/sec (for a hydrogen–*n*-hexane mixture) and the Knudsen diffusion coefficient $D_{KB} = 0.0202$ cm²/sec (for *n*-hexane at 10 Torr).

EXPERIMENTAL

Apparatus

The gas chromatographic measurements were carried out with a Pye Model 64 heated dual flame-ionization detector programmed chromatograph (Series 104, Pye Unicam, Cambridge, Great Britain). It was equipped with a 0–1-mV recorder (Honeywell, Electronik 194). The columns employed were 170 × 0.4 cm I.D. glass tubes and nitrogen was used as the carrier gas at a flow-rate of approximately 30 ml/min. The samples were introduced with a 10-μl Hamilton microsyringe. The injection port and detector temperatures were maintained at 200°.

The thermal stabilities of polymers were determined gravimetrically using the simplified quartz spring sorption balance of McBain and Bakr[13]. The sensitivity of the spring was 10 mg/mm and the temperature was increased at a constant rate of about 1°/min. Steadily flowing nitrogen was used instead of evacuation. The changes in the weight of the resin were followed with a cathetometer (Pye) with an accuracy of ± 0.05 mm.

The adsorption measurements were performed with a Sorptomatic 1826 apparatus (Carlo Erba, Milan, Italy) equipped with a digital reduction unit.

Chemicals

Benzene, pyridine, methanol, ethanol, 1-butanol, 1,4-dioxane, 2-butanone, acetic acid, *n*-butyl acetate and nitromethane (all reagent grade, except nitromethane) were supplied by Lachema (Brno, Czechoslovakia). Ethylene dimethacrylate and 2-

hydroxyethyl methacrylate (both pure) were products from Dental (Prague, Czechoslovakia), and benzoyl peroxide from Argon (Lodž, Poland). *n*-Hexane, *n*-octane, *n*-nonane, *n*-decane (all 99.4–99.8 %, GC analysis), 1-nitropropane, 2-pentanone (both at least 97 %, GC analysis), 4-vinylpyridine, N-vinyi-2-pyrrolidone and α,α'-azobisisobutyronitrile (all pure, GC analysis), were supplied by Fluka (Buchs, Switzerland). Methane (purity at least 99 %), was supplied by Schuchardt (Munich, G.F.R.) and *n*-heptane (reagent grade) by VEB Jenapharm-Laborchemie (Apolda, G.D.R.). Squalane was a product of May & Baker (Dagenham, Great Britain), while 1-iodobutane, 2-methyl-2-pentanol, divinylbenzene (40 %) and *cis*-hydrindane were from our laboratory stock. 2-Cyanoethyl methacrylate was synthesized according to the literature[14,15].

Preparation of porous polymers

Poly[(2-cyanoethyl)methacrylate] (CEM) was prepared[16] by copolymerization of 2-cyanoethyl methacrylate with ethylene dimethacrylate using *n*-butyl acetate as a diluent and benzoyl peroxide as initiator at 68–70°.

Poly[(2-hydroxyethyl)methacrylate] (HEM) was synthesized from 2-hydroxyethyl methacrylate and ethylene dimethacrylate with xylene as diluent at 90°.

Poly(4-vinylpyridine) (PYR) was obtained by polymerizing 4-vinylpyridine with divinylbenzene in *n*-heptane at 80°.

Poly(N-vinylpyrrolidone) (PON) was prepared by copolymerization of N-vinyl-2-pyrrolidone in *n*-heptane at 75–80°.

In the last three instances, α,α'-azobisisobutyronitrile was used as initiator of the polymerization. The resulting products were crushed and fractionated on sieves and the fraction of particle size 0.2–0.4 mm was extracted with methanol for 16 h and dried at elevated temperature.

The B.E.T. surface area was measured with nitrogen at the temperature of liquid nitrogen and the pore distribution was calculated from the desorption branch of the isotherm using the Roberts[17] method. The results are summarized in Table I.

TABLE I

B.E.T. SURFACE AREAS AND MAXIMA OF PORE RADII DISTRIBUTIONS OF POROUS POLYMERS UNDER STUDY

Polymer	*S* (m^2/g)	*Most frequent pore radii (nm)*
HEM	15	61
CEM	24	76[12]
PYR	51	80
PON	50	58

Column packings and specific retention volumes

The fractions of individual porous polymers of particle size 0.2–0.4 mm were chosen as column packings. Amounts of 10.10 g of CEM, 8.75 g of HEM, 5.85 g of PYR and 4.90 g of PON were pre-conditioned for 16 h at 160° with the carrier gas flowing and used both for determining the retention volumes of selected substances and for calculating McReynolds constants[18] at 142° in all instances.

RESULTS AND DISCUSSION

A series of polymer packings was synthesized based on commercial or specially prepared monomers and suitable crosslinking agents. Special care was taken to develop a polymerization procedure that would yield materials with a relatively low surface area and broad pores; some results on the relationships between surface area and pore size distributions have been reported previously[12]. The monomers were selected according to their expected ability to associate with various solutes by means of hydrogen bonds (HEM), proton-accepting coordination (CEM, PYR) or charge-transfer complexing (PON).

Firstly, their thermal stabilities were measured thermo-gravimetrically and Fig. 2 shows a graph of loss of weight *versus* temperature. PYR was found to be the most stable polymer, being usable up to 250°; higher temperatures can be tolerated during a temperature-programmed run. The upper limit for HEM and PON was *ca.* 220°; the value for HEM is in accordance with a literature report[19] for a similar material. The relatively low thermal stability of CEM has been mentioned previously[20].

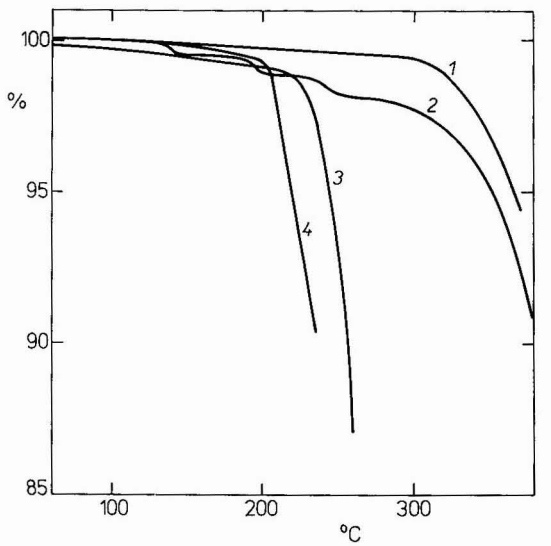

Fig. 2. Plot of loss of weight of porous polymers *versus* temperature. Heating rate, *ca.* 1°/min. 1 = PYR (0.29630 g); 2 = PON (0.20610 g); 3 = HEM (0.29600 g); 4 = CEM (0.77728 g).

The traditional classification of GC stationary phases according to their polarity is vague and, in general, "polarity" is an ill-defined term because various solvation (in GLC) or adsorption (in GSC) mechanisms are neglected. The concept of polarity is usually derived from the affinity of a given substance for another (polar) substance. Therefore, the McReynolds constants (ΔI), which provide the best information about the selectivity of various stationary phases, were used in this study. An advantage of these constants is their clear physical meaning as the relative adsorption equilibrium constants $\Delta I \approx \log(K_A^X/K^{squalane})$ of a solute A on a stationary phase X with respect to a standard (20% loading) squalane stationary phase. Table II shows

the values of ΔI on our polymer packings arranged according to decreasing adsorption ability towards polar compounds, which was defined as the average of the ΔI values for the first five substances listed in Table II. It is evident that PON can be considered to be the stationary phase with the highest polarity. It is worth noting that the McReynolds constants differ significantly from those obtained on the other investigated stationary phases. Therefore, PON is not suitable for the separation of related substances but it is of use in fractionating groups of compounds. On the basis of the capability of charge-transfer complex formation between the pyrrolidone functional groups chemically incorporated on to the polymer matrix and aromatic compounds, PON was successfully used[12] for determining trace amounts of non-aromatics in aromatic hydrocarbons. HEM and CEM showed comparable adsorption abilities in spite of the different natures of their functional groups and assumed adsorption mechanisms. Different behaviour was shown by PYR; its adsorption ability was in general lower and it gave large differences in the ΔI values for some test substances.

TABLE II

SELECTED McREYNOLDS CONSTANTS AT 142°

The absolute values of the retention indices observed on the Squalane column at 142° are as follows: benzene, 692; 1-butanol, 638; 2-pentanone, 671; 1-nitropropane, 664; pyridine, 756; 2-methyl-2-pentanol, 746; 1-iodobutane, 855; 1,4-dioxane, 705; *cis*-hydrindane, 1032.

Solute	ΔI			
	PON	*HEM*	*CEM*	*PYR*
Benzene	3180	275	269	58
1-Butanol	5720	522	476	156
2-Pentanone	4150	372	404	166
1-Nitropropane	6000	566	603	292
Pyridine	5530	551	481	183
2-Methyl-2-pentanol	4800	–	349	208
1-Iodobutane	5230	205	188	445
1,4-Dioxane	3640	424	450	95
cis-Hydrindane		58	19	34

However, the McReynolds constants do not answer every question concerning the applicability of a stationary phase to practical separation problems. Therefore, the specific retention volumes of selected compounds were calculated and expressed relative to those for *n*-heptane. Their values are given in Table III together with the corresponding boiling points.

The specific retention volumes were correlated with some properties of the polymers studied. Firstly, the effect of the surface area and porosity on the retention behaviour was investigated. With compounds, the sorption of which is predominantly due to non-specific interactions[21], the retention volumes depend primarily on surface area (see Tables I and III). However, the retention volumes of *n*-alkanes on CEM are smaller than those on HEM although their surface areas are reversed. This probably results from the fact that HEM possesses about 20% of its total surface area in pores smaller than 5 nm, whereas no microporous structure was found with CEM[22]. If specific interactions (*e.g.*, hydrogen bonding or complex formation) between the component and the adsorbent are expected to be the main contribution to the adsorption,

TABLE III

SPECIFIC RETENTION VOLUMES OF SELECTED COMPOUNDS ON SOME POROUS POLYMER PACKINGS AND SQUALANE

Temperature, 142°; carrier gas, nitrogen.

Compound	*B.p.* (°C)	*Specific retention volume*				
		HEM	*CEM*	*PYR*	*PON*	*Squalane*
n-Hexane	68	0.61	0.60	0.53	0.67	0.52
n-Heptane	98.4	1.00	1.00	1.00	1.00	1.00
n-Octane	125.5	1.83	1.73	1.86	1.04	1.92
n-Nonane	150.8	3.11	2.30	3.55	1.09	3.60
n-Decane	174.1	5.44	5.07	6.51	1.13	6.64
cis-Hydrindane	167.7	4.78	5.47	6.55	0.67	8.48
Benzene	80.1	4.61	4.13	1.37	3.50	0.96
Pyridine	115.5	30.67	18.27	4.49	11.22	1.44
1-Iodobutane	130	7.72	6.40	0.16	10.31	2.72
Ethanol	78.5	3.67	3.73	0.96	2.05	0.20
1-Butanol	117.5	13.56	9.47	3.37	10.27	0.68
2-Methyl-2-pentanol	121.5	–	8.53	4.92	7.21	1.24
2-Butanon	79.6	4.56	5.33	1.40	2.54	0.48
2-Pentanon	102	7.00	7.60	2.37	5.27	0.84
1,4-Dioxane	101	11.33	11.73	1.88	4.31	1.04
Acetic acid	118.5	46.77	33.33	–	–	–
Nitromethane	100.8	10.50	14.93	1.76	2.85	0.28
1-Nitropropane	131	19.89	21.47	5.00	11.73	0.80
V_g (*n*-heptane) (ml/g)	–	2.27	1.65	18.33	15.49	21.45

then the relative retention is markedly increased on polymers that are capable of stronger bonding. The retentions of all polar solutes are in accord with this concept, particularly nitromethane, nitropropane and pyridine.

From a comparison of the specific surface areas and the maxima of the pore

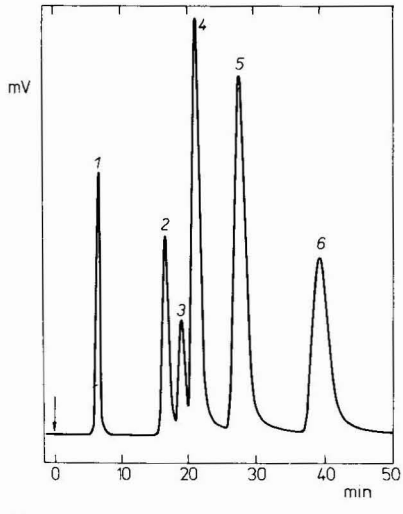

Fig. 3. Chromatogram of *n*-C_1–C_5 fatty acids and water at the optimal carrier gas flow-rate[20]. 1 = Water; 2 = acetic acid; 3 = formic acid; 4 = propionic acid; 5 = butyric acid; 6 = valeric acid.

distribution[23,24] of our sorbents with commercially available sorbents, it is clear that the differences in each are about one order of magnitude. The large surface area and narrower pores can be assumed to cause a relatively strong sorption of solutes on commercial packings. If reasonable retentions are to be achieved, the column has to be operated at considerably higher temperatures, even when low-boiling compounds are being analysed. However, as has already been pointed out previously[12], the chemical homogeneity of the surface may lead to a higher selectivity of our low-surface-area packings compared with commercial packings.

The porous polymers considered in this paper were tested in actual analyses. For instance, CEM was found to be a very convenient column packing for the separation of fatty acids and water[20,25,26] (Fig. 3) and also for determining water in compounds containing carbonyl groups[27]. PON was employed for the group analysis of trace non-aromatic fractions in aromatic hydrocarbons[12] and PYR proved excellent for the determination of water in aniline solutions with simultaneous separation of its derivatives (Fig. 4).

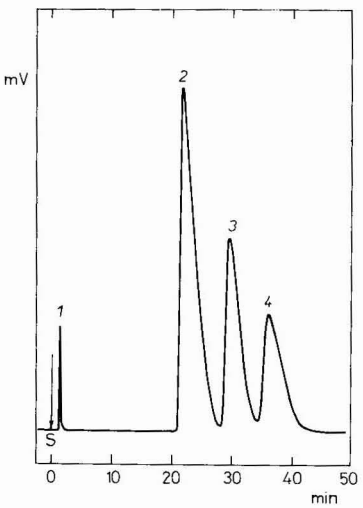

Fig. 4. Separation of water, aniline and its derivatives. Column, 170 × 0.4 cm I.D.; PYR, 0.2–0.4 mm; column temperature, 188°; carrier gas (hydrogen) flow-rate, 30 ml/min. 1 = Water; 2 = N,N-dimethylaniline; 3 = aniline; 4 = N-methylaniline.

REFERENCES

1 O. L. Hollis, *Anal. Chem.*, 38 (1966) 309.
2 O. L. Hollis and W. V. Hayes, *J. Gas Chromatogr.*, 4 (1966) 235.
3 O. L. Hollis, W. V. Hayes, in A. B. Littlewood (Editor), *Gas Chromatography 1966*, Institute of Petroleum, London, 1967, p. 57.
4 E. Kučera, *J. Chromatogr.*, 19 (1965) 237.
5 M. Kubín, *Collect. Czech. Chem. Commun.*, 30 (1965) 1104.
6 M. Kubín, *Collect. Czech. Chem. Commun.*, 30 (1965) 2900.
7 P. Schneider and J. M. Smith, *A.I.Ch.E. J.*, 14 (1968) 762.
8 R. H. Ewell, J. M. Harrison and L. Berg, *Ind. Eng. Chem.*, 36 (1944) 871.
9 R. S. Drago and K. F. Purcell, in T. C. Waddington (Editor), *Non-Aqueous Solvent Systems*, Academic Press, London, 1965, p. 211.

10 H. Kopecká and P. Schneider, to be published.
11 C. N. Satterfield, *Mass Transfer in Heterogeneous Catalysis*, M.I.T. Press, Cambridge, Mass., 1970.
12 M. Kraus and H. Kopecká, *J. Chromatogr.*, 124 (1976) 360.
13 J. W. McBain and A. M. Bakr, *J. Amer. Chem. Soc.*, 48 (1926) 690.
14 J. H. Haslam, *U.S. Pat.*, 2,822,348 (1958).
15 E. C. Kendal and B. McKenzie, *Org. Syn.*, Collect. Vol. 1 (1941) 256.
16 I. Gavrilová and M. Kraus, *Czech. Pat.*, 160,232 (1974).
17 B. F. Roberts, *J. Colloid Interface Sci.*, 23 (1966) 266.
18 W. O. McReynolds, *J. Chromatogr. Sci.*, 8 (1970) 685.
19 J. Lukáš, J. Hradil, M. Křiváková and J. Čoupek, *J. Chromatogr.*, 114 (1975) 335.
20 L. Kalusová and R. Komers, *J. Chromatogr.*, 91 (1974) 133.
21 A. V. Kiselev, in A. Goldup (Editor), *Gas Chromatography 1964*, Institute of Petroleum, London, 1965, p. 239.
22 R. Komers and D. Tomanová, *Chem. Prům.*, 21 (1971) 559.
23 *Chromosorb Century Series, Porous Polymer Supports*, Johns-Manville, New York, 1974.
24 K. I. Sakodynskii and L. I. Panina, *Zh. Anal. Khim.*, 27 (1972) 1024.
25 M. Zdražil, *Collect. Czech. Chem. Commun.*, 39 (1974) 1488.
26 A. Heyberger, D. Balcarová, J. Bulička and J. Procházka, *Collect. Czech. Chem. Commun.*, 39 (1974) 1663.
27 R. Komers and Z. Šír, *Collect. Czech. Chem. Commun.*, 42 (1977) 3576.

Journal of Chromatography, 148 (1978) 53–59

CHROM. 10,399

SOME SORPTION PROPERTIES OF A NEW TYPE OF ACTIVE CARBON

V. PATZELOVÁ, J. JANSTA and F. P. DOUSEK

J. Heyrovský Institute of Physical Chemistry and Electrochemistry, Czechoslovak Academy of Sciences, 121 38 Prague 2, Máchova 7 (Czechoslovakia)

SUMMARY

The sorption properties of a new type of active carbon, prepared by decomposition of polytetrafluoroethylene by lithium amalgam, were tested under chromatographic conditions with various types of adsorbates. It was found that aliphatic hydrocarbons penetrate into the carbon skeleton. The high heats of adsorption for these molecules are the result of very close contact between the adsorbent and adsorbate.

Polar substances exhibit a physical adsorption that can be partially suppressed by the reaction product (LiF crystals) present in the carbon skeleton. This adsorbent was classified as a type I adsorbent according to Kiselev's classification.

INTRODUCTION

Active carbon was one of the first adsorbents employed in gas adsorption chromatography. In addition to materials formed by the thermal decomposition of natural substances, chiefly cellulose, others have appeared, prepared under similar conditions from, for example, polyvinylidene chloride —the saran active charcoals[3]. While with active carbons of the first type the porosity is chiefly determined by meso- and macropores, mainly due to additional treatment, saran active charcoals have an extensively developed microporous structure. On this basis, some workers explained certain sorption properties of saran active charcoals by the molecular sieve effect[2–4]. Walker[5] tested the sorption properties using gas–solid chromatography technique. Carbosieve, produced by Supelco (Bellefonte, Pa., U.S.A.) for chromatographic purposes[6], is also based on a saran charcoal. The specific surface area of saran charcoals is about 1072 $m^2 \cdot g^{-1}$, the mean radius of the micropores being 1.24 nm (ref. 5).

Kiselev and Yashin[7] studied the sorption properties of graphitized thermal carbon black and the use of its separation properties. They showed that dispersion forces are almost exclusively operative in the adsorption of any adsorbate. It has been stated that thermal carbon blacks are the most homogeneous adsorbents known[8].

In this work, the sorption properties of a new type of active carbon (JADO), prepared by electrochemical reduction of polytetrafluoroethylene (PTFE) by lithium amalgam at a low temperature[9], were studied by gas chromatography. The work was

intended to clarify the nature of the interactions of the adsorbent with various types of adsorbate.

EXPERIMENTAL

The preparation of active carbon powder by the electrochemical reduction of PTFE by alkali metal amalgams was described in detail earlier[9,10]. As the gas chromatographic column packing, JADO 1017 was prepared with a particle size of 0.3 mm. The non-porous PTFE particles, irregular hexahedrons in shape, were degreased and dried *in vacuo* at 150°. The resulting PTFE crumbs were then contacted with lithium amalgam in a glass apparatus at 25°, *in vacuo* and with stirring. After 60 min, the PTFE particles were covered with a 3-μm black layer of reaction products, a solid mixture of carbon and lithium fluoride. The treated PTFE crumbs were then separated from the partially depleted lithium amalgam and washed several times with boiling water that had been acidified with hydrochloric acid in order to extract the lithium fluoride from the carbon skeleton. The washed PTFE crumbs covered with a layer of the JADO carbon were dried first in air and then *in vacuo* at 150°. For comparison, a sample was also prepared containing 90% of the reaction product, lithium fluoride (JADO 1051). The fully extracted sample (without lithium fluoride) was designated JADO 1053.

The experiments were carried out on a CHROM 4 laboratory chromatograph using a thermal conductivity detector.

The retention volumes were measured for each substance over a temperature range of 80° in 7° steps. The temperature intervals were selected according to the nature of the individual adsorbates. The flow-rate of the helium carrier gas was 30–40 $cm^3 \cdot min^{-1}$. With symmetrical elution curves, the retention volumes were calculated from the average peak maximum times measured with an accuracy of $\pm$ 0.2 sec, obtained as the mean of the retention times measured in quadruplicate at each temperature. The elution curves for polar substances were not symmetrical at lower temperatures and therefore the retention volumes for these substances were determined not from the maxima but from the first statistical moment of the elution curve. All experiments were carried out on the same column (0.58 m $\times$ 3 mm I.D.).

The heats of adsorption were computed from the dependence of the corrected retention volumes (V_{corr}) on the reciprocal temperature[11] using a simple program.

The following adsorbates were used: methane, ethane, propane, ethene, propene, water, methanol, ethanol and benzene.

RESULTS AND DISCUSSION

For the purpose of testing the sorption properties of JADO carbon, the heats of adsorption (ΔH) were calculated from the chromatographic data for the JADO 1053 sample (without lithium fluoride) and even for JADO 1051 (90% lithium fluoride). In addition to the adsorbates exhibiting only non-specific interactions (saturated hydrocarbons), adsorbates capable of specific interactions due to π-electron bonds (ethene, propene) and hydroxyl group (water, alcohols) were used. The calculated ΔH values are given inTables I and II respectively and data for other types of adsorbates are given for comparison.

TABLE I

HEATS OF ADSORPTION FOR HYDROCARBONS (kJ · mole^{-1})

Adsorbate	*Adsorbent*			
	JADO 1053	*JADO 1051*	*Graphitized thermal carbon black*[12]	*NaX zeolite*[13]
CH_4	24.3 ± 0.5	23.3 ± 0.6	11.3	18.8
C_2H_6	34.6 ± 1.0	33.2 ± 0.8	18.0	25.9
C_3H_8	45.0 ± 0.8	45.7 ± 0.8	24.7	33.0
C_2H_4	33.1 ± 1.1	32.0 ± 1.5	16.7	38.5
C_3H_6	44.9 ± 0.7	45.6 ± 0.8	23.4	50.2

TABLE II

HEATS OF ADSORPTION FOR WATER, METHANOL, ETHANOL AND BENZENE (kJ · mole^{-1})

Adsorbate	*Adsorbent*				
	JADO 1053	*JADO 1051*	*Graphitized thermal carbon black*[14]	*Activated charcoal*[15]	*Heat of condensation*
H_2O	51.5 ± 2.2	47.3 ± 4.3	–	46.9	41.4
CH_3OH	60.3 ± 2.1	47.7 ± 3.7	42.7	54.8	35.1
C_2H_5OH	65.8 ± 1.9	56.1 ± 4.5	50.6	62.8	38.9
C_6H_6	53.1 ± 2.3	49.9 ± 3.1	45.2	61.5	30.8

Interaction with hydrocarbons

The following conclusions can be drawn from the values in Table I.

(i) The heats of adsorption for saturated hydrocarbons are about 1 kJ higher than those for the corresponding unsaturated hydrocarbons. The absence of active sites capable of specific interaction with π-electron bonds (see ΔH on NaX zeolite) confirms the energetic homogeneity of this adsorbent. The ΔH values for both types of hydrocarbons on JADO carbon increase linearly with increasing number of carbon atoms in a molecule, the increment per CH_2 group being about 10 kJ.

(ii) The differences in ΔH values for extracted and unextracted JADO carbon do not exceed the range of experimental errors. The presence of lithium fluoride in the carbon skeleton does not lead to any steric hindrance for the hydrocarbon molecules, limiting contact with the adsorbent. Neither the shapes of the elution curves (see Fig. 1) nor the values of the retention volumes (see Fig. 2) exhibit any changes of a diffusional character.

(iii) ΔH values on JADO carbon for the hydrocarbons considered are about double those on the even surface of graphitized carbon black, and are close to the values for microporous saran charcoal with a pore diameter commensurate with the effective molecular diameter of the adsorbate[16].

Interaction with water, methanol and ethanol

The results in Table II can be summarized as follows.

(i) The ΔH values are systematically higher in comparison with the values for another type of charcoal (differences for water 4.6 ± 2.2 kJ·mole^{-1}, for methanol

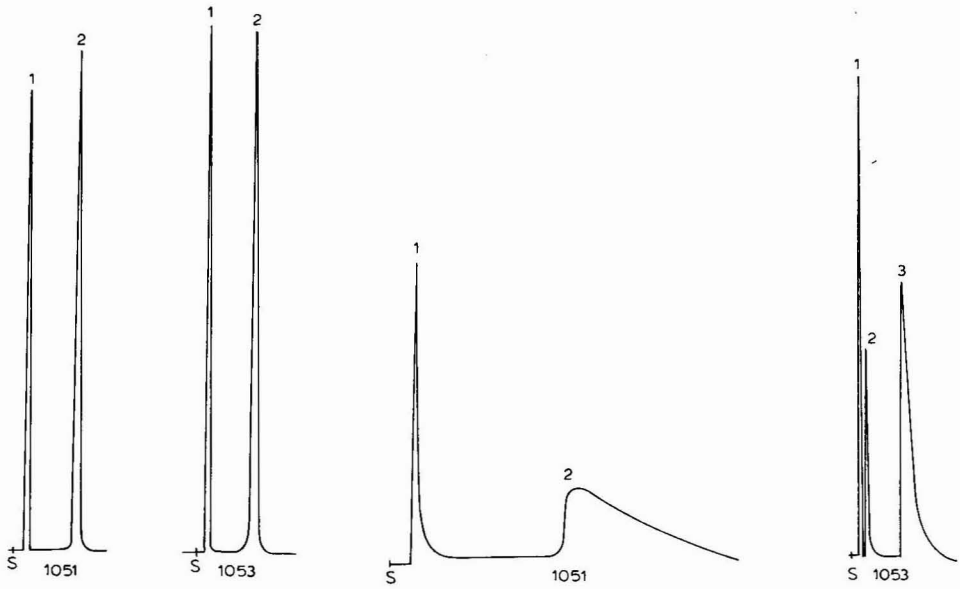

Fig. 1. Elution curves for ethane and propane on JADO 1053 (LiF extracted) and on JADO 1051 (LiF unextracted). Column, 0.58 m long, I.D. 3 mm; helium flow-rate, 40 $cm^3 \cdot min^{-1}$; sample size, 12 μl; temperature, 97°. Retention volumes on JADO 1051: 1, ethane 13.1 cm^3; 2, propane 83.0 cm^3. Retention volumes on JADO 1053: 1, ethane 12.2 cm^3; 2, propane 78.4 cm^3.

Fig. 2. Elution curves for water and alcohols on JADO 1053 (LiF extracted) and on JADO 1051 (LiF unextracted). Column, 0.58 m long, I.D. 3 mm; helium flow-rate, 40 $cm^3 \cdot min^{-1}$; sample size, 0.17 μl on JADO 1053 and 0.5 μl on JADO 1051; temperature, 191°. Retention volumes on JADO 1051: 1, water 25.3 cm^3; 2, ethanol 175.1 cm^3. Retention volumes on JADO 1053: 1, water 8.6 cm^3; 2, methanol 17.8 cm^3; 3, ethanol 46.1 cm^3.

5.5 ± 2.1 kJ·mole^{-1} and for ethanol 3.0 ± 1.9 kJ·mole^{-1}). These differences are not so important from the point of view of specific interactions.

(ii) The influence of lithium fluoride present in the JADO 1051 sample, causing a decrease in the ΔH values instead of increasing them owing to the presence of ionic crystals, was unexpected. The extent to which this influence is suppressed by the fine dispersion of lithium fluoride crystals [by small-angle scattering of X-rays, the determined average length of the edge of the lithium fluoride cubic crystal is 3.29 nm (ref. 17)] and by the decrease in the effective area of the surface cannot be stated on the basis of the above experiments. The shapes of elution curves for polar compounds (see Fig. 3), in a similar manner to the values of the retention volumes (see Fig. 2), indicate the remarkable influence of lithium fluoride crystals on the rate of diffusion into the cavities of the carbon skeleton. The presence of lithium fluoride in the cavities leads to pronounced steric hindrance for these adsorbates. The heats of adsorption on such modified JADO carbon (JADO 1051) approach the values measured on the even surface of graphitized carbon black.

Relationship between the structure and sorption properties of JADO carbon

As follows from our previous work[9], JADO carbon exhibits a highly developed porous structure. The specific surface area determined by the BET method is 2 600 $m^2 \cdot$

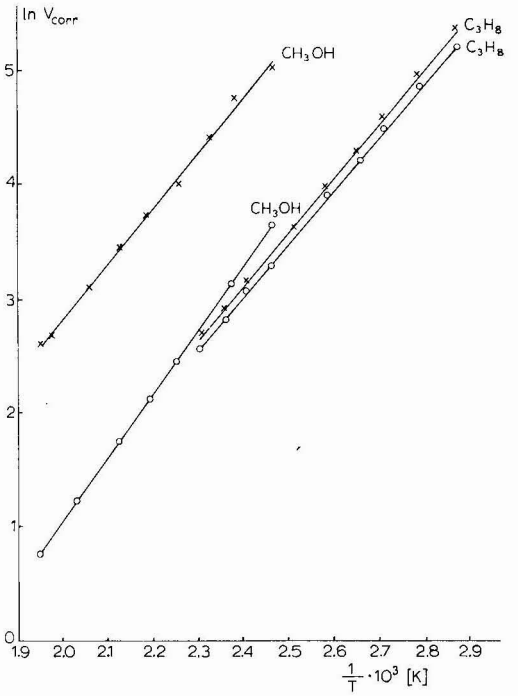

Fig. 3. Dependence of ln V_{corr} on reciprocal temperature for propane and methanol on JADO 1051 (×) and JADO 1053 carbon (○).

g^{-1}, which represents a sorption capacity of 1.25 g of argon per gram of JADO carbon. These values agree with our knowledge of the structure acquired from electron microscopic and small-angle X-ray scattering data[17]. It was found that the structure of the JADO carbon is amorphous.

The high specific surface area and the unique cavity diameters are given by the structure, which can be illustrated schematically as shown in Fig. 4. Carbon fibres join the nodules of 1.1 ± 0.35 nm in diameter. A "bead" carbon structure is created, the local orientation of the carbon chains being pre-terminated by the primary structure of PTFE. The distance between the centres of neighbouring nodules in the chain is 1.9 ± 0.3 nm and the diameter of the cavities in the carbon skeleton is 2.3 ± 0.3 nm. The lithium fluoride crystals are situated in these cavities and their formation during the electrochemical reaction is manifested by a 20% expansion in the primary PTFE volume. The cavities differ from the pores in a rigid matrix, their diameter being of the same order as the wall thickness of the carbon skeleton. The value of the calculated cavity diameter was also given indirectly by the adsorption measurements[9].

We conclude that there are two mechanisms of interaction on JADO carbon, depending on the nature of the adsorbate. Aliphatic hydrocarbons penetrate the carbon skeleton, this interaction being similar to the solvation observed, for example, in interaction of benzene with Porapak[18]. The presence of lithium fluoride crystals in the cavities does not affect this interaction. High ΔH values for hydrocarbons are caused by the very close contact between the adsorbent and adsorbate, similar to that which takes place during the adsorption in micropores.

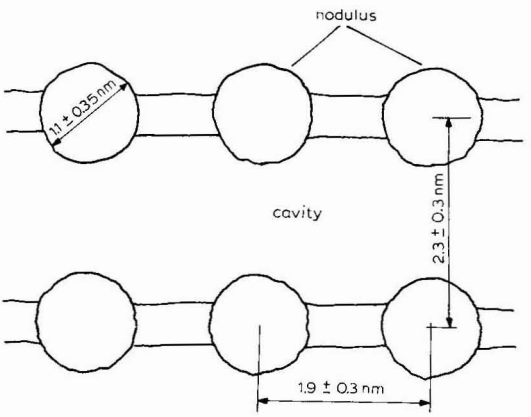

Fig. 4. Scheme of structural elements of JADO carbon.

Alcohols and water are adsorbed in the cavities of the carbon skeleton; the ΔH values for these adsorbates indicate that only physical adsorption without a pronounced contribution of specific interactions occurs. For these adsorbates, the accessibility of the cavities is reduced by the presence of lithium fluoride crystals. A similar effect was also observed for benzene.

CONCLUSIONS

(i) The JADO carbon does not have a significantly heterogeneous surface. It can be classified as a type I adsorbent according to Kiselev's classification.

(ii) The molecules of aliphatic hydrocarbons penetrate the carbon skeleton, the nature of the interaction being similar to solvation.

(iii) The molecules of polar compounds are adsorbed in the cavities of the carbon skeleton.

(iv) The presence of lithium fluoride crystals in cavities does not cause any increase in the specificity of the interaction for any of the adsorbates tested. It acts only to produce steric hindrance for the molecules that diffuse into the cavities.

ACKNOWLEDGEMENTS

Thanks are due to Dr. Z. Pelzbauer of the Institute of Macromolecular Chemistry, ČSAV, for his valuable contributions during discussions of this work. We also thank Dr. M. Pšeidlová for her technical assistance.

REFERENCES

1 C. Pierce, J. W. Wiley and R. N. Smith, *J. Phys. Chem.*, 53 (1949) 669.
2 A. Bayley and D. H. Everett, *Nature (London)*, 211 (1966) 1082.
3 J. R. Dacey and D. G. Thomas, *Trans. Faraday Soc.*, 50 (1954) 740.
4 J. J. Kipling and R. B. Wilson, *Trans. Faraday Soc.*, 56 (1960) 557.
5 P. L. Walker, Jr., *Miner. Ind.*, 35, No. 4 (1966) 1.
6 *Supelco Bull.*, No. 712 (1971).

7 A. V. Kiselev and Ya. J. Yashin, *Gas Adsorption Chromatography*, Plenum Press, New York, 1969.
8 W. R. Smith and D. G. Ford, *J. Phys. Chem.*, 65 (1965) 3587.
9 J. Jansta, F. P. Dousek and V. Patzelova, *Carbon*, 13 (1975) 377.
10 F. P. Dousek and J. Jansta, *Electrochim. Acta*, 20 (1975) 1.
11 R. I. Gale and R. A. Beebe, *J. Phys. Chem.*, 68 (1964) 555.
12 N. N. Avgul, A. V. Kiselev and D. P. Poshkus, *Adsorption of Gases and Vapours on Homogeneous Surfaces*, Khimia, Moscow, 1974.
13 A. V. Kiselev, *Discuss. Faraday Soc.*, 40 (1965) 205.
14 L. D. Belyakova and A. V. Kiselev, *Anal. Chem.*, 36 (1964) 1517.
15 A. B. Lamb and A. S. Coolidge, *J. Amer. Chem. Soc.*, 42 (1929) 1146.
16 V. Patzelová, O. Kadlec and P. Seidl, *J, Chromatogr.*, 91 (1974) 313.
17 Z. Pelzbauer, J. Baldrián, J. Jansta and F. P. Dousek, *Carbon*, in press.
18 V. Patzelová and J. Volková, *J. Chromatogr.*, 65 (1972) 255.

Journal of Chromatography, 148 (1978) 61–68

CHROM. 10,400

CHROMATOGRAPHIC PROPERTIES OF TUFFS CONTAINING SOME ZEOLITES

T. G. ANDRONIKASHVILI, G. V. TSITSISHVILI, Sh. D. SABELASHVILI, T. A. CHUMBURIDZE and L. G. EPRIKASHVILI

Institute of Physical and Organic Chemistry, Academy of Sciences of the Georgian S.S.R., Tbilisi (U.S.S.R.)

SUMMARY

The separating properties of tuffs containing clinoptilolite and mordenite as adsorbents in gas chromatography were studied, using argon–oxygen–nitrogen–methane–carbon monoxide as a model mixture. It was shown that the treatment of tuffs containing clinoptilolite with hydrochloric acid improves the separation of the oxygen–nitrogen mixture but does not separate oxygen–argon. It was found that natural tuffs containing mordenite have better separation abilities than synthetic sodium mordenite. The enrichment of natural mordenite with calcium or strontium cations improves the separation of oxygen–nitrogen, while the introduction of strontium and barium cations into the zeolite structure improves the separation of argon–oxygen. The temperature of the thermal activation of the specimens greatly influences the separating ability of tuffs containing mordenite.

INTRODUCTION

At present, zeolites of Types A and X[1,2] are most widely used in gas chromatography, and the possibility of using some other types of zeolites as adsorbents has been studied less[3–5].

Recently, interest in zeolites of natural origin has increased considerably, mainly relating to tuffs containing clinoptilolite and mordenite[6]. The content of a zeolite in tuffs in some instances may reach 85%[7]. Both clinoptilolite and mordenite are high-silica zeolites: the Si:Al ratio in clinoptilolite is 4.25–5.00, while in mordenite it is 4.17–5.00 (ref. 6). The cation composition (calcium, potassium, sodium and magnesium) in these zeolites varies, depending on the conditions of their formation.

The kinetic diameters (σ) of the free apertures of clinoptilolite and mordenite cavities are 3.5 and 3.9 Å, respectively. In gas chromatography, these types of zeolites are used mainly for the separation of gaseous systems in which the components, as a result of the size of their critical diameters, can penetrate the adsorbent channels[8–14]. Most studies have been devoted to the development of methods for the efficient separation of air into oxygen and nitrogen by using natural zeolites.

The purpose of our studies was to investigate the separating properties of

tuffs containing clinoptilolite and mordenite, both natural ones and those subjected to acidic or cationic modification, as adsorbents in gas chromatography.

EXPERIMENTAL

The samples were tuffs containing clinoptilolite from the Dzegvi deposit in the Georgian S.S.R. (the Khekordula region) and tuffs containing mordenite from Ratevani in the Bolnisi region of the Georgian S.S.R.

Tuffs containing 80–85% of clinoptilolite were treated at room temperature with hydrochloric acid, the concentration of which was varied in the range 0.05–5.0 *N*. The changes in the main oxide content of tuffs containing clinoptilolite on acid treatment are given in Table I. The results show that if the concentration of the acid does not exceed 0.25 *N*, mainly decationization of clinoptilolites takes place, as the content of alumina in the specimens is not changed. More concentrated acid (1–5 *N*) causes dealuminization of the specimens as well, as shown by a sharp decrease in the alumina content. The content of mordenite in tuffs varies within the range 40–50%.

TABLE I

CHANGES IN THE MAIN OXIDE COMPOSITION OF TUFFS CONTAINING CLINOPTILOLITE ON ACID TREATMENT

The absolute content of SiO_2 during the acid treatment of tuffs containing clinoptilolite remains virtually unchanged.

Concentration of HCl (N)	*Al_2O_3 (%)*	*Fe_2O_3 (%)*	*CaO (%)*	*MgO (%)*	*Na_2O (%)*	*K_2O (%)*
—	12.85	1.65	3.92	1.50	3.34	1.68
0.05	12.80	1.56	3.00	1.30	1.68	0.80
0.10	12.80	1.56	3.20	1.34	2.08	0.70
0.25	12.14	1.50	3.00	1.30	1.98	—
1.00	10.05	1.08	2.50	0.94	—	0.60
5.00	7.60	0.60	2.35	0.68	1.50	0.09

Rock containing mordenite has the following chemical composition: SiO_2, 70.70; TiO_2, 0.20; Al_2O_3, 9.25; Fe_2O_3, 3.85; FeO, 0.38; MnO, 0.03; Mg, 0.88; CaO, 3.36; Na_2O, 1.60; K_2O, 1.29; P_2O_5, 0.20; SO_3, 0.14; H_2O^+, 4.41; H_2O^-, 4.11%. Cation-exchange modification of these tuffs was obtained in two ways: (1) replacement of the initial cations (mainly Ca^{2+}) in mordenite with sodium cations by treatment of tuffs containing zeolites with 0.5 *N* sodium hydroxide solutions (once) and then with 25% sodium chloride solution (six times) at 85°; after these treatments, metal cations from the corresponding solutions of chlorides were introduced into the zeolite structure[15]; (2) by direct treatment of tuffs with the corresponding solutions of chlorides.

Specimens with high contents of exchange cations were used. All of the specimens were characterized by the conservation of the crystal lattice, except for mordenite containing barium, which was characterized by some weakening of the anion framework.

Tuffs containing zeolites were crushed and the fraction of particle size 0.5–1 mm was packed into chromatographic columns. The granules of the tuff containing clinoptilolite, after previous dehydration by heating at 300° for 5 h, were loaded into the column (1 m × 4 mm I.D.) of a Tsvet-64 chromatograph and were re-activated by heating at 300° for 2 h in a flow of the carrier gas (helium). The temperature of the column was varied in the range 25–140°, the flow-rate of the carrier gas was 20–50 ml/min and a thermal conductivity detector was used. Tuffs containing mordenite were loaded into the column (50 cm × 5 mm I.D.) of a Carlo Erba Model GV chromatograph. The specimens were activated in the column in a flow of the carrier gas (helium) at two temperatures (300° and 450°) for 1 h. The column temperature was 20°, the flow-rate of the carrier gas was usually 100 ml/min and a thermal conductivity detector was used. The model system was a mixture of argon, oxygen, nitrogen, methane and carbon monoxide.

RESULTS AND DISCUSSION

Measurement of the specific retention volumes of different components of the model system showed that those of argon and particularly of methane on the original (untreated) clinoptilolite are extremely small (Table II), presumably because molecules of argon and methane are unable to penetrate the channels of clinoptilolite owing to their geometrical sizes. The critical diameter of an argon molecule is 3.83 Å and that of methane is 4 Å, while the diameter of the free apertures of natural clinoptilolite is about 3.5 Å.

TABLE II

SPECIFIC RETENTION VOLUMES V_g (ml/g) OF ARGON, OXYGEN, NITROGEN, METHANE AND CARBON MONOXIDE ON A TUFF CONTAINING CLINOPTILOLITE AND SPECIMENS TREATED WITH ACID

Temperature of column, 25°; carrier gas flow-rate, 20 ml/min.

Concentration of HCl (N)	*Component*				
	Ar	O_2	N_2	CH_4	*CO*
–	3.20	6 1	15.6	2.0	66.6
0.05	4.6	6.1	17.1	4.3	90.5
0.10	5.6	6.9	23.1	7.8	188.1
0.25	6.3	7.0	24.0	20.0	188.1
1.00	5.7	6.1	17.0	28.0	118.3
5.00	3.6	3.6	5.9	4.8	30.0

Treatment of clinoptilolite specimens with acid caused an increase in the specific retention volumes of all of the compounds studied. However, the increases depended not only on the concentration of the acid used, but also on the size of the adsorbate molecules. The highest specific retention volumes of oxygen, nitrogen, argon and carbon monoxide were obtained on the specimens treated with 0.25 *N* hydrochloric acid, and that of methane on specimens treated with 1 *N* acid (Table II). A further increase in the acid concentration resulted in a sharp decrease in the specific retention volumes of all of the compounds studied.

These results can probably be explained as follows. Treatment of clinoptilolite with acid of concentration below 1 *N* causes partial decationization of the specimen, promoting broadening of the free apertures of the zeolite. This in turn leads to an increase in the adsorption rate, creating favourable contions for the establishment of adsorption equilibrium in the chromatographic process. The overall result is an increase in the retention volumes of the compounds studied, and this can be seen particularly clearly with methane. On the other hand, the use of acid of higher concentration leads to dealuminization of the specimens, which causes a decrease in the number of Lewis adsorption centres and also leads to partial amorphism of the zeolite. The result in this instance is some weakening of interactions in the adsorbate–adsorbent system, leading to a decrease in the specific retention volumes of the compounds studied. On clinoptilolite in the original (untreated) form the separation of the system mixture methane–oxygen–nitrogen–carbon monoxide takes place in that order of elution, caused by methane diffusing on the "external" surface of the zeolite. Treatment of the specimen with 1 *N* acid results in a reversed order of elution, *viz.*, oxygen–nitrogen–methane–carbon monoxide. The separation of the mixture argon–oxygen–nitrogen takes place on the original clinoptilolite specimen, but the separation of oxygen–nitrogen is very poor. On other specimens of natural tuffs containing clinoptilolite, the separation of oxygen–nitrogen does not take place[9,13] and in some instances the components were even eluted in the order nitrogen–oxygen[9]. Probably a nitrogen molecule, having a larger critical diameter (3 Å) than that of oxygen (2.8 Å), cannot penetrate the zeolite free apertures and moves on the "external" surface of the adsorbent. An assumption is made that it is connected with the different ratios of calcium and potassium cations per unit cell of clinoptilolite.

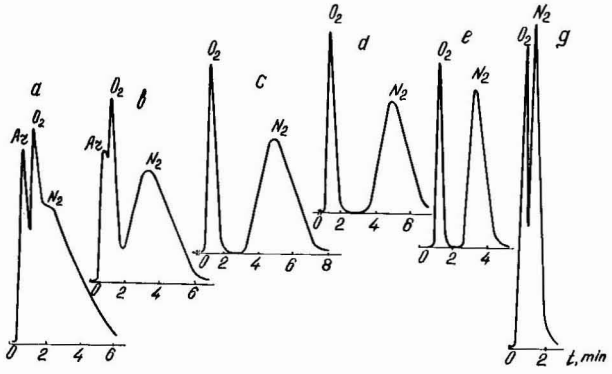

Fig. 1. Chromatograms of the separation of argon–oxygen–nitrogen on the original specimen of clinoptilolite and on specimens modified with acid. a, Original specimen; b, c, d, e, g, specimens treated with 0.05, 0.1, 0.25, 1.0 and 5.0 *N* hydrochloric acid, respectively. Column temperature, 25°; carrier gas flow-rate, 50 ml/min.

Treatment of clinoptilolite with 0.1–1 *N* hydrochloric acid considerably improves the separation of oxygen–nitrogen but gives no separation of argon–oxygen. A further increase in the hydrochloric acid concentration makes the separation of oxygen–nitrogen worse (Fig. 1). Calculations of the criteria of separation

K_1* and δ** (ref. 16) of the oxygen–nitrogen mixture clearly show that they depend to a considerable extent on the concentration of the acid used for the treatment of clinoptilolite, the temperature of heating of the chromatographic column and the carrier gas flow-rate (Table III).

TABLE III

CRITERION OF SEPARATION (K_1, δ) OF O_2–N_2 ON NATURAL CLINOPTILOLITE AND ON SPECIMENS TREATED WITH HYDROCHLORIC ACID

Concentration of HCl (N)	*Flow-rate of carrier gas (ml/min)*	*Temperature of column (°C)*					
		25	*40*	*60*	*80*	*100*	*120*
—	20	0.63	0.69	0.75	—	—	—
	50	0.22	0.24	0.25	—	—	—
0.05	20	1.10	0.95	0.94	0.91	0.75	0.71
	50	0.78	0.76	0.76	0.71	0.65	0.50
0.10	20	2.00	1.80	1.55	1.37	0.96	0.88
	50	1.57	1.46	0.97	0.96	0.91	0.80
0.25	20	2.17	1.98	1.73	1.36	0.97	0.88
	50	1.75	1.52	0.99	0.97	0.93	0.78
1.00	20	2.20	1.87	1.88	0.97	0.88	—
	50	1.91	1.54	0.99	0.95	0.82	0.60
5.00	20	0.90	0.78	0.40	—	—	—
	50	0.63	0.38	—	—	—	—

As can be seen from Table III, the best separation of oxygen–nitrogen is obtained on specimens modified with 0.1–1 *N* acid at a chromatographic temperature of 25° and a carrier gas flow-rate of 20 ml/min. Determination of the heats of adsorption of argon, oxygen, nitrogen, methane and carbon monoxide from chromatographic data showed that the acid modification of tuffs containing clinoptilolite considerably increases the heats of adsorption of argon and particularly of methane in comparison with the original specimens, while the heats of adsorption of nitrogen, oxygen and carbon monoxide change only slightly (Table IV). These results again confirm the above assumption that on the natural specimen, molecules of argon and methane diffuse on the "external" surface of clinoptilolite, while the acid treatment of tuffs allows molecules of these substances to be adsorbed in the zeolite cavities. Treatment of clinoptilolite with 5 *N* hydrochloric acid, causing partial destruction of the clinoptilolite crystal lattice, promotes a decrease in the heats of adsorption of argon, oxygen, nitrogen, methane and carbon monoxide.

Synthetic mordenites (NaM) have a better separating ability with respect to the oxygen–nitrogen mixture[17,18] than a well known type of zeolite such as NaX (13X).

* $K_1 = \dfrac{\Delta l}{\mu_{0.5(1)} + \mu_{0.5(2)}}$

where Δl is the distance between the maxima of two chromatographic peaks and $\mu_{0.5(1)}$ and $\mu_{0.5(2)}$ are the peak widths at half-height. The absolute value of K_1 is always > 1.

** $\delta = \dfrac{h_m - h_{\min}}{h_m}$

where h_m is the average height of both peaks and $h_{\min}$ is the minimum height of both peaks. The absolute value of δ is always < 1.

TABLE IV

HEATS OF ADSORPTION (kcal/mole) OF ARGON, OXYGEN, NITROGEN, METHANE AND CARBON MONOXIDE ON NATURAL AND MODIFIED TUFFS CONTAINING CLINOPTILOLITE

Concentration of HCl (N)	*Component*				
	Ar	O_2	N_2	CH_4	*CO*
0.00	1.65	3.30	4.90	1.09	6.59
0.05	2.77	3.30	4.95	1.38	7.03
0.10	3.00	3.23	5.19	1.43	8.91
0.25	3.30	3.37	4.95	4.12	8.12
1.00	3.00	3.29	5.00	5.60	7.92
5.00	2.80	2.80	3.96	2.80	6.75

On the other hand, it is known that enrichment of these zeolites with cations of alkaline earth metals and the use of thermal activation permit their separating abilities with respect to the above mixture to be almost doubled[19].

Studies of the chromatographic properties of tuffs containing mordenites showed that they are characterized by good separating properties with respect to the oxygen–nitrogen mixture and they are not worse than the synthetic mordenite NaM[12,19]. In terms of its cation composition, tuffs containing mordenite from the deposits of the Geogian S.S.R. can be considered as a form enriched with calcium cations.

The introduction of cations of barium or strontium into the structure of natural mordenite by the first method of exchange causes a sharp decrease in the specific retention volumes of argon and methane (Table V). Probably large cations of strontium and barium, when the first method of exchange is used, occupy positions in the inner channels of mordenite, while nitrogen, oxygen and carbon monoxide penetrate these channels.

A sharp decrease in the specific retention volumes of nitrogen and oxygen takes place on barium forms of tuffs containing mordenite, obtained by the first

TABLE V

SPECIFIC RETENTION VOLUMES V_g (ml/g) OF ARGON, OXYGEN, NITROGEN, METHANE AND CARBON MONOXIDE ON TUFF CONTAINING MORDENITE AND SPECIMENS SUBJECTED TO CATION MODIFICATION

Component	*Original natural specimen*		*MgM***	*CaM**	*CaM***	*SrM**	*SrM***	*BaM**	*BaM***
	Temperature of activation (°C)								
	300	*450*	*450*	*450*	*450*	*450*	*450*	*450*	*450*
Argon	1.1	2.3	2.4	1.2	2.0	0.2	2.8	0.2	1.2
Oxygen	1.3	3.4	2.8	3.2	3.7	4.9	5.5	2.3	15.5
Nitrogen	3.4	42.0	29.0	34.5	51.0	61.0	87.4	1.9	18.7
Methane	3.4	11.1	8.1	0.2	0.8	0.2	2.0	0.4	3.9
Carbon monoxide	25.6	660.0	–	553.2	783.2	579.3	826.8	49.6	273.5

* Specimens obtained by the first method of ion exchange.

** Specimens obtained by the second method of ion exchange.

method of exchange, in comparison with the original form. In addition, inversion of the elution order of oxygen and nitrogen occurs on this cation-exchanged form.

Calculations of the criteria of separation showed that the best separation of the oxygen–nitrogen mixture takes place on natural mordenite and also on the specimens enriched with cations of calcium and strontium by the first method of exchange (Table VI). The separation of argon–oxygen on mordenite containing strontium improves on increasing the flow-rate of the carrier gas (at 50 ml/min, $\delta = 0.50$, while at 200 ml/min, $\delta = 0.75$). For barium-substituted tuffs containing mordenite, on the contrary, an increase in the carrier gas flow-rate results in a poorer separation of this mixture (Fig. 2).

TABLE VI

CRITERIA OF SEPARATION (K_1, δ) OF O_2–N_2 AND Ar–O_2 ON TUFF CONTAINING MORDENITE AND CATION-MODIFIED SPECIMENS

Temperature of activation of the specimen, 450°; column temperature, 20°; carrier gas flow-rate, 100 ml/min.

Mixture	*Tuff containing mordenite*	*Synthetic mordenite (NaM)*	*MgM****	*CaM**	*CaM****	*SrM**	*SrM****	*BaM**	*BaM****
Ar–O_2				0.11	—	0.64	—	0.45	0.11
O_2–N_2	1.0	1.0	0.67	0.98	1.1	1.2	1.4	—	0.39

* Specimens obtained by the first method of ion exchange.
** Specimens obtained by the second method of ion exchange.

Evidently, large barium cations in the structure of mordenite, owing to steric effects, prevent the diffusion of argon molecules into zeolite channels, while oxygen molecules can freely penetrate them. At a low flow-rate of the carrier gas, oxygen molecules move more slowly in mordenite channels, interacting with the cations of the zeolite framework, while argon molecules diffuse on the "external" surface of mordenite and the carrier gas has less influence on the velocity of their motion.

With strontium forms of mordenites, the steric factor of strontium cations is lower than that of barium cations and therefore, at low flow-rates of the carrier gas, argon penetrates, although with difficulty, the channels of the zeolite, making the separation of the argon–oxygen mixture worse. At high flow-rates of the carrier gas,

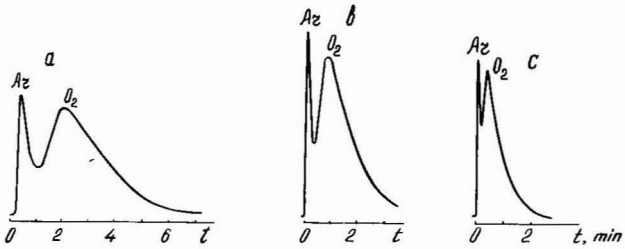

Fig. 2. Chromatograms of the separation of argon-oxygen on natural barium-modified mordenite (BaM) activated at 450°, at room temperature and different flow-rates of the carrier gas: (a) 25; (b) 50; (c) 100 ml/min.

the argon molecules have no time to penetrate the mordenite channels, which are blocked by strontium cations, and diffuse on the external surface. The difference between the retention times of argon and oxygen is increased and the separation of this mixture is improved.

The results obtained show that tuffs containing clinoptilolite treated with acid and also mordenite-containing rocks can be used successfully in adsorption processes for the separation of gaseous mixtures with the purpose of obtaining fractions enriched with some component, particularly air enriched with oxygen.

REFERENCES

1 G. V. Tsitsishvili and T. G. Andronikashvili, *Uspekhi Khromatografii*, Nauka, Moscow. 1972, p. 226.
2 C. Vidal-Madjar and G. Guiochon, *Separ. Purif. Methods*, 2 (1973) 1.
3 T. G. Andronikashvili, G. V. Tsitsishvili and L. Ya. Laperashvili, *Chromatographia*, 5 (1975) 223.
4 F. Wolf and P. König, *Z. Chem.*, 9 (1974) 367.
5 G. V. Tsitsishvili, T. G. Andronikashvili, Sh. D. Sabelashvili and N. A. Osipova, *Chromatographia* 130 (1977) 13.
6 D. Breck, *Zeolite Molecular Sieves*, Mir, Moscow, 1976, p. 195.
7 G. V. Gvakharia, N. I. Skhirtladze, T. V. Batiashvili and R. A. Akhvlediani, G. A. Mikadze, *Dokl. Akad. Nauk SSSR*, 205 (1972) 179.
8 G. V. Tsitsishvili T. G. Andronikashvili, Sh. D. Sabelashvili and Z. I. Koridze, *Dokl. Akad. Nauk SSSR*, 194 (1970) 1346.
9 G. V. Tsitsishvili, Sh. D. Sabelashvili Z. I. Koridze, E. K. Kvantaliani and T. G. Andronikashvili, *Izv. Akad. Nauk SSSR, Neorg. Mater.*, 9 (1973) 1394.
10 Sh. D. Sabelashvili, A. Yu. Krupennikova, Z. I. Koridze and T. G. Andronikashvili, *Soobshch. Akad. Nauk Gruz. SSR*, 73 (1974) 373.
11 K. Torii, M. Asaka and H. Yamazaki, *Kogyo Kagaku Zasshi*, 72 (1969) 661.
12 G. V. Tsitsishvili, N. I. Skhirtladze, T. A. Chumburidze and T. G. Andronikashvili, *Dokl. Akad. Nauk SSSR*, 225 (1975) 587.
13 I. M. Galabova, L. N. Petkova and R. Nikolov, *Dokl. Bolg. Akad. Nauk*, 29, 3 (1976) 383.
14 I. M. Galabova, G. Haralampiev, R. Nikolov and L. Petkova, *Dokl. Bolg. Akad. Nauk*, 28 (1976) 387.
15 Y. Nishimura and H. Takahashi, *Kolloid-Z.Z. Polym.*, B245, (1971) 415.
16 *Gas Chromatography, Trudy I Vses. Konf.*, Izd. Akad. Nauk SSSR, Moscow, 1960, pp. 108 and 237.
17 F. Wolf, P. König and K. Grüner, *Z. Chem.*, 1 (1975) 36.
18 G. V. Tsitsishvili, T. A. Chumburidze and T. G. Andronikashvili, *Soobshch. Akad. Nauk Gruz. SSR*, 80 (1975) 369.
19 T. G. Andronikashvili, T. A. Chumburidze and G. V. Tsitsishvili, *Izv. Akad. Nauk GSSR, Ser. Khim.*, 1 (1975) 399.

Journal of Chromatography, 148 (1978) 69–74

CHROM. 10,401

FERRITE PRESSURE TRANSDUCER IN SYRINGE PUMPS USED IN HIGH-PERFORMANCE LIQUID CHROMATOGRAPHY

ANDRZEJ BYLINA and KAROL LEŚNIAK

Institute of Physical Chemistry, Polish Academy of Sciences, Kasprzaka 44/52, 01-224 Warszawa (Poland)

and

STEFAN ROMANOWSKI

Institute of Tele and Radio Technology, Ratuszowa 11, 03-450 Warszawa (Poland)

SUMMARY

A ferrite pressure transducer acting as a constant flow device was applied to a high-performance liquid chromatographic syringe pump, and permitted high stability and reproducibility of chromatographic results in isocratic elution to be obtained and a *Y–t* recorder to be applied.

INTRODUCTION

It is well known that syringe pumps used in high-performance liquid chromatography (HPLC) have many advantages in comparison with other types. Martin *et al.*[1] described the influence of the fluid compressibility on the chromatographic peaks recorded as a function of time. This problem cannot be neglected in the case of real fluids closed in a syringe pump with a volume of 250–500 ml and a back-pressure of up to several hundred atmospheres. Theoretical considerations[1] and experimental values[2] have been presented recently.

Such effects can be avoided when constant-displacement syringe-type pumps are used, by modifying the driving system. The ideal, but so far non-existing, solution would be to place a flow meter in the head of the pump and to feed its signals back to the motor. In others words, a flow meter should not be sensitive to the changes in the density of liquids caused by the back-pressure. Meanwhile, one can apply a pressure transducer based on Darcy's equation:

$$\dot{Q}_0 = \frac{kS}{\bar{\eta}L} \cdot \Delta p_\infty$$

where k, S, $\bar{\eta}$ and L are constants when Δp_∞ is the pressure under steady-state conditions and Q_0 is the set flow-rate. Transducers of these types were recently described by Van Lenten and Rothman[3] and by Achener *et al.*[4].

TABLE I

TYPES OF PRESSURE TRANSDUCER

Type of transducer	*Example*	*Pressure range (atm)*	*Remarks*
Piezoresistive	Manganine	$> 20{,}000$	Large size, depending on temperature
Semiconductor junction	Zener diode	$> 20{,}000$	For high pressures
Ultrasonic propagator		$\geqslant 19{,}000$	Large size
Magneto-elastic ferrite	Torroidal core	$\leqslant 2000$	Chemically resistant, thermally stable, small size
Others	Bourdon tube, membrane[5]		Connected with other transducers, not expensive

EXPERIMENTAL

For electrical measurements of hydrostatic pressure, various methods can be used and a comparison of these methods is given in Table I. We believe that, for measurements of pressure and for the feed-back connection to the pump in HPLC, a ferrite transducer is the most suitable. A torroidal-shaped core (Fig. 1A) made from nickel–zinc ferrite as the pressure transducer was used. The chemical composition and specially developed technology enabled us to obtain a rectangular hysteresis loop and pressure sensitivity[6]. Rectangular and current pulses (Fig. 1B), which are necessary for magnetizing the core, induce the voltage pulses in the measuring coil (Fig. 1C). The amplitude, U_m, of these pulses can be described approximately as follows:

$$U_m = KAZ_p \cdot \frac{\Delta B}{t_s}$$

where K is a constant depending on the impulse shape, Z_p the number of coils in the measuring circuit, A the area of the cross-section, ΔB the change in magnetic induction of the core and t_s the response time of the transformer. Changes in the hydrostatic pressure acting on the ferrite core result in changes in ΔB and t_s, *i.e.*, changes in

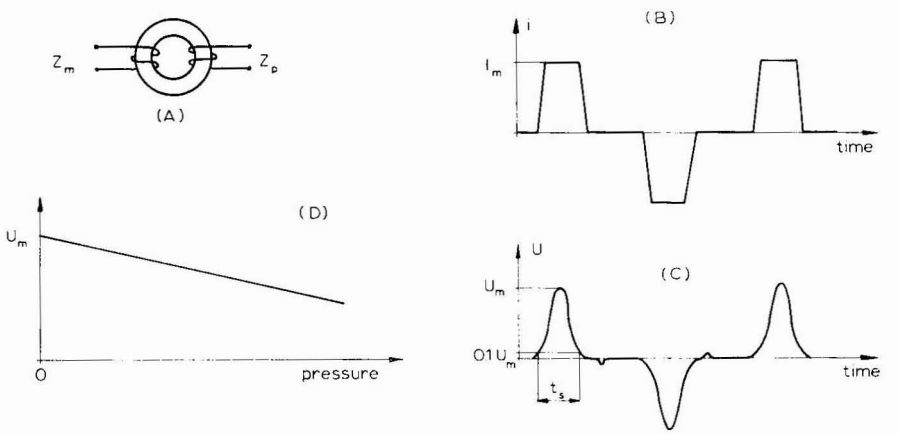

Fig. 1. (A) Ferrite core. (B) Magnetizing current pulses. (C) Voltage pulses in the measuring coil. (D) Pressure characteristics of the ferrite core.

the output amplitude due to the inverse magnetostrictive effect (Fig. 1D). When the hydrostatic pressure increases, the output voltage pulses, U_m, consequently decrease. The characteristic of the ferrite transducer is shown in Fig. 1D to be linear in the range 0–400 atm. A torroidal core with O.D. 2 mm, I.D. 1.3 mm and height 0.9 mm as a pulse transformer was used[7]. There are two coils for the input Z_m and the output Z_p.

A schematic diagram of the transducer connected with the syringe pump (driven by the stepping motor) is shown in Fig. 2. Rectangular pulses are generated by the generator and fed into the transformer. The amplitude of the output pulses U_m, depending on the pressure, is converted by the peak detector into the d.c. voltage U_p. Next, the characteristic of the ferrite transducer is reversed and for the pressure $\Delta p = 0$ the d.c. voltage $U_p = 0$. The signal U_p is compared with the reference voltage, U_{ref}, which can be derived from the potentiometer. When $U_p > U_{ref}$, the signal from the comparator causes the gate G to close, *i.e.*, the pulses from the voltage-to-frequency (V/F) converter used normally to drive the stepping motor are switched off. At this moment, the stepping motor stops, which is indicated by a light. When $U_p < U_{ref}$, the gate is open for pulses from the V/F converter. In this instance, the stepping motor is on and the light is off. The pressure which stops the motor can be adjusted according to U_{ref}. The potentiometer Q_r sets the piston speed. The voltage behind the peak detector permits the measurement and recording of the pressure. The transducer is placed in the head of the pump. A high-pressure valve is located between the column and the output of the pump and enables stop-flow injection to be used. When U_p reaches U_{ref}, corresponding to the steady-state pressure, the constant flow mode for the syringe pump is obtained.

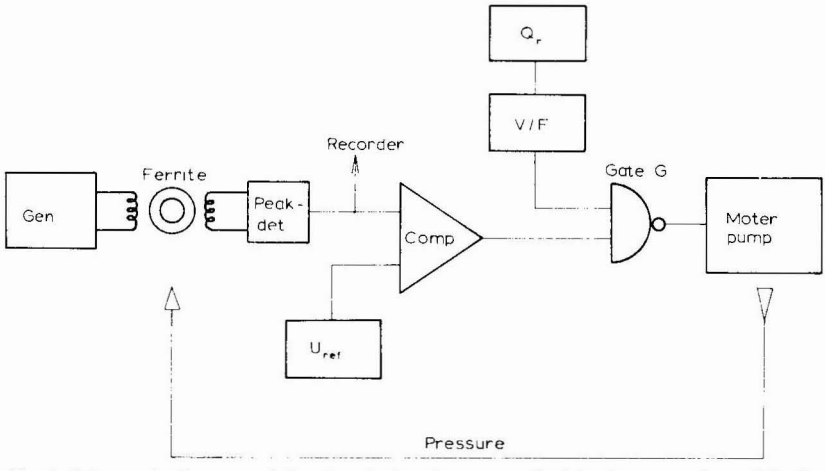

Fig. 2. Schematic diagram of the electrical and pressure feed-back connection of the ferrite transducer to the driving system.

The action of the transducer was examined on a home-made constant-displacement syringe pump liquid chromatograph fitted with a UV detector. The syringe volume was 250 ml, the highest back-pressure 400 atm and the highest flow-rate 6 ml/min. A column of length 250 mm and I.D. 3 mm packed with Merckosorb SI-60, particle diameter 5 μm, was used. The flow-rate was measured as a function of time using a recording balance.

The signals from the balance, the pressure manometer, the UV detector and the clock were recorded or printed out.

RESULTS AND DISCUSSION

The correlation between the flow-rate and the back-pressure was measured; according to the Darcy equation, this should be linear. The results obtained (100–300 points printed at 0.5- or 1-sec intervals) were analyzed using the least-squares method according to the equation

$$Q(t) = a\Delta p(t) + b$$

where $Q(t)$ is the flow-rate calculated from the mass flow and the density of *n*-hexane. The measurements were carried out with an initial pump volume of 50 ml and an initial pressure of zero. In the instance, when the set flow-rate is 2 ml/min, the pressure increased to about 150 atm. The mass of the *n*-hexane eluent was measured with an accuracy of 1 mg and the pressure with an accuracy of 0.1 atm.

The negative b values (Table II) can be regarded as a result of the difference in the input and the output flow-rates, because of the compressibility and viscosity of *n*-hexane in the column. In the simple form of the Darcy equation, this influence of the pressure on the flow-rate is neglected. The same discrepancy with the theoretical data was observed earlier[4] by measuring the time (t_{99}) needed for steady-state flow conditions to be attained.

TABLE II

CONSTANTS OBTAINED IN THE EQUATION $Q(t) = a\Delta p(t) + b$

Q_0 (ml/min)	$a \times 10^4$ (ml/min.atm)	$b \times 10^2$ (ml/min)
0.5	134.8 ± 6.7	−0.9 ± 1.5
1	130.4 ± 2.7	−1.4 ± 1.3
2	133.6 ± 2.3	−2.3 ± 2.9

The high-pressure valve and electronic feed-back of the pressure manometer to the motor were applied in order to give stop-flow injection and to obtain a constant flow-rate. When a new column and/or mobile phase is used and Q_0 is set, then a considerable time is needed in order to attain steady-state flow. To permit the use of the valve, U_{ref} has to be adjusted such that $U_{ref} = U_p$. The opening and closing of the valve in connection with stop-flow injection does not change the pressure in the syringe pump. The phenomena that occur during the closing and opening of the valve are represented in Fig. 3. The 3-sec delay is needed in order to obtain a constant flow-rate after opening the valve and no change in pressure is observed. The long-term drift of the pressure read on the manometer is not greater than 0.5 atm at a level of 150 atm and 0.2 atm at 40 atm.

It is important in chromatography to demonstrate the influence of the fluid compressibility in the pump on the chromatograms recorded as functions of time and volume. The signal from the UV detector, the mass flow-rate and time were recorded

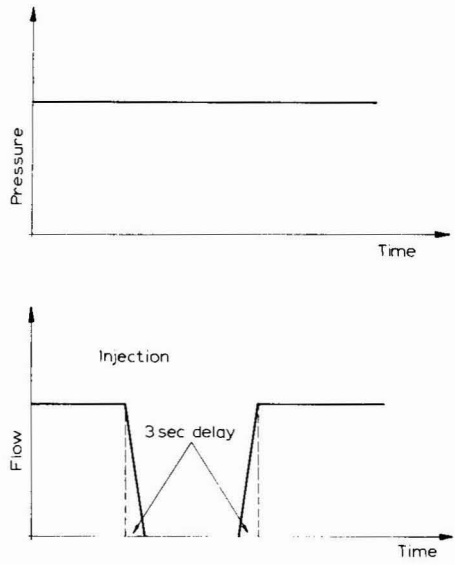

Fig. 3. Flow and pressure characteristics in the stop-flow injection mode.

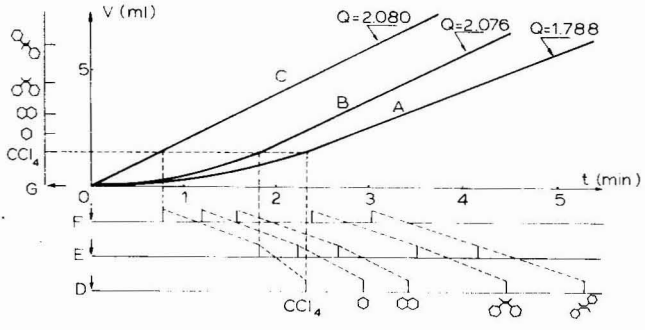

Fig. 4. A, B and C represent the effluent volumes on the time scale; C was obtained using the pressure device. D, E and F show the retention times of the substances analyzed under conditions A, B and C, respectively. G represents the true retention volume of the substances analyzed.

simultaneously. Fig. 4 shows the dependence of the effluent volume on time. Curves A and B were obtained for the initial volumes of the pump, $V_0 = 250$ and 50 ml, respectively, where Q_0 was set 2 ml/min and the starting pressure was zero. Curve C is a straight line and depicts the situation when the stop-flow injection mode is employed, using the constant-flow device.

Chromatographic analyses of a mixture of carbon tetrachloride, benzene, naphthalene and *cis*- and *trans*-stilbene were carried out and the retention data were recorded. These were always constant on the volume scale (*cf.*, G in Fig. 4). However, the retention times on chromatograms D, E and F were different and depended on the starting conditions (*i.e.*, initial volumes, pressures, etc.). The broken lines pass through the peaks of the same substances. The true capacity factors for all of the substances could be calculated only from plot C, which was obtained with the use of the

constant-flow device. This means that in the constant flow-rate mode, a Y–t recorder can be applied.

CONCLUSION

The equipment described enables one to obtain high stability and reprodúcibility of chromatographic results in isocratic elution and a Y–t recorder can be used. We consider that owing to the expansion of the liquid along the column, small differences between the set flow-rate (Q_0) and the flow-rate actually recorded (Q) can be observed even when the constant flow-rate device is used.

REFERENCES

1 M. Martin, G. Blu, C. Eon and G. Guiochon, *J. Chromatogr.*, 112 (1975) 399.
2 S. R. Abbott, J. R. Berg, P. Achener and R. L. Stevenson, *J. Chromatogr.*, 126 (1976) 421.
3 F. J. van Lenten and L. D. Rothman, *Anal. Chem.*, 48 (1976) 1430.
4 P. Achener, S. R. Abbott and R. L. Stevenson, *J. Chromatogr.*, 130 (1977) 29.
5 F. McDonald, *Basic Liquid Chromatography*, Varian Aerograph, Walnut Creek, Calif., 1971, pp. 10–18.
6 R. Neswald, *Electronic Products*, 3 (1970) 53.
7 S. Romanowski, S. Goldberg and G. Wasiak, *Pomiary Autom. Kontrola*, 4 (1975) 161.

Journal of Chromatography, 148 (1978) 75–77

CHROM. 10,484

GLASS COLUMNS WITH A SEPTUMLESS INJECTOR FOR HIGH-PERFORMANCE LIQUID CHROMATOGRAPHY

VRATISLAV SVOBODA and IMRICH KLEINMANN

Institute for Research, Production and Application of Radioisotopes, 17004 Prague 7 (Czechoslovakia)

SUMMARY

A construction of columns made from thick-walled glass tubes is described. The joints between the glass column and metal head are deformable. An injector is built into the column head. These columns were used at pressures up to 10 MPa and temperatures up to 80°.

INTRODUCTION

The use of hard glass as a column material in high-performance liquid chromatography (HPLC) has many advantages. Its surface is very smooth and chemically resistant and the columns are transparent, so that it is easy to follow mechanical compression of column bed and any changes in its colour. However, these advantages are offset by the fragility of glass. Because glass has a relatively low expansion coefficient, it is difficult to make a pressure-tight seal between stainless steel and glass.

A successful construction of glass columns was described by Stahl and Schuppe[1,2]. They used glass tubes of I.D. 2.3 mm and O.D. 9 mm, sealed to the stainless steel outlet and inlet parts by Viton O-rings and cylindrical inserts made from Kel-F. Both ends of the column were held together by a stainless-steel tube, surrounding the whole column and acting as a pressure shield. The pressurized eluent not only flows through the column but also surrounds the glass column, permitting pressures up to 30 MPa to be attained.

Tesařík and Kaláb[3] tested glass tubes for use as columns in liquid chromatography, and found that pressures up to about 60 MPa are necessary for their rupture. They characterized the tension in pressurized tubes by a dimensionless constant, A:

$$A = \frac{(D/d)^2 + 1}{(D/d)^2 - 1}$$

where D is the outer and d the inner diameter of the tube. If A is less than *ca.* 1.55, the tube should be suitable for application in liquid chromatography.

EXPERIMENTAL

We used glass tubes with I.D. 3.5 mm and O.D. 10 mm, made from SIAL glass, with $A = 1.28$.

In the first construction, the ends of tubes were cemented to brass or stainless-steel heads with epoxy resin. After several weeks of daily use the glass broke, usually at some distance from the seal. This effect was not overcome by temperature annealing the tubes and fire-polishing their ends, presumably because of tension in the glass due the difference in the thermal expansion coefficients of metal and glass.

Our aim was to construct a column that could be operated from room temperature to about 80°. Therefore, we had to avoid any firm joint between metal and glass. Further, in order to decrease the void volumes, we incorporated the injector into the column head.

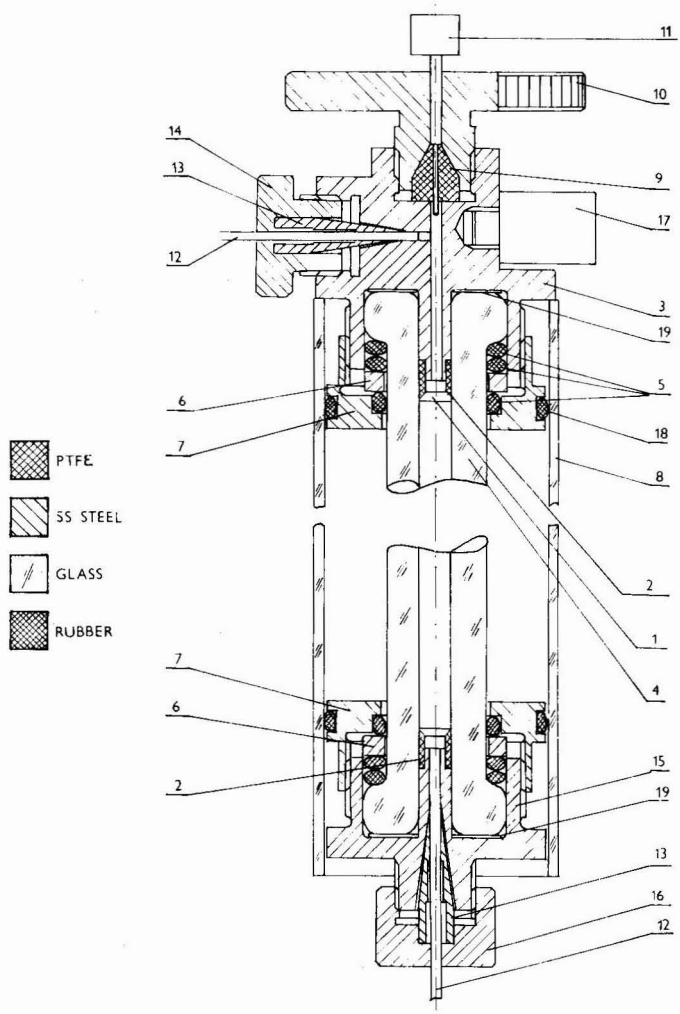

Fig. 1. Construction of column.

The final version of the construction is illustrated in Fig. 1*. A conical surface of glass or metal frit (1) is pressed against a polytetrafluoroethylene seal (2), forming a deformable joint between the inlet channel of the column head (3) and the glass column (4). The tube is fabricated with a very precise inner diameter (3.45 mm) and has two rounded rims on both ends. Between the glass tube rim, column head (3) and and washer (6) and nut (7) are inserted three rubber O-rings (5) and a plastic washer (19). A shaft (17) is used for mounting the column head on a stand.

The septumless injector is closed by a shaft (11) and a seal (9). When a sample is to be injected, the screw (10) is lifted, the shaft (11) is replaced with a syringe needle and the seal is re-tightened by the screw (10). The eluent is fed into the column by a capillary (12); the joint is made tight by a conical ferrule (13). A similar connection is made on the lower end of the column, but the shapes of the nuts (15) and (16) are different. The glass thermostating jacket (8) is simply held by an O-ring (18) in the groove of the nut (7).

The eluent comes into contact only with stainless steel, polytetrafluoroethylene and glass and it can therefore be used for most commonly used systems.

RESULTS AND DISCUSSION

These columns have been used routinely in our laboratory for more than 2 years with pressures up to 2.5 MPa and in some instances up to 10 MPa. No breakages of the glass column were observed. Because the column bed can be observed constantly, changes in the bed volume are easily detected. Operation at temperatures up to 80° caused no problems. It is difficult to make a quantitative estimation of influence of glass on the temperature of eluent in the column in comparison with columns made of stainless steel. Obviously, the heat transfer through a thick glass wall is less efficient than that through a relatively thin steel wall, but this may be not be very important. Firstly, the eluent flows through narrow bores in the metallic column head, which is kept at the same temperature as the column itself. Secondly, in both metallic and glass columns the most difficult part of the heat transfer is radially into the column bed, and in this respect both designs are equivalent.

Because the trend in HPLC in recent years has been towards smaller particles and pressures below 10 MPa, and because the interior surface of a stainless steel tube even if initially very smooth, may become corroded or eroded very easily, we believe, that there is a future for glass columns in this field.

ACKNOWLEDGEMENTS

We are indebted to Mrs. H. Samešová, Mr. J. Pankrác and Mr. J. Špirk for their assistance.

REFERENCES

1 K. G. Stahl and E. Schuppe, *GIT Fachz. Lab.*, 15 (1971) 28.
2 K. G. Stahl and E. Schuppe, *GIT Fachz. Lab.*, 17 (1973) 563.
3 K. Tesařík and P. Kaláb, *Chem. Listy*, 69 (1975) 1078.

* Patent applied for (PV-2693-77).

Journal of Chromatography, 148 (1978) 79–97

CHROM. 10,395

GRADIENT ELUTION IN LIQUID CHROMATOGRAPHY

VIII. SELECTION OF THE OPTIMAL COMPOSITION OF THE MOBILE PHASE IN LIQUID CHROMATOGRAPHY UNDER ISOCRATIC CONDITIONS

P. JANDERA, M. JANDEROVÁ and J. CHURÁČEK

Department of Analytical Chemistry, University of Chemical Technology, Pardubice (Czechoslovakia)

SUMMARY

The influence of the composition of the mobile phase on resolution in liquid chromatography is considered from both the theoretical and the practical points of view. Different theoretical models for adsorption and ion-exchange chromatography are compared and an approach is suggested that permits calculations of the composition of the mobile phase that is necessary in order to achieve the separation required. The factors limiting the application of the mathematical approach presented are discussed. The theoretical conclusions are supported by several practical examples of chromatographic separations on silica and alumina.

INTRODUCTION

Since the comeback of liquid chromatography in the late 1960s, considerable effort has been devoted to the improvement of liquid chromatographic separations. A dramatic increase in resolution was achieved by the development of efficient column packing materials and rational instrumental design. Many papers devoted to the improvement of column and system efficiencies have been published, but far less attention has been paid to the possibilities of improving resolution by appropriate control of the composition of the mobile phase, which has been adjusted by trial and error methods until acceptable separations were achieved. Few attempts have been made to calculate the optimal composition of the mobile phase for the resolution required. The work of Snyder and Saunders[1], in which the conditions for gradient elution in adsorption chromatography were calculated in order to maintain a constant width of all peaks during the elution, is a rare exception.

If any calculations of this type are to be performed, the relationship between the composition of the mobile phase and some characteristic representing the retention of the solute in the system (such as the capacity ratio) must be known. In an earlier paper[2], we suggested a simple equation to describe this relationship:

$$k' = k'_0 c^{-n} \qquad (1)$$

where k' is the capacity ratio of the solute, c is the concentration of the stronger eluting component in a binary mobile phase and k'_0 and n are experimental constants. This equation has been shown to be valid in a number of practical separations by adsorption and ion-exchange chromatography[3–6].

Based on Snyder's theory of adsorption chromatography[7], an equation can be written[2] for the capacity ratio in a mixture of two solvents a and b:

$$\log k' = \log k'_a - \frac{A_s}{n_b} \cdot \log [c(10^{\bar{\alpha} n_b (\varepsilon^\circ_b - \varepsilon^\circ_a)} - 1) + 1] \tag{2}$$

where A_s and n_b represent the effective molecular area of an adsorbed molecule of the sample solute and that of the more polar solvent b, respectively, ε°_a and ε°_b denote the solvent strength parameters of the two solvents a and b, respectively, $\bar{\alpha}$ is the adsorbent surface activity function and k'_a refers to the capacity ratio of sample solute in the pure solvent a.

Eqn. 2 can be rearranged into the form

$$k' = (a + bc)^{-n} \tag{3}$$

where $a = k'^{-\frac{n_b}{A_s}}_a$, $b = k'^{-\frac{n_b}{A_s}}_a \cdot (10^{\bar{\alpha} n_b (\varepsilon^\circ_b - \varepsilon^\circ_a)} - 1)$, $n = \frac{A_s}{n_b}$ and a, b and n are experimental constants which should not depend on the concentration of solvents a and b in the mobile phase. If the sample solutes are very strongly retained in the less polar solvent a (usually a hydrocarbon), k'_a is very high and the parameter a is very small and can be neglected. Then eqn. 3 is simplified to eqn. 1.

Recently, Scott[8] published another simple equation for the capacity ratio in binary solvent systems, which can be written in the form:

$$k' = (a + bc)^{-1} \tag{4}$$

Eqn. 4 is identical with eqn. 3 if $n = 1$, which holds provided that $A_s = n_b$, *i.e.*, if an adsorbed molecule of the sample solute occupies the same area of the adsorbent surface as a molecule of the more polar solvent. This simplified assumption, however, is generally not fulfilled. The differences in the number of polar functional groups in the solute molecules and/or solvation effects may cause differences in the area of the adsorbent occupied by various molecules. Consequently, the exponent n often deviates considerably from unity and eqn. 4 is no longer valid. In a previous study on the adsorption chromatography of azo compounds on silica in different binary solvent systems[5], we found that n varied in the range 0.5–2.5, depending on the nature of the solute and solvents used.

The adsorption chromatography of four steroids on alumina in *n*-propanol–*n*-heptane[9] is described here to illustrate some practical limitations of the mathematical models discussed. The experimental values of n for lumisterol, tachysterol, calciferol and ergosterol (Tables II–IV) are within the range 1.1–1.5. The compounds are only slightly retained in mobile phases that contain more than 1% of *n*-propanol. To compare the application of eqns. 1 and 4 to the above practical system, the relationship between $1/k'$ and c is plotted in Fig. 2, while the plot of log k' *versus* log c is shown in Fig. 1. The relationship between $1/k'$ and c is approximately linear for ergosterol and possibly for calciferol, but there are large deviations for lumisterol

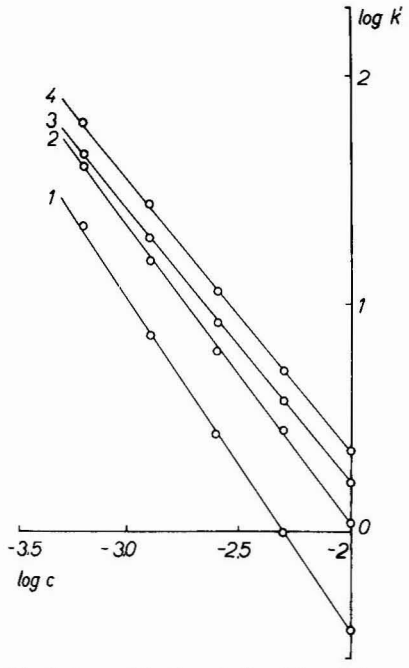

Fig. 1. Logarithmic relationships between capacity ratios (k') of lumisterol (1), tachysterol (2), calciferol (3) and ergosterol (4) and the concentration of *n*-pronapol (c, vol.-% $\times 10^{-2}$) in *n*-heptane used as the mobile phase in chromatography on LiChrosorb ALOX T. Experimental conditions are given in Table II. The relationships should be linear if eqn. 1 applies.

and tachysterol, which indicates that eqn. 4 cannot be applied to them. All of the logarithmic relationships in Fig. 2 are linear, which demonstrates the validity of eqn. 1, which is more suitable than eqn. 4 for describing the system.

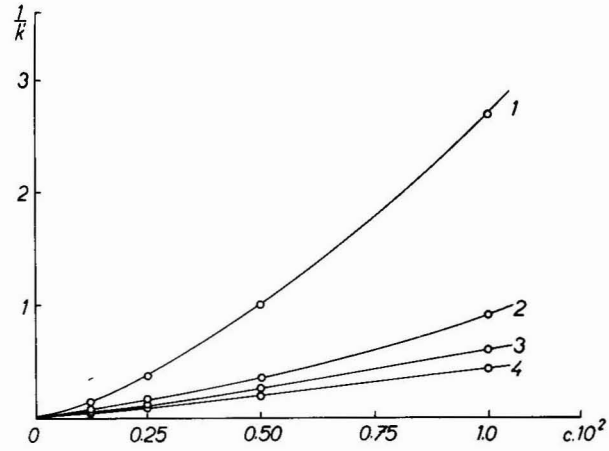

Fig. 2. Reciprocal relationships between capacity ratios (k') of lumisterol (1), tachysterol (2), calciferol (3) and ergosterol (4) and concentration of *n*-propanol (c, vol.-% $\times 10^{-2}$) in *n*-heptane used as the mobile phase in chromatography on LiChrosorb ALOX T. Experimental conditions are given in Table II. The relationships should be linear if eqn. 4 applies.

In ion-exchange chromatography, $n = 1$ is to be expected theoretically, provided that exchange between the monovalent ions takes place. If the charge of the solute ion and/or that of the counter ion differ from unity, then n will differ from unity[2] and eqn. 4 cannot be expected to be followed. Anion-exchange chromatography of guanosine 5′-mono-, di- and triphosphates on Perisorb AN in aqueous solutions of potassium dihydrogen phosphate as the mobile phase[10] represents a practical example of an ion-exchange system in which the solutes have different

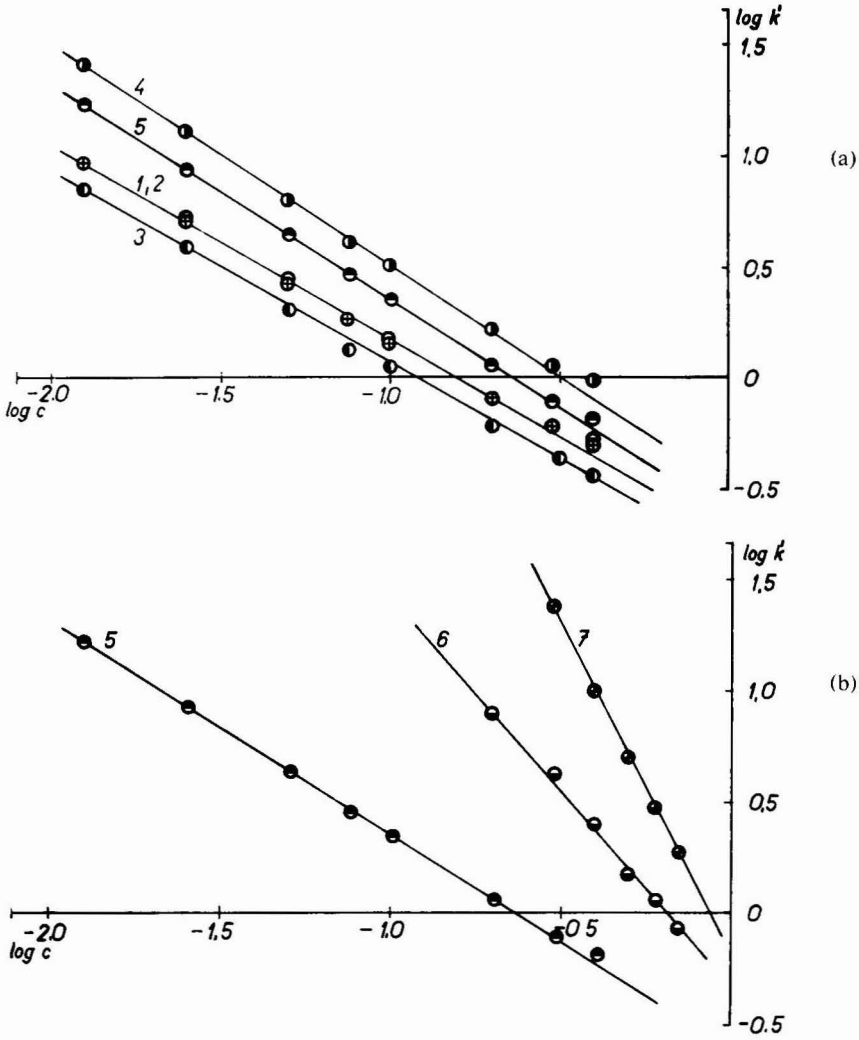

Fig. 3. Logarithmic relationships between capacity ratios (k') of nucleotides and concentration of potassium dihydrogen phosphate (c, molarity) in the mobile phase (aqueous, pH = 3.15) in anion-exchange chromatography on a column (905 × 2.3 mm) packed with Perisorb AN (30–40 μm). Numbers of compounds: (a) 1 = thymidine 5′-monophosphate; 2 = ribothymidine 5′-monophosphate; 3 = deoxyuridine 5′-monophosphate; 4 = deoxyguanosine 5′-monophosphate; 5 = guanosine 5′-monophosphate; (b) 5 = guanosine 5′-monophosphate; 6 = guanosine 5′-diphosphate; 7 = guanosine 5′-triphosphate. The relationships should be linear if eqn. 1 applies.

values of n. The experimental values in this system are very close to those predicted theoretically: 0.96 for monophosphate (theoretical value 1), 1.85 for diphosphate (theoretical value 2) and 3.03 for triphosphate (theoretical value 3). The relationship between log k' and log c (where c is the molarity of potassium dihydrogen phosphate) is plotted in Fig. 3, while Fig. 4 shows the relationship between $1/k'$ and c for the compounds studied. The graphs in Fig. 3 are linear, which shows that eqn. 1 applies well, while those for diphosphate and triphosphate in Fig. 4 are not linear. As would be expected, the plot for monophosphate is linear in the mobile phase that is less than 0.3 M in potassium dihydrogen phosphate. Fig. 4 also shows clearly that the term a in eqn. 4 is very close to zero.

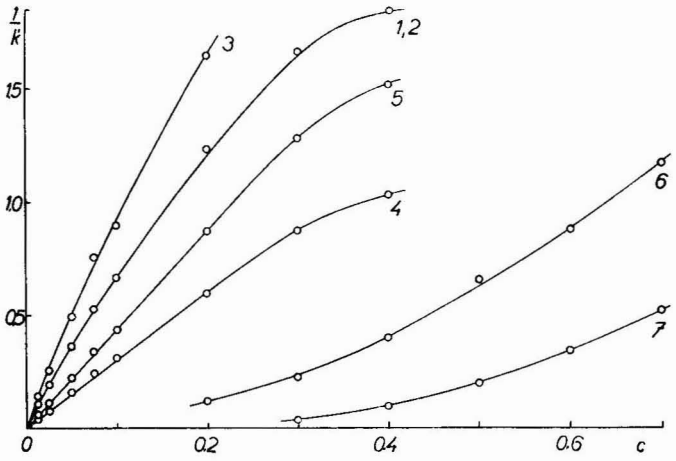

Fig. 4. Relationships between reciprocal of capacity ratios (k') of nucleotides and concentration of potassium dihydrogen phosphate (c, molarity) in the mobile phase (aqueous, pH = 3.15) in chromatography on Perisorb AN. Experimental conditions and compounds as in Fig. 3. The relationships should be linear if eqn. 4 applies.

It can be concluded that the relationship between the capacity ratio and the concentration of the binary mobile phase in adsorption and ion-exchange chromatography can generally be expressed by eqn. 3. If the molecules of the solute are placed on the surface of the column packing material in the same manner as the molecules of the stronger eluting component in the mobile phase (the same area of the adsorbent surface occupied by an adsorbed molecule; the same charge of the exchanging ions in ion-exchange chromatography), the simplified eqn. 4 can be used instead of eqn. 3. It is difficult to predict the chromatographic systems for which this assumption is fulfilled. In systems in which the solutes are strongly retained from the less efficient eluting component of the mobile phase, the term a in eqn. 3 is very close to zero and the simple eqn. 1 is valid. This applies to a number of ion-exchange systems and to the adsorption chromatography of polar compounds on silica or alumina using mobile phases that contain hydrocarbons as the less polar component.

INFLUENCE OF THE COMPOSITION OF THE MOBILE PHASE ON RESOLUTION

Considering the relationship between the capacity ratio, k', and the concentration, c, of the more efficient eluting component in the mobile phase (eqn. 3), we can write the following equations for the retention volume, V_R, peak width, w, and separation factor, $\alpha = V'_{R_2}/V'_{R_1}$:

$$V_R = V_m[1 + (a + bc)^{-n}] \tag{5}$$

$$w = \frac{4V_m}{\sqrt{N}}[1 + (a + bc)^{-n}] \tag{6}$$

and

$$\alpha = \frac{(a_1 + b_1c)^{n_1}}{(a_2 + b_2c)^{n_2}} \tag{7}$$

where the subscripts 1 and 2 relate to compounds 1 and 2, N is the plate number, V_m is the column void volume (the volume of the mobile phase in the column) and the coefficients a and b and the exponent n are experimental constants characteristic of the nature of the adsorbent, the components of the mobile phase and the compound being chromatographed.

The constants a, b and n are related to the capacity ratio in the pure stronger eluting component of the mobile phase, k'_0, and to the capacity ratio in the less efficient component, k'_∞:

$$k'_0 = (a + b)^{-n} \tag{8}$$

and

$$k'_\infty = a^{-n} \tag{8a}$$

Further, eqns. 5–8 a have a real physical meaning if $a \geqslant 0$. As c denotes the concentration of the stronger eluting component in the mobile phase, $k'_\infty > k'_0$ and $b \geqslant 0$; $n \geqslant 0$.

If we accept the commonly used simplified definition of the resolution of two compounds 1 and 2 as

$$R_s = \frac{V_{R_2} - V_{R_1}}{w_2} \tag{9}$$

we can derive the equation for the influence of the composition of the mobile phase on resolution:

$$R_s = \frac{\sqrt{N_2}}{4} \cdot \frac{(a_2 + b_2c)^{-n_2} - (a_1 + b_1c)^{-n_1}}{1 + (a_2 + b_2c)^{-n_2}} \tag{10}$$

which can be expressed in a more illustrative form as

$$R_s = \underset{\text{I}}{\frac{\sqrt{N_2}}{4}} \cdot \underset{\text{II}}{(1 - \alpha^{-1})} \cdot \underset{\text{III}}{\frac{1}{(a_2 + b_2c)^{n_2} + 1}} \tag{10a}$$

Here, three common terms for different contributions to the resolution can be distinguished: I, efficiency; II, selectivity; and III, capacity.

If the number of plates does not depend significantly on the composition of the mobile phase, the concentration of the more efficient component in the mobile phase influences the resolution by means of terms II and III. As the concentration c increases, the capacity term decreases. The selectivity term is minimal (zero) if $\alpha = 1$, and in this instance, no separation of the compounds 1 and 2 occurs. Generally, a composition of the mobile phase can be found, where $\alpha = 1$ and $R_s = 0$, from the following equation:

$$c_{(\alpha=1)} = \frac{(a_2 + b_2 c_{(\alpha=1)})^{\frac{n_2}{n_1}} - a_1}{b_1} \tag{11}$$

From this equation, the concentration c cannot be expressed in an explicit form.

The concentration $c_{(\alpha=1)}$ has a real meaning [$c_{(\alpha=1)} > 0$] if the following condition holds true:

$$a_2{}^{n_2} > a_1{}^{n_1} \tag{11a}$$

If $n_1 \approx n_2$, eqn. 11 can be simplified to the explicit form

$$c_{(\alpha=1)} = \frac{a_2 - a_1}{b_1 - b_2} \qquad (n_1 \approx n_2) \tag{11b}$$

The concentration range of a binary mobile phase can be divided into two parts, with opposite elution sequences of the two compounds. As long as $c < c_{(\alpha=1)}$, the compound with the lower value of the exponent n (if $n_1 = n_2$ and $a_1 \neq 0$ and/or $a_2 \neq 0$, the compound with the lower value of b) is eluted first, while if $c > c_{(\alpha=1)}$ the opposite occurs.

The concentration c always lies in the range between $c = 0$ and $c = c_{mp}$, where c_{mp} is a maximum possible concentration, which is either the pure more efficient eluting component of the mobile phase, or its saturated solution in the less efficient eluting agent. If $c_{(\alpha=1)} < 0$, or $c_{(\alpha=1)} > c_{mp}$, the elution sequence of the two compounds does not change over the whole concentration range. Thus, a reversal of the elution sequence with changing composition of the mobile phase can occur only if the concentration $c_{(\alpha=1)}$ is within practical limits [$0 < c_{(\alpha=1)} < c_{mp}$].

On the other hand, it can be proved that at a certain composition of the mobile phase, the resolution can reach a maximum value. The concentration of the more efficient eluting component in the mobile phase for maximum resolution, c_{max}, can be found by solving the equation

$$dR_s/dc = 0 \tag{12}$$

The equation for c_{max} can be written in the following implicit form:

$$c_{max} = \frac{1}{b_1} \cdot \left\{ \frac{1}{\frac{n_1 b_1}{n_2 b_2} \cdot \frac{(a_2 + b_2 c_{max})}{(a_1 + b_1 c_{max})^{(n_1+1)}} \cdot [1 + (a_2 + b_2 c_{max})^{n_2}] - 1} \right\}^{\frac{1}{n_1}} - \frac{a_1}{b_1} \tag{13}$$

The numbers of compounds in this equation should be chosen so that $n_1 > n_2$, otherwise eqn. 13 yields no solution.

The above conclusions hold true for concentrations $c > c_{(\alpha=1)}$, where the increasing concentration leads to an increase in the selectivity term (II) and to a simultaneous decrease in the capacity term (III). In the concentration range where $c < c_{(\alpha=1)}$, the increase in concentration is followed by a decrease in both the capacity and selectivity terms, so that maximal resolution is achieved for $c = 0$.

Thus, according to the sequence of $c = 0$, c_{max}, $c_{(\alpha=1)}$ and c_{mp}, six different situations can be distinguished. These situations are illustrated by plots of R_s *versus* c in Figs. 5 and 6 and of k' *versus* c in Figs. 7 and 8 (for clarity, the curves are approximated by lines).

(1) $0 < c_{mp} < c_{(\alpha=1)} < c_{max}$. This situation is shown in Figs. 5(1) and 7(1). Over the whole concentration range accessible, the compound with a higher value of n is eluted later than the compound with lower n. The resolution decreases with increasing concentration over the whole concentration range, so that maximal resolution is achieved at $c = 0$.

(2) $0 < c_{(\alpha=1)} < c_{mp} < c_{max}$ [Figs. 5(2) and 7(2)]. The elution sequence is the same as in (1) and the resolution decreases with increasing concentration as long as

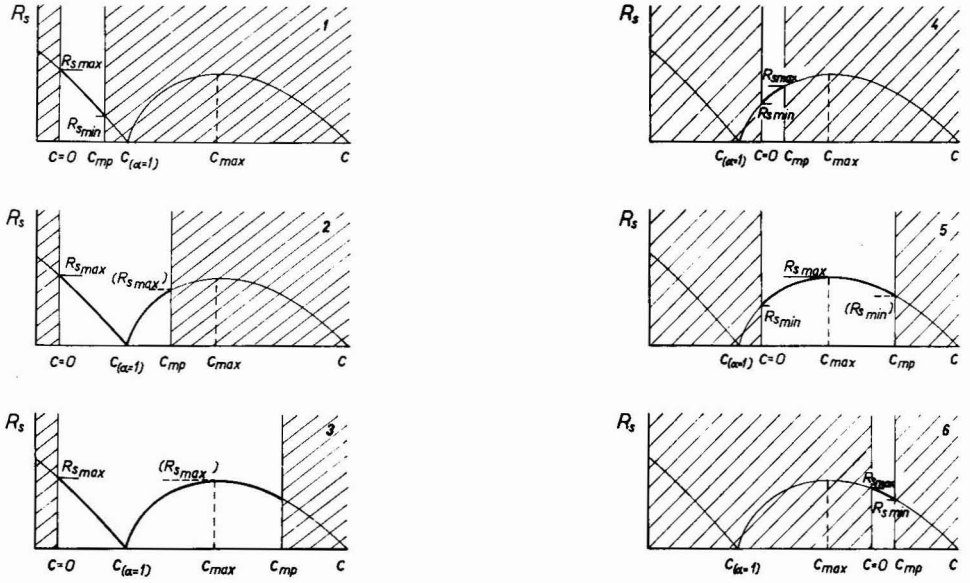

Fig. 5. Representative relationships between resolution (R_s) and concentration (c) of the more efficient eluting agent in the mobile phase. (1) Instance 1, $0 < c_{mp} < c_{(\alpha=1)} < c_{max}$; (2) instance 2, $0 < c_{(\alpha=1)} < c_{mp} < c_{max}$; (3) instance 3, $0 < c_{(\alpha=1)} < c_{max} < c_{mp}$. $c_{(\alpha=1)}$ – Concentration at which $\alpha = 1$; c_{max} = concentration corresponding to the maximum on the R_s *versus* c curve; c_{mp} = maximal practically available concentration; $R_{s\,max}$ = maximal resolution; $R_{s\,min}$ = minimal resolution.

Fig. 6. Representative relationships between resolution (R_s) and concentration (c) of the more efficient eluting agent in mobile phase. (4) Instance 4, $c_{(\alpha=1)} < 0 < c_{mp} < c_{max}$; (5) instance 5, $c_{(\alpha=1)} < 0 < c_{max} < c_{mp}$; (6) instance 6, $c_{(\alpha=1)} < c_{max} < 0 < c_{mp}$. Symbols as in Fig. 5.

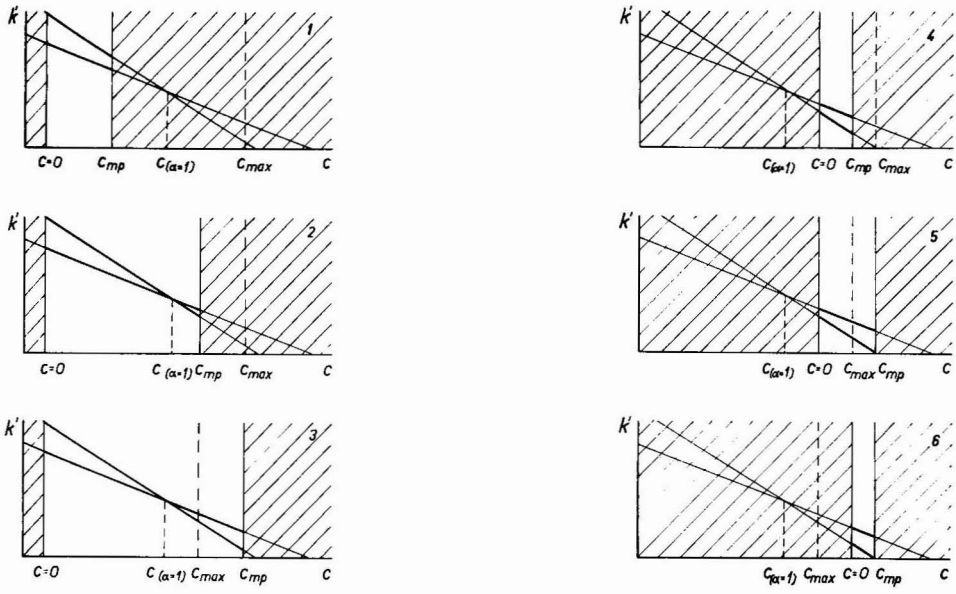

Fig. 7. Representative relationships between capacity ratios (k') and concentration (c) of the more efficient eluting agent in the mobile phase. For clarity, the curves are simplified as lines. (1) instance 1, $0 < c_{mp} < c_{(\alpha=1)} < c_{max}$; (2) instance 2, $0 < c_{(\alpha=1)} < c_{mp} < c_{max}$; (3) instance 3, $0 < c_{(\alpha=1)} < < c_{max} < c_{mp}$. Symbols as in Fig. 5.

Fig. 8. Representative relationships between capacity ratios (k') and concentration (c) of the more efficient eluting agent in the mobile phase. For clarity, the curves are simplified as lines. (4) Instance 4, $c_{(\alpha=1)} < 0 < c_{mp} < c_{max}$; (5) instance 5, $c_{(\alpha=1)} < 0 < c_{max} < c_{mp}$; (6) instance 6, $c_{(\alpha=1)} < c_{max} < < 0 < c_{mp}$. Symbols as in Fig. 5.

$c < c_{(\alpha=1)}$. At $c_{(\alpha=1)}$, $R_s = 0$. For $c > c_{(\alpha=1)}$, the elution sequence reverses (the compound with higher n is eluted first) and the resolution increases with rising concentration up to $c = c_{mp}$. The higher of the two values of the resolution at $c = 0$ and $c = c_{mp}$, respectively, gives the maximal resolution that can be obtained. The speed of chromatographic separation at $c = c_{mp}$ is much higher than that at $c < c_{(\alpha=1)}$.

(3) $0 < c_{(\alpha=1)} < c_{max} < c_{mp}$ [Figs. 5(3) and 7(3)]. This situation is similar to (2), but in the concentration range where $c > c_{(\alpha=1)}$ maximum on the R_s *versus* c curve is achieved. Thus, the resolution decreases from $c = 0$ to $c_{(\alpha=1)}$, where $R_s = 0$, then the elution sequence is reversed and the resolution increases to a maximal value at c_{max}. Increasing the concentration above c_{max} leads to a further decrease in resolution up to c_{mp}. The higher of the two values of the resolution at $c = 0$ and $c = c_{max}$, respectively, gives the maximal resolution that can be obtained. The chromatographic separation at c_{max} is much faster than that at $c < c_{(\alpha=1)}$.

(4) $c_{(\alpha=1)} < 0 < c_{mp} < c_{max}$ [Figs. 6(4) and 8(4)]. The compound with a higher value of n is eluted first over the whole accessible concentration range. The resolution increases with increasing concentration and acquires a maximal value at $c = c_{mp}$.

(5) $c_{(\alpha=1)} < 0 < c_{max} < c_{mp}$ [Figs. 6(5) and 8(5)]. The elution sequence is the same as in (4). The resolution increases with increasing concentration from 0 to

c_{max}, where maximal resolution is achieved. A further increase in concentration above c_{max} leads to a decrease in resolution.

(6) $c_{(\alpha=1)} < c_{max} < 0 < c_{mp}$ [Figs. 6(6) and 8(6)]. The elution sequence is the same as in (4). The resolution decreases with increasing concentration from its maximal value at $c = 0$ to the minimal value at c_{mp}. The decrease in resolution over the whole concentration range is similar to that in (1), but there the elution sequence was reversed in relation to the values of n.

A practical chromatographic system involving the separation of two compounds can easily be attributed to one of the above instances by comparing the known value of c_{mp} with calculated values of $c_{(\alpha=1)}$ (eqn. 11) and c_{max} (eqn. 13). If $c_{(\alpha=1)} < 0$ or $c_{max} < 0$, the eqns. 11 and 13 give no solution (instances 4–6).

The maximal resolution that can be obtained in a given system (or the maximal tolerable ratio $R_s/\sqrt{N}$) can be calculated from eqn. 10 by introducing $c = 0$, $c = c_{max}$ or $c = c_{mp}$. This calculated value of the ratio $R_s/\sqrt{N}$ must not be exceeded, otherwise eqn. 10 yields no solution or no solution with a practical meaning.

The concentration necessary in order to obtain a required resolution can be calculated after rearranging eqn. 10 into the following two forms:

$$c = \frac{1}{b_1} \cdot \left[\left(1 - \frac{4R_s}{\sqrt{N_2}}\right)(a_2 + b_2 c)^{-n_2} - \frac{4R_s}{\sqrt{N_2}} \right]^{-\frac{1}{n_1}} - \frac{a_1}{b_1} \tag{14}$$

and

$$c = \frac{1}{b_2} \cdot \left\{ \frac{\sqrt{N_2}}{4R_s} \left[1 - \frac{(a_2 + b_2 c)^{n_2}}{(a_1 + b_1 c)^{n_1}} \right] - 1 \right\}^{\frac{1}{n_2}} - \frac{a_2}{b_2} \tag{14a}$$

If the compounds are numbered so that $n_1 > n_2$, the solutions of eqns. 14 and 14a give the concentrations for the required R_s at each side from the maximum R_s ($R_{s\,max}$) on the R_s *versus* c curve. Eqns. 14 and 14a cannot be expressed in an explicit form and mathematical solution by an approximation method is required. Eqn. 14 gives the concentration for the required R_s on the lower concentration side from the maximum on the R_s *versus* c curve, while eqn. 14a gives the corresponding concentration higher than c_{max}. The values of the first approximation of concentration used when eqns. 14 and 14a are being solved must be chosen from the appropriate region in order to obtain a solution. Hence the first approximation, c_I, for eqn. 14 should be chosen so that $c_{(\alpha=1)} < c_I \leqslant c_{max}$ and c_I for eqn. 14a should not be lower than c_{max}; $c_I \geqslant c_{max}$.

If we use eqn. 14a with the inverse sequence of the parameters n, *i.e.*, $n_1 < n_2$, we obtain the solution for the left branch of the R_s *versus* c curve [for concentrations lower than $c_{(\alpha=1)}$]. Here again, the first approximation c_I should be chosen so that $0 < c_I < c_{(\alpha=1)}$.

In all calculations using eqns. 14 and 14a, care must be taken that the value of $R_s/\sqrt{N_2}$ does not fall outside the range limited by the minimal and maximal values given by concentrations $c = 0$, c_{max} and c_{mp} (this range should be considered individually in each of the instances 1–6).

In some instances, when the numbers of plates for the two compounds 1 and 2

being chromatographed differ considerably, the simplified definition of resolution according to eqn. 9 may no longer be satisfactory and a more rigorous equation for resolution should be considered:

$$R_s = 2 \cdot \frac{V_{R_2} - V_{R_1}}{w_2 + w_1} \tag{15}$$

Introducing eqn. 5, we can derive the relationship between resolution and the concentration of the more efficient eluting agent in the mobile phase in the following form:

$$R_s = \frac{(a_2 + b_2c)^{-n_2} - (a_1 + b_1c)^{-n_1}}{2\,[N_2^{-\frac{1}{2}} + N_2^{-\frac{1}{2}}(a_2 + b_2c)^{-n_2} + N_1^{-\frac{1}{2}} + N_1^{-\frac{1}{2}}(a_1 + b_1c)^{-n_1}]} \tag{16}$$

It can be shown that eqn. 11 for $c_{(\alpha=1)}$ and eqn. 13 for $c_{\max}$ apply in this instance as well as for the simplified definition of resolution. All of the other considerations and conclusions also remain valid, only eqns. 14 and 14a for the concentration at which a required resolution can be achieved acquire somewhat altered forms; eqn. 17 must be used instead of eqn. 14 and eqn. 17a instead of eqn. 14a:

$$c = \frac{1}{b_1}\left[\frac{1 + \frac{2R_s}{\sqrt{N_1}}}{(a_2 + b_2c)^{-n_2}\left(1 - \frac{2R_s}{\sqrt{N_2}}\right) - 2R_s\left(\frac{1}{\sqrt{N_2}} + \frac{1}{\sqrt{N_1}}\right)}\right]^{\frac{1}{n_1}} - \frac{a_1}{b_1} \tag{17}$$

and

$$c = \frac{1}{b_2}\left[\frac{1 - \frac{2R_s}{\sqrt{N_2}}}{(a_1 + b_1c)^{-n_1}\left(1 + \frac{2R_s}{\sqrt{N_1}}\right) + 2R_s\left(\frac{1}{\sqrt{N_2}} + \frac{1}{\sqrt{N_1}}\right)}\right]^{\frac{1}{n_2}} - \frac{a_2}{b_2} \tag{17a}$$

If the compounds are very strongly retained on the column in the mobile phase containing only the pure less efficient eluting agent, then a in eqn. 3 is close to zero and can be neglected. Then, eqn. 1 can be used to describe the relationship between the capacity ratio, k', and the concentration, c, of the more efficient eluting agent in the mobile phase. Taking into account the simplified definition of resolution (eqn. 9), we can write the relationship between resolution, R_s, and concentration, c, in the following form:

$$R_s = \frac{\sqrt{N_2}}{4} \cdot \frac{k'_{02}c^{-n_2} - k'_{01}c^{-n_1}}{1 + k'_{02}c^{-n_2}} \tag{18}$$

or, after rearrangement:

$$R_s = \underset{\text{I}}{\frac{\sqrt{N_2}}{4}} \cdot \underset{\text{II}}{(1 - \alpha^{-1})} \cdot \underset{\text{III}}{\frac{k'_{02}}{k'_{02} + c^{n_2}}} \tag{18a}$$

where

$$\alpha = \frac{k'_{02}}{k'_{01}} \cdot c^{(n_1 - n_2)} = \alpha_0 c^{(n_1 - n_2)} \tag{19}$$

and terms I (efficiency), II (selectivity) and III (capacity) are as in eqn. 10a.

All of the considerations concerning the influence of concentration on resolution remain unchanged, except that the equations for $c_{(\alpha=1)}$ and c_{max} acquire the following forms:

$$c_{(\alpha=1)} = \alpha_0^{\frac{1}{n_2 - n_1}} \tag{20}$$

and

$$c_{max} = \left(\alpha_0^{-1} \cdot \frac{n_1}{n_2} \cdot c_{max}^{n_2} + k'_{01} \cdot \frac{n_1 - n_2}{n_2} \right)^{\frac{1}{n_1}} \tag{21}$$

Eqn. 21 must be solved by an approximation method.

The two compounds are very strongly retained on the column if $c = 0$, and therefore the resolution at $c = 0$ has no practical meaning. To calculate the maximal practical value of the resolution on the lower concentration side from $c_{(\alpha=1)}$ of the R_s *versus* c curve, the resolution (and the minimal practical concentration) must be calculated on the basis of the maximal value of k' ($k' = 20$, for instance) which can be allowed considering the time of analysis.

The values of k' for the two compounds become extremely large as the concentration c is decreased to zero ($k'_1 \to \infty$, $k'_2 \to \infty$). Hence any intersection of the two $\log k' = f(\log c)$ lines must be found in the region where $c \geqslant 0$. In this instance, the number of different situations is limited to the instances 1–3 (see above discussion and Figs. 5–8), as the situations shown in instances 4–6 are not possible.

The concentration necessary in order to obtain a required resolution can be calculated from eqns. 22 [$c_{(\alpha=1)} < c < c_{max}$] and 22a ($c > c_{max}$) if $n_1 > n_2$, and from eqn. 22a [$c < c_{(\alpha=1)}$] if $n_2 > n_1$:

$$c = \left[\left(1 - \frac{4R_s}{\sqrt{N_2}} \cdot \frac{k'_{02} + c^{n_2}}{k'_{02}} \right) \alpha_0 \right]^{\frac{1}{n_2 - n_1}} \tag{22}$$

$$c = \left\{ \left[\frac{\sqrt{N_2}}{4R_s} (1 - \alpha_0^{-1} c^{(n_2 - n_1)}) - 1 \right] k'_{02} \right\}^{\frac{1}{n_2}} \tag{22a}$$

If the more correct definition equation for R_s is considered (eqn. 15), then eqns. 22 and 22a acquire the following forms:

$$c = \left[\frac{k'_{01} \left(1 + \frac{2R_s}{\sqrt{N_1}} \right)}{c^{-n_2} k'_{02} \left(1 - \frac{2R_s}{\sqrt{N_2}} \right)} - \frac{}{- 2R_s \left(\frac{1}{\sqrt{N_2}} + \frac{1}{\sqrt{N_1}} \right)} \right]^{\frac{1}{n_1}} \tag{23}$$

and

$$c = \left[\frac{k'_{02}\left(1 - \frac{2R_s}{\sqrt{N_2}}\right)}{c^{-n_1}k'_{01}\left(1 + \frac{2R_s}{\sqrt{N_2}}\right) + 2R_s\left(\frac{1}{\sqrt{N_2}} + \frac{1}{\sqrt{N_1}}\right)} \right]^{\frac{1}{n_2}} \tag{23a}$$

Assuming that eqn. 1 applies and the two parameters n are close one to another ($n_1 \approx n_2 \approx n$), the separation factor, α, does not depend on concentration:

$$\alpha = \frac{k'_{02}}{k'_{01}} = \alpha_0 \tag{24}$$

and the equation for resolution is further simplified:

$$R_s = \underset{\text{I}}{\frac{\sqrt{N_2}}{4}} \cdot \underset{\text{II}}{(1 - \alpha_0^{-1})} \cdot \underset{\text{III}}{\frac{k'_{02}}{k'_{02} + c^{n_2}}} \tag{25}$$

Here, the selectivity term II is constant and a change in concentration can influence the resolution by means of the capacity term III only. In this situation, no intersection of the two lines $\log k'_2 = \mathrm{f}(\log c)$ and $\log k'_1 = \mathrm{f}(\log c)$ can be found in the whole concentration range and the elution sequence is given by the sequence of the values of k'_0. Hence, the compound with a larger k'_0 value is eluted later and should have the subscript 2 ($k'_{02} > k'_{01}$). The resolution decreases with increasing concentration over the whole concentration range from the maximal value at $c = 0$ to the minimal value at c_{mp}, as in instance 1. (Fig. 5); the two parallel lines $\log k' = \mathrm{f}(\log c)$ also decrease with increasing concentration. The concentration necessary in order to obtain a required resolution can be calculated by solving the following equation, which is expressed in an explicit form:

$$c = \left\{ \frac{\sqrt{N_2}}{4R_s}\left[k'_{02}\left(1 - \frac{4R_s}{\sqrt{N_2}}\right) - k'_{01}\right] \right\}^{\frac{1}{n}} \tag{26}$$

[the maximal value of $R_s/\sqrt{N_2}$ must not exceed $(k'_{02} - k'_{01})/4\,k'_{02}$].

Considering the more correct definition of R_s (eqn. 15), eqn. 26 acquires the form:

$$c = \left[\frac{k'_{02} - k'_{01} - 2R_s\left(\frac{k'_{01}}{\sqrt{N_1}} + \frac{k'_{02}}{\sqrt{N_2}}\right)}{2R_s\left(\frac{1}{\sqrt{N_1}} + \frac{1}{\sqrt{N_2}}\right)} \right]^{\frac{1}{n}} \tag{27}$$

In all of the above relationships and derivations, the number of theoretical plates, N, is assumed not to depend on the composition of the mobile phase. This condition may not be strictly true and the number of plates can depend to some

extent on the capacity ratios of sample compounds. If the form and the constants of the relationship between N and k' are known, this relationship can be introduced into the above equations instead of a constant value of N. Thus, if a linear relationship between the number of plates and capacity ratio of compounds to be separated can be accepted[5], such as

$$N = C + Dk' = C + D(a + bc)^{-n} \tag{28}$$

eqn. 28 can be used for substituting N. This approach leads to more complex forms of the above derived equations; however, this is not a serious drawback if we consider that the solution is to be made by some approximation method in any case.

PRACTICAL EXAMPLES

A few practical examples will be given in order to demonstrate the applicability of the above theoretical considerations.

The first example[11] is the separation of 3-chloro-5-nitro-4-hydroxydiphenyl (compound A) and 2-fluorophenol (compound B) on a 904 × 2.3 mm column packed with Porasil A (37–75 μm), using mixtures of *n*-propanol and *n*-heptane as the mobile phase. The conditions of separation are given in Table I, together with experimentally found values of k'_0 and n. The two compounds are so strongly retained in pure *n*-heptane that $a_1 \approx a_2 \approx 0$ and eqn. 1 applies. The number of theoretical plates for the two compounds does not change significantly with concentration. In this system, $c_{mp} = 1$ (pure *n*-propanol), $c_{(\alpha=1)} = 0.0278$ (calculated from eqn. 20) and $c_{max} = 1.7415$ (calculated from eqn. 21). Hence $0 < c_{(\alpha=1)} < c_{mp} < c_{max}$, which corresponds to instance 2. In mobile phases that contain less than 2.78 vol.-% of *n*-propanol, compound A is eluted first, while the elution sequence is reversed in mobile phases that contain higher amounts of *n*-propanol. The resolution $R_s = 1.0$ can be obtained at two different concentrations, $c_1 = 0.0197$ and $c_2 = 0.0413$, as calculated from eqns. 22 and 22a, respectively. The experimental and calculated

TABLE I

EXPERIMENTAL PARAMETERS n, k'_0 AND N, CALCULATED VALUES OF IMPORTANT CONCENTRATIONS OF *n*-PROPANOL IN *n*-HEPTANE AND CORRESPONDING RESOLUTION AND OTHER RETENTION CHARACTERISTICS IN CHROMATOGRAPHY OF 3-CHLORO-5-NITRO-4-HYDROXYDIPHENYL (COMPOUND A) AND 2-FLUOROPHENOL (COMPOUND B) ON A COLUMN PACKED WITH PORASIL A, 37–75 μm (904 × 2.3 mm; $V_m = 3.05$ ml)

Conditions: flow-rate of mobile phase, 1.07 ml/min; pressure, 2.5 MPa; instrument, Waters ALC-100; detection, UV (254 nm). $n_A = 0.045$; $k'_{0A} = 1.206$; $N_A \approx 500$; $n_B = 0.968$; $k'_{0B} = 0.0441$; $N_B \approx 500$. Instance 2; $0 < c_{(\alpha=1)} < c_{mp} < c_{max}$.

c (vol. % × 10^{-2})	$R_{s_{A,B}}$	V_{R_A} (ml)	V_{R_B} (ml)	w_A (ml)	w_B (ml)
0.0197	1.000	7.43	9.05	1.33	1.62
0.0278 [$c_{(\alpha=1)}$]	0.000	7.37	7.37	1.32	1.32
0.0413	1.000	7.29	5.99	1.30	1.07
1.0000 (c_{mp})	2.94	6.72	3.18	1.20	0.57
1.7415 (c_{max})	2.955	—	—	—	—

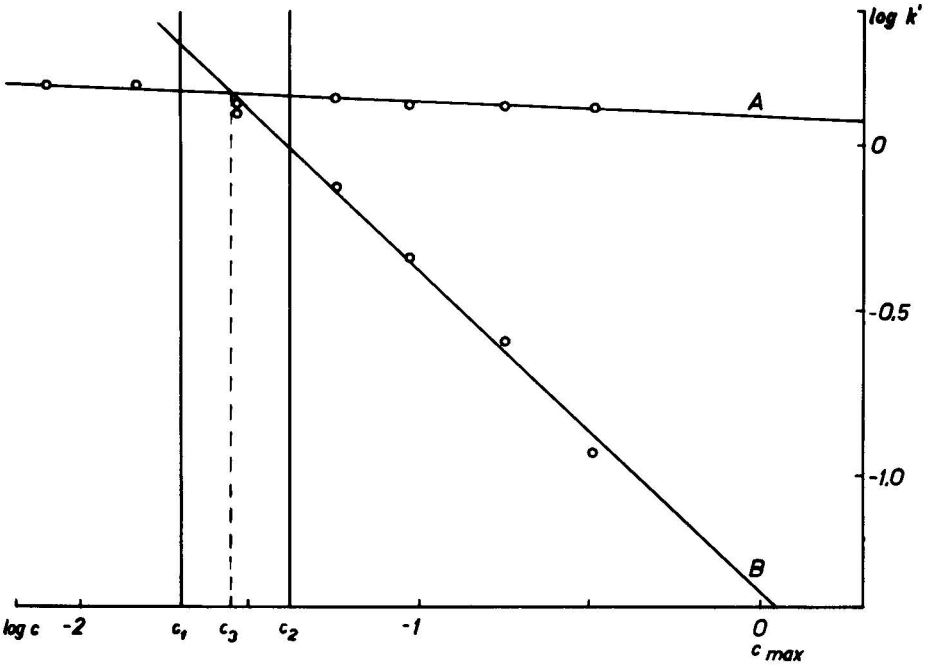

Fig. 9. Relationship between capacity ratios (k') of 3-chloro-5-nitro-4-hydroxydiphenyl (A) and 2-fluorophenol (B) and concentration (c, vol.-% $\times$ 10^{-2}) of n-propanol in n-heptane used as the mobile phase. The points represent experimental values; the lines were evaluated using linear regression analysis. Operating conditions as in Table I.

plots of log k' *versus* log c for compounds A and B are shown in Fig. 9, together with concentrations c_1, c_2 and $c_3 = c_{(\alpha=1)}$.

The second example concerns the chromatography of the steroids compounds[9] lumisterol (compound A) and tachysterol (compound B) on a column packed with LiChrosorb ALOX T alumina (20 μm), also in a mobile phase composed of n-heptane and n-propanol, with a resolution $R_s = 1.5$. Here $a_1 \approx a_2 \approx 0$ and eqn. 1 again applies. The number of theoretical plates does not change significantly with variation in the composition of the mobile phase. The conditions of separation are given in Table II, together with experimentally found values of n and k'_0 for compounds A and B. Here, $c_{mp} = 1$ (pure n-propanol), $c_{(\alpha=1)} = 0.00002$ (calculated from eqn. 20) and $c_{max} = 0.00206$ (calculated from eqn. 21). Hence $0 < c_{(\alpha=1)} < c_{max} < c_{mp}$, which corresponds to instance 3. The resolution $R_s = 1.5$ cannot be achieved for $c < c_{(\alpha=1)}$ and the elution sequence where tachysterol is eluted ahead of lumisterol is not practical owing to extremely large retention volumes. $R_s = 1.5$ can be achieved at two concentrations (one on each side of the maximum on the R_s *versus* c curve), which are calculated from eqns. 22 and 22a: $c_1 = 0.00078$ and $c_2 = 0.00206$. Other retention characteristics under these conditions are given in Table II. The R_s *versus* c curve is plotted in Fig. 10 as the curve for $R_{s_{1,2}}$ (the curve is calculated on basis of the values of n_A, n_B, k'_{0A}, k'_{0B} and N_B; the experimental values of R_s are plotted as points).

In the third example, tachysterol and calciferol are to be separated with a

TABLE II

EXPERIMENTAL PARAMETERS n, k' AND N, CALCULATED VALUES OF IMPORTANT CONCENTRATIONS OF n-PROPANOL IN n-HEPTANE AND CORRESPONDING RESOLUTION AND OTHER RETENTION CHARACTERISTICS IN CHROMATOGRAPHY OF LUMISTEROL (COMPOUND A) AND TACHYSTEROL (COMPOUND B) ON A COLUMN PACKED WITH LICHROSORB ALOX T, 30 μm (596 × 2.3 mm; V_m = 2.30 ml).

Conditions: flow-rate of mobile phase, 1.93 ml/min; pressure, 5.0 MPa; instrument, Waters ALC-100; detection, UV (254 nm). n_A = 1.463; k'_{0A} = 0.000428; N_A = 131; n_B = 1.284; k'_{0B} = 0.00298; N_B = 165. Instance 3; $0 < c_{(\alpha=1)} < c_{max} < c_{mp}$.

c (vol. % × 10^{-2})	$R_{s_{A,B}}$	V_{R_A} (ml)	V_{R_B} (ml)	w_A (ml)	w_B (ml)
0.0000195 [$c_{(\alpha=1)}$]	0.000	7653	7653	2675	2386
0.000783	1.500	36.78	69.09	12.85	21.54
0.002064 (c_{max})	1.622	10.65	21.54	3.72	6.72
0.004596	1.500	4.89	9.18	1.71	2.86
1.0000 (c_{mp})	0.008	2.30	2.31	0.80	0.72

resolution R_s = 1.0 under the same conditions (column, mobile phase, flow-rate) as in the second example. Here again, $a_1 \approx a_2 \approx 0$ and eqn. 1 applies. The conditions of separation and the parameters necessary for calculations are given in Table III. The calculated values are $c_{(\alpha=1)}$ = 0.00013 (eqn. 20) and c_{max} = 0.0047 (eqn. 21); c_{mp} = 1 and $0 < c_{(\alpha=1)} < c_{max} < c_{mp}$, which is again the situation referred to in instance 3, as in the second example. The maximal resolution that can be obtained at c_{max} is 0.769 [operation at $c < c_{(\alpha=1)}$ involves extremely long retention times and is not practical] and therefore the required resolution cannot be achieved with the plate number given in the conditions of the experiments. If a resolution R_s = 0.75 is accepted, this resolution is achieved at c_1 = 0.00308 and c_2 = 0.00701 (eqns. 22

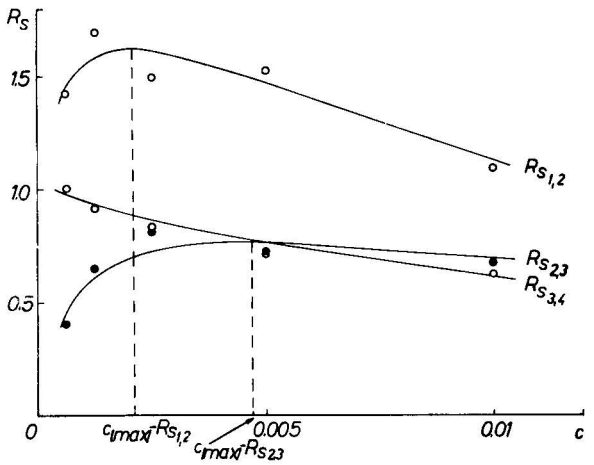

Fig. 10. Relationships between resolution (R_s; defined by eqn. 9) of steroids and concentration (c, vol.-% × 10^{-2}) of n-propanol in n-heptane used as the mobile phase. $R_{s_{1,2}}$ = resolution of lumisterol and tachysterol; $R_{s_{2,3}}$ = resolution of tachysterol and calciferol; $R_{s_{3,4}}$ = resolution of calciferol and ergosterol; c_{max} = concentration corresponding to the maximum on the R_s *versus* c curve. The points represent experimental values; the curves were calculated from the parameters n_A, n_B, k'_{0A}, k'_{0B}, N_A and N_B (eqn. 18a). Operating conditions as in Table II.

and 22a). Hence in the concentration range from 0.3 to 0.7% of *n*-propanol, the resolution does not change significantly and is near to the maximal value. The corresponding R_s *versus* c curve is plotted in Fig. 10 as the curve for $R_{s2,3}$ and the calculated retention characteristics are given in Table III.

TABLE III

EXPERIMENTAL PARAMETERS n, k' AND N, CALCULATED VALUES OF IMPORTANT CONCENTRATIONS OF *n*-PROPANOL IN *n*-HEPTANE AND CORRESPONDING RESOLUTION AND OTHER RETENTION CHARACTERISTICS IN CHROMATOGRAPHY OF TACHYSTEROL (COMPOUND A) AND CALCIFEROL (COMPOUND B) ON A COLUMN PACKED WITH LICHROSORB ALOX T.

Operating conditions as in Table II. $n_A = 1.284$; $k'_{0A} = 0.00298$; $N_A = 165$; $n_B = 1.189$; $k'_{0B} = 0.00698$; $N_B = 175$. Instance 3, $0 < c_{(\alpha=1)} < c_{max} < c_{mp}$.

c (vol. % × 10^{-2})	$R_{s_{A,B}}$	V_{R_A} (ml)	V_{R_B} (ml)	w_A (ml)	w_B (ml)
0.0001289 ($c_{(\alpha=1)}$)	0.000	679.4	679.4	211.8	205.4
0.003082	0.750	13.80	17.85	4.30	5.40
0.004697 (c_{max})	0.769	8.99	11.72	2.80	3.54
0.007007	0.750	6.30	8.15	1.96	2.46
1.0000 (c_{mp})	0.013	2.31	2.32	0.72	0.70

The last example concerns the separation of calciferol and ergosterol under the same conditions as in the two preceding examples. The parameters $a_1 \approx a_2 \approx 0$ and calculations based on eqn. 1 were used. The conditions of separation and the parameters necessary for the calculations are given in Table IV. Eqn. 20 yielded the concentration $c_{(\alpha=1)} = 1{,}070{,}600$ and thus it was not necessary to calculate c_{max}. Here, $0 < c_{mp} < c_{(\alpha=1)} < c_{max}$, which is the situation in the instance 1. The resolution decreases with increasing concentration over the whole concentration range, as is shown in Fig. 10 (curve for $R_{s3,4}$). Thus, $R_s = 0.75$ can be achieved at $c = 0.00536$.

If the four compounds lumisterol, tachysterol, calciferol and ergosterol are to be separated on the same column packed with LiChrosorb ALOX T, the optimal composition of the mobile phase can be chosen on basis of the above calculated values. The resolution of lumisterol and tachysterol is higher than that of tachysterol and calciferol and that of calciferol and ergosterol over the whole practical concentration range and, as the first two compounds are eluted first, their separation does not need

TABLE IV

EXPERIMENTAL PARAMETERS n, k'_0 AND N, CALCULATED VALUES OF IMPORTANT CONCENTRATIONS OF *n*-PROPANOL IN *n*-HEPTANE AND CORRESPONDING RESOLUTION AND OTHER RETENTION CHARACTERISTICS IN CHROMATOGRAPHY OF CALCIFEROL (COMPOUND A) AND ERGOSTEROL (COMPOUND B) ON A COLUMN PACKED WITH LICHROSORB ALOX T

Operating conditions as in Table II. $n_A = 1.189$; $k'_{0A} = 0.00698$; $N_A = 175$; $n_B = 1.205$; $k'_{0B} = 0.00872$; $N_B = 190$. Instance 1, $0 < c_{mp} < c_{(\alpha=1)} < c_{max}$.

c (vol. % × 10^{-2})	$R_{s_{A,B}}$	V_{R_A} (ml)	V_{R_B} (ml)	w_A (ml)	w_B (ml)
0.005362	0.750	10.34	13.22	3.13	3.84
1.0000 (c_{mp})	0.006	2.32	2.32	0.70	0.67
1,070 600 [$c_{(\alpha=1)}$]	0.000	–	–	–	–

to be considered. The resolution of tachysterol and calciferol is in the range 0.75–0.77 for concentrations of 0.3–0.7 vol.-%. The same resolution of calciferol and ergosterol can be achieved at $c = 0.005$. This concentration, *i.e.*, 0.5% *n*-propanol in *n*-heptane, is acceptable for separation, as the same resolution is achieved for the last three eluted compounds. To increase the resolution, a longer column or a lower flow-rate of the mobile phase should be used. Fig. 11 shows the separation of a mixture containing lumisterol (3), tachysterol (5) and calciferol (6) in 0.5% (A), 0.25% (B) and 0.125% *n*-propanol (C) in *n*-heptane. The improved resolution of compounds 5 and 6' and the impaired resolution of compounds 3 and 5 with increasing concentration of *n*-propanol in the mobile phase is clearly demonstrated (for comparison, see Fig. 10).

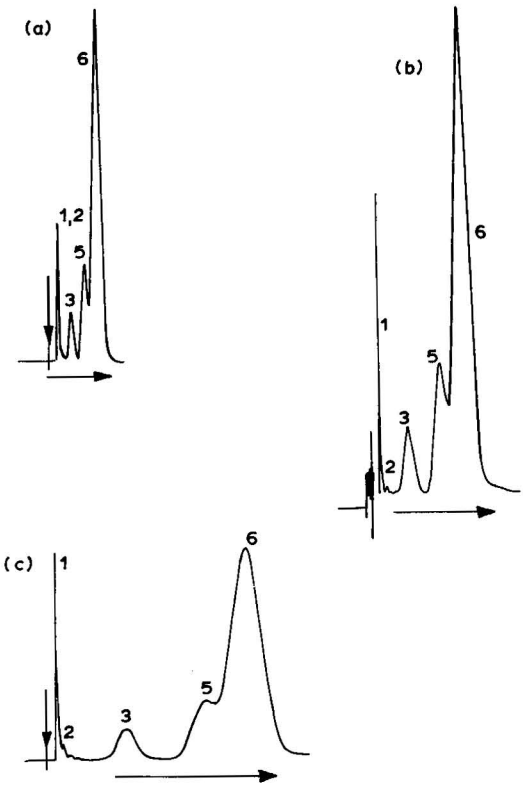

Fig. 11. Chromatographic separation of a mixture containing lumisterol (3; *ca.* 5 μg), tachysterol (5; *ca.* 8 μg) and calciferol (6; *ca.* 30 μg) on LiChrosorb ALOX T in a mobile phase containing different concentrations of *n*-propanol in *n*-heptane (A, 0.5 vol.-%; B, 0.25 vol.-%; C, 0.125 vol.-%). Compounds 1 and 2 are impurities. Flow-rate of mobile phase, 1.93 ml/min; chart speed, 2.5 mm/min; detector sensitivity, 0.64 a.u.f.s. (A) and 0.32 a.u.f.s. (B and C). Other conditions as in Table II.

CONCLUSIONS

It has been demonstrated that the experimentally found dependence of the resolution of two compounds on the concentration of the more efficient eluting agent in the mobile phase can acquire various shapes in the practically available concentration

range. Depending on the values of the parameters a, b (or k_0') and n, different sequences of four important concentrations occur, according to which the R_s *versus* c curve may be descending or ascending or may have a maximum or a minimum. These four important concentrations are as follows: $c = 0$; $c_{(\alpha=1)}$, the concentration at which $\alpha = 1$; c_{max}, the concentration at which the maximum on the R_s *versus* c curve is reached; and c_{mp}, the highest practically available concentration. These concentrations and the corresponding resolution should be calculated prior to any further theoretical predictions of the influence of c on R_s. The methods of calculation differ, depending on whether $a = 0$ for $a \neq 0$ and $n_1 \neq n_2$ or $n_1 = n_2$. If the required resolution is within the practically allowed limits ($R_{s\,min} < R_s < R_{s\,max}$), it is possible to calculate the concentration (or concentrations) at which it can be reached. In the chromatography of a multicomponent mixture, comparison of the concentration regions in which the resolution of two neighbouring compounds is achieved can lead to a rational choice of the composition of the mobile phase, which permits good separations in a reasonable time.

REFERENCES

1 L. R. Snyder and D. L. Saunders, *J. Chromatogr. Sci.*, 7 (1969) 195.
2 P. Jandera and J. Churáček, *J. Chromatogr.*, 91 (1974) 207.
3 P. Jandera and J. Churáček, *J. Chromatogr.*, 93 (1974) 17.
4 P. Jandera and J. Churáček, *J. Chromatogr.*, 104 (1975) 257.
5 P. Jandera, M. Janderová and J. Churáček, *J. Chromatogr.*, 115 (1975) 9.
6 P. Jandera and J. Churáček, in preparation.
7 L. R. Snyder, *Principles of Adsorption Chromatography*, Marcel Dekker, New York, 1968.
8 R. P. W. Scott, *J. Chromatogr.*, 122 (1976) 35.
9 P. Jandera, M. Janderová and J. Churáček, in preparation.
10 J. Churáček, P. Jandera, M. Janderová and F. Všianský, in preparation.
11 P. Jandera, J. Churáček, M. Janderová and M. Zdvihal, in preparation.

Journal of Chromatography, 148 (1978) 99–110

CHROM. 10,402

GENERATION OF ELECTRICITY IN LOW-CONDUCTIVITY LIQUIDS AS A DETECTION PRINCIPLE IN LIQUID CHROMATOGRAPHY

K. ŠLAIS and M. KREJČÍ

Institute of Analytical Chemistry, Czechoslovak Academy of Sciences, 662 28 Brno (Czechoslovakia)

SUMMARY

A detection principle is described that is based on the measurement of streaming current. Relationships are presented that describe the generation of electricity in low-conductivity liquids during their flow through a capillary or a porous bed. By virtue of the theory of an electrical double layer, the dependence of the magnitude of the electrical current transported by the liquid on the composition of the mobile phase and the nature of the phase interface is derived. The response, *i.e.*, the electrical current, has the character of a mass-sensitive response. The detection principle is non-selective and non-destructive.

INTRODUCTION

Despite the rapid development of instrumentation associated with liquid chromatography in recent years, the detector still remains a limiting factor in the utilization of this method for trace analysis. In most instances the sensitivity of liquid chromatographic detectors still does not reach that usual in gas chromatography. Mostly it is the stability of temperature, such as with refractive index detectors, or the requirement of a small volume of the measuring cell, such as with spectrophotometric detectors, that sets limits to further increases in the sensitivity of the present detectors.

We have employed a detection principle which is new in chromatography, *viz.*, the measurement of streaming currents in capillaries, orifices or adsorption beds[1]. After the phenomenon has been mastered theoretically with respect to the conditions of liquid chromatography, the principle may have some promise, especially owing to the great variability of the detection system (sorption surface–mobile phase), the technical simplicity of the design and electronics, and, in some instances, its high sensitivity and small contribution to zone spreading.

THEORETICAL

A streaming current is produced by the transport of a liquid that possesses an electrical charge. As a result of sorption equilibrium, a difference in the solute concentrations in the liquid phase and the interface boundary is established. At the same

time, there is also established a difference in the concentrations of charged particles, *i.e.*, ions, so that the liquid and the interface boundary carry electrical charges of opposite signs. The distribution of charge about the interface boundary can be described by virtue of the theory of an electrical double layer, with regard to the special properties of liquids of low conductivity and low dielectric constant. According to contemporary concepts[2–6], the dependence of the potential in a liquid on the distance from the boundary can be characterized schematically as shown in Fig. 1. On contacting a surface that has a potential φ_s with a liquid, the adsorption of potential-determining ions or dissociation of surface groups leads to a change in the potential to a value φ_0. According to Stern's assumptions[7], on such a modified surface ions and molecules are adsorbed owing to non-electrostatic forces (forces of specific adsorption), to form an immobile part of the electrical double layer. This part of the double layer can be considered as a plane condenser of a thickness d constituting the distance between the surface and the plane of the centres of ions occurring closest to the surface. The potential of the outer side of this layer is usually denoted by φ_d. Behind this plane there is usually considered a share plane behind which the liquid is allowed to move relative to the interface boundary. The potential at this plane is usually called the ζ potential.

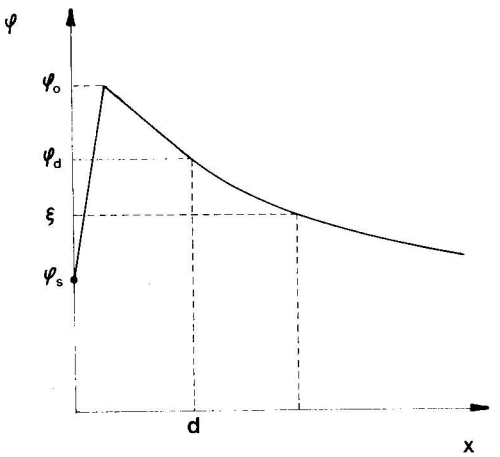

Fig. 1. Variation of potential with the distance from the surface. For symbols, see text.

The components of the liquid that occurs at a distance greater than d from the surface are influenced by electrostatic forces only. In dilute solutions of electrolytes, for calculating the distribution of potential or charge within this region of the liquid it is possible to apply the Gouy–Chapman theory of the diffusion part of electrical double layer[8,9]. The calculation is based on the equilibrium of diffusional and conductive charge fluxes between the boundary and the electrolyte. By solving the so-called linearized Poisson–Boltzman equation[10–12], we obtain the dependence of the course of the potential in a liquid on the distance from the plane surface in the form

$$\varphi = \varphi_d \exp(-\kappa x) \tag{1}$$

where $\kappa^{-1} = \sqrt{D\tau}$ is the so-called Debye–Hückel thickness of the ionic atmosphere, $\tau = \varepsilon/\varkappa$ is the relaxation time of the liquid, ε and $\varkappa$ being the permittivity and conductivity of the liquid and D being the diffusion coefficient of ions in the liquid. In the further treatment, we shall consider liquids with conductivities of $\varkappa < 10^{-9}\ \Omega^{-1}\cdot m^{-1}$ and relative permittivities of $\varepsilon_r < 5$. For these cases we have relaxation times $\tau > 10^{-2}$ sec and the parameter $\kappa^{-1} > 10\ \mu m$. As the plane at which we consider that $\varphi = \zeta$ is much closer than 10 μm to the surface, it is possible to introduce[13,14], with sufficient precision, $\zeta = \varphi_d$ and/or $\zeta = \varphi_0$ if specific adsorption does not occur in the system.

On solving the linearized Poisson–Boltzman equation for a liquid in a capillary of radius a, we obtain for the dependence of the potential on the distance r from the centre of the capillary[15 17]

$$\varphi = \varphi_d \cdot \frac{I_0(\kappa r)}{I_0(\kappa a)} \tag{2}$$

As it is possible to employ the Debye approximation[10,18] for the liquid considered, the relationship between the volume density of charge at the surface, q_s, and φ_d can be expressed as

$$q_s = \frac{2\,C_0F^2}{RT} \cdot \varphi_d \tag{3}$$

On introducing a mean density of charge by[15,17]

$$q_{av} = \frac{2\pi \int_0^a q\, r\, dr}{\pi a^2} \tag{4}$$

the dependence of the distribution of charge in the cross-sectional plane of the capillary on the distance from the centre of the capillary can be expressed as[15]

$$q/q_{av} = \frac{\kappa a}{2} \cdot \frac{I_0(\kappa r)}{I_1(\kappa a)} \tag{5}$$

The dependence is illustrated in Fig. 2. It can be seen that for $\kappa a < 0.3$ the charge in the capillary can be considered, with a precision better than 5%, to be distributed uniformly over the cross-sectional plane[15,17].

The above derivation of the distribution of charge density in a liquid applies to the case of a liquid which does not move. For liquids that are moving, it is necessary to consider the charge transfer brought about by diffusion, conductivity, convection and surface reaction[16,19,20]. For a uni–univalent electrolyte, the cations and anions of which have the same diffusivities, the charge transfer is described by the equation

$$j = -D \bigtriangledown q - \varkappa \bigtriangledown \varphi + uq \tag{6}$$

where u is a local liquid velocity, $j = shq$ is a local surface reaction rate, s is the hydraulic surface of the adsorbent per unit volume (m^{-1}) and h is the mass-transfer

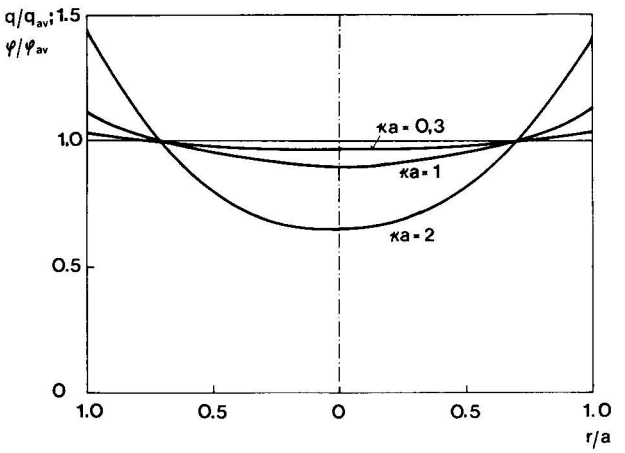

Fig. 2. Distribution of charge in low-conductivity liquids in tubes.

coefficient[21,22]. Provided that the charge is distributed uniformly over the cross-sectional area of the capillary of diameter a, and if, according to Gavis and co-workers[15,22],

$$D = \frac{\partial q}{\partial r}\Big|_{y,\, r=a} = \frac{F h}{n_+}(C_{-0} - C_{-s}) \tag{7}$$

where F is the Faraday constant, n_+ is the transfer number of the cation, C_{-0}, C_{-s} are concentrations of the anions in the liquid and at the surface, respectively, and y is the length of the capillary, by solving eqn. 6 we can express the dependence of the charge density q in the moving liquid on the coordinate y by the relationship[23,24]

$$q = \frac{sh\tau}{1 + sh\tau} 2F(C_{-0} - C_{-s})\left[1 - \exp - (1 + sh\tau)\frac{y}{\bar{u}\tau}\right] \tag{8}$$

The boundary condition quoted in eqn. 7 and the solution of eqn. 8 involve the assumption of preferential adsorption of negative ions at the interface boundary. Further, in deriving eqn. 8, it has been assumed that the entering liquid is not charged and that the transfer numbers of the cations and anions are 0.5. Eqn. 8 describes the dependence of the charge density in the liquid on the length of the capillary, the relaxation time, the rate of charge transfer through the boundary and phase equilibrium of the ions. In the equation, the local velocity, u, can be replaced with an average linear velocity, $\bar{u}$, as a uniform distribution of charge over the capillary cross-section has been considered[15,22]. In deriving this equation, the effect of changes of charge density on the conductivity of the liquid has also been neglected. As will be shown later, for particular values of the individual quantities eqn. 8 can be simplified.

Eqn. 8 indicates the dependence of the charge density on the concentration of the ions of the component considered in the solution. The dependence of the charge density on the analytical concentration of a component i, c_i, can be derived from the dependence of the charge density on the potential of the phase interface. According

to the Debye approximation[3], and if the charge is distributed uniformly over the capillary cross-section, q_{av} can be expressed as

$$q_{av} = \frac{2C_0 F^2}{RT} \cdot \varphi_d \tag{9}$$

where $C_0 = C_{-0} = C_{+0}$ is the concentration of the ions in the bulk liquid ($\varphi = 0$).

Denoting the potential of the surface covered by a monolayer of component i and the potential of the non-covered surface by φ_i and φ_0, respectively, the dependence of φ_d on the coverage θ_i can be described by

$$\varphi_d = (\varphi_i - \varphi_0)\,\theta_i + \varphi_0 \tag{10}$$

As a change in the concentration c_i of the components also brings about a change in the permittivity of the liquid, which influences the degree of dissociation of ionizable components of the solution[25,26], the concentration C_0 is a function of c_i, and the coverage θ_i is also a function of c_i. Therefore, the dependence of the average charge density, q_{av}, on the concentration of the component, c_i, can be written in the differential form as

$$\mathrm{d}q = \frac{2F^2}{RT}(\varphi_i - \varphi_0)\left(\theta_i \cdot \frac{\partial C_0}{\partial c_i} + C_0 \cdot \frac{\partial \theta_i}{\partial c_i}\right)\mathrm{d}c_i \tag{11}$$

The dependence of the electrical conductivity of the liquid on the change of its permitivity has an exponential form[25–27], and as the relationship

$$\varkappa = \frac{2C_0 F^2 D}{RT} \tag{12}$$

holds for a uni–univalent electrolyte with the cations and anions having the same diffusivity, we can derive

$$\partial C_0/\partial c_i = C_0 A \tag{13}$$

where A is a constant characteristic of the solvent and solute. Further, for the linear region of the adsorption isotherm we have

$$\frac{\partial \theta_i}{\partial c_i} = K_{di}/c_{si}^0 \tag{14}$$

where $K_{d\,i} = c_{s\,i}/c_i$ is the distribution constant and c_{si}^0 is the maximum surface concentration of component i. In eqn. 11, for $K_{d\,i}/c_{s\,i} \geqslant A$, we shall have $\theta_i \cdot \partial C_0/\partial c_i \ll C_0 \cdot \partial\theta_i/\partial c_i$ and, employing eqns. 12 and 11, we can write the dependence of the average charge on the concentration of the component as

$$\frac{\mathrm{d}\,q_{av}}{\mathrm{d}\,c_i} = \frac{\varkappa}{D} \cdot \frac{\varphi_i - \varphi_0}{c_{si}^0} \cdot K_{di} \tag{15}$$

When evaluating the response of the detection system with respect to its dependence on the composition of the mobile phase, solute concentration and chemical nature of the surface, it is necessary to start from eqns. 8 and 15.

RESULTS AND DISCUSSION

If the charge is distributed uniformly in the liquid, which has been assumed in deriving eqns. 8 and 15, then the streaming current, I_{str}, can be expressed as the product of charge density, q, and volumetric liquid flow rate, F_m:

$$I_{str} = dQ/dt = F_m q \tag{16}$$

where Q is the overall charge in the volume of liquid having flowed through. It is evident that the response of this detection system in liquid chromatography is the electrical current, I_{str} (A), and the peak area is equal to the electrical charge, Q (A · sec). The detection system is of mass-sensitivity character. Further, this detection system does not require any converter of the analytical property to the response. The streaming current can be measured directly with an electrometric amplifier and/or, in some instances, directly with a recording millivoltmeter. The properties of the electrometric amplifier are determined by the requirement that the imput resistance of the amplifier should be sufficiently small compared with the resistance of the liquid within the space in which the measurement is carried out; however, the sensitivity of the arrangement is proportional to the magnitude of the input resistance. Depending on the mobile phase system employed, the input resistance of the electrometric amplifier varies within the range 10^6–10^{10} Ω.

The properties of the detection system were proved experimentally by employing a laboratory-made liquid chromatograph (an MC-300 pump, Mikrotechna, Prague, Czechoslovakia, and/or an DMP 1515 pump, Orlita, Giessen, G.F.R.; pressure-shock dampers according to Locke[28]; a septum inlet port; an HP 305 syringe, Hamilton, Reno Nev., U.S.A.; a 250 × 2 mm I.D. column; and silica gel, 30–40 μm, Lachema, Brno, Czechoslovakia).

A schematic diagram of the electrokinetic detector with a capillary as the detection element is shown in Fig. 3. In Fig. 3a, the streaming current is generated in a bundle of about 200 glass capillaries (1) with inner diameters of about 20 μm, the outer diameter of the bundle being about 1 mm. Bundles of capillaries of length 20 and 100 mm were tried. The bundle of capillaries was connected to the column via a PTFE seal (2) and the liquid was drained off by a PTFE capillary (3). The streaming current was picked up from the capillary bundle by means of a copper wire (0.2 mm in diameter) wound over the full length of the bundle and led via a connector (4) to a 33B-2 Vibron electrometer (Electronic Instruments, Surrey, Great Britain) (5). Input resistances of 10^9–10^{10} Ω were employed. Lower alcohols were separated using *n*-hexane–isopropanol (95:5) as the mobile phase, and the effect of the length of the capillaries on the magnitude of the streaming current, depending on the mobile phase flow-rate, was studied.

On analyzing the quantities in eqn. 8, it can be shown that with the geometry of the capillaries and the mobile phase employed, the equation can be simplified to

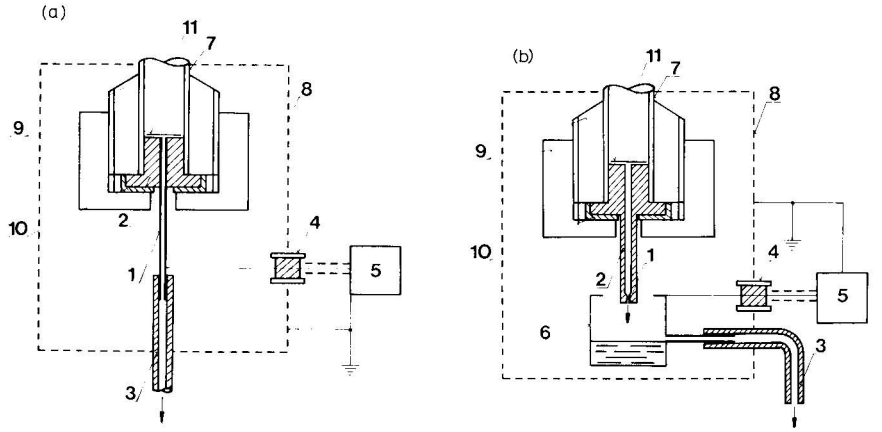

Fig. 3. (a) Schematic representation of the electrokinetic detector with a bundle of about 200 capillaries (1) of about 10 cm in length and 20 μm in diameter, made by drawing a glass tube packed with glass capillaries. 2 = PTFE seal of the column; 3 = PTFE capillary for draining off the mobile phase; 4 = connector; 5 = electrometric amplifier; 7 = chromatographic column; 8 = earthed shielding; 9 = screw closure of the column; 10 = metal washer to the column closure; 11 = filter-paper. (b) Schematic representation of the electrokinetic detector with a PTFE jet (1) of I.D. 20 μm and length 1 mm. 6 = Effluent collector; other components as in (a).

obtain the form derived by Gavis and Koszman[15]. Because $s = 2/a$ and $h = D/\delta$, $s\,h\tau \ll 1$ for the system employed and eqn. 8 assumes the form

$$q = s\,h\,\tau\,2F(C_{-0} - C_{-s})\,[1 - \exp - y/\bar{u}\tau] \qquad (8a)$$

If further $y \gg \bar{u}\tau$, it is possible to neglect the exponential term in eqn. 8a. The results of the measurements are shown in Fig. 4. In compliance with the above-mentioned

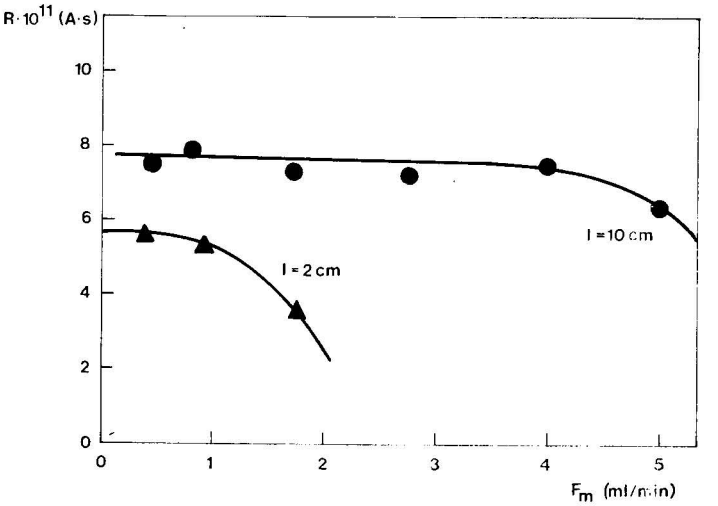

Fig. 4. Dependence of response (R) of the electrokinetic detector shown in Fig. 3a on the volumetric flow-rate (F_m) of mobile phase and the length (l) of the glass capillary bundle. Mobile phase, *n*-heptane–isopropanol (95:5); 1-μl sample of ethanol. Vibron M 33B-2 electrometric amplifier with a 10^9 input resistance; each point represent an average value of three measurements.

assumption, it can be seen that the interval within which the response is independent of the flow-rate of the mobile phase increases with increasing length of the capillary. Under these circumstances, the response $Q = \int I_{str}\,dt = R$ is independent of the flow-rate of the mobile phase and has the character of a mass-sensitive response.

If a condition opposite to that quoted above applies, *i.e.*, $y \ll \bar{u}\tau$, it is possible to obtain, by using the first two terms of the expansion of the exponential term[15] in eqn. 8a, an expression for the case of a very short capillary (orifice):

$$q = \frac{y\,s\,h}{\bar{u}} \cdot 2F(C_{-0} - C_{-s}) \tag{8b}$$

Under these conditions, the response has a concentration-sensitive character.

An arrangement with a very short capillary is shown in Fig. 3b. A capillary (1) of about 20 μm in diameter and 1 mm in length was a part of the PTFE seal (2). In contrast to the case shown in Fig. 3a, the streaming current is picked up from a stainless-steel holder of mobile phase (6), which is electrically insulated both from the jet and from the earthed shield. The liquid is drained off via a PTFE capillary (3). The holder (6) is connected, via a connector (4), to the electrometric amplifier (5). In separating the isomers of nitroaniline, *n*-hexane–isopropanol (85:15) was employed as the mobile phase. The dynamic linear range of response towards *m*-nitroaniline was about 10^3; the result is shown in Fig. 5.

As it has been derived[17,29], eqn. 16 holds for any shape of capillary cross-section. Hence it is possible to use also a porous bed for generating the streaming current and to study the dependence of the response on the chemical nature of the surface and/or on the distribution constant according to eqn. 15. When applying eqn. 8 to the flow through a porous bed formed by beads of about 10 μm in diameter, it is possible to assume that, for velocities up to about 10 cm/sec, the following conditions are fulfilled: $sh\tau \gg 1$ and $hsy/\bar{u} \gg 1$ for $y > 1$ mm. At the same time, in order to be able to neglect the effect of axial diffusion, it is necessary that the condition $\bar{u} \gg 30\,D/y$ also be fulfilled[30]. The magnitude of the hydraulic surface[31] is a function of the particle diameter, $s = 6/d_p$, and the mass-transfer coefficient, h, in a region for which $0.04 < Re < 30$, can be expressed by the relation[31] $h = 5.4\,(D/d_p)\,Re^{1/3}\,Sc^{1/4}$, for instance. Hence, the exponential term in eqn. 8 can be neglected and, as we consider the ion concentrations C_+ and C_- to be distributed symmetrically about the concentration C_0, we can assume that

$$q = q_s = q_{av} \tag{17}$$

(*cf.* Fig. 2 for the condition $\kappa a \ll 1$).

From eqns. 15, 16 and 17, we obtain for the sensitivity of the detection system

$$\frac{d\,I_{str}}{d\,c_i} = \frac{\varkappa}{D} \cdot \frac{(\varphi_i - \varphi_0)}{c^0_{si}} \cdot K_d\,F_m \tag{18}$$

For a chosen chromatographic system, the right-hand side of eqn. 18 is constant. The mobile phase is characterized by $F_m\varkappa/D$ and the stationary phase and solute by $(\varphi_i - \varphi_0)K_d/c^0_{si}$.

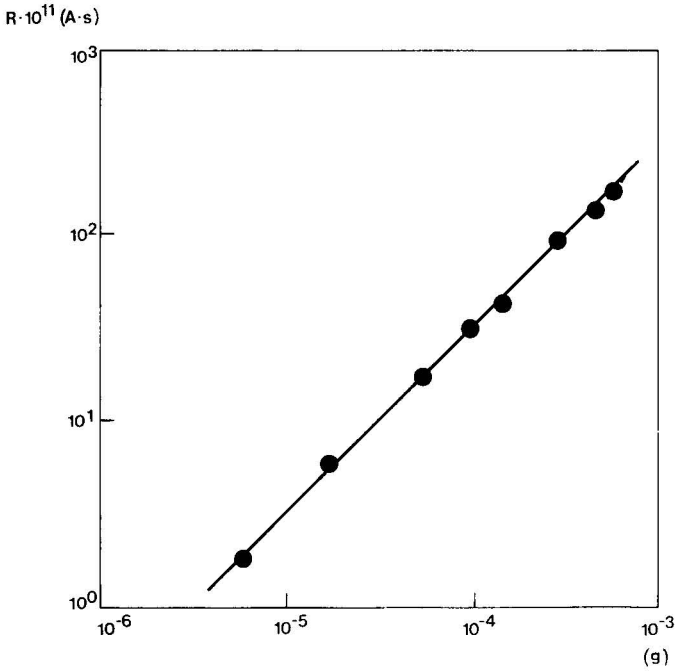

Fig. 5. Dependence of the response (R) of the electrokinetic detector shown in Fig. 3b on the amount of *m*-nitroaniline injected into the chromatographic column. Mobile phase, *n*-hexane–isopropanol (85:15); flow-rate, 0.6 ml/min; Vibron M 33B-2 electrometer with a $10^9\,\Omega$ input resistance; each point represents an average value of three measurements.

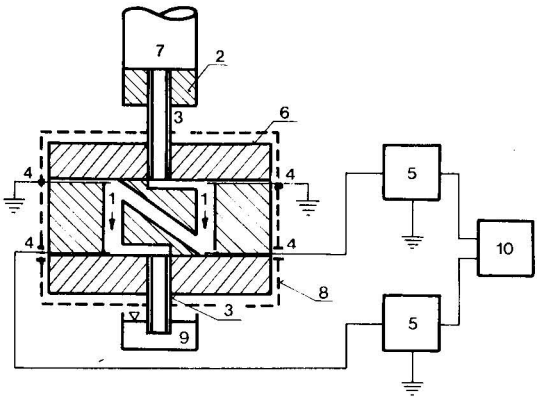

Fig. 6. Schematic representation of the electrokinetic detector with two sorbent-packed cells as sensing elements. 1 = Cells packed with an adsorbent; 2 = PTFE seal of the column; 3 = PTFE capillary for the introduction and drain-off of the effluent; 4 = platinum contacts; 5 = electrometric amplifiers; 6 = PTFE body of the detector; 7 = column; 8 = earthed shielding; 9 = mobile phase waste; 10 = two-pen recorder.

A schematic representation of the electrokinetic detector with two cells filled with a sorbent is shown in Fig. 6. The cells, of length 2 mm and I.D. 1 mm, were drilled out in an electrically shielded PTFE block. The connecting channels directed the flow of column effluent through the cell with silica gel into the cell with pellicular alumina[32] and to the detector outlet. Both cells were earthed at the inlet of the liquid. The contacts for earthing and for the outlet of the current to the electrometric amplifier consisted of platinum wire of diameter 0.1 mm. The adsorbent was held within the cells by plugs of quartz-wool. The effect of the chemical nature of sorbent is apparent from Fig. 7, which shows chromatograms of nitroaniline isomers. The chromatograms reflect not only the different sensitivities of the two cells employed but also, with the water peak, an opposite polarity of the response.

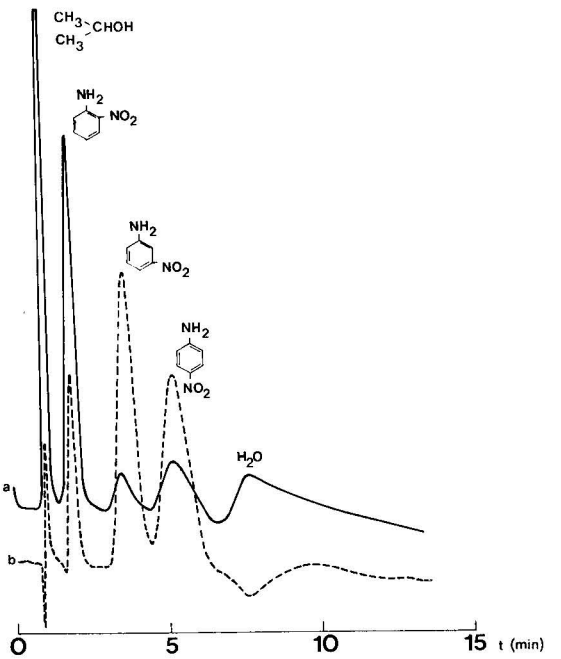

Fig. 7. Chromatogram obtained with the electrokinetic detector shown in Fig. 6 with the use of different sorbents packings in the cells. a, Silica gel, 12–25 μm (Lachema, Brno, Czechoslovakia); b, pellicular alumina, 10–20 μm (see ref. 32); mobile phase, *n*-hexane–isopropanol (85:15); sample, 0.3 mg of a mixture of nitroanilines dissolved in isopropanol.

The detection principle described can be used for mobile phases with an electrical conductivity of about $10^{-9}\ \Omega^{-1}\cdot m^{-1}$ and less. This requirement is fulfilled with a large number of mobile phases, from paraffinic hydrocarbons, through aromatic and chlorinated hydrocarbons, to mixtures of hydrocarbons with alcohols, organic acids and bases. It can be assumed that the detection principle described might also be used with liquids of higher electrical conductivity, provided that a technique for measuring the streaming potential is employed.

The construction of the detector is very simple. The analytical property employed is the streaming current, which is a directly measured response of the system.

The instantaneous response, I_{str}, is appreciably dependent on the flow-rate of the mobile phase, which has to be kept constant. The dependence of the response on the temperature of the detection system is insignificant. The arrangement belongs to the category of non-selective detectors and is not suitable for gradient techniques.

LIST OF SYMBOLS

a	tube radius	m
C_+, C_-	concentration of positive or negative ions	$\text{mole}\cdot\text{m}^{-3}$
C_0	concentration of discharging ion in bulk of fluid	$\text{mole}\cdot\text{m}^{-3}$
C_s	concentration of discharging ion at boundary	$\text{mole}\cdot\text{m}^{-3}$
c_i	concentration of non-electrolyte species i	$\text{mole}\cdot\text{m}^{-3}$
$c_{s\,i}$	surface concentration of non-electrolyte species i	$\text{mole}\cdot\text{m}^{-2}$
$c_{s\,i}^0$	monolayer capacity for species i	$\text{mole}\cdot\text{m}^{-2}$
D	molecular diffusivity of charge	$\text{m}^2\cdot\text{sec}^{-1}$
d_p	particle diameter	m
F	Faraday number	$96{,}500\ \text{A}\cdot\text{sec}\cdot\text{mole}^{-1}$
F_m	volume flow-rate	$\text{m}^3\cdot\text{sec}^{-1}$
h	mass-transfer coefficient	$\text{m}\cdot\text{sec}^{-1}$
I_{str}	streaming current	A
I_0, I_1	Bessel functions of the first kind of order zero and one, respectively	
K_d	distribution constant	m
l	length of capillary	m
n_+	transfer number of cation	dimensionless
q	charge density	$\text{A}\cdot\text{sec}\cdot\text{m}^{-3}$
q_{av}	charge density averaged over the tube radius	$\text{A}\cdot\text{sec}\cdot\text{m}^{-3}$
q_s	charge density at the boundary	$\text{A}\cdot\text{sec}\cdot\text{m}^{-3}$
R	gas constant	$8.31\ \text{V}\cdot\text{A}\cdot\text{sec}\cdot\text{mole}^{-1}\cdot{}^\circ\text{K}^{-1}$
Re	Reynolds number, $\bar{u}d_p/\nu$	dimensionless
r	spatial variable in radial direction	m
s	specific surface area	m^{-1}
Sc	Schmidt number, ν/D	dimensionless
T	absolute temperature	°K
u	local flow velocity	$\text{m}\cdot\text{sec}^{-1}$
$\bar{u}$	average flow velocity	$\text{m}\cdot\text{sec}^{-1}$
x	spatial variable normal to boundary	m
y	spatial variable in axial direction	m
δ	effective thickness of diffusion layer, $\delta = D/h$	m
ε	permittivity of liquid, $\varepsilon = \varepsilon_r\varepsilon_0$	$\text{A}\cdot\text{sec}\cdot\text{V}^{-1}\cdot\text{m}^{-1}$
ε_0	permittivity of free space	$8.854\cdot10^{-12}\ \text{A}\cdot\text{sec}\cdot\text{V}^{-1}\cdot\text{m}^{-1}$
ε_r	relative permittivity of liquid	dimensionless

ζ	zeta potential	V
θ_i	coverage of boundary with species i	dimensionless
κ	Debye–Hückel reciprocal distance	m^{-1}
$\varkappa$	conductivity of liquid	$A \cdot V^{-1} \cdot m^{-1}$
ν	kinematic viscosity of liquid	$m^2 \cdot sec^{-1}$
τ	relaxation time of liquid	sec
φ	potential	V
φ_d	electric potential at the outer Stern plane	V
φ_0	thermodynamic potential	V
φ_i	potential at the outer Stern plane of boundary covered with monolayer of species i	V

REFERENCES

1 M. Krejčí and K. Šlais, *Czech. Pat. Appl.*, 81, 037, 1975.
2 S. S. Dukhin and B. V. Derjaguin, in E. Matijević (Editor), *Surface and Colloid Science*, Vol. 7, *Electrokinetic Phenomena*, Wiley, New York, 1974.
3 A. W. Adamson, *Physical Chemistry of Surfaces*, Interscience, New York, 1960, pp. 179–228.
4 J. T. Davies and E. K. Rideal, *Interfacial Phenomena*, Academic Press, New York, 1963, pp. 108–150.
5 D. A. Haydon, *Recent Prog. Surf. Sci.*, 1 (1964) 94.
6 A. L. Smith, *J. Colloid Interface Sci.*, 55 (1976) 525.
7 O. Stern, *Z. Elektrochem.*, 30 (1924) 508.
8 O. Gouy, *J. Phys. Radium*, 9 (1910) 457.
9 D. L. Chapman, *Philos. Mag.*, 25 (1913) 475.
10 S. S. Dukhin and B. V. Derjaguin, in E. Matijevič (Editor), *Surface and Colloid Science*, Vol. 7, *Electrokinetic Phenomena*, Wiley, New York, 1974, pp. 14–23.
11 D. A. Haydon, *Recent Prog. Surf. Sci.*, 1 (1964) 95.
12 A. W. Adamson, *Physical Chemistry of Surfaces*, Interscience, New York, 1960, pp. 179–183.
13 S. S. Dukhin and B. V. Derjaguin, in E. Matijevič (Editor), *Surface and Colloid Science*, Vol. 7, *Electrokinetic Phenomena*, Wiley, New York, 1974, pp. 23–32 and 100–107.
14 A. Kitahara, *Prog. Org. Coat.*, 2 (1973/74) 81.
15 J. Gavis and I. Koszman, *J. Colloid Sci.*, 16 (1961) 375.
16 G. Touchard and P. Dumargue, *Electrochim., Acta*, 20 (1975) 125.
17 T. S. Sørensen and J. Koefoed, *J. Chem. Soc. Faraday Trans. II*, 70 (1974) 665.
18 P. Debye and E. Hückel, *Phys. Z.*, 24 (1923) 185.
19 Ref. 2, pp. 274–276.
20 R. Alkire and R. Plichta, *J. Electrochem. Soc.*, 120 (1973) 1060.
21 R. Alkire and B. Gracon, *J. Electrochem. Soc.*, 122 (1975) 1594.
22 I. Koszman and J. Gavis, *Chem. Eng. Sci.*, 17 (1962) 1013 and 1023.
23 V. V. Zakharchenko, N. I. Kryachko, E. F. Mazhara, V. V. Sevrikov and N. D. Gavrilenko, *Elektrizatsiya Zhidkostei i ee Predotvrashchenie*, Khimiya, Moscow, 1975, pp. 13–24.
24 S. A. Bobrovskii, *Autoreferat Diss. M.*, MINKh i GP, Moscow, 1969.
25 L. P. Hammet, *Physical Organic Chemistry*, McGraw-Hill, New York, 1970.
26 Ch. Reichardt, *Lösungsmittel-Effekte in der organische Chemie*, Verlag Chemie, Weinheim/Bergstr., 1969, p. 40.
27 A. Klinkenberg and J. L. van der Minne, *Electrostatics in the Petroleum Industry*, Elsevier, Amsterdam, 1958, p. 84.
28 J. C. Locke, *J. Gas Chromatogr.*, 5 (1967) 202.
29 Ref. 2, pp. 113–118.
30 G. Razumney, H. S. Wroblowa and G. L. Schrenk, *J. Electroanal. Chem.*, 69 (1976) 299.
31 F. Coeuret, *Electrochim. Acta*, 21 (1976) 185 and 203.
32 P. Kaláb, K. Tesařík, D. Kouřilová and J. Pajurek, *Chem. Listy*, in press.

Journal of Chromatography, 148 (1978) 111–116

CHROM. 10,472

A CONDUCTIMETRIC DETECTOR WITH A WIDE DYNAMIC RANGE FOR LIQUID CHROMATOGRAPHY

VRATISLAV SVOBODA and JAROSLAV MARŠÁL
Institute for Research, Production and Application of Radioisotopes, 17004 Prague 7 (Czechoslovakia)

SUMMARY

A conductimeter with an alternating symmetrical square wave measuring voltage (1 V, 2.5 kHz) and logarithmization circuit has been constructed and its application studied using a symmetrical cell of 3 μl internal volume. Its dynamic range is about six orders of magnitude. No manual switching of ranges is necessary and therefore unattended operation as an on-line chromatographic detector is possible. Examples of inorganic salts chromatographed on a Sephadex G-10 column are presented.

INTRODUCTION

The concentration of inorganic compounds in effluents from liquid chromatography columns may change very rapidly, sometimes by even more than four orders of magnitude within several seconds. This effect is very pronounced in gel chromatography, when peaks of salts are highly asymmetric with steep shoulders or fronts, probably owing to ion exclusion effects.

When using a conductimeter with a linear scale, *i.e.*, with the signal proportional to the conductivity of the solution, then the dynamic range is limited at the lower end by the noise and drift of the recording chain and frequent switching of ranges is therefore necessary. This is usually performed manually and is not only time consuming but also susceptible to human errors. If it is done automatically, then the reading of the graphical record may become complicated in regions of rapid ascent or descent of the effluent conductivity. We have therefore tried to construct an instrument in which the signal is approximately proportional to the logarithm of the measured conductivity.

Flow-through conductimetric detectors are frequently used in liquid chromatography, but optimization of their design has never been thoroughly studied[1]. Most conductimetric detectors described recently[2–5] were built so as to minimize the cell volume. This is most pronounced in detectors for isotachophoresis, where sharp boundaries of zones have to be measured quickly and with minimal distortion. In order to offset the influence of the fluctuation of the regulated high-voltage source, a conductimeter operating at high frequency (above 100 kHz) was developed[2]. However, at these frequencies the ohmic conductivity of electrolytes is lower than the

d.c. conductivity. Obviously, this detector could also be used in high-performance liquid chromatography (HPLC), its advantage being the higher immunity to electrical noise.

Conductimetric cells constructed specifically for use in HPLC were described by Pecsok and Saunders[3] and later by Tesařík and Kaláb[4]. Their designs were very similar in both basic characteristic and performance. Cells formed an integral part of columns; their dead volume was low (5 and 2.5 μl, respectively) and their cell constants were near to unity (0.55 and 0.8 cm^{-1}, respectively). The cells had to be isolated from metallic columns, or were adapted for use with glass columns only. For measurement of resistivity commercial instruments with several manually switchable linear ranges were used in both instances (Radiometer CDM2e and Radelkis OK-102/1). For testing a short column packed with glass beads was used and deionized water was used as the solvent. The minimal detectable concentrations of potassium chloride (signal equal to twice the peak-to-peak noise amplitude) were $5 \cdot 10^{-8}$ and $1.5 \cdot 10^{-7}$ mole$\cdot l^{-1}$, respectively.

Jackson[5] studied the use of a high-frequency conductimetric detector with external electrodes; however, the dead volume was very high (*ca.* 2 ml). The minimal detectable concentration with this instrument was probably similar to those mentioned above.

EXPERIMENTAL

The conductivity, G, measured by the electronic circuit is determined by the specific electrical conductivity of the measured solution and by the cell constant of the measured solution and by the cell constant of the measuring cell. Hence the cell design may affect to some extent the range of specific conductivities measurable by a particular instrument.

In our instrument, the range of measurable conductivities extends from about 10^{-8} S to more than 10^{-2} S. For measurement a rectangular alternating voltage with amplitude ± 1 V and frequency 2.5 kHz is used. The output voltage in this range is proportional to a function approximating to the logarithm of the conductivity.

The electronic circuitry is illustrated in Fig. 1. The instrument consists of three principal parts: a generator of alternating voltage (OA1), a logarithmic alternating current–voltage converter (OA2) and a d.c. amplifier (OA3).

For generation of the logarithmic function use is made of the fact that for most transistors the relationship between the base-emitter current and voltage is nearly logarithmic. Hence the alternating measuring voltage of ± 1 V from the generator is carried to the positive input of the operational amplifier OA2. Owing to the back-loop, virtually the same voltage is also on the other input of OA2. The resistance of the condenser C_V can, in the range of conductivities applying here, be neglected and therefore for the current flowing through the cell, I_x, and the generator voltage, U_A, we have

$$I_x \approx U_A \cdot G_x \tag{1}$$

At the output from OA2 we then have an alternating voltage with amplitude given by

$$U_b = \pm (U_A + k \log I_x + k) \tag{2}$$

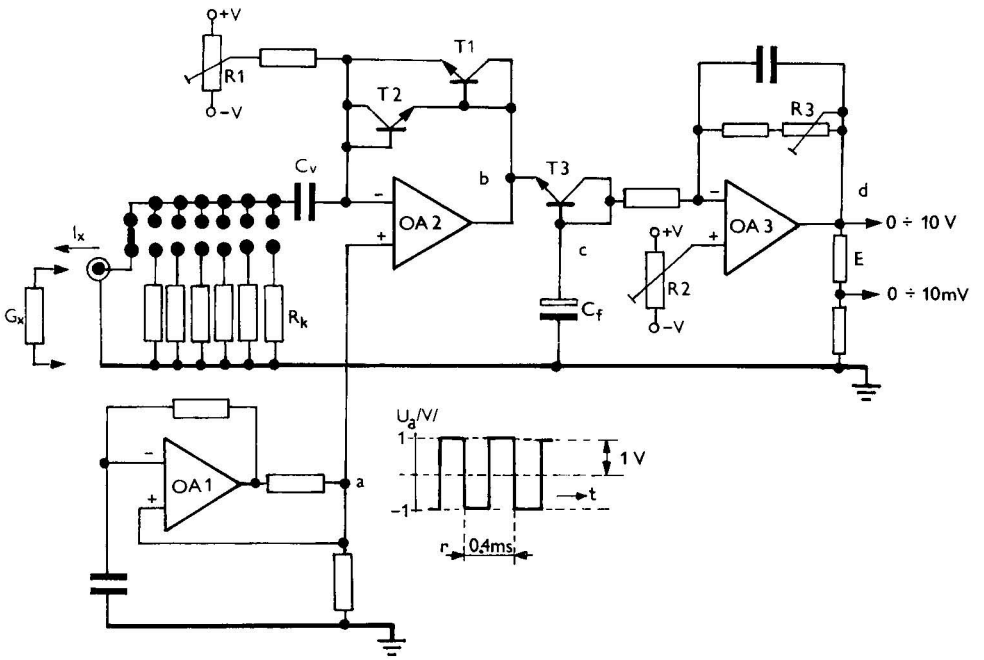

Fig. 1. Wiring diagram of conductimeter. OA1, OA2, OA3 are operational amplifiers, T1, T2, T3 transistors, and R1, R2, R3 potentiometers.

and after rectification we obtain

$$U_c = -(U_A + k \log I_x + k - U_T) \tag{3}$$

After amplification of this signal by OA3 we finally obtain the output voltage:

$$U_d = A \log I_x + B \tag{4}$$

The constants A and B are set by potentiometers R_2 and R_3 so that the output voltage ranges from 0 to +10 V (see Fig. 2). The temperature drift of the base-emitter voltage

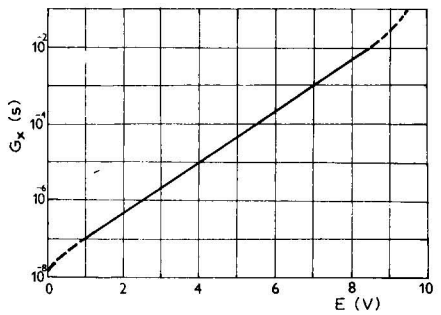

Fig. 2. Calibration curve of conductimeter. G_x = measured conductivity (S), E = output voltage (V).

of transistors T_1 and T_2 is compensated for by temperature drift of the voltage on transistor T_3.

The correct functioning of the instrument can be checked by a set of fixed resistors, R_k, which can be selected by a switch.

A d.c. power supply of ± 12 V is used. The whole electronic unit is built on a single printed circuit board of dimensions 100 × 160 mm. On the front panel of the instrument are located only two switches: an on–off switch and an external–internal calibration switch. More detailed information on the construction of the circuit is available from the authors on request.

Because of the extreme simplicity of the design, the instrument is very dependable. Two instruments have been in use in our laboratory for more than 2 years, during which period only one repair of a calibration switch was needed.

The conductimetric cell (Fig. 3) is symmetric, both outer electrodes being earthed and the internal electrode being attached to the voltage source. The electrodes are made of stainless steel and isolators of polytetrafluoroethylene. The total volume of this detector is about 3 μl and this can easily be reduced further if necessary.

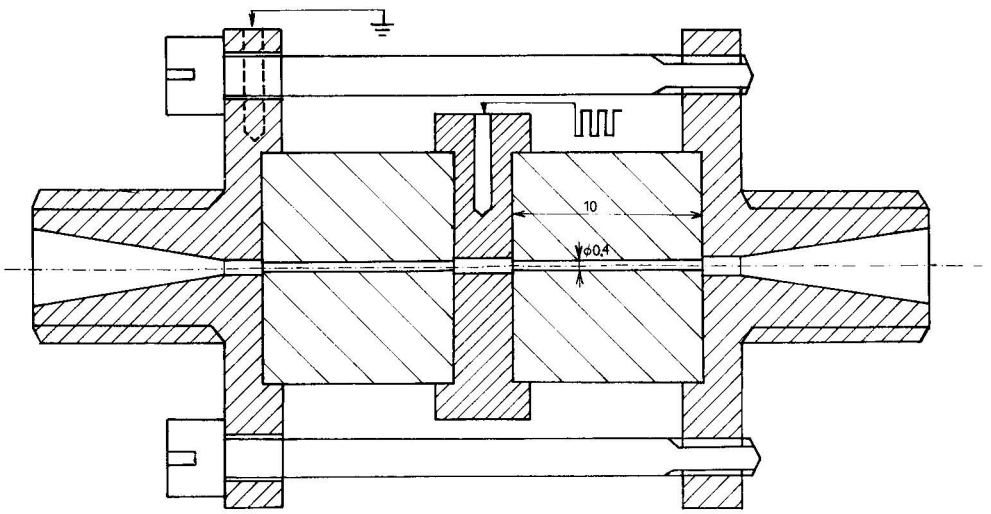

Fig. 3. Diagram of conductimetric cell. Materials used: stainless steel and PTFE. Dimensions in mm.

RESULTS AND DISCUSSION

A typical chromatogram of sodium perchlorate on Sephadex G-10 is illustrated in Fig. 4. This is a characteristic example of a peak with a steep front edge; the total change in conductivity ranges from about $4 \cdot 10^{-8}$ to $1.5 \cdot 10^{-2}$ S, *i.e.*, just about the whole range of our instrument. Fig. 5 illustrates a set of chromatograms recorded with various amounts of potassium chloride injected on a Sephadex G-10 column, and is an example of a peak with a steep shoulder. In curve 6 the full range of the instrument is used for recording. Thus with the same instrument setting two peaks representing amounts of sample differing by a factor 10^4 can be recorded and quanti-

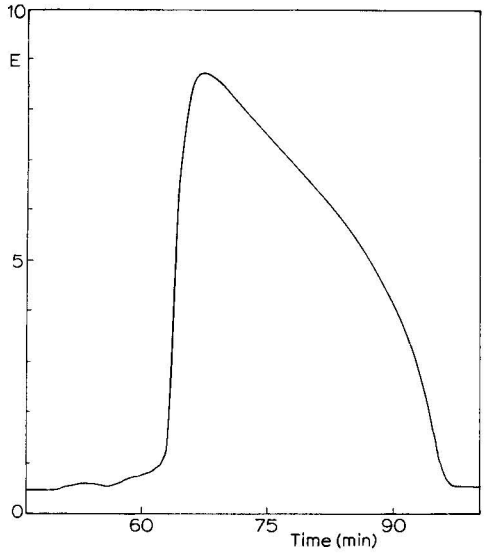

Fig. 4. Shape of a peak with steep front edge. Column dimensions, 1000 × 4 mm, packed with Sephadex G-10; eluent, 0.01 *M* ammonia solution in water; pumping speed 10 ml/h; sample, 61 mg sodium perchlorate.

tatively evaluated. This is a major advantage over the previously described conductimeters[2–5], with which unattended recording over a wide dynamic range was virtually impossible. The relationship between amount of sample and peak area is non-linear, even when the pen deflection is strictly proportional to the measured conductivity[3,4]. Therefore, even in these instances a calibration graph constructed over the whole range of concentration s_U is necessary.

The symmetrical construction of the conductimetric cell led to a suppression of ground-loop currents and high-frequency pick-up, both of which increase the drift and noise. Therefore, metallic columns can be used and all connections can be made

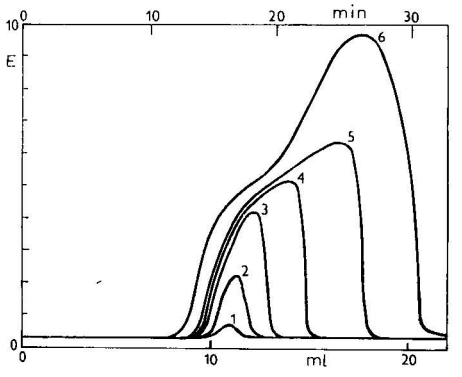

Fig. 5. Influence of sample amount on the peak shape. Column dimensions, 1260 × 4.8 mm, packed with Sephadex G-10, eluent $1 \cdot 10^{-5}$ *M* Tris in water, pumping speed 0.67 ml/min. Various amounts of KCl: 1: 10 μg, 2: 50 μg, 3: 250 μg, 4: 1 mg, 5: 5 mg, 6: 100 mg. Vertical axis: 0–10 V (see Fig. 2).

by using common stainless-steel capillaries with ferrules. In contrast to previous designs we could therefore increase the cell constant to *ca.* 4.10^2 cm^{-1}. This further permits an increase in the precision of measurements at high concentrations, which are important with many samples of biological interest. The upper measuring limit of our instruments probably extends to about two orders of magnitude higher than those described previously[3,4]. On the other hand, we do not believe that in most experiments in which conductimetric detectors are used deionized water is the solvent of choice. Usually, even in gel filtration or ion-exclusion chromatography, the pH of the solvent has to be maintained either above or below 7. Therefore, the conductivity of the solvent in most instances is higher than that of conductimetric water and the published ultimate minimal detectable concentrations are mostly only of academic interest. Even so, the maximum concentration of potassium chloride in peak 1 (Fig. 5) is only $1.2 \cdot 10^{-7}$ mole·ml^{-1} (the measured amount of potassium chloride within the detector is about 27 ng) and the minimal detectable concentration, owing to the very low noise of the whole measuring chain, is about $6 \cdot 10^{-6}$ mole·l^{-1}. The total dynamic range is about six orders of magnitude, which is about two orders of magnitude greater than that reported earlier[4].

There is no point in comparing the absolute amplitude of the noise and the output from the amplifier, as was done in earlier papers[3,4], because of the different (and unpublished) electronic gains.

The advantages of the detector can be used fully only in eluents with relatively low concentrations of ionizable components (*e.g.*, 0.001 *M* ammonia, formic acid in water) and therefore it can be expected to be applied mainly in gel filtration and ion-exclusion chromatography.

REFERENCES

1 M. Krejčí, Z. Pechan and Z. Deyl, in Z. Deyl, K. Macek and J. Janák (Editors), *Liquid Column Chromatography*, Elsevier, Amsterdam, 1975, p. 148.
2 S. Stankoviansky, P. Čičmanec and D. Kaniansky, *J. Chromatogr.*, 106 (1975) 131.
3 R. L. Pecsok and D. L. Saunders, *Anal. Chem.*, 40 (1968) 1765.
4 K. Tesařík and P. Kaláb, *J. Chromatogr.*, 78 (1973) 357.
5 A. Jackson, *J. Chem. Educ.*, 42 (1965) 447.

Journal of Chromatography, 148 (1978) 117–125

CHROM. 10,478

INFLUENCE OF THE TEMPERATURE FIELD ON A PERMITTIVITY DETECTOR IN LIQUID CHROMATOGRAPHY

VLADIMÍR SLAVÍK

Institute of Analytical Chemistry, Czechoslovak Academy of Sciences, Brno (Czechoslovakia)

SUMMARY

A dual detector, based on a heterodyne principle with two variable oscillators, reacts both to observed changes in the real component of the complex permittivity and to a range of interferences. The most significant interference is caused by temperature fluctuations, and its analysis leads to an electrical equivalent diagram of the circuit of the detector. The analysis shows the requirements for the optimal arrangements of electrical, thermal and hydraulic relationships. These requirements were considered in the construction of the permittivity detector, with the help of which a sensitivity for the volume fraction $m_x \approx 3 \cdot 10^{-6}$ of benzene in *n*-heptane was achieved.

INTRODUCTION

Changes in the real component, ε', of the complex permittivity are used for the detection of substances eluted at the outlet of the separation column of a liquid chromatograph. The permittivity detector developed operates with two radiofrequency oscillators, the frequency of which is influenced by the value of ε' of the dielectric that

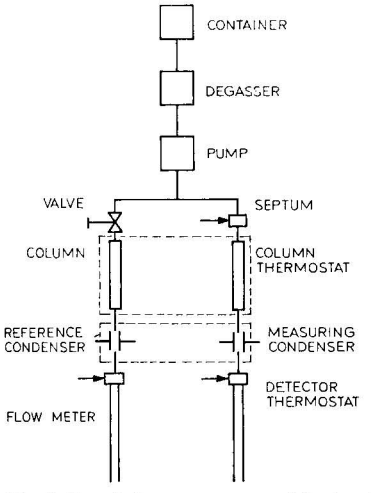

Fig. 1. Parallel arrangement of hydraulic circuit.

fills the flow-through condenser at a particular moment. According to the parallel configuration in Fig. 1, the eluent, together with the gradually eluted substances, flows through the measuring condenser in the right arm, whereas in the left arm the eluent alone flows through the reference condenser.

Fig. 2 shows a block diagram of the detector with two oscillators, O_1 and O_2, whose frequencies, f_1 and f_2, are influenced by the flow-through condensers C_1 and C_2. High-frequency voltages from the separating amplifiers, Z, are brought to the frequency mixer, S, and to the low-frequency filter, F, behind which the converter, f/U, and the chromatogram recorder with the suppressing voltage source[1-3], K, are connected.

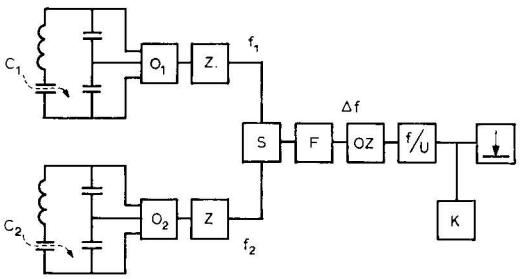

Fig. 2. Diagram of heterodyne detector.

The detector should reach the highest possible sensitivity towards changes in ε' with peaks lasting approximately 1 sec, which is why the working frequency of the oscillators was set at *ca.* 50 MHz.

INSTRUMENTATION

Interfering influences on the permittivity detector

Apart from the desirable changes in frequency, there are also further influences that create noise and zero drift. Increases in the detector sensitivity are usually limited by these particular interfering influences, the most significant of which are fluctuations in the electrical parameters and in the temperature.

To exclude the interfering influences, an arrangement is required that effects their stabilization, and in which the electrical equivalent diagram of the interferences in the detector can be considered as a parametrically balanced bridge, while on the other hand the equivalent diagram of the circuit with a measured value can be represented by an unbalanced bridge, the output of which represents the chromatogram on the recorder.

Equivalent thermal circuit

To acquire an idea of the features of a thermal circuit of the detector, which is not easy to survey, it is useful to employ an analogy with an electric circuit. An electrical equivalent connection is used for this purpose, with elements representing the elements of the thermal circuit.

In this analogy, the thermal leakage (equal to the reciprocal of the thermal resistance) is represented by the conductivity, G, and the thermal flow, $(dQ/dt)_{term.}$,

where Q is the quantity of electricity, is represented by the flow of the electric current, I_{el}:

$$I_{el} = \left(\frac{dQ}{dt}\right)_{el} \approx \left(\frac{dQ}{dt}\right)_{term.} \tag{1}$$

The driving force of the thermal flow is formed by the temperature gradient $(T_2 - T_1)$, represented by the difference in electrical potential $(E_2 - E_1)$, or the electrical voltage, U (V):

$$U_{el} = (E_2 - E_1)_{el} \approx (T_2 - T_1)_{term.} \tag{2}$$

The electrical conductivity, G, which is equivalent to $1/R$, corresponds to the thermal conductivity:

$$G_{el} = \frac{I}{U} \approx \frac{dQ}{(T_2 - T_1)\, dt_{term.}} \tag{3}$$

Fig. 3a shows an electrical equivalent diagram of a thermal circuit of a heterodyne detector. The diagram is slightly simplified; it does not include the temperature dependences of either the oscillator coil or the transistor and other circuit elements. Capacitances C_V and C_N represent the thermal capacities of the flow-through condensers in the oscillator circuits. G_1 represents the thermal leakage between the condenser and the transistor as a source of heat; G_2 represents the thermal leakage between the condenser and the outer parts, which are formed mainly by the capillaries for the inlet and outlet of liquid. The conductivity G_3 represents the thermal leakage between the measuring condenser and the heating element.

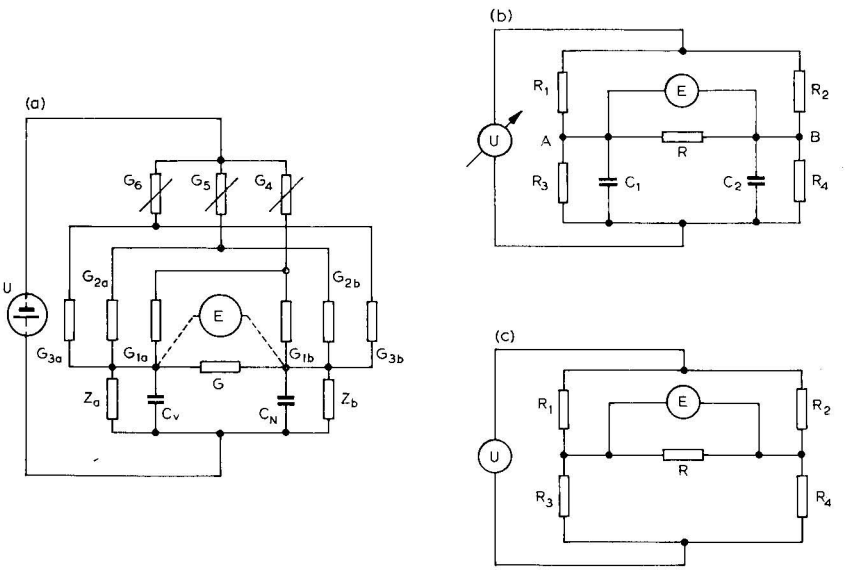

Fig. 3. (a) Electrical equivalent diagram of the thermal circuit. (b) Simplified equivalent diagram. (c) Equivalent diagram for the stabilized state.

The thermal situation of the arm with the measuring condenser, designated with a subscript a, is similar to the situation of the arm with the reference condenser, designated with a subscript b. Conductivities G_4, G_5 and G_6 represent the routes of the thermal interference as variable thermal leakages, common to both bridge arms connected to the hypothetical source of the temperature difference U. For the detector it is assumed that the temperature of the condensers is higher than that of the surroundings. In practice, this means an essential simplification of the whole chromatograph. Conductivities Z then represent the thermal losses of the condensers into the surroundings, through which all of the heat brought into the condensers by means of G_1, G_2 and G_3 is drawn off. Most of the heat is drawn off through the walls of the detector box, by analogy designated as leakages Z_a and Z_b.

It follows from the equivalent diagram that the disturbance interferences affect both thermal capacitances C_V and C_N symmetrically only when the capacities and their respective leakages are symmetrical. Thus $C_V = C_N$, $G_{1a} = G_{1b}$, $G_{2a} = G_{2b}$, $G_{3a} = G_{3b}$ and $Z_a = Z_b$. The thermal leakage, G, between C_V and C_N, *i.e.*, between the flow-through condensers, should be as high as possible, so that only a negligibly small temperature gradient would arise on it due to the equalizing thermal flow.

If the thermal leakages are symmetrical, the electrical equivalent diagram can be simplified as shown in Fig. 3b, which is valid for variable interferences and a dynamic state. Fig. 3c is even more simplified, and shows the stabilized state where the thermal capacities can be neglected. It follows from these illustrations that there is a temperature difference in the capacities of the condensers between points A and B. However, the value of the temperature difference is constant, and equal to zero, only when the thermal bridge is balanced:

$$\frac{R_1}{R_2} = \frac{R_3}{R_4} \tag{4}$$

If for the leakages

$$\frac{R_1}{R_2} = \frac{R_3}{R_4} = 1 \tag{5}$$

and for the capacitances

$$C_1 = C_2 \tag{6}$$

then the balance and the zero difference in the condenser temperatures is also maintained under unstable conditions caused by the variable power source.

Arrangement for optimal thermal stability

It is important that the eventual changes in temperature should be nearly zero and very slow. Their time constant, $\tau = R\,C$, depends on the values of the capacity and the resistor through which the capacity is fed. If there is a resistor of resistance R_3 (namely the thermal leakage Z_a) connected parallel to the capacitance C_1, the effective resistance decreases to a value given by the resistances of the parallel-connected resistors R_1 and R_3. The time constant then is

$$\tau = C \cdot \frac{R_1 R_3}{R_1 + R_3} \tag{7}$$

In order to acquire very slow temperature changes, it is necessary to reach the minimum thermal loss leakage, Z, which corresponds to a maximal R_3, which requires very good thermal isolation against the surroundings. A low voltage of the condenser C in the equivalent electrical circuit corresponds to a low degree of heating of the detector, and this can be acquired with the given thermal leakage R_3 with the help of the large resistance R_1 that corresponds to a low thermal input. As the result of the requirement of an equivalence of temperatures of both flow-through condensers, there arises the necessity for an efficient thermal leakage between the condensers C_V and C_N. They should be placed on a plate of good thermal conductivity, as close to each other as possible.

Changes in temperature of the flow-through condensers of both oscillators occur in two ways: by the influence of the linear expansion of the material on the one hand, and by the influence of the temperature dependence of the permittivity of the liquid that is filling the condenser on the other.

If we assume that only small temperature changes occur, so that the temperature dependences can be taken as linear, than the term for the condenser capacity is as follows:

$$C = \varepsilon_r' C_V \tag{8}$$

where ε_r' is the real component of the relative complex permittivity of the measured liquid and C_V is the capacity of the empty measuring condenser.

The influence of the temperature change from T_o to T is expressed by

$$C_V = C_{Vo} [1 + TK_c (T - T_o)] \tag{9}$$

$$\varepsilon_r' = \varepsilon_{ro}' [1 + TK_c (T - T_o)] \tag{10}$$

where

$$TK_c = \frac{dC}{C\,dT} (°K^{-1}) \tag{11}$$

is the temperature coefficient of the capacity of the empty condenser, which is dependent on the construction and the materials used.

$$TK_{\varepsilon'} = \frac{d\varepsilon'}{\varepsilon'\,dT} \tag{12}$$

which is the temperature coefficient of the liquid that is filling the condenser.

By substituting eqns. 9 and 10 into eqn. 8, we obtain

$$C = \varepsilon_{ro}' C_o [1 + TK_c (T - T_o) + TK_{\varepsilon'} (T - T_o) + TK_c TK_{\varepsilon'} (T - T_o)^2] \tag{13}$$

For low values of TK_c and TK_ε', it is possible to neglect the square at the end of the eqn. 13 and we obtain

$$C \approx \varepsilon_{ro}' C_o [1 + (TK_c + TK_{\varepsilon'}) (T - T_o)] \tag{14}$$

The condenser capacity thus depends on the sum of the temperature coefficient of the empty condenser and that of the real component of the complex permittivity of the liquid.

The real relationships are more complicated[4], but the result of this problem, however, remains essentially the same.

It is possible to give some actual data for the temperature coefficients. The real components, ε'_r, of the complex permittivity of some substances (otherwise the dielectric constant) and the temperature coefficients, $TK_{\varepsilon'}$, for the change of ε' with temperature are given in Table I.

TABLE I

TEMPERATURE COEFFICIENTS FOR SOME AROMATIC COMPOUNDS

Compound	ε'_r *(20 °C)*	$TK_{\varepsilon'} = \frac{d\varepsilon'}{\varepsilon' dT}$
Cyclohexane	2.0148	$7.796 \cdot 10^{-4}$
Benzene	2.2463	$7.158 \cdot 10^{-4}$
Chlorobenzene	5.6895	$3.059 \cdot 10^{-3}$
Nitrobenzene	35.72	$5.180 \cdot 10^{-3}$

The temperature coefficient of the capacity of the empty condenser was measured on samples of coaxial flow-through condensers. With the brass type it was found that $TK_c = 1.60 \cdot 10^{-3}\ °K^{-1}$, while for a coaxial condenser made of chrome stainless steel, type 17022, $TK_c = 3.0 \cdot 10^{-4}\ °K^{-1}$.

A comparison of TK_c with $TK_{\varepsilon'}$, shows that both temperature dependences affect the measuring error to nearly the same extent, which is why it is important to devote attention to decreasing TK_c by using a suitable construction of the condenser and to stabilize carefully the detector temperature in order to restrict the influence of both temperature coefficients.

Arrangement for optimal electrical stability

Changes in temperature are the cause of the fluctuation of the capacity and also of the output detector signal, although they are not the only cause. The dependence of the oscillator frequency on the supply voltage and on the electrical symmetry of both oscillators is also significant. Apart from this, such electrical asymmetry causes an asymmetry of the Joule heat, which in turn leads to temperature asymmetry. For this reason, it is advisable to secure symmetry and stability of the detector not only by its design but also by setting identical inputs during its operation.

Arrangement for optimal hydraulic relationships

The influence of interference factors has already been discussed; their suppression requires a symmetrical bridge arrangement. Should such an arrangement of the detector lead to better stability and sensitivity, the symmetry must be retained with considerable care in all respects: geometrically, electrically, thermally and also in the liquid flow that causes thermal effects.

Requirement of temperature stability

As has been derived before, the temperature coefficient of the condenser capacity and also of the real component, ε', of the complex permittivity of the substances under consideration are $TK \approx 10^{-3}$ (relative)/$°K^{-1}$.

If there are changes ε' with a sensitivity of, *e.g.*, 10^{-6} (relative) to be followed by the detector, then the temperature should not fluctuate by more than

$$\Delta T = \frac{\Delta\varepsilon'}{\varepsilon' TK} = \frac{10^{-6}}{10^{-3}} = 10^{-3}\ ^{\circ}\mathrm{K}$$

Owing to the symmetrical bridge arrangement, the real factor demanded is lower; however, in spite of this the requirement of increasing sensitivity leads to the need for temperature stabilization in the region of a few thousandths of a degree.

Arrangement of the chromatograph

In contrast to Fig. 1, a series hydraulic arrangement of the chromatograph with two separately thermostated boxes is shown in Fig. 4. The mobile phase flows from the container through the thermal degasser, through a pump and the pulse damper, to the filter and the needle valve, with the help of which the liquid flow is adjusted. The mobile phase enters the column thermostat, the heat exchanger and the saturation column, from where it passes into the detector thermostat and into the reference flow-through condenser. From there it returns through the column thermostat for feeding the sample. Then it enters the separation column, the measuring flow-through condenser, then again through the thermostat to the flow meter and out.

In order to attain good symmetry, both flow-through condensers are connected to the inlet and outlet capillaries that serve at the same time as heat exchangers in the thermostat. For better heat transfer a special silicone vaseline (Unisillicon TK SBA,

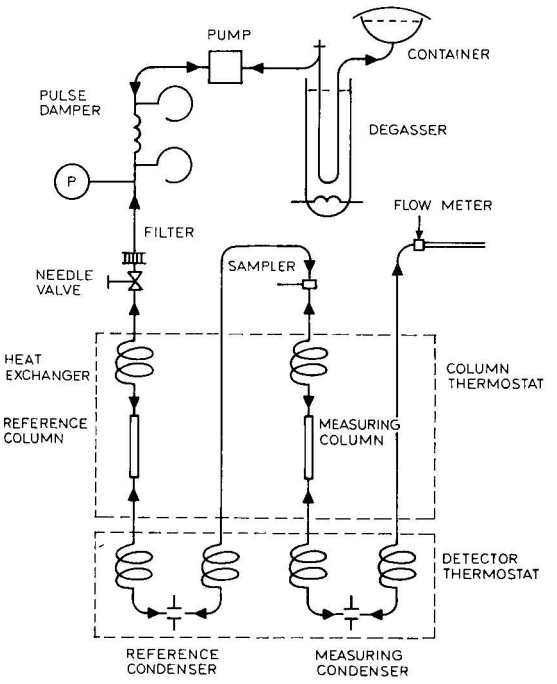

Fig. 4. Liquid chromatograph with detector condensers.

Klüber Lubrication, Vienna, Austria) with good thermal conductivity is used, being coated between the surface of the capillaries and the copper block of the thermostat.

Detector

It was our aim to achieve the best possible stability of the output signal while maintaining the optimal thermal, electrical and hydraulic stability.

The electrical input of the oscillator was reduced in the all-transistor concept of the detector to 20 mW, which is *ca.* 100–1000-fold less than in a similar electron-tube version[2]. Both oscillators were of the Clapp-type, with separator stages, and a mixer with a stabilized power supply for the thermistor bridge. The total input of the detector parts built in a copper block with a mass of 5300 g was 1.5 W. The copper block, together with the heating elements covering both opposite walls, is placed in an isolation case made of polystyrene foam with external dimensions of 140 × 165 × 200 mm.

Temperature controller

The detector is thermostated by a commercial controller, Type DHS (Eurotherm, Worthing, Great Britain). It is a universal transistor controller with adjustable PID* (three-term controller), adjustable maximum output and reference voltage set in four decade switches with a resolution of 2 μV. The controller also contains an auxiliary disturbance compensator that quickly compensates the fluctuation of the line voltage before it causes temperature changes.

The inlet of the regulator is connected to the outlet of a Wheatstone bridge with a thermistor, Type NRZ 1001.3K/El-R (Pramet, Šumperk, Czechoslovakia). Its exchangeability is better than 1 °C.

The power supply for the thermistor bridge is stabilized by a zener dipole (Tesla KZZ82), which is placed together with the Manganin resistors of the bridge in the thermostated case of the detector. The setting of the proportional term of the controller was optimal when the stabilization coefficient of the whole regulation circuit was 2100.

RESULTS

The whole power consumption of the detector causes a temperature rise of not more than 5 °C, so that even in summer it is possible to work with this detector at the highest temperature of 35 °C without using any cooling system. This leads to the advantage of a simple temperature control[5] without cooling, even for studying biological materials.

Under these conditions, the fluctuation of the block temperature was measured with the help of a platinum resistance miniature sensor (Type P3, Degussa, Hanau, G.F.R.). Fig. 5 shows the recording of the temperature of the detector with a sensitivity of 0.003 °K/mm. Ten minutes after switching on, the temperature was stabilized within an error of 0.01 °K and after approximately half an hour the temperature was steady with a hardly noticeable fluctuation of less than 10^{-3} °K.

* PID = Proportional Integral Derivative.

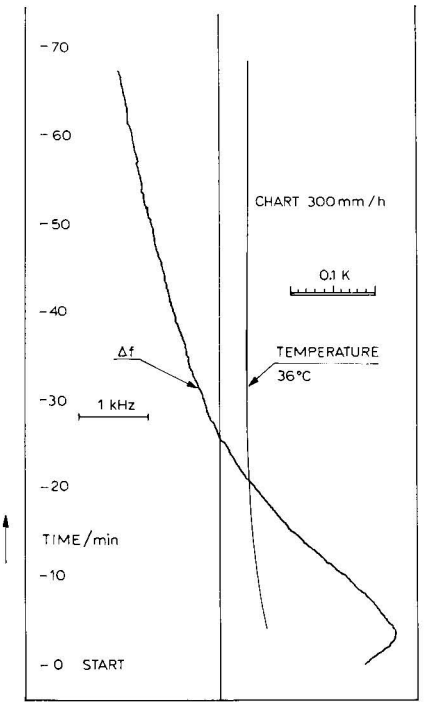

Fig. 5. Recording of temperature and frequency drift.

The other line represents the output signal of the detector. Its drift lasts slightly longer than the temperature stabilization.

The operating model of this detector was constructed without the use of any contact surface protection. Under good conditions there was a noise of less than $\pm$ 7 Hz. Holding that the smallest detectable peak is twice as great as the noise band, the smallest detectable volume fraction of benzene in *n*-heptane is $m_x = 3 \cdot 10^{-6}$ (relative).

REFERENCES

1 A. J. Slavin, *Cryogenics*, 4 (1972) 121.
2 R. Vespalec and K. Hána, *J. Chromatogr.*, 65 (1972) 53.
3 S. Haderka, *J. Chromatogr.*, 91 (1974) 167.
4 J. Provaz, *Teplotní Kompensace Kmitočtu Vysokofrekvenčních Obvodů*, SNTL, Prague, 1958.
5 J. Chlup, *Sdělovací Tech.*, 8 (1975) 299.

Journal of Chromatography, 148 (1978) 127–141

CHROM. 10,477

CONTRIBUTION TO THE CHOICE OF OPTIMAL GEOMETRIC CONDITIONS FOR PREPARATIVE LIQUID CHROMATOGRAPHY

A. W. J. DE JONG, H. POPPE and J. C. KRAAK

Laboratory for Analytical Chemistry, University of Amsterdam, Nieuwe Achtergracht 166, Amsterdam (The Netherlands)

SUMMARY

Column technology for preparative liquid chromatography is discussed. The choice of the optimal particle size is considered. A derivation is presented that shows that operation in the rising part of the plate height curve results in an improved throughput when the plate number and pressure drop are specified.

The influence of the injection mode on the preparative performance is also discussed. Experimental results pertaining to three injection modes are given. A proposed flow-surrounded conical disperser system was found to be superior for difficult separations.

INTRODUCTION

General interest in preparative column liquid chromatography has increased remarkably since the introduction of columns with highly improved performance, brought about by the application of totally porous microparticulate material and suitable packing techniques. The success of modern column technology in the analytical field may lead to its exploitation for preparative purposes, as the columns concerned have high efficiencies and high specific loading capacity (amount of sample per unit amount of packing).

Although the choice of optimal conditions in analytical liquid chromatography is now clear, as a result of both theoretical considerations and practical experience, we feel that for preparative applications a number of questions remain.

Bombaugh and Almquist[1] and Wehrli[2] introduced the throughput as the main performance parameter for a preparative liquid chromatography system (the amount of pure material collected per unit time). The factors that determine the maximum obtainable throughput are:

(a) Geometric and kinetic parameters, such as column and particle dimensions, injection mode and velocity of the eluent. These aspects are more or less universal.

(b) The composition of the original mixture and the requirements with respect to yield and purity of the product. These aspects are specific to the problem at hand.

(c) Parameters of the phase system chosen, such as the selectivity factor and

the usable range of the distribution isotherm. These aspects are specific to the compounds in the mixture and the phase system chosen.

The factors mentioned under (b) and (c) were discussed by Wehrli[2] and Wehrli *et al.*[3]. They showed that high selectivity factors, when suitably exploited, can increase the throughput considerably. Selectivity adjustment is therefore of great value.

Difficult situations arise, however, if one has to separate a complex mixture on a preparative scale and there is no possibility of influencing the selectivity or, as usually occurs with complex mixtures, the selectivity for one pair can be improved only at the expense of the selectivity for another pair. High numbers of theoretical plates are then necessary in order to avoid contamination of products with closely eluting compounds. Improvement of the throughput in those instances can be obtained only by adjusting the general geometric and kinetic factors, taking into account such limitations as the available pressure drop, the required plate number and the maximal cross-section of the column that which is practically feasible.

A number of workers have considered these general factors: the column diameter and efficiency were studied by Wolf[4], Godbille and Devaux[5,6] and Wehrli[2]; the effect of particle size was discussed by Wehrli[2] and Scott and Kucera[7]; and injection mode and recycling were studied by Wehrli[2] and Conroe[8].

The aim of this study was to investigate further the effect of two factors, the particle size and the injection mode, on the performance with respect to efficiency, loadability and throughput, because we felt that existing discussions in the literature left a number of crucial questions unanswered or reached conflicting conclusions. Particular attention was paid to the effect of peak tailing, caused by irregularities in the packing at the column wall, (local) overloading or the injection profile, as this effect often diminishes the throughput obtainable at a specified purity of the product.

The work was carried out using a normal silica adsorption system, as this is the most popular for preparative work.

THEORETICAL

Of decisive importance in both production-scale and analytical work is the amount per unit time. It may seem that in semi-preparative applications, such as structure elucidation, it is the amount per load which is the important parameter, but the time required to process one load determines how many samples can be treated per day or per week, so that the ultimate characteristic is the same in both cases instances, *i.e.*, the throughput (number of grams of material of a specified purity obtained per second).

An optimal choice of conditions has to be made with respect to the phase system and phase ratio, column dimensions, particle diameter, specific load (grams of material per gram of column packing) on the column and volume of the sample. Whatever phase system is chosen, it will have a limited linear range in the distribution isotherm; the concentration in the mobile phase corresponding to a specified deviation from this linearity will be denoted by $c_{i,m}^{\max}$. The concentration of the eluate must certainly be less than $c_{i,m}^{\max}$, as the solution in the first part of the column can only be more concentrated. An upper limit to the eluting concentration, $\alpha c_{i,m}^{\max}$, α being dependent on the dispersive processes within the column, and having a value between 0 and 1, will exist.

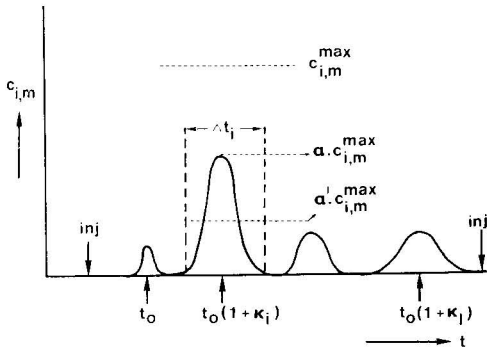

Fig. 1. Chromatogram, collection and injection interval.

At the time of elution of the peak maximum, we will obtain a momentary production rate of $w\alpha c_{i,m}^{max}$. However, averaged over the peak collection time of Δt_i sec, for compound i, the production rate, T_i', will be (see Fig. 1):

$$T_i' = \frac{w\alpha \cdot \int_{\Delta t_i} \frac{c_{i,m}}{\alpha c_{i,m}^{max}} \cdot dt}{\Delta t_i} \cdot c_{i,m}^{max} \tag{1}$$

For a gaussian peak and a collection time corresponding to 4 σ_t (95% yield), this "peak-averaged" production rate would be

$$T_i' = \frac{\sqrt{2\pi}}{4} \cdot w\alpha \cdot 0.95 \cdot c_{i,m}^{max} \tag{2}$$

The production rate, averaged over a long period, will depend on the injection frequency. For a complicated mixture, which completely fills the chromatogram, an injection is possible every $t_0(1 + \kappa_l)$ sec, where t_0 is the unretained retention time and κ_l is the capacity ratio of the last eluting compound. In that case, the "long-time-averaged" production rate or throughput will be

$$T_i = \frac{\alpha \cdot \int_{\Delta t_i} \frac{c_{i,m}}{\alpha c_{i,m}^{max}} \cdot dt}{t_0(1 + \kappa_l)} \cdot wc_{i,m}^{max} \tag{3}$$

The integral expression is a time, which in general will not deviate more than a factor of two or three from Δt_i itself.

If a gaussian time distribution is observed, this results in

$$T_i = \frac{\alpha \sqrt{2\pi} \cdot 0.95 \cdot \sigma_{t,i}}{t_0(1 + \kappa_l)} \cdot wc_{i,m}^{max} = \frac{\sqrt{2\pi}}{\sqrt{N}} \cdot 0.95 \cdot \alpha \cdot \frac{1 + \kappa_i}{1 + \kappa_l} \cdot wc_{i,m}^{max} \tag{4}$$

where N is the number of theoretical plates. In both equations, the important product $wc_{i,m}^{max}$ plays the dominant role; the other factors are either fixed numerical values,

such as $\sqrt{2\pi}$, or are dictated by the phase system and mixture at hand (α, κ_i and κ_1 for instance). We now include numerical factors such as $\sqrt{2\pi}$ and 0.95 in α and obtain

$$T_i = \alpha' N^{-\frac{1}{2}} \cdot \frac{(1 + \kappa_i)}{(1 + \kappa_1)} \cdot w c_{i,m}^{\max} \tag{5}$$

For simple mixtures, the sample injection repetition frequency can be higher, as pointed out by a number of workers[2,8,9]. The simplest case is that of a binary mixture, in which a sample can be injected every $\Delta t_i + \Delta t_j$. For a gaussian peak shape, this results in

$$T_i = \frac{\alpha \cdot \int_{\Delta t_i} \frac{c_{i,m}}{\alpha c_{i,m}^{\max}} \cdot \mathrm{d}t}{\Delta t_i + \Delta t_j} \cdot w c_{i,m}^{\max} = \alpha' \cdot \frac{(1 + \kappa_i)}{(2 + \kappa_i + \kappa_j)} \cdot w c_{i,m}^{\max} \tag{6}$$

which shows that in that case the required plate number has no influence.

The aim of optimization in preparative liquid chromatography, a maximum production rate or throughput, can now be simplified to maximum $c_{i,m}^{\max}$ and w. The constraints within which we must realize this are, of course, set by the specified purity of the product; there should be a possibility of choosing the Δt_i interval for the collection of compound i in such a way that the compound produced is of sufficient purity and with expensive products, in an acceptable yield. Optimization towards large w values should, of course, be effected while observing this constraint.

The allowable width or the collection interval, Δt_i, while specifying the yield or purity, is determined by (a) peak broadening due to dispersive effects in the column, in the simplest and mostly used description fully characterized by the plate number; (b) peak broadening due to non-linearity of the distribution isotherm; and (c) external peak broadening, particularly the volume and injection profile of the feed solution. The second effect will not be discussed here, mainly because a general quantitative description of the effect of this phenomenon, when operating together with dispersion and external broadening, is not available. In fact, we already took this effect into consideration in a crude manner while assuming a $c_{i,m}^{\max}$ value that should not be surpassed. This crude and somewhat arbitrary simplification may raise some doubts, but can be made plausible in the following way.

In the absence of dispersion and external broadening effects, the shape of the elution curve can be completely described by the distribution isotherm:

$$t_{\text{elution}}(c_{i,m}) = t_0 \left(1 + q \cdot \frac{\mathrm{d}c_{i,s}}{\mathrm{d}c_{i,m}}\right) \tag{7}$$

where q is the phase ratio. With two or more compounds chromatographed together, the situation is more complicated, because different solutes will influence each other's distribution behaviour, and without careful detailed study nothing can be said about the elution function that can be expected. However, also in this instance a $c_{i,m}^{\max}$ value will also undoubtedly exist; when we operate the column with ever-increasing loads of i and j, there will be a case where the $q \cdot (\mathrm{d}c_{i,s}/\mathrm{d}c_{i,m})$ value of one compound will be equal to the infinite dilution value of another one.

With the combined effects of non-linearity and dispersion, the $c_{i,m}^{max}$ value will be lower, but the extent cannot be calculated with theories available at present, and this in any event will require detailed knowledge of the distribution isotherms of i and j in the presence of each other. A liberal choice of a high $c_{i,m}^{max}$ value would require a high plate number and low injection volumes. Nevertheless, for the present discussion, which aims at the elucidation of the role of dispersion and external volumes, we can take $c_{i,m}^{max}$ as chosen, and consider its effect in the throughput via eqn. 1 and its effect on the maximum allowable other dispersive effect as given *a priori*.

Whatever the concentration load on a column may be, a certain plate number will be required in order to obtain sufficient purity. On the other hand, a certain maximum pressure will be given. With reasoning similar to that presented by Knox and Saleem[10] and Kraak *et al.*[11], we have

$$T_i = \alpha' N^{-\frac{1}{2}} \cdot \frac{1 + \kappa_i}{1 + \kappa_l} \cdot w c_{i,m}^{max} = \alpha' N^{-\frac{1}{2}} \cdot \frac{1 + \kappa_i}{1 + \kappa_l} \cdot \frac{vD}{d_p} \cdot \varepsilon A c_{i,m}^{max} \tag{8}$$

where $v = vd_p/D$, D is the diffusion coefficient, v is the migration velocity of the mobile phase, d_p is the particle diameter, ε is the porosity of the bed with respect to the mobile phase, and A is the area of the cross section of the column.
On the other hand, we have a pressure limitation, giving

$$\Delta p = \varphi \cdot \frac{vL\eta}{d_p^2} = \varphi D \eta d_p^{-2} N h v \tag{9}$$

where Δp is the pressure drop, φ is the shape factor of permeability, L is the column length, η is the viscosity of the mobile phase, $h = H/d_p$, and H is the plate height. Solving for d_p:

$$d_p = \varphi^{+\frac{1}{2}} D^{\frac{1}{2}} \eta^{\frac{1}{2}} \Delta p^{-\frac{1}{2}} N^{\frac{1}{2}} h^{\frac{1}{2}} v^{\frac{1}{2}} \tag{10}$$

Substituting into eqn. 8, we obtain

$$T_i = \alpha' \varphi^{-\frac{1}{2}} D^{\frac{1}{2}} \eta^{-\frac{1}{2}} \Delta p^{\frac{1}{2}} N^{-1} \left(\frac{v}{h}\right)^{\frac{1}{2}} \varepsilon A \, c_{i,m}^{max} \cdot \frac{1 + \kappa_i}{1 + \kappa_l} \tag{11}$$

Thus, while adapting d_p and L to the required plate number and the pressure limitation, T_i will be dependent on a number of physical parameters, which we can regard as constants, as soon as the phase system and column diameter are chosen, but proportional to the expression $v^{\frac{1}{2}}/h^{\frac{1}{2}}$, giving the effect of the choice of the operating point in the plate height curve.

Clearly, we must work under conditions such that v/h is as high as possible. All liquid chromatography dispersion theories give $h(v)$ expressions which for large changes of v can be approximated by

$$h = 2\,\alpha/v + \beta + \gamma v$$

The throughput, T_i, is therefore expressed by a proportionality as follows:

$$T_i \propto \frac{v^{\frac{1}{2}}}{(2\,\alpha/v + \beta + \gamma v)^{\frac{1}{2}}} = t(v)$$

Fig. 2 gives $t(\nu)$ as a function of ν, for $\alpha = 0.75$, $\beta = 3$ and $\gamma = 0.03$. Optimal kinetic conditions for preparative liquid chromatography are therefore obtained on the ascending branch of the H/v curve, in the region where the major part of the plate height is caused by intra-particle mass transfer. This suggests particle sizes in the range 30–100 μm, plate heights of millimetres and column lengths of several metres. In analytical columns, this leads to long retention times, as is universally known. In preparative liquid chromatography this drawback is more than compensated for by an increase in the allowable sample load, keeping the concentration of the solute constant.

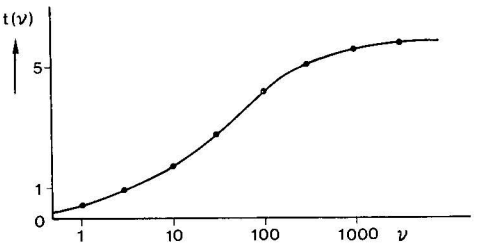

Fig. 2. Dependence of the factor $t(\nu) = (\nu/h)^{\frac{1}{2}}$ on the reduced velocity, ν. Assumed parameters for the plate height curve: $\alpha = 0.75$, $\beta = 3$ and $\gamma = 0.03$.

A similar discussion to that presented above was given by Scott and Kucera[7]. However, they assumed *a priori* that the working point is in the ascending part of the H/v curve, and therefore did not compare this point with other points nearer to the minimum in the H/v curve. Some results of their theoretical discussion do not agree with ours, *e.g.*, the effect of the phase ratio and the effect of using a longer column with increased particle sizes. In our treatment, "solvent economy" is not affected by this process, as $c_{i,m}^{\max}$ remains the same.

From eqn. 11, it can be seen that the cross-sectional area of the column has a direct proportional influence on the throughput. The above discussion, given for a fixed value of this area, therefore may seem useless, as an increase in the throughput can always be obtained by simply increasing the diameter of the column. The efficiency will be maintained because column performances in this respect do not change provided that the linear velocity is not changed[2,12,13]. The following limitations exist, however, for increase in column diameter:

(a) the realization of sufficient mechanical strength of the column, necessary for operating at high pressures, becomes increasingly difficult;

(b) heat dissipated within the column by friction cannot be conducted to the walls in columns with large cross-sections. Wider columns, especially when filled with small particles, are practically adiabatic.

EXPERIMENTAL

Apparatus

The experiments were carried out on a home-made liquid chromatograph constructed from a double-headed reciprocating pump (Orlita Type AE-10-4.4), a flow-through Bourdon-type manometer serving as a pulse damper and a variable-wavelength UV detector (Zeiss PM 4). The columns had a length of 25 cm and were

made of stainless-steel 316 tubing of I.D. 10–20 mm and O.D. 16–36 mm. The inside surfaces of the tubes were smoothed by honing. Three types of column-top terminators were used in combination with a sampling valve (Valco HPSV CV-6 UHPa) for introduction of the sample. In one injection mode (FSCD) a second pump (Orlita Type ZB-De) was used for feeding the injection flow. The column-end terminators had a conical shape with a top angle of 150°; a disc of PTFE wool prevented transport of packing material into the outlet tubing. All connections between the different parts of the chromatograph were made of 0.3–0.5-mm I.D. capillary tubing and 1/16-in. zero dead volume Swagelock connectors.

Materials

The materials used were 2,2,4-trimethylpentane, acetone, tetrabromoethane, chloroform, butanol-1 (Merck, Darmstadt, G.F.R.), silica gel SI 60 (Merck), ground and classified in particle size (d_p) ranges of 5–8 and 20–25 μm by means of an air classifier (Alpine MZR, Augsburg, G.F.R.). The test solutes were toluene, *o*-nitrotoluene and 2,4-dimethylphenol.

Procedures

The columns were filled by a balanced-density slurry technique. About 20% (w/w) of silica slurry in a mixture of chloroform and tetrabromoethane of sp. gr. 2.10 was placed into the metal stock tube (20 mm I.D., 100 cm length, wall thickness of 8 mm) to which the column was connected. The slurry was pumped into the column at a very high fluid velocity with a high-pressure, high-capacity pump (Burdoza, Giessen, G.F.R., Type V410) with 2,2,4-trimethylpentane at an ultimate pressure of 800 bar. After packing, the columns were washed with several column volumes of acetone and finally eluted with the eluent (trimethylpentane containing 1% of butanol-1) until the capacity ratios became constant.

For the calculation of the column efficiencies two methods for measuring the standard deviation were used: (i) half of the peak width at 0.607 of the maximal peak height (denoted by $H_{0.6}$ and $N_{0.6}$) and (ii) the peak width at 0.1 of the maximal height divided by 4.3 (denoted by $H_{0.1}$ and $N_{0.1}$).

In the loadability experiments the wavelength was adapted to the amount of injected sample in such a way that a linear response was obtained.

RESULTS AND DISCUSSION

Sample introduction

As was shown by Wehrli[2], the method of sample introduction significantly influences the column loadability. He showed that for large-diameter columns the loadability increases if the sample is simultaneously injected at different points on the cross-section of the column. In order to measure the effect of the method of sample introduction more extensively, three injection modes were tested with respect to band spreading, peak symmetry and column loadability. In all three modes a sample valve was used in combination with different column-top terminators (Fig. 3).

The in-column syringe injection as used by Knox and Parcher[14], creating conditions for the so-called infinite-diameter column, was omitted from the experiments because a lower loadability can be expected as only a fraction of the total bed is used by the sample. This simplest way of introducing the sample is shown in Fig.

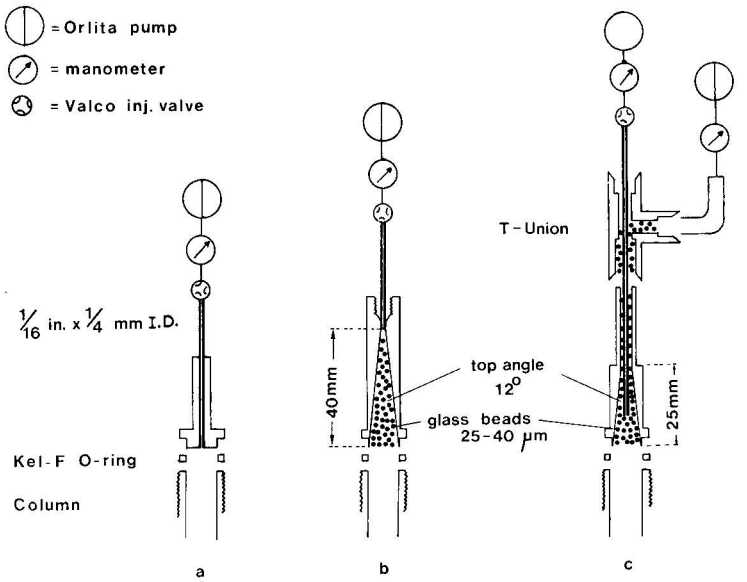

Fig. 3. Schematic representation of three column-top terminators.

3a and involves a spot injection in the middle of the cross-section of the column top. Although column efficiencies were found to be in close agreement with the values expected theoretically, all compounds investigated appear as peaks with some tailing in the 5–10% peak height range. The asymmetry factor, defined as the ratio of the peak width at 0.1 of the peak height of the front and back of the peak, decreases with increasing fluid velocity (Fig. 4). The asymmetry can be caused by a number of effects. Firstly, as a result of the forced stream lines in the first part of the column packing some stagnant mobile phase areas exist (*i.e.*, dead corners). During the injection, mass transport from the moving eluent to these stagnant areas occurs by diffusion or (perhaps) by reflection of the injection plug against the column packing as a result of the jet stream-like injection induced by the interruption of the flow during the switching of the valve. The release of the compounds from the stagnant areas into the moving eluent is slow as it is a diffusion-controlled process. This consequently leads to an asymmetric injection profile and to tailing peaks. At very low and high flow-rates, however, the asymmetry caused by the diffusion of the compounds into the stagnant areas must be small, as at low flow-rates the mass transport by diffusion is large enough to obtain equilibrium while at very high flow-rates the injection plug moves so fast along the stagnant areas that no significant mass transfer can occur.

The second reason for peak tailing might be the irregularities in the packing near the wall (*i.e.*, the so-called wall effect), which causes differences in flow-rates across the column. Another reason, column overloading, could be excluded in our experiments as no significant overloading occurred by injection the same amount of sample into an analytical column.

To avoid stagnant eluent areas, a conical column top, filled with glass beads, was installed between the column packing and injection valve (Fig. 3b). The glass-bead filled conical top first prevents the occurrence of stagnant eluent areas and

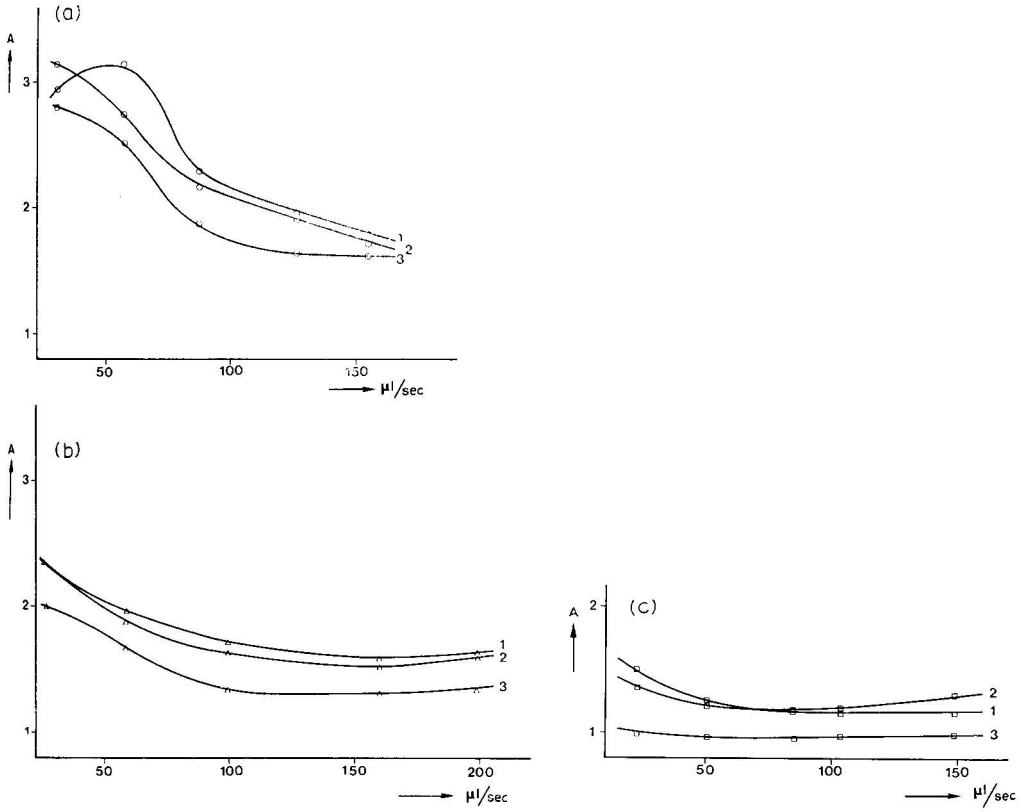

Fig. 4. Asymmetry (A) as function of the flow-rate for different injection modes. Column: 250 × 10 mm I.D., SI 60, d_p = 5–8 μm. Eluent: 2,2,4-trimethylpentane + 1% (v/v) butanol-1. Injection volume: 50 μl. Solutes: (1) toluene (κ = 0); (2) *o*-nitrotoluene (κ = 0.30); (3) 2,4-dimethylphenol (κ = 3.26). (a) Central injection; (b) conical disperser; (c) flow-surrounding conical disperser.

secondly might distribute the sample more equally across the separation column, diminishing local sample overloading at higher sample loads. As can be seen from Fig. 4, the asymmetry factors are indeed significantly smaller with the conical injection mode than with the flat injection mode. This experiment confirms that the stagnant eluent areas and inhomogeneous sample introduction act as a source of peak tailing.

Despite the improvement in the symmetry, tailing is still observed with the conical injection mode. The remaining tailing must be attributed to the so-called wall effects. In order to diminish the wall effects, a flow-surrounding injection system, similar in principal to that described by Webber and McKerrell[12], was tested (Fig. 3c). The system described by Webber and McKerrel is comparable with syringe injection in the eluent stream as eluent flows continuously through the column and forces the injection plug to move in certain flow lines away from the wall (*i.e.*, the surrounding flow injection leads to an infinite-diameter column). Thus, in this injection mode one can expect small loadabilities as only a small part of the packing is effectively used by the samples. To improve the loadability, the flow-surrounding system was combined with the conical glass-bead filled column inlet. By this means the sample

is more spread out when injected into the column packing, diminishing the risk of local overloading. Primary experiments with this injection mode showed that smaller asymmetry factors were obtained than with the other injection modes (Fig. 4c). It was found, however, that the ratio of the flow-rates of the injection and surrounding flow can influence the asymmetry significantly (Fig. 5). As was noticed with the other injection modes, smaller asymmetry factors were found at higher total flow-rates. For the retained compound 2,4-dimethylphenol almost perfect gaussian peaks were found at flow-rates above 50 μl/sec. The less retained compounds have some larger asymmetry factors (*ca.* 1.2) but are still much better than those obtained with the flat and conical injection system. The small remaining tailing even with the conical flow-surrounding system indicates that other effects, such as the geometrical shape of the column-end terminator, contribute. A more systematic investigation in this respect will be necessary in future.

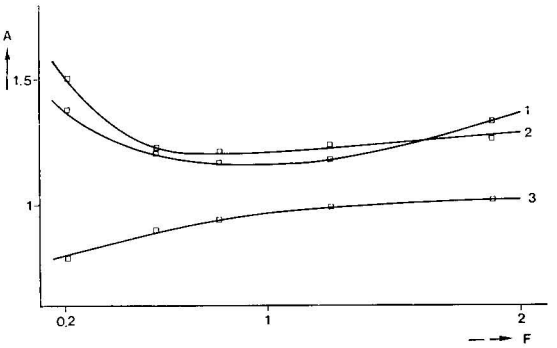

Fig. 5. Effect of the ratio of injection- and flow-surrounding flow (F) on the asymmetry factors (A) of the flow-surrounding conical disperser injection mode at constant total flow-rate. Conditions as in Fig. 4; total flow-rate, 85 μl/sec.

Column performance

The large-diameter columns were packed by a balanced-density slurry technique, as previously described[11], and H *versus* v plots were constructed for the three injection systems (Fig. 6a). The theoretical plate heights of the test compounds were calculated from the peak width at 0.607 of the peak height and their retention times. As can be seen from Fig. 6a, highly efficient 1-cm I.D. columns can be packed and there is no significant difference between the three injection modes. Such H *versus* v plots, based on the peak width measurements at 0.607 of the peak height or by drawing tangents, are valuable for characterizing roughly the performance of analytical columns. In preparative work, however, where one wishes to collect pure samples within the shortest collection interval, Δt_i, possible, these plots are less accurate as they ignore to a large extent the effect of tailing in the lower regions of the peak height. H *versus* v plots based on the measurement of peak standard deviations in the lower region of the peak heights (*i.e.*, 5–10%) are more realistic as they incorporate the surplus of resolution needed as the result of tailing to separate two compounds in such a way that pure fractions can be collected. Fig. 6b shows the H *versus* v plots for the three injection modes, calculated with peak widths measured at 0.1 of the peak height. The plots demonstrate clearly that significant differences in column efficiency exist if the

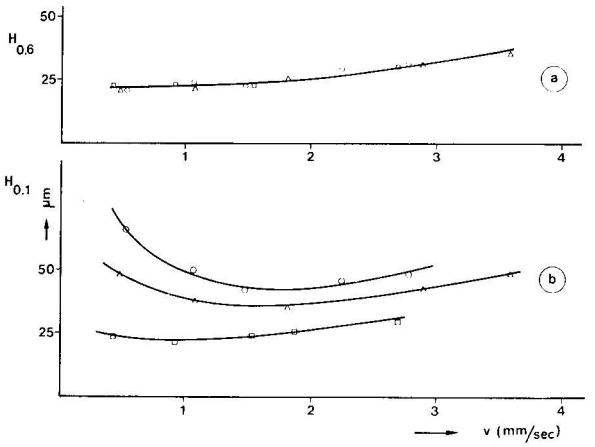

Fig. 6. *H versus v* curves with the three injection modes. Conditions as in Fig. 4; solute, 2,4-dimethylphenol. (a) H calculated with σ_t measurements at 0.607 of the peak height ($H_{0.6}$); (b) H calculated with σ_t measurements at 0.1 of the peak height ($H_{0.1}$). ○, Central injection; △, conical disperser; □, flow-surrounding conical disperser.

effect of tailing is included in the calculations. At these low sample concentrations the conical flow surrounding system is by far superior. The FSCD system gives an increase of about 20–100% in the effective resolution (taking into account the effect of the lower parts of the peak curves compared with the other injection modes).

In order to investigate if an increase in the column diameter influences the column efficiency, columns of I.D. 1, 1.5 and 2 cm were packed using the balanced-density slurry technique described and *H versus v* plots were constructed (Fig. 7). No significant decrease in efficiency was observed indicating that the packing procedure used is very suitable and gives reproducible packing characteristics.

Loadability aspects

In all experiments so far, very low sample concentrations were used in order to characterize the injection modes and column efficiency. For preparative work, however, a high production rate is necessary. One way of increasing the production

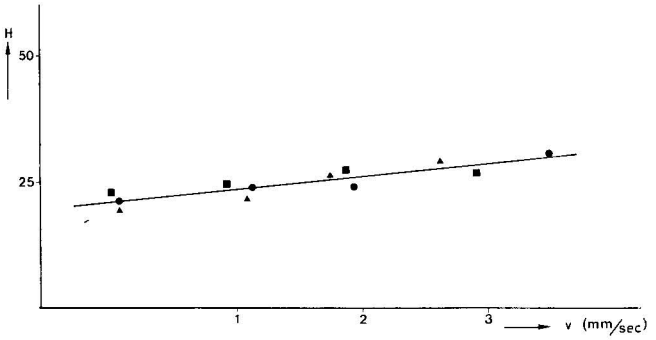

Fig. 7. Influence of the inner diameter of the column on the efficiency. Conditions as in Fig. 6a; central injection. I.D.: ●, 10 mm; ▲, 16 mm; ■, 20 mm.

rate is to increase the amount of sample injected or to increase the injection volume with a fixed sample concentration. The effect of sample loading on the number of theoretical plates measured with the three injection modes described and calculated from standard deviation measurements at 0.607 of the peak height is shown in Fig. 8a. Up to a certain concentration (amount) no significant decrease in column efficiency (*i.e.*, $H_{0.6}$) is found. At larger concentrations, however, the column is highly overloaded and the efficiency decreases drastically. As can be seen from Fig. 8a, no remarkable difference in the loadability curve is found for the flat and conical injection systems when calculated at 0.607 of the peak height. With the conical surrounding-flow injection system, however, the loadability (*i.e.*, maximum amount of sample that produces no change in N) is a factor of 2–3 smaller. This indicates that the sample injected with the conical surrounding-flow system uses only a fraction of the column packing and is close to an infinite-diameter column as obtained if syringe injection into the packing is used. If one includes, however, the effect of the lower parts of the peak curves in the N calculations by measurement of the peak width at 0.1 of the peak height (*i.e.*, $N_{0.1}$), the loadability curve up to 1 mg on a 1-cm I.D. column with the

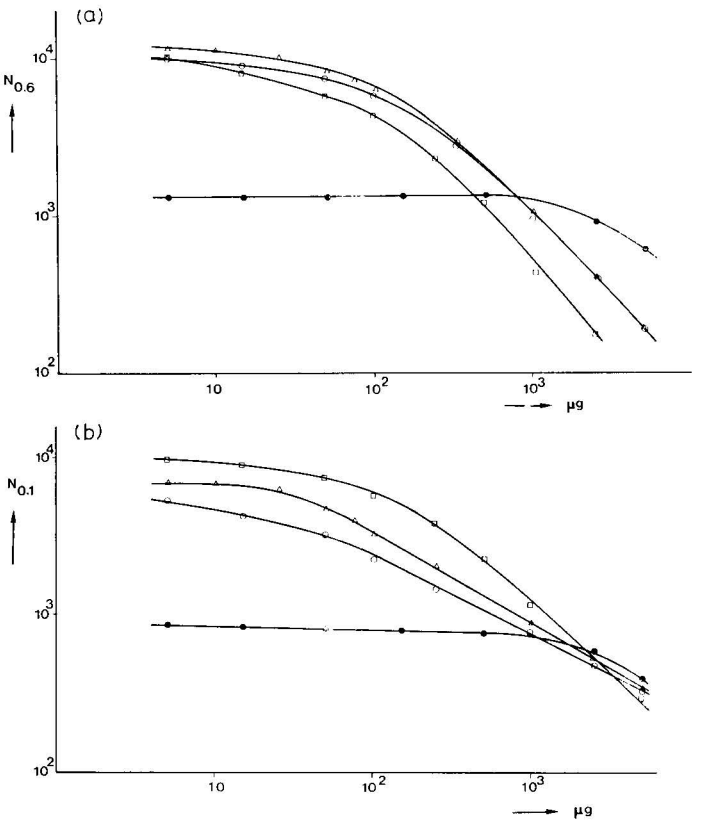

Fig. 8. Column loadability *versus* column efficiency. Conditions as in Fig. 4a; flow-rate, 85 µl/sec; solute, 2,4-dimethylphenol. (a) N calculated with σ_t measurements at 0.607 of the peak height ($N_{0.6}$); (b) N calculated with σ_t measurements at 0.1 of the peak height ($N_{0.1}$). ○, ●, Central injection; △, conical disperser; □, flow-surrounding conical disperser. d_p: □, △, ○, 5–8 µm; ●, 20–25 µm.

FSCD system is significantly better than those of the other injection systems, as can be seen in Fig. 8b. Only at larger sample concentrations is the performance of the FSCD system lower. The effect of the injection volume, containing a fixed amount of sample (250 μg), on the column efficiency calculated from the peak width at 0.6 ($N_{0.6}$) and 0.1 ($N_{0.1}$) of the peak height is shown in Fig. 9. The number of theoretical plates (*i.e.*, $N_{0.6}$) measured with the FSCD system is lower compared to the other injection systems as the column is highly overloaded when this amount of sample is injected. Fig. 9a shows that no decrease in efficiency occurs up to an injection volume of 1 ml. At larger injection volumes the peak shape is completely determined by the injection profile and the efficiency decreases drastically. With respect to peak symmetry, the injection systems perform in the order FSCD > conical > flat. Taking into account the effect of the peak tailing (*i.e.*, $N_{0.1}$), the FSCD system seems to be significantly better than the others, despite the fact that the column is overloaded, as is shown in Fig. 9b.

Another way of increasing the production rate is to increase the speed of separation as more sample can be injected in the same period of time. In practice, however, the pressure is limited and hence so is the speed of separation. As was derived

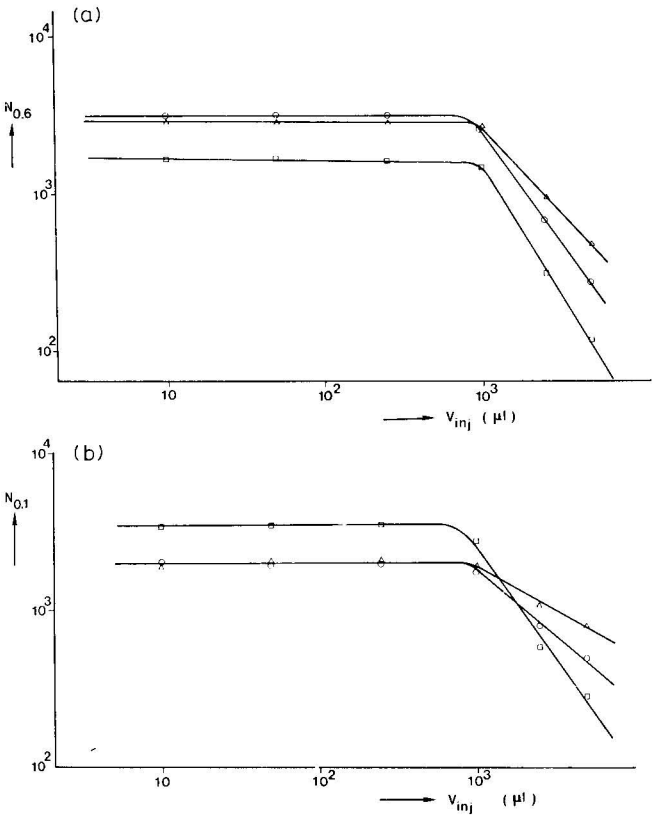

Fig. 9. Dependence of the column efficiency on the injection volume. Conditions as in Fig. 8; solute, 250 μg of 2,4-dimethylphenol. (a) N calculated with σ_t measurements at 0.607 of the peak height ($N_{0.6}$); (b) N calculated with σ_t measurements at 0.1 of the peak height ($N_{0.1}$). For designation of symbols, see Fig. 8.

theoretically, the production rate is dependent on the particle size, and is determined by the amount of sample injected and the speed of separation (*i.e.*, proportional to v/h). The result of the theoretical derivation of the production rate at limited pressure drop predicts higher production rates with long columns filled with large-diameter particles than on shorter columns filled with small particles.

In order to verify this result in practice, v/h *versus* v plots were constructed with small (5–8 μm) and larger (20–25 μm) particles (Fig. 10). This plot shows that if the pressure drop is limited and a fixed number of theoretical plates is required in order to obtain a complete separation, indeed a larger production rate is obtained on longer columns with larger particles, as v/h is largest with the large-diameter particles.

The loadability for the test compound on the column packed with 20–25-μm particles was found to be significantly larger than on the small particle diameter columns (see Fig. 8). An explanation for this effect has not yet been found.

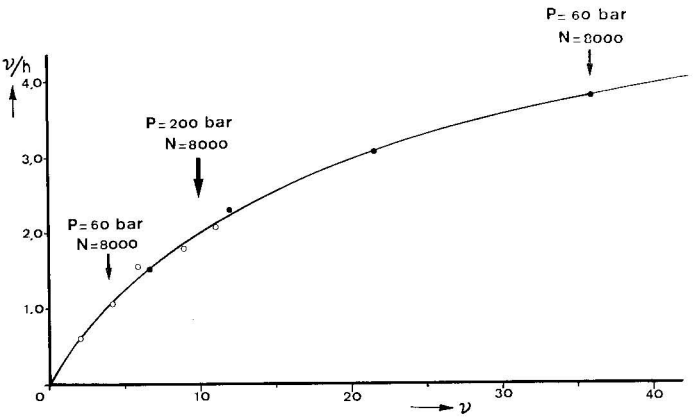

Fig. 10. v/h versus v curve. Conditions as in Fig. 6a. d_p: ○, 5–8 μm; ●, 20–25 μm.

CONCLUSIONS

(i) The production rate or throughput and solvent economy depends firstly on the usable range of the distribution isotherm. Further work, characterizing different phase systems, is necessary.

(ii) Theoretically, very long columns packed with relatively large particles give an improved throughput. The realization of this concept, together with the use of coupled columns, should be investigated.

(iii) The choice of the injection system will depend on the separation problem at hand. For difficult separations, the proposed FSCD system is to be preferred.

(iv) Columns with high efficiency and suitable for high pressures with an I.D. of 20 mm can be constructed.

(v) The characterization of column performance by measuring the peak width at 0.6 of the peak height or via tangents gives no insight into the performance of columns for preparative work.

ACKNOWLEDGEMENTS

Thanks are due to Mr. K. Camstra and Mr. P. J. de Quack for the construction of the main parts of the equipment and to Mr. F. Smedes for careful experimental work.

REFERENCES

1 K. J. Bombaugh and P. W. Almquist, *Chromatographia*, 8 (1975) 109.
2 A. Wehrli, *Z. Anal. Chem.*, 277 (1975) 289.
3 A. Wehrli, U. Hermann and J. F. K. Huber, *J. Chromatogr.*, 125 (1976) 59.
4 J. P. Wolf, *Anal. Chem.*, 45 (1973) 1248.
5 E. Godbille and P. Devaux, *J. Chromatogr. Sci.*, 12 (1974) 564.
6 E. Godbille and P. Devaux, *J. Chromatogr.*, 122 (1976) 317.
7 R. P. W. Scott and P. Kucera, *J. Chromatogr.*, 119 (1976) 467.
8 K. E. Conroe, *Chromatographia*, 8 (1975) 119.
9 J. A. Atteberry, *Chromatographia*, 8 (1975) 121.
10 J. H. Knox and M. Saleem, *J. Chromatogr. Sci.*, 7 (1969) 614.
11 J. C. Kraak, H. Poppe and F. Smedes, *J. Chromatogr.*, 122 (1976) 147.
12 T. J. N. Webber and E. H. McKerrell, *J. Chromatogr.*, 122 (1976) 243.
13 J. J. DeStefano and H. C. Beachell, *J. Chromatogr. Sci.*, 8 (1970) 434.
14 J. H. Knox and J. F. Parcher, *Anal. Chem.*, 41 (1969) 1599.

Journal of Chromatography, 148 (1978) 143–149

CHROM. 10,476

PROPERTIES OF MICRO-PACKED COLUMNS AND OF POROUS-LAYER OPEN-TUBULAR COLUMNS WITH GRAPHITIZED THERMAL CARBON BLACK

Th. WELSCH, W. ENGEWALD and J. POERSCHMANN
Department of Chemistry, Karl-Marx-University, Liebigstrasse 18, 701 Leipzig (G.D.R.)

SUMMARY

The properties of porous-layer open-tubular (PLOT) columns and of so-called micro-packed columns with graphitized thermal carbon black not coated with a liquid phase were compared by means of characteristic parameters such as HETP, permeability, capacity ratio and the *C* term in the Van Deemter equation.

It was found that micro-packed columns with graphitized thermal carbon black are useful for efficient and rapid separations and for the determination of the retention data of low-boiling isomers.

INTRODUCTION

Gas adsorption chromatography with graphitized thermal carbon black (GTCB) using classical packed columns is suitable for the separation of structural and geometrical isomers that have only very small differences in their physical properties. Moreover, retention data obtained on GTCB not coated with a liquid phase together with semi-empirical calculations of adsorption energy give useful information for the identification of separated compounds. For the solution of difficult separation problems, it is desirable to improve the separating power of GTCB columns. From the theoretical point of view two types of columns are applicable: porous-layer open-tubular (PLOT) columns[1,2] and so-called micro-packed columns[3–8]. Their applicability in gas–solid chromatography (GSC) with unmodified GTCB was examined in this work.

EXPERIMENTAL

Preparation of micro-packed columns

For filling small-diameter glass tubes with GTCB particles we used a technique similar to that described for the preparation of classical packed columns[9] using a variable-speed electric motor as a vibrator. The treatment of the column with ultrasonic waves proposed by Cramers *et al.*[3] was unsuitable in this instance.

The connection of the columns to the injection and detection system of a

Varian instrument was achieved with Swagelok T-pieces modified as an inlet splitter and a make-up gas inlet, respectively.

Preparation of PLOT columns

The preparation of PLOT columns with GTCB was similar to the procedure described by Vidal-Madjar *et al.*[10] using ultrasonically stabilized suspensions of about 20% GTCB dust in a low-boiling alkyl halide and a home-made capillary drying oven after Jennings *et al.*[11]. In this manner we produce PLOT columns with a length of 10 m and a GTCB layer of 10–20 μm.

RESULTS AND DISCUSSION

Properties of micro-packed columns

Micro-packed columns with GTCB possess high efficiency and good permeability, as shown in Table I in which the experimental values for the permeability (K) of some typical micro-packed columns are compared with values calculated according the equation given by Kozeny-Carman[12] and by Halász[13].

TABLE I

EXPERIMENTAL AND CALCULATED PERMEABILITIES (K) AND MINIMAL HETP VALUES FOR TYPICAL MICRO-PACKED COLUMNS WITH GTCB

Carrier gas, hydrogen; column temperature, 120°; $HEPT_{min}$ determined for *n*-hexane.

Column		*Particle size*	$K_{exp.}$	$K_{Koz.-Car.}$	$K_{Halász}$	$HETP_{min}$
Length (m)	*I.D. (mm)*	*(mm)*	*($cm^2 \times 10^{-7}$)*	*($cm^2 \times 10^{-7}$)*	*($cm^2 \times 10^{-7}$)*	*(mm)*
1.5	0.80	0.16–0.20	2.10	2.00	3.14	0.44
1.5	0.45	0.16–0.20	1.92	2.00	3.14	0.37
1.5	0.80	0.09–0.125	0.84	0.73	1.13	0.28
1.5	0.45	0.09–0.125	0.82	0.73	1.13	0.23
2.7	0.45	0.09–0.125	0.77	0.73	1.13	0.21
1.7	0.28	0.06–0.08	0.27	0.31	0.50	0.13

The measured values on vibrational packed columns agree well with the values calculated by the Kozeny-Carman equation, although in our work the pellets were not completely spherical and the ratio of particle diameter (d_p) to column diameter (d_c) was between 0.15 and 0.40 (see Figs. 1b and 1c). In agreement with the theory but contrary to the results of Rijks *et al.*[5], we found only a slight dependence of permeability on the column diameter. The K values calculated by the Halász equation are higher than the experimental values. Nevertheless, the Halász equation is helpful for estimating the permeability.

The minimal HETP values depend not only on the particle diameter but also on the column diameter. This could be explained by irregularities in packing and/or by random effects. From the fact that in these instances nearly the same permeability results, it follows that irregularities in the packing influence the efficiency to a greater extent than the permeability. This is also reflected by the plots of HETP values *versus*

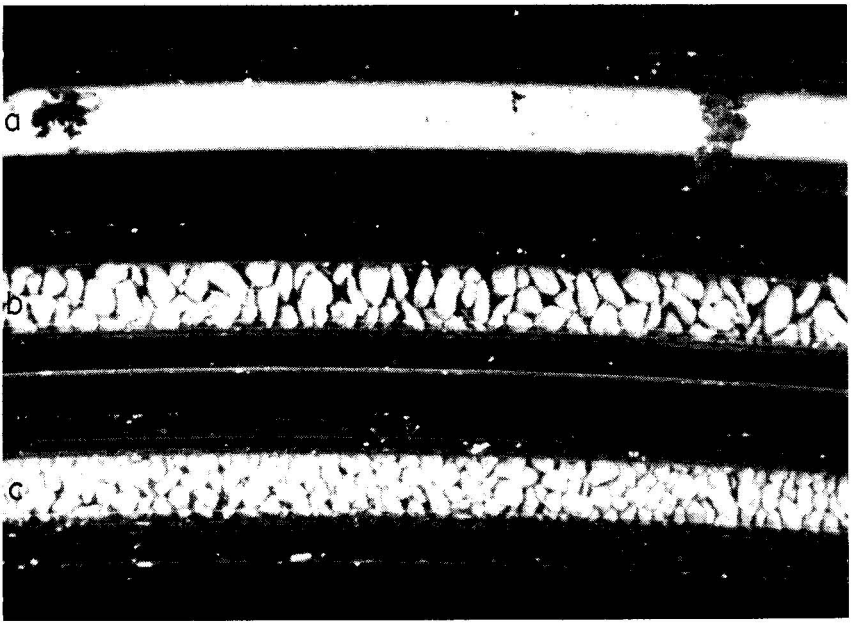

Fig. 1. Microphotographs of 0.45-mm I.D. columns filled with GTCB Sterling MT (Phase Separations, Solingen, G.F.R.). (a) PLOT column; (b) and (c) micro-packed columns with particle sizes of 0.16–0.20 and 0.09–0.12 mm, respectively.

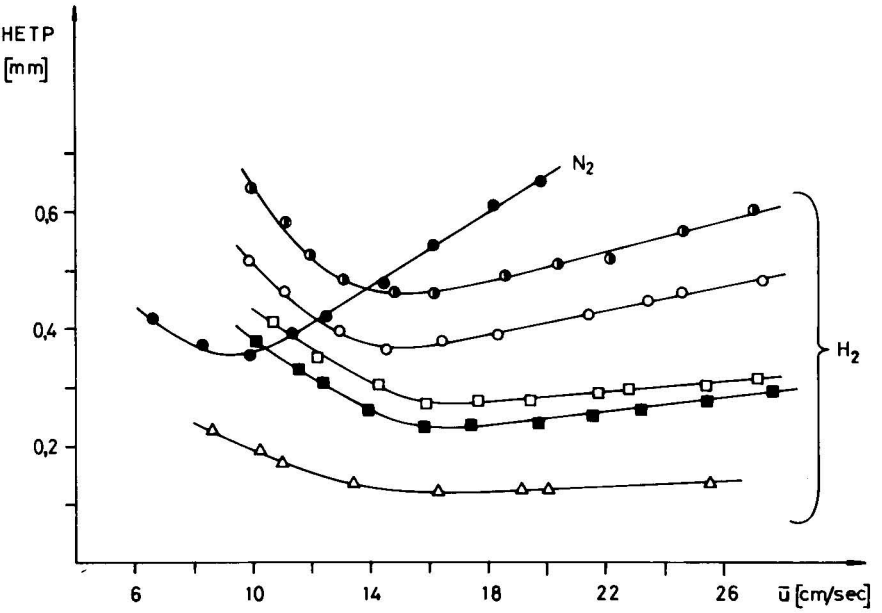

Fig. 2. Plots of HETP *versus* average linear gas velocity of the carrier gas measured for *n*-hexane ($k' \approx 19$) at 120° for different micro-packed columns. ●, ◑, Length = 1.5 m, I.D. = 0.8 mm, d_p = 0.16–0.20 mm; ○, length = 1.5 m, I.D. = 0.45 mm, d_p = 0.16–0.20 mm; □, length = 1.5 m, I.D. = 0.8 mm, d_p = 0.09–0.125 mm; ■, length = 1.5 m, I.D. = 0.45 mm, d_p = 0.09–0.125 mm; △, length = 1.7 m, I.D. = 0.28 mm, d_p = 0.06–0.08 mm.

average linear gas velocity for columns of different diameters with different particle sizes and different carrier gases (Fig. 2).

A comparison of columns with different particle sizes showed that the *C* term in the Van Deemter equation decreases as the particle diameter decreases. The *B* term decreases simultaneously because a decrease in particle size produces an increase in the pressure drop and thus a smaller diffusion coefficient. With decreasing particle size the minimal height equivalent to a theoretical plate also decreases, in accordance with eqn. 1 given by Huber *et al.*[14], provided that the diffusion coefficient of the components in the mobile phase is greater than the diffusion coefficient of the components in the GTCB particles. This assumption is confirmed by the very different slopes of the ascending part of the Van Deemter curve when hydrogen and nitrogen were used.

The usefulness of high-efficiency micro-packed columns with GTCB for the separation of low-boiling mixtures is shown in Figs. 3 and 4.

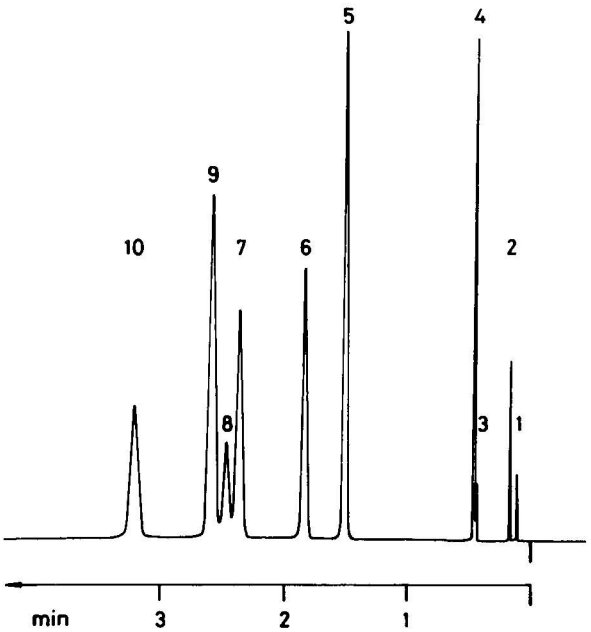

Fig. 3. Analysis of a mixture of gaseous hydrocarbons on a micro-packed column with GTCB. Column length, 1.7 m; I.D., 0.28 mm; GTCB, Sterling MT, particle size 0.06–0.08 mm; column temperature, 40°; carrier gas, hydrogen; inlet pressure, 7.2 bar. Peaks: 1 = methane; 2 = ethane; 3 = propene; 4 = propane; 5 = isobutane; 6 = 1-butene; 7 = isobutene; 8 = *n*-butane; 9 = *cis*-2-butene; 10 = *trans*-2-butene.

Properties of PLOT columns

The column efficiency expressed as the HETP (Table II) is unsatisfactory. The measured *C* term in the Van Deemter equation corresponds to the value obtained by Vidal-Madjar *et al.*[10], while the permeability is slightly poorer. Although the thickness of the GTCB layer is greater in our work, the k' values are not sufficient for a good separation of low-boiling mixtures.

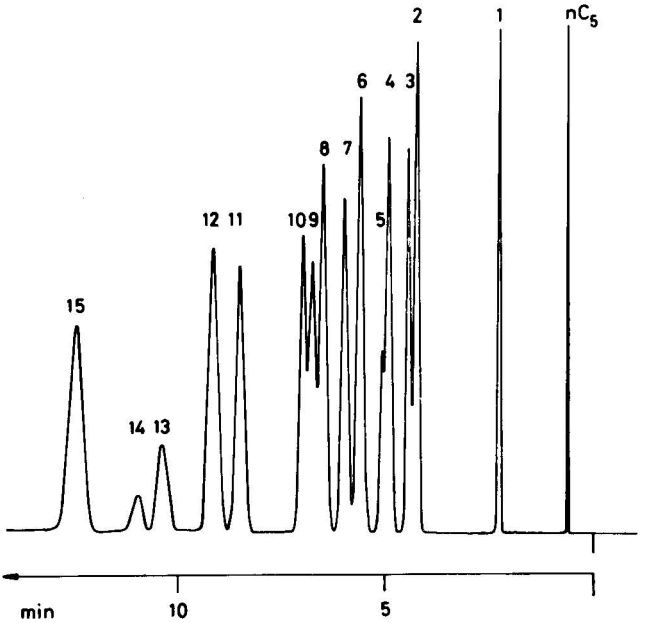

Fig. 4. Analysis of a mixture of isooctanes on a micro-packed column with GTCB. Column length, 2.7 m; I.D., 0.45 mm; GTCB, Sterling MT, particle size 0.09–0.125 mm; column temperature, 150°; carrier gas, hydrogen; inlet pressure, 5 bar. Peaks (with retention indices in parentheses): 1 = 2,2,3,3-tetramethylbutane (619); 2 = 2,2,3-trimethylpentane (676); 3 = 2,2,4-trimethylpentane (679); 4 = 3-methyl-3-ethylpentane (689); 5 = 2,3,4-trimethylpentane (691); 6 = 3,3-dimethylhexane (701); 7 = 2,2-dimethylhexane (706); 8 = 2,4-dimethylhexane (713); 9 and 10 = diastereomeric 3,4-dimethylhexane (716 and 719); 11 = 3-ethylhexane (737); 12 = 2,5-dimethylhexane (743); 13 = 4-methylheptane (754); 14 = 3-methylheptane (759); 15 = 2-methylheptane (770).

Moreover such columns exhibit some disadvantages:

(a) The preparation procedure is very time consuming.

(b) The reproducible production of a uniform layer is difficult. During the evaporation of the solvent some parts of the capillary column remain vacant (see Fig. 1a) or some GTCB particles break away and lead to obstructions.

(c) The retention characteristics of the GTCB can be changed by the suspension liquid. Trace amounts of thermal decomposition products of alkyl halides deposited on the surface of the GTCB and change their adsorption properties.

(d) The sample capacity is very low and high splitting ratios are necessary.

Comparison of different types of column

Table II compares some typical types of GTCB columns by means of the HETP, C term of the Van Deemter equation, optimal average linear gas velocity ($\bar{u}_{opt}$), inlet pressure for this velocity ($p_{i_{opt}}$), permeability (K), partition ratio for n-hexane (k'), resolution between n-hexane and 3-methylhexane (R) and gross retention time for the last peak, 3-methylhexane (t_{ms}). It can be seen that the micro-packed columns Nos. 2 and 3 exhibit good parameters. Their $HETP_{min}$ values are smaller than those of a packed and of a PLOT column. In addition the C term of column No. 3 is the smallest of all, thus permitting a much higher "working velocity" of carrier gas to be

TABLE II

COMPARISON OF DIFFERENT TYPES OF GTCB COLUMNS

Carrier gas, hydrogen; column temperature, 120° (40° for PLOT column).

No.	*Type of column*	*Length (m)*	*I.D. (mm)*	*Particle size (mm)*	$HETP_{min}$ *(mm)*	C *(sec* $\times$ 10^{-4}*)*	$\bar{u}_{opt}$ *(cm/sec)*	$P_{i_{opt}}$ *(bar)*	K *(10^{-7} cm²)*	k'	R	t_{ms} *(min)*
1	Packed	1.5	1.65	0.16–0.20	0.65	32	11.2	0.65	2.3	15.0	6.1	6.9
2	Micro-packed	1.5	0.80	0.16–0.20	0.44	15	15.5	1.20	2.1	16.8	7.7	5.9
3	Micro-packed	1.5	0.45	0.09–0.125	0.23	5	16.4	4.20	0.8	17.6	10.5	5.8
4	PLOT	10.0	0.45	—	1.20	13	26.5	0.24	141	7.1	8.1	9.6

applied without loss of resolution. This type of column is therefore very useful in the so-called high-speed GSC.

The partition ratio is nearly the same for classical packed and micro-packed columns. The resolution for micro-packed column No. 3 is 1.7 times higher than that obtained with the packed column with a shorter analysis time. Hence for the same resolution, the analysis time for a micro-packed column is much smaller. A drawback of this type of column may be the inlet pressure, which limited the column length by necessitating the use of a commercial instrument.

As mentioned above, the PLOT column has a poorer minimal HETP value than the micro-packed column, and even a significant increase in length does not compensate for this effect. With a longer analysis time the resolution obtained on the PLOT column is higher than that with columns Nos. 1 and 2, but lower than that of the micro-packed column No. 3*. The good permeability should allow the use of high "working velocities" at a low pressure drop. The limiting factor is, however, the relatively high C term in the Van Deemter equation.

CONCLUSIONS

The so-called micro-packed columns represent a good compromise in GSC with GTCB between resolution, analysis time and sample capacity. Particularly for the analysis of low-boiling mixtures they have certain advantages over PLOT columns: the preparation time is very short; $HETP_{min}$ is smaller; the C term in the Van Deemter equation is small; the resolution that can be obtained in a given time is better; the sample capacity is greater; and the unchanged adsorption properties of GTCB permit the precise and accurate determination of retention data.

REFERENCES

1 C. Horváth, *Dissertation*, Frankfurt/Main, 1963.
2 L. S. Ettre and J. E. Purcell, *Advan. Chromatogr.*, 10 (1974) 1.
3 C. A. Cramers, J. Rijks and P. Boček, *J. Chromatogr.*, 65 (1972) 29.
4 V. G. Berezkin, L. A. Shkolina and A. T. Svyatoshenko, *J. Chromatogr.*, 99 (1974) 111.
5 J. A. Rijks, C. A. Cramers and P. Boček, *Chromatographia*, 8 (1975) 482.
6 F. Bruner, P. Ciccioli, G. Bertoni and A. Liberti, *J. Chromatogr. Sci.*, 12 (1974) 758.
7 F. Bruner, P. Ciccioli and G. Bertoni, *J. Chromatogr.*, 90 (1974) 239.
8 S. Cirendini, J. Vermont, J. C. Gressin and C. L. Guillemin, *J. Chromatogr.*, 84 (1973) 21.
9 J. Tranchant (Editor), *Practical Manual of Gas Chromatography*, Elsevier, Amsterdam, 1969, p. 118.
10 C. Vidal-Madjar, J. Ganansia and G. Guiochon, in R. Stock (Editor), *Gas Chromatography 1970*, Institute of Petroleum, London, 1971, p. 20.
11 W. G. Jennings, K. Yabumoto and R. H. Wohleb, *J. Chromatogr. Sci.*, 12 (1974) 344.
12 G. Deininger, *Ber. Bunsenges. Phys. Chem.*, 77 (1973) 145.
13 I. Halász, *Ber. Bunsenges. Phys. Chem.*, 77 (1973) 140.
14 J. F. K. Huber, H. H. Lauer and H. Poppe, *J. Chromatogr.*, 112 (1975) 377.

* The comparison is not quite exact, as the k' value of the peak in question is smaller on the PLOT column (the capacity ratio on the PLOT column was measured at a temperature that was 80° lower).

Journal of Chromatography, 148 (1978) 151–157

CHROM. 10,520

DIRECT DETERMINATION OF SPECIFIC SURFACE AREAS AND ROUGHENING FACTORS OF GLASS CAPILLARIES

Z. SUPRYNOWICZ, A. GORGOL and J. WÓJCIK

Department of Physical Chemistry, Institute of Chemistry, M. Curie-Skłodowska University, Lublin, Nowotki 12 (Poland)

SUMMARY

In order to promote the spreading of stationary phases, the inside surface of glass open-tubular columns can be modified chemically or physically (surface roughening). The measure of surface roughening after an etching process is the Wenzel coefficient, defined as the ratio of the cosines of the contact angles or the specific surface areas after and before etching.

A method for the direct determination of the specific surface areas of glass capillaries is described. The method is based on the thermal desorption of nitrogen with the use of a microcatharometer. The results of measurements of specific surface areas of glass open-tubular columns etched with "etching ether" are presented.

INTRODUCTION

The presence of a thin, homogeneous layer of stationary phase is necessary for satisfactory operation and high efficiencies of glass open-tubular columns. Many methods for the preparation of high-efficiency open-tubular columns with up to 8000 theoretical plates per metre have been described[1–5]. However, the preparation of a reproducible glass surface is not easy in view of its good wettability by polar stationary phases. This is connected with the poor wettability of high-energy surfaces by most organic liquids[6]. High-energy surfaces undergo ready adsorption and hydration, which change their properties to those of low-energy surfaces (autophobic effect)[7]. Using the so-called critical surface tension (CST) as a measure of the wettability of a solid surface, it was shown that CST for smooth, clean glass surfaces is $\leqslant 30$ dyne/cm and the surface tensions of typical stationary phases are in the range 30–50 dyne/cm. According to the definition of CST these values lead to non-wettability of the glass surfaces[2]. For these reasons, the inside surfaces of glass open-tubular columns have to be modified physically[1–5] and/or chemically[8,9] (surface roughening).

The chemical modification involves changing the chemical character of the glass surface by adsorption or chemical binding with active hydroxyl groups, followed by increasing or decreasing the CST of a given surface to the surface tension of the particular stationary phase concerned. On this basis, the concept of the chemical compatibility of solid surfaces and stationary phases has been proposed[8,9].

Physical modifications include all processes for increasing the specific surface area, *e.g.*, etching with inorganic acids and bases, or gases such as hydrogen chloride and hydrogen fluoride. Contact with water or aqueous solutions leads to irreversible changes of the glass surface that are difficult to control and that can be explained in terms of hydration and ageing processes[7,8]. Gaseous hydrogen chloride or hydrogen fluoride, the latter commonly evolved from the so-called "etching ether", are usually used[1–5,8].

The possibilities of directly coating the inside surface of capillaries with fine salt particles (analogous to preparing procedures for PLOT columns) such as sodium chloride[3] or crystallisation of insoluble salts (barium carbonate)[10] have been reported. Such modified glass surfaces were shown according to Wenzel[11] to have decreased contact angles and are able to create thin, homogeneous liquid films. The Wenzel coefficient (r), defined as the ratio of cosines of the contact angles ($\cos\theta'/\cos\theta$) or the specific surface areas (A'/A) after and before etching was used as the measure of surface roughening:

$$r = \frac{\cos\theta'}{\cos\theta} = \frac{A'}{A} \tag{1}$$

Nečasová and Tesařík[12] introduced another measure of the wettability of a glass surface, the so-called "wettability coefficient", defined as the ratio of the interfacial tensions after (γ_e') and before (γ') the modification process:

$$k_w = \frac{\gamma_e'}{\gamma'} \tag{2}$$

Both interfacial tensions can be calculated from the Young equation, using the surface tensions measured by the capillary rise method for a liquid with a zero contact angle (methanol)[12]. The wettability coefficient seems to be a very characteristic value but its usefulness has not yet been fully verified. Actual contact angle measurements can be carried out for a flat surface[2], which is not a convenient choice and may give results that are not equivalent to the contact angles that exist in capillaries.

The measurement of specific surface area seems to be a simple method for the determination of the surface roughening and Wenzel's coefficient. The most popular method for this measurement is the classical B.E.T. method, with static weight or volumetric pressure measurement[13]. Faster and better characterization of adsorption under dynamic conditions can be achieved by the Nelson and Eggersten method[14], based on the low-temperature thermal desorption of nitrogen or argon. A modification of the last method, proposed by Engelhard and Engelbrecht[15], permitted the measurement, by changing the measurement temperature range ($-190°$ to $-70°$), of the specific "effective" surface area; the surface can be covered with an adsorption or a liquid layer.

The measurement of specific surface area is a non-destructive method and can be carried out so as to give an average value for the full length of a capillary or for any part of it. The adsorbate pressure gradient and the very small volume in which adsorption takes place complicate the determination of the specific surface area of a capillary by the thermal desorption method, which may explain the lack of suitable apparatus in the literature.

In this work, investigations of the low-temperature processes of nitrogen and argon adsorption–desorption in thin capillaries were carried out.

EXPERIMENTAL

A simple apparatus for the measurement of specific surface areas and determination of surface roughening factors was constructed (Fig. 1). The apparatus consists of a pressurised adsorbate gas mixture supply (1), two flow restrictors (2), a measured capillary (3) in a cooling bath (4), a calibration injector (7), measurement (5) and reference (6) cells of the microcatharometric detector (6-μl cell volume), a retarding tube (8) and two damping (buffer) capillaries (9). A Model 21 S recorder (Laboratorní Přístroje, Prague, Czechoslovakia) was used.

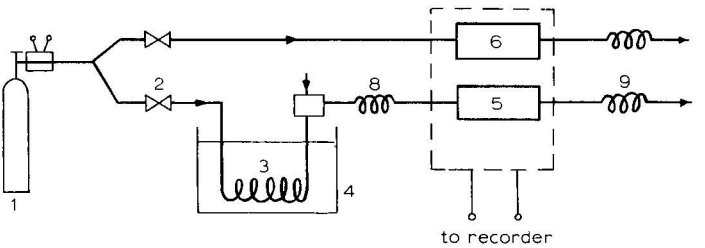

Fig. 1. Schematic diagram of the apparatus for specific surface area measurements: 1, Nitrogen–hydrogen mixture supply; 2, flow regulators; 3, capillary; 4, low-temperature bath (liquid nitrogen); 5, measurement cell of the detector; 6, reference cell of the detector; 7, calibration injector; 8, retarding tube; 9, damping (buffer) capillaries.

The measurements are based on a Wheatstone bridge; through the measurement and reference cells flow two independent streams of a 10% (v/v) nitrogen–hydrogen mixture. The adsorption process takes place at the temperature of liquid nitrogen and the desorption process at room temperature. Both processes change the balance of the Wheatstone bridge, which causes a detector signal that is proportional to the surface area.

The retarding glass tube (8, Fig. 1), with an inside diameter a few times larger than that of the capillary, is connected in the measurement stream between the capillary and detector in order to eliminate the irregular peak shape of the desorption curve.

Fig. 2 shows three typical examples of desorption curves, which were obtained with different lengths (volumes) of the retarding tube. For the determination of specific surface area the desorption curves were used. The microcatharometer was of the flow-through type and consisted of two tungsten wires, each 20 μm in diameter and of 30 Ω resistance.

The surface under the desorption curve in each instance was directly proportional to the specific surface area of the capillary. The regular shape (Fig. 2c) is suitable for integration purposes and can be achieved by an appropriate choice of the dimensions of the retarding tube. However, this causes a longer measurement time.

The total volume of the measurement stream is very small, both in itself and relative to the volume of the cooled capillary. This difference influences the shape of

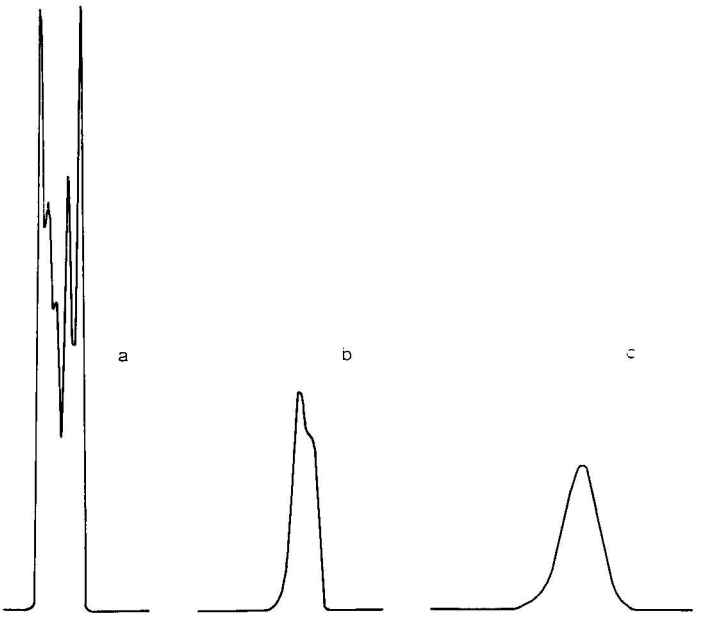

Fig. 2. Typical examples of desorption curves obtained with different lengths (volumes) of retarding tube of I.D. 1.0 mm: a, 15 m; b, 25 m; c, 35 m.

the desorption peak and results in baseline noise. To eliminate this noise, damping capillaries (9, Fig. 1) were used.

Connections with low temperature gradients were used to connect the capillaries into the measurement stream. The measurement parameters were as follows: flow-rate of adsorbate mixture, 3 ml/min, which corresponds to a linear velocity of *ca.* 100 cm/sec for a 0.25-mm I.D. capillary; detector sensitivity, 1500 mV/ml·mg, achieved at a current of 340 mA; limit of detection, 30 ppm of nitrogen, for a 10% (v/v) nitrogen–hydrogen mixture. The maximal adsorbate concentration during the measurements on hydrogen fluoride etched capillaries was *ca.* 1000 ppm.

RESULTS AND DISCUSSION

To estimate the usefulness of the apparatus, simple measurements using smooth-walled capillaries of different lengths were carried out.

Fig. 3 (Table I) shows the linear relationship between the specific surface area and capillary length. Line 1 represents the geometrical surface area of the inside capillary walls, calculated from its dimensions, and line 2 the results calculated from the desorption peaks using the Temkin[16] equation (eqn. 3) and the B.E.T. adsorption isotherm:

$$a_m = a\left(1 - \frac{p}{p_s}\right)\left[1 + \frac{\left(\frac{p_s}{p}\right) - 1}{C}\right] \tag{3}$$

$$A = a_m N_A w_m \tag{3a}$$

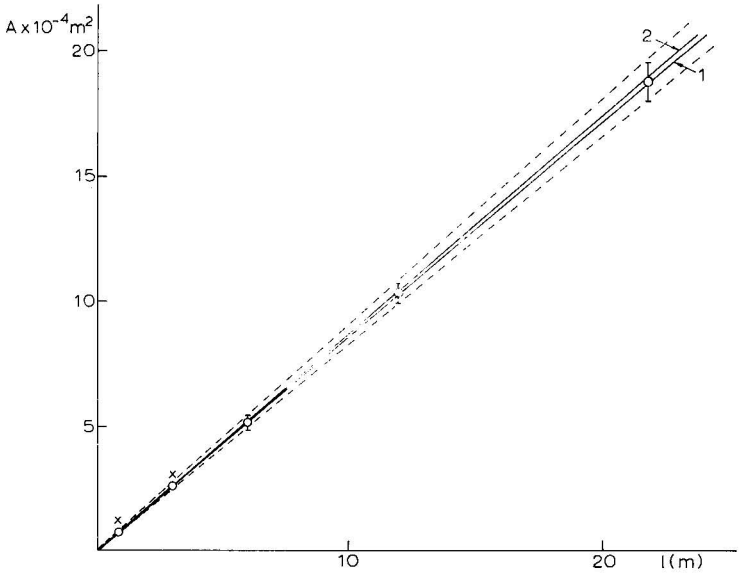

Fig. 3. Relationship between specific surface area and smooth-wall capillary length (numerical data from the Table I).

TABLE I

COMPARISON OF SPECIFIC SURFACE AREAS CALCULATED FROM GEOMETRICAL CAPILLARY DIMENSIONS AND DETERMINED BY MEANS OF THE THERMAL DESORPTION METHOD

Measured capillary length (m)	*Geometrical surface area, A_g ($m^2 \times 10^4$)*	*Measured surface area, A_m ($m^2 \times 10^4$)*	A_m/A_g
0.82	0.71	0.81	1.17
3	2.58	2.98	1.15
6	5.16	5.26	1.019
12	10.3	10.35	1.005
21.9	18.8	18.9	1.005

where

a = amount of nitrogen adsorbed (mole/m);
a_m = amount adsorbed in monolayer (monolayer capacity) (mole/m);
C = constant in the B.E.T. equation;
p = actual nitrogen pressure in the mixture (N/m^2);
p_s = pressure of nitrogen-saturated vapour at the temperature of adsorption (n/m^2);
A = specific surface area (m^2/m);
N_A = Avogadro constant (molecules/mole);
w_m = settling surface area of one adsorbate molecule (m^2/molecule).

The Tiomkin equation (the use of the coordinates of a single adsorption point) introduces a systematic error of *ca.* 5%, due to the simplifications involved. The error

in calculations of geometrical surface areas due to inaccuracies in the measurement of the inside diameter of a capillary and the variation in the inside diameter along the length of a capillary is $\pm 4\%$ (see the area between the broken lines in Fig. 3).

It can be seen that the geometrical and measured specific surface areas agree within the limits of experimental error (Fig. 3). As one of the calculation parameters is the ratio of adsorbate pressures, p/p_s, the pressure gradient for a long capillary should be taken into account. For this purpose, the original B.E.T. equation (eqn. 4) has been modified, assuming that the inlet pressure is higher than the outlet pressure and that the whole adsorption process is a sum of many individual processes without a pressure gradient (p = constant, (eqn. 5):

$$\frac{\frac{p}{p_s}}{a\left(1-\frac{p}{p_s}\right)} = \frac{1}{a_m C} + \frac{C-1}{a_m C}\cdot\frac{p}{p_s} \tag{4}$$

$$a = \frac{a'_m p_s}{(p_{in} - p_0)}\left[\frac{1}{C-1}\cdot\ln\frac{1+(C-1)\frac{p_0}{p_s}}{1+(C-1)\frac{p_{in}}{p_s}} + \ln\frac{1-\frac{p_0}{p_s}}{1-\frac{p_{in}}{p_s}}\right] \tag{5}$$

where a'_m is the monolayer capacity with pressure gradient correction, p_{in} is the nitrogen inlet pressure and p_0 is the nitrogen outlet pressure.

Comparison of eqns. 4 and 5 shows that the error due to neglecting the pressure gradient is significant only for long capillaries. For example, it is *ca.* 7% for a capillary of length 60 m and I.D. 0.33 mm. The calculations for short capillaries up to 20 m long can be performed without a pressure gradient correction (eqns. 3 or 4). Eqns. 4 and 5 allow the adsorption isotherm to be determined and permit a more precise determination of the specific surface area, for which two or three measurements at different concentrations of the nitrogen–hydrogen mixture are necessary.

The Wenzel coefficient can be determined as the ratio of two specific surface areas, after and before the glass capillary modification process (eqn. 1).

The use of the method described may give interesting information about the "effective" specific surface area, after coating the inside capillary wall with a thin film of a stationary liquid or another liquid, such as water; the determination can be carried out by changing the desorption temperature from room temperature to $-70°$.

The method and the apparatus described can be used generally for the determination of specific surface areas, roughening factors and "effective" specific surface areas in very thin capillaries, or in open-tubular columns, including PLOT (SCOT) columns, without their destruction. The homogeneity of surface roughening along the length of a capillary can also be tested. Measurements of specific surface areas and determinations of roughening factors for some capillaries of different lengths and made of different types of glasses etched by the same method were carried out. For the same capillaries the wettability coefficients were determinated by means of Nečasová and Tesařík's method[12]. The results are given in Table II.

Three types of glass (two soda-lime and one borosilicate glass) were etched

TABLE II

SPECIFIC SURFACE AREAS, ROUGHENING FACTORS, ROUGHENING HOMOGENEITY FACTORS AND WETTABILITY COEFFICIENTS FOR DIFFERENT TYPES OF GLASS CAPILLARIES ETCHED WITH "ETCHING ETHER" AT 380°

Type of glass	*A' ($m^2 \times 10^4/m$)*		*A ($m^2 \times 10^4/m$), geometrical surface area*	*r*	*Roughening homogeneity coefficient, r_h*	*γ'_c (dyne/cm)*	*γ' (dyne/cm)*	*k_w*
	Measured							
	Full length of capillary	*1-m section*						
Soda-lime, type I	56.7	54.4	10.68	5.3	1.04	20.46	19.85	1.031
Soda-lime, type II	81.09	79.0	10.36	7.8	1.03	20.08	19.63	1.023
Borosilicate (Sovirel)	32.14	32.9	7.85	4.1	0.98	20.83	21.33	0.977

with "etching ether" at 380°. The capillaries were subsequently flushed with oxygen at 380° in order to remove carbon residues. The specific surface areas of the etched capillaries were measured on the apparatus described and specific surface areas of smooth-walled capillaries were calculated from their geometrical dimensions. It can be seen from Table II that there is a close correlation between the roughening factors and wettability coefficients. Because a roughening factor of about 4 corresponds to a wettability coefficient of about 1, this value seems to be the most suitable for promoting the spreading of stationary liquids. The roughening homogeneity factor (r_h) is the ratio of the specific surface area per metre calculated from the measurement for the full capillary length to the specific surface area measured for a 1-m section of the same capillary. The closer to unity this roughening homogeneity factor is, the better is the homogeneity of roughening (Table II).

REFERENCES

1 M. Novotný and A. Zlatkis, *Chromatogr. Rev.*, 14 (1971) 1.
2 G. Alexander and G. A. F. M. Rutten, *J. Chromatogr.*, 99 (1974) 81.
3 J. J. Franken, G. A. F. M. Rutten and J. A. Rijks, *J. Chromatogr.*, 126 (1976) 117.
4 F. J. Onuska and M. E. Comba, *J. Chromatogr.*, 126 (1976) 133.
5 J. Krupčík, M. Kristín, M. Valachovičová and Š. Janiga, *J. Chromatogr.*, 126 (1976) 147.
6 H. W. Fox, E. F. Hare and W. A. Zisman, *J. Phys. Chem.*, 59 (1955) 1097.
7 E. F. Hare and W. A. Zisman, *J. Phys. Chem.*, 59 (1955) 335.
8 M. Novotny and K. D. Bartle, *Chromatographia*, 7 (1974) 122.
9 K. D. Bartle and M. Novotný, *J. Chromatogr.*, 94 (1974) 35.
10 K. Grob, *Fortschritte in der Gas- und Flüssigkeits-Chromatographie*, Plenary Lecture, Leipzig, G.D.R., November, 1976.
11 R. Wenzel, *Ind. Eng. Chem.*, 28 (1936) 988.
12 M. Nečasová and K. Tesařík, *J. Chromatogr.*, 79 (1973) 15.
13 S. Brunauer, P. H. Emett and E. Teller, *J. Amer. Chem. Soc.*, 60 (1938) 309.
14 F. M. Nelson and F. T. Eggersten, *Anal. Chem.*, 30 (1958) 1387.
15 H. Engelhard and B. P. Engelbrecht, *Chromatographia*, 4 (1971) 66.
16 M. J. Temkin, *Zh. Fiz. Khim.*, 29 (1955) 1610.

Journal of Chromatography, 148 (1978) 159–167

CHROM. 10,417

COMPARISON OF INTERPOLATION METHODS FOR THE INTERPRETATION OF RETENTION DATA IN GAS CHROMATOGRAPHY

L. SOJÁK
Institute of Chemistry, Comenius University, Bratislava (Czechoslovakia)
and
M. S. VIGDERGAUZ
Institute of Organic and Physical Chemistry, Academy of Sciences of the U.S S.R., Kazan (U.S.S.R.)

SUMMARY

On the basis of high-precision measurements of the retention times of alkylbenzenes, the accuracies of the determinations of linear and logarithmic retention indices were compared, and the correlation between the structure and the retention of isomers of these two interpolation characteristics was investigated. The linear retention index can be measured more accurately than the logarithmic value. Fine correlations between structure and retention are different for the two types of retention indices; logarithmic retention indices are more suitable for these correlations.

INTRODUCTION

Retention quantities can be divided into absolute, relative and interpolation types[1]. Interpolation characteristics enable one to determine the elution moment of the maximum sorbate zone in the range of elution moments of the maximum zones of two standards. The most widespread is the logarithmic shape of the interpolation elution characteristics with standards created by two neighbouring *n*-alkanes, z and $z+1$, introduced by Kováts[2] as the retention index, I. Vigdergauz[3] suggested a linear shape for the interpolation characteristics, *i.e.*, the linear retention index, J. The analogous function (multiplied by 100) under the name of the arithmetical retention index was recommended by Harbourn[4].

The linear retention indexis calculated on the basis of the measured retention times of the sorbate x (t_{R_x}) and *n*-alkanes with z and $z+1$ carbon atoms in the molecules (t_{R_z}, $t_{R_{z+1}}$), or by measuring the respective distances between the ordinates of the maxima of peaks on the chromatogram [$\Delta l_{(x,z)}$ and $\Delta l_{(z+1,z)}$]:

$$J = \frac{t_{R_x} - t_{R_z}}{t_{R_{z+1}} - t_{R_z}} + z = \frac{\Delta l_{(x,z)}}{\Delta l_{(z+1,z)}} + z$$

The analytical relationship between the quantities J and I has the following form[5]:

$$J = \frac{\sigma^{\delta I/100} - 1}{\sigma - 1}$$

where

$$\sigma = \frac{t'_{R_{z+1}}}{t'_{R_z}} = \frac{t_{R_{z+1}} - t_{R_z}}{t_{R_z} - t_{R_{z-1}}}$$

and

$$\delta I = I - 100\,z$$

Hence the difference between the values $100J$ and I depends on the value of the coefficient σ, *i.e.*, on the selectivity of the sorbent for a homologous series of *n*-alkanes with $I \geqslant 100\,J$. The value of σ varies between 1.4 and 3.4 for commonly used liquid phases, with the higher values corresponding to non-polar phases and room temperature[1]. The maximum of the difference $I - 100\,J$ within this range, which corresponds to $\delta I = 50$–60, increases from 4.2 to 15.0 units. For squalane the maximum of the difference $I - 100\,J$ increases from 8 to 16 units when the temperature is decreased from 100° to 0° and for polypropylene glycol from 7 to 14 units[6].

A survey of the use of linear retention indices for describing separations in gas chromatography was published by Vigdergauz[1]. In comparison with logarithmic retention indices, for determining the values of linear retention indices there is no need for logarithmic calculations or the determination of the elution time of the non-sorbing gas (t_0). Apart from the simple determination involved, the linear retention index also fulfils some of the other requirements of retention characteristics, for example the quantity J can be expressed with the help of the separation and activity coefficients of the sorbate and standards under consideration[1].

The possibility of correlations with the structure of compounds being analysed is a significant feature of the logarithmic retention index. With linear retention indices these relationships have not yet been studied, even if the validity of such relationships is assumed. This paper is devoted to a comparison of the accuracies of the determinations of linear and logarithmic retention indices on the basis of high-precision measurements of the retention times of alkylbenzenes, and to a comparison of fine correlations between the structures and retentions of alkylbenzene isomers using these two interpolation characteristics.

EXPERIMENTAL

Forty-seven aromatic hydrocarbons were studied by capillary gas chromatography: benzene and C_7–C_{15} alkylbenzenes on three stationary phases of different polarity [squalane (SQ), acetyltributyl citrate (ATC) and 1,2,3-tris(cyanoethoxy)-propane (TCEP)] at two temperatures. A device securing a high accuracy of measurement was used for measuring retention times[7]. For the calculation of J values the same

TABLE I

LINEAR RETENTION INDICES OF ALKYLBENZENES ON SQUALANE, ACETYLTRIBUTYL CITRATE AND 1,2,3-TRIS(CYANOETHOXY)PROPANE

Carrier gas: for SQ, 4.0 atm hydrogen; for ATC, 1.0 atm nitrogen; for TCEP, 1.0 atm nitrogen.

Compound	*Squalane*		*Acetyltributyl citrate*		*1,2,3-Tris(cyanoethoxy)propane*	
	$J_{80.8}$	$J_{95.4}$	$J_{81.5}$	$J_{95.2}$	$J_{84.7}$	$J_{94.2}$
Benzene	6.3459	6.3849	7.7450	7.7834	11.309	11.497
Toluene	7.4163	7.4581	8.7711	8.8098	12.230	12.411
Ethylbenzene	8.3213	8.3634	9.6622	9.7046	12.998	13.159
1,4-Xylene	8.4576	8.5025	9.7458	9.7842	13.091	13.266
1,3-Xylene	8.4788	8.5231	9.7893	9.8295	13.117	13.267
1,2-Xylene	8.6980	8.7548	10.0794	10.1093	13.624	13.894
Isopropylbenzene	9.0078	9.0344	10.2495	10.2803	13.235	13.425
n-Propylbenzene	9.2195	9.2595	10.5148	10.5564	13.531	13.771
1-Methyl-3-ethylbenzene	9.3353	9.3753	10.6282	10.6654	13.764	14.008
1-Methyl-4-ethylbenzene	9.3561	9.4001	10.6336	10.6720	13.781	14.029
1-Methyl-2-ethylbenzene	9.4842	9.5348	10.8961	10.9474	14.209	14.421
1,3,5-Trimethylbenzene	9.5314	9.5762	10.7954	10.8349	13.975	14.150
tert.-Butylbenzene	9.5796	9.6345	10.9978	11.0223	13.782	14.024
1,2,4-Trimethylbenzene	9.7286	9.7865	11.0542	11.0817	14.393	14.625
Isobutylbenzene	9.7627	9.8233	11.0635	11.0906	13.676	13.936
sec.-Butylbenzene	9.7724	9.8343	11.0882	11.1181	13.775	14.012
1-Methyl-3-isopropylbenzene	9.9650	10.0049	11.1855	11.2104	14.046	14.206
1,2,3-Trimethylbenzene	10.0306	10.0658	11.3234	11.3695	15.041	15.248
1-Methyl-4-isopropylbenzene	10.0311	10.0587	11.2257	11.2571	14.100	14.272
1-Methyl-2-isopropylbenzene	10.0723	10.1024	11.3649	11.4003	14.426	14.652
1,3-Diethylbenzene	10.1669	10.1996	11.4251	11.4589	14.317	14.523
1-Methyl-3-propylbenzene	10.2040	10.2395	11.4470	11.4834	14.289	14.498
n-Butylbenzene	10.2172	10.2577	11.5164	11.5593	14.349	14.554
1,2-Diethylbenzene	10.2468	10.2888	11.5931	11.6383	14.706	14.991
1-Methyl-4-propylbenzene	10.2477	10.2887	11.4825	11.5242	14.338	14.552
1,4-Diethylbenzene	10.2538	10.2954	11.5182	11.5604	14.424	14.656
1-Methyl-2-propylbenzene	10.3024	10.3491	11.6448	11.6927	14.737	15.005
1,3-Dimethyl-5-ethylbenzene	10.3388	10.3756	11.5867	11.6216	14.506	14.746
1,4-Dimethyl-2-ethylbenzene	10.4438	10.4900	11.7774	11.8211	14.980	15.164
1-Methyl-3-*tert.*-butylbenzene	10.4735	10.5156	11.8143	11.8499	14.468	14.684
1,3-Dimethyl-4-ethylbenzene	10.5075	10.5584	11.8489	11.8985	15.036	15.226
2-Phenyl-2-methylbutane	10.5270	10.5934	11.9060	11.9687	14.407	14.635
1,2-Dimethyl-4-ethylbenzene	10.5566	10.6097	11.9222	11.9723	15.085	15.289
1,3-Dimethyl-2-ethylbenzene	10.5573	10.6142	12.0144	12.0436	15.324	15.577
1-Methyl-4-*tert.*-butylbenzene	10.6029	10.6586	11.9404	11.9911	14.584	14.826
2-Phenylpentane	10.6320	10.6870	12.0052	12.0321	14.506	14.751
1,2-Dimethyl-3-ethylbenzene	10.7427	10.8083	12.1297	12.1661	15.487	15.729
1,2,4,5-Tetramethylbenzene	10.9969	11.0324	12.2222	12.2633	15.646	15.780
1,2,3,5-Tetramethylbenzene	11.0352	11.0714	12.2790	12.3227	15.724	15.964
1,3-Diisopropylbenzene	11.1034	11.1300	12.3296	12.3527	14.611	14.805
n-Pentylbenzene	11.1893	11.2288	12.4917	12.5325	15.133	15.332
1,2,3,4-Tetramethylbenzene	11.2111	11.2653	12.5823	12.6452	16.264	16.550
1,3-Dimethyl-5-*tert.*-butylbenzene	11.3708	11.4010	12.6492	12.6733	15.176	15.385
1,4-Diisopropylbenzene	11.3876	11.4301	12.6697	12.7071	15.030	15.187
1,3,5-Triethylbenzene	11.8392	11.8750	13.1026	13.1183	15.498	16.016
Pentamethylbenzene	12.4143	12.4897	13.8709	13.9519	17.469	17.871
1,3,5-Triisopropylbenzene	12.7650	12.7737	14.0365	14.0359	15.550	15.698

values of t_R were used as were used for the I values that were used for comparison[8]. The calculated values of the linear retention indices of alkylbenzenes on SQ at 80.8° and 95.4°, on ATC at 81.5° and 95.2° and on TCEP at 84.7° and 94.2° are shown in Table I.

RESULTS AND DISCUSSION

Accuracy of measurement of linear and logarithmic retention indices

The standard deviations for linear and logarithmic retention indices of alkylbenzenes on SQ, ATC, TCEP are compared in Table II.

TABLE II

COMPARISON OF MEAN STANDARD DEVIATIONS OF LINEAR AND LOGARITHMIC RETENTION INDICES ON SQUALANE, ACETYLTRIBUTYL CITRATE AND 1,2,3-TRIS-(CYANOETHOXY)PROPANE

Squalane				*Acetyltributyl citrate*				*1,2,3-Tris(cyanoethoxy)propane*			
80.8°		*95.4°*		*81.5°*		*95.2°*		*84.7°*		*94.2 °C*	
I	*100 J*	*I*	*100 J*	*I*	*100 J*	*I*	*100 J*	*I*	*100 J*	*I*	*100 J*
0.03	0.03	0.03	0.03	0.09	0.06	0.05	0.04	0.22	0.13	0.21	0.12

The standard deviations of the values of $100\,J$ and I were identical (*ca.* 0.03) for the most accurate measurements on squalane. On ATC and especially on TCEP the standard deviations of J were significantly smaller. The differences in the accuracies of the values of J and I are due to the fact that errors caused by the inaccuracy of the determination of t_0 do not affect J. Further, when determining J, errors arising from errors in the determination of the differences $t_{R_x} - t_{R_z}$ and $t_{R_{z+1}} - t_{R_z}$ are less dependent on the fluctuations in the operating conditions in the range from injection to t_{R_z} than when determining I. In this connection, a significant influence of column ageing on the accuracy of I was found on ATC and especially on TCEP, *e.g.*, the retention indices of alkylbenzenes on TCEP decreased by 0.3 unit in 1 day[8].

It follows from the comparison of the accuracies of the linear and logarithmic retention indices that the former can be measured more accurately than (or at least as accurately as) the latter.

Correlations between structure and retention indices

A number of dependences between the structures of alkylbenzenes and their retentions expressed as logarithmic retention index have been demonstrated previously[9–11]. Our aim was to establish correlations between values of ΔJ and $\mathrm{d}J/\mathrm{d}T$ and the structures of alkylbenzenes using linear retention indices.

Difference in retention indices on two stationary phases. Semenčenko *et al.*[12], by correlating the differences in the linear indices of oxygen-containing compounds on polyethylene glycol 6000 (PEG) and Apiezon L (APL) ($\Delta J = J^{\mathrm{PEG}} - J^{\mathrm{APL}}$), and J^{APL} achieved the group identification of esters, acids, peroxides and primary, secondary and tertiary alcohols, in a similar manner to results with logarithmic retention indices. The identification of isomers on the basis of such dependences is usually difficult. However, through correlations between accurate values of ΔI and the structures of alkylbenzene

isomers, characteristic dependences have been found[11]. These dependences have not been confirmed by comparing the corresponding correlations of ΔJ values on SQ, ATC, TCEP for mono-, di-, tri-, tetra- and pentaalkylbenzenes, not only for the corresponding differences in the separate values of $\delta(\Delta J)$ or $\delta(\Delta I)$, but sometimes also for the characteristic sequence of their quantities for the respective positional and configurational isomers. For example, it can be seen from Table III that the values of ΔI for trialkylbenzenes increase in the order 1,3,5- < 1,2,4- < 1,2,3-trialkylbenzenes; the values of $\Delta J_1 = J^{ATC} - J^{SQ}$, however, increase in the order 1,3,5- < 1,2,3- < 1,2,4-trimethylbenzene. Similar differences can be seen from Table III for other alkylbenzenes.

TABLE III

COMPARISON OF DIFFERENCES IN RETENTION INDICES, ΔJ AND ΔI VALUES, AND STRUCTURES OF ALKYLBENZENES AT 80°

$\Delta J_1 = J^{ATC} - J^{SQ}$; $\Delta I_1 = I^{ATC} - I^{SQ}$; $\Delta J_2 = J^{TCEP} - J^{SQ}$; $\Delta I_2 = I^{TCEP} - I^{SQ}$.

Alkylbenzene	$100\,\Delta J_1$	ΔI_1	$100\,\Delta J_2$	ΔI_2
1,3,5-Trimethylbenzene	126.2	121.8	436.0	425.2
1,2,4-Trimethylbenzene	132.6	127.7	455.3	455.8
1,2,3-Trimethylbenzene	129.0	136.3	490.9	488.8
1,3-Dimethyl-5-ethylbenzene	124.6	123.4	405.1	404.3
1,3-Dimethyl-4-ethylbenzene	133.9	128.1	443.8	432.3
1,4-Dimethyl-2-ethylbenzene	133.2	128.7	444.8	432.6
1,2-Dimethyl-4-ethylbenzene	136.3	129.1	443.0	434.4
1,2-Dimethyl-3-ethylbenzene	138.7	136.7	462.8	462.7
1,3-Dimethyl-2-ethylbenzene	145.7	136.8	464.5	462.0
1,3,5-Trimethylbenzene	126.2	121.8	436.0	425.2
1,3,5-Triisopropylbenzene	127.2	123.4	271.3	273.2
1,3,5-Triethylbenzene	126.4	126.0	340.4	358.7
1,3,5-Trimethylbenzene	126.2	121.8	436.0	425.2
1,3-Dimethylbenzene	130.9	126.2	456.7	446.3
Methylbenzene	135.3	130.9	472.6	476.4
1,3,5-Triethylbenzene	126.4	126.0	340.4	358.7
1,3-Diethylbenzene	125.6	128.2	404.9	405.2
Ethylbenzene	133.9	132.0	460.0	448.2
1,3,5-Triisopropylbenzene	127.2	123.4	271.3	273.2
1,3-Diisopropylbenzene	122.5	126.3	341.3	343.7
Isopropylbenzene	124.0	131.4	413.5	418.5

Fig. 1 shows the dependence of the difference in the values of $I^{SQ}_{80.8} - 100J^{SQ}_{80.8}$ on I^{SQ}_{80} for alkylbenzenes. It can be seen that this difference increases from zero for an alkylbenzene eluted with an *n*-alkane z up to a maximum value of 10.2 units corresponding to an alkylbenzene with a retention index $I = 100\,z + 50$, then it decreases to zero for an alkylbenzene eluted with an *n*-alkane $z+1$. Hence the smallest values of J compared with I are shown by alkylbenzenes eluted in the middle between neighbouring *n*-alkanes. Similar dependences were determined on SQ even at a temperature of 95.4° as well as on ATC and TCEP at both temperatures. Fig. 2 shows the dependence of the value of the difference $I - 100\,J$ on the values of I on SQ, ATC and TCEP at two temperatures. It can be seen that $I - 100\,J$ increases with decreasing

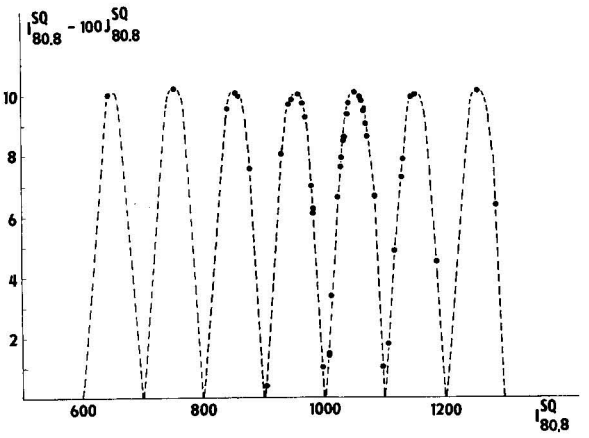

Fig. 1. Dependence of the difference $I^{SQ}_{80.8} - 100\,J^{SQ}_{80.8}$ on $I^{SQ}_{80.8}$ for alkylbenzenes.

polarity of the stationary phase in the series TCEP > ATC > SQ and with decreasing column temperature.

It follows from the above results that the deviations in correlations of the values of ΔJ and ΔI are the greater the nearer to the middle of the *n*-alkanes *z* and *z*+1 the given sorbate is eluted, the less polar is the stationary phase and the lower is the temperature.

Temperature increments of retention indices. The dependences between the linear and logarithmic retention indices and the column temperature were studied by Saha and Mitra[6]. It follows from their results[1] that the dependence between *J* and column temperature can be approximated by a straight line, in a similar manner to the temperature dependence of *I*, and that the slope $\mathrm{d}(100J)/\mathrm{d}T$ is usually greater than $\mathrm{d}I/\mathrm{d}J$. It is assumed that the values of $\mathrm{d}J/\mathrm{d}T$ are specific for materials of a certain structure in the same way as the values of $\mathrm{d}I/\mathrm{d}T$, which means that they can be used for purposes of identification with the same results.

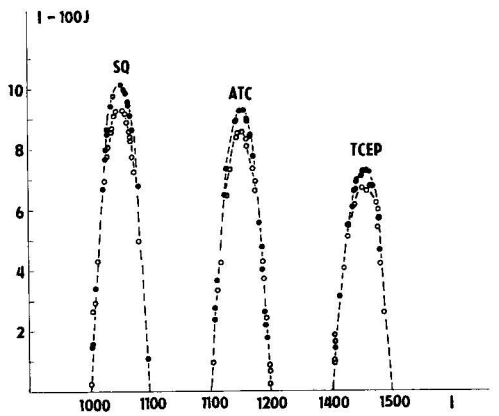

Fig. 2. Dependence of the difference $I - 100\,J$ on *I* for squalane (SQ), acetyltributyl citrate (ATC) and 1,2,3-tris(cyanoethoxy)propane (TCEP) at two temperatures. SQ: ●, 80.8°; ○, 95.4. ATC: ●, 81.5°; ○, 95.2°. TCEP: ●, 84.7°; ○, 94.2°.

The temperature increments of the retention indices (dI/dT) of the alkylbenzenes reflect the fine structural differences of isomers[10]. These correlations were not confirmed for values of dJ/dT. Table IV compares the values of $100\ dJ/dT$ and dI/dT with the structures of trialkylbenzenes. It can be seen that the orders of the dI/dT values for the positional isomers of trialkylbenzenes on all three stationary phases are identical: 1,3,5- < 1,2,4- < 1,2,3-trialkylbenzenes. For the values of dJ/dT on SQ, however, there is the following sequence: 1,2,3- < 1,3.5- < 1,2,4-trimethylbenzene, on ATC 1,2,4- < 1,3,5- < 1,2,3- and on TCEP 1,3,5- < 1,2,3- < 1,2,4-trimethylbenzene. Similar differences in the values of $100\ dJ/dT$ and dI/dT can also be seen in Table IV for some other alkylbenzenes.

TABLE IV

COMPARISON OF TEMPERATURE INCREMENTS, $100\ dJ/dT$ AND dI/dT VALUES, AND STRUCTURES OF ALKYLBENZENES ON SQUALANE, ACETYLTRIBUTYL CITRATE AND 1,2,3-TRIS(CYANOETHOXY)PROPANE

Alkylbenzene	*SQ*		*ATC*		*TCEP*	
	100 dJ/dT	*dI/dT*	*100 dJ/dT*	*dI/dT*	*100 dJ/dT*	*dI/dT*
1,3,5-Trimethylbenzene	0.310	0.239	0.290	0.206	1.83	2.20
1,2,4-Trimethylbenzene	0.400	0.288	0.200	0.264	2.44	2.38
1,2,3-Trimethylbenzene	0.240	0.337	0.340	0.312	2.20	2.65
1,3-Dimethyl-5-ethylbenzene	0.250	0.218	0.250	0.182	2.53	2.18
1,4-Dimethyl-2-ethylbenzene	0.320	0.260	0.320	0.229	1.94	2.32
1,3-Dimethyl-4-ethylbenzene	0.350	0.281	0.360	0.249	2.00	2.46
1,2-Dimethyl-4-ethylbenzene	0.360	0.286	0.370	0.253	2.15	2.49
1,3-Dimethyl-2-ethylbenzene	0.400	0.309	0.210	0.287	2.66	2.63
1,2-Dimethyl-3-ethylbenzene	0.450	0.329	0.270	0.303	2.55	2.73
1,3,5-Triisopropylbenzene	0.060	0.015	0.040	0.074	1.55	1.28
1,3,5-Triethylbenzene	0.250	0.167	0.110	0.117		2.20
1,3,5-Trimethylbenzene	0.310	0.239	0.290	0.206	1.83	2.20
1,3,5-Trimethylbenzene	0.310	0.239	0.290	0.206	1.83	2.20
1,3-Dimethylbenzene	0.300	0.245	0.290	0.213	1.58	2.07
Methylbenzene	0.290	0.245	0.280	0.213	1.91	2.03
1,3,5-Triethylbenzene	0.250	0.167	0.110	0.117		2.20
1,3-Diethylbenzene	0.220	0.244	0.250	0.201	2.20	2.19
Ethylbenzene	0.290	0.265	0.310	0.225	1.69	2.14
1,3,5-Triisopropylbenzene	0.060	0.015	0.040	−0.074	1.55	1.28
1,3-Diisopropylbenzene	0.180	0.195	0.170	0.137	2.04	1.94
Isopropylbenzene	0.180	0.264	0.220	0.214	2.00	2.11

Fig. 3 shows the dependence of the difference $dI^{SQ}/dT - 100\ dJ^{SQ}/dT$ on $I^{SQ}_{80.8}$ for alkylbenzenes. It can be seen that this difference gradually changes with increasing retention of alkylbenzenes between the alkanes z and $z+1$ from positive to negative values. Alkylbenzenes eluted immediately after n-alkane z have the greatest positive values of difference (the values of $100\ dJ/dT$ are significantly lower than dI/dT). Alkylbenzenes eluted immediately before n-alkane $z+1$ have the greatest negative values of the difference (the values of $100\ dJ/dT$ are significantly higher than dI/dT). Alkylbenzenes with a retention index $I^{SQ}_{80.8} \approx 100\ z + 40$ have $d(100\ dJ)/dT \approx$ $\approx dI/dT$. A similar course of the dependence of the difference $dI/dT - 100\ dJ/dT$ on

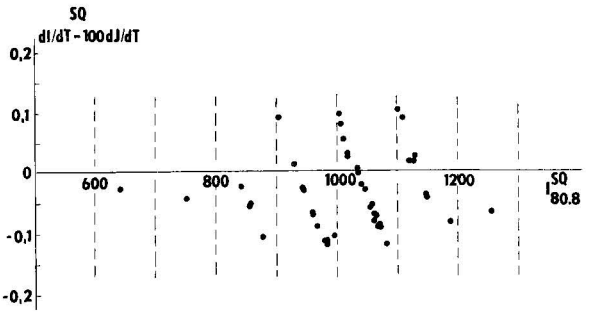

Fig. 3. Dependence of the difference $dI^{SQ}/dT - 100\,dJ^{SQ}/dT$ on $I^{SQ}_{80.8}$ for alkylbenzenes.

I was determined on SQ also for a temperature of 95.2° and was also confirmed on ATC and TCEP at both temperatures. On TCEP, on which the temperature increments of the retention indices are an order of magnitude higher than on ATC and SQ, at 94.2°, $100\,dJ/dT \approx dI/dT$ for alkylbenzenes with $I^{TCEP}_{94.2} \approx 100\,z + 60$.

The dependences of the difference $dI/dT - 100\,dJ/dT$ on I show that the correlations found between structure and dI/dT are not valid for values of $100\,dJ/dT$, because the dependence of the positions of the peak maxima between neighbouring n-alkanes also has to be considered. Deviations between the correlations of structure and temperature increments for linear and logarithmic retention indices are the greater the closer the analysed compounds are eluted to the n-alkane z or $z+1$.

The correlation found between structure and the pressure variation coefficients of retention indices (dI/dP)[10] for alkylbenzenes on TCEP, could not be confirmed for values of dJ/dP owing to the dependence of J on the positions of the peak maxima between the n-alkanes z and $z+1$. For examples, the values of dI/dP are less for 1,4- than for 1,2-alkylbenzenes, but dJ/dP for 1-methyl-4-ethylbenzene is greater than that for 1-methyl-2-ethylbenzene.

CONCLUSION

The relationship between linear retention indices and the structures of alkylbenzenes was studied on three stationary phases at two temperatures under the conditions of high-efficiency and high-precision capillary gas chromatography. The results were compared with those published previously for logaritmic retention indices. It was found that under identical experimental conditions, the linear retention index can be measured more accurately than the logarithmic value. Fine correlations between the structures of alkylbenzenes and values of the temperature increments of the retention indices, and also the differences in the retention indices on two stationary phases, show that the differences in these dependences are different for the linear and logarithmic retention indices. These differences are due to the fact that for structural correlations of linear retention indices the dependence of the positions of the peak maxima of the sorbate between two neighbouring n-alkanes must also be considered. As the relationships between structure and linear retention indices are more complicated than those of logarithmic retention indices, the latter interpolation characteristics are more suitable when using the correlation between structure and retention behaviour as a means of identification.

REFERENCES

1 M. S. Vigdergauz, *Zh. Anal. Khim.*, 31 (1976) 2222.
2 E. Kováts, *Helv. Chim. Acta*, 41 (1958) 1915.
3 M. S. Vigdergauz, in H. G. Struppe (Editor), *Gas-Chromatographie 1968*, Akademie-Verlag, Berlin, 1968, p. 625.
4 A. G. Douglas, *J. Chromatogr. Sci.*, 7 (1969) 583.
5 M. S. Vigdergauz and A. A. Martynov, *Chromatographia*, 4 (1971) 463.
6 N. C. Saha and C. D. Mitra, *Technology (India)*, 8 (1971) 3.
7 J. A. Rijks and C. A. Cramers, *Chromatographia*, 7 (1974) 99.
8 L. Soják and J. A. Rijks, *J. Chromatogr.*, 119 (1976) 505.
9 L. Soják, J. Janák and J. A. Rijks, *J. Chromatogr.*, 135 (1977) 71.
10 L. Soják, J. Janák and J. A. Rijks, *J. Chromatogr.*, 138 (1977) 119.
11 L. Soják, J. Janák and J. A. Rijks, *J. Chromatogr.*, 142 (1977) 177.
12 L. V. Semenčenko, F. I. Lapteva and V. I. Pachomova, in M. S. Vigdergauz (Editor), *Uspekhi Gazovoj Khromatografii*, Vol. 3, Kazan, 1973, p. 28.

Journal of Chromatography, 148 (1978) 169–173

CHROM. 10,403

DETECTION OF NITROGEN AND SULPHUR IN SUBSTANCES SEPARATED BY PAPER AND THIN-LAYER CHROMATOGRAPHY

JAROSLAV FRANC and JAROSLAV POUR

Research Institute of Organic Syntheses, 532 18 Pardubice-Rybitví (Czechoslovakia)

SUMMARY

A procedure has been developed for the detection of sulphur and nitrogen in substances separated by paper and thin-layer chromatography, using a single apparatus for both elements. The substances are pyrolysed together with the chromatographic support, and the sulphur products are converted into hydrogen sulphide and the nitrogen products into ammonia on a platinum gauze in a stream of hydrogen. The hydrogenation products are then suitably detected.

INTRODUCTION

The Lassaigne test for sulphur, nitrogen and the halogens is used as one of identification methods for unknown compounds[1,2]. In paper and thin-layer chromatography, it is often necessary to decide whether the substances separated contain nitrogen, sulphur or a halogen. As microgram amounts of substances are usually applied to the start of the chromatogram, the components separated sometimes occur in amounts of fractions of microgram and it is then not simple to detect sulphur, nitrogen and the halogens.

The only paper on this problem describes the detection of chlorine, bromine, sulphur and molybdenum in substances on chromatograms using X-ray fluorescence[3]. The instrumentation is expensive and unavailable in most laboratories. Moreover, nitrogen cannot be detected by this method. Hence a simple method is required that is capable of detecting sulphur, nitrogen and the halogens by a single procedure, with only small modifications (*i.e.*, using a single apparatus).

Attempts to solve this problem have been described. For the detection of nitrogen, methods based on the modified Lassaigne test have been proposed[4,5], usually using other detection reagents after alkaline fusion. Other methods convert the nitrogen present into nitrous acid, which is then detected[6], or heat the nitrogen-containing substance in a capillary with a mixture of calcium and zinc oxides, detecting the ammonia formed by an acid–base indicator[7]. Nitrogen is also determined photometrically in a phenolic oxidizing medium[8]. An ultramicro method based on the Dumas method cannot be used for this purpose[9–12].

Sulphur can be detected in several ways. Sulphur is converted into sulphur dioxide, which is either titrated coulometrically[13] or oxidized with potassium per-

manganate and determined according to the Pregl method[14]. On an ultramicro scale, sulphur is oxidized with a mixture of copper(II) and boric oxides and the sulphur trioxide formed is detected with *p*-rosaniline[15].

In many methods, sulphur is reduced to hydrogen sulphide. For example, the test sample is heated with sodium carbonate and potassium hexacyanoferrate(III)[16]. In another procedure, the sample is heated with mercury, oxidized with perchloric acid and the sulphur dioxide formed is reduced with hypophosphorous acid, the hydrogen sulphide being detected with 4-(2-pyridyl)resorcinol[17]. Huber *et al.*[18] converted hydrogen sulphide into methylene blue. Sulphur is often reduced by metals to hydrogen sulphide, *e.g.*, by magnesium[19], potassium[20] and sodium[21]. Sulphur was also converted into barium sulphate, which was reduced to barium sulphide with hydrogen, liberating hydrogen sulphide on acidification[22]. Kristen[23] converted sulphur to sulphur dioxide and reduced the latter to hydrogen sulphide with a stream of hydrogen in a quartz tube. Feigh and Stark[24] developed a spot test, based on heating the sample with benzoin in a capillary. In a method developed by Widmark[25], the sample is decomposed with a mixture of calcium and zinc oxides and lead(II) acetate is used for the detection. Widmark[26] also modified the Lassaigne reaction. Sulphur was also converted into hydrogen sulphide on platinum foil[27]. Further older papers can be found in a review by Kainz[28].

Most of the above work is not suitable for the detection of nitrogen and sulphur in microgram samples, because of either insufficient sensitivity or difficult manipulation on the microscale. Moreover, no method permits the detection of sulphur, nitrogen and the halogens in a single procedure.

In addition to the last requirement, the method must be relatively simple, rapid and sufficiently sensitive. These requirements are met by the present method, in which the test sample, together with the chromatographic support, is pyrolysed in a stream of hydrogen and the mixture of pyrolysis products is led over a platinum gauze heated at 950–1000°. Hydrogen sulphide, ammonia and the hydrogen halides are formed from sulphur, nitrogen and the halogens, respectively. Sulphur is detected from the coloration of a silica gel column soaked with lead(II) acetate and nitrogen from the coloration due to the reaction of ammonia with phenol and 2,6-dibromoquinonechloroimine. The detection of halogens will be published elsewhere.

EXPERIMENTAL

The apparatus is shown in Fig. 1. The test sample is placed in a platinum boat on a thermocouple (4) in the pyrolysis furnace (3). A stream of hydrogen flows from a cylinder (1), through a gas purifier (2) and a three-way stop-cock (8) over the sample and then into the hydrogenation furnace (5), which contains a quartz tube containing platinum gauze heated at 950–1000°, and then through other three-way stop-cock (7) into the detection device (6). Nitrogen is reduced to ammonia, the halogens to the hydrogen halides, sulphur to hydrogen sulphide and carbon to methane.

The detection device (6) is varied depending on the element being detected (Fig. 2). For the detection of sulphur, a glass tube (I.D. 1.5 mm) is used, packed with silica gel soaked with a 0.5% solution of lead(II) acetate. The presence of sulphur is shown by a black-brown coloration of the column.

Nitrogen is detected using a glass tube containing a strip of filter-paper

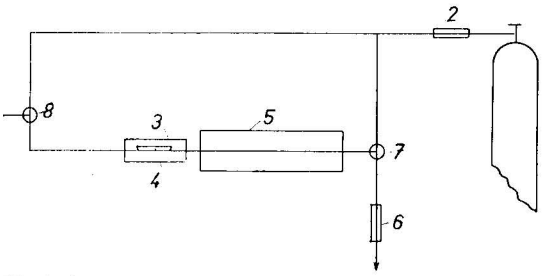

Fig. 1. Apparatus for the detection of nitrogen and sulphur. For description, see text.

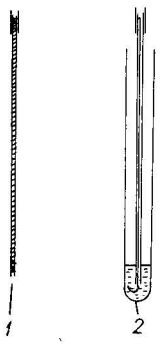

Fig. 2. Detection devices: 1, for sulphur; 2, for nitrogen.

(150 × 2.5 mm) soaked with a mixture of a 1 % aqueous solution of phenol and a 1 % solution of 2,6-dibromoquinonechloroimine in ethanol. These solutions are mixed immediately before the experiment, are placed in a small test-tube and the glass tube is placed so that the filter-paper is partly immersed in the solution. The presence of ammonia is shown by an intense blue coloration of the paper. If sulphur, nitrogen and a halogen are present simultaneously, the device for detection of nitrogen is preceded by a vent containing caustic asbestos, in which hydrogen sulphide and the halides are trapped. Samples obtained by scraping from a thin-layer chromatogram or cut from a paper chromatogram require no pre-treatment and are placed directly in the furnace (3). However, a blank determination must always be carried out, both with Silufol and without it, in order to check that the apparatus is clean.

The three-way stop-cock (7) is placed beyond the furnace (5) so that carrier gas can be flushed backwards during placement of the sample, as even small amounts of air polluted with nitrogen-containing substances seriously interfere in the detection of nitrogen.

RESULTS AND DISCUSSSION

As with any sensitive micro-scale method, great care must be exercised not to pollute the sample with nitrogen or sulphur. Sulphur usually originates only from the chromatographic plate or paper, but nitrogen often comes from atmospheric pollution with ammonia or nitrogen oxides. A length of the platinum gauze of 20 cm was found to be optimal for the detection of both nitrogen and sulphur.

The time changes in the coloration of the silica gel column with lead(II) acetate and of the paper strip with a mixture of 2,6-dibromoquinonechloroimine and phenol must be monitored as the colour intensity increases faster in the presence of sulphur and nitrogen than in the blank determination. This is especially important with small amounts of these elements, *i.e.*, when the difference between the sample and the blank is small (see Fig. 3).

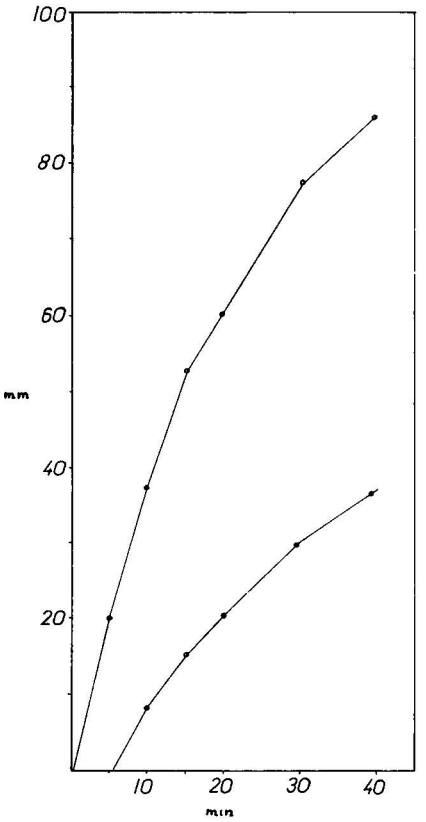

Fig. 3. Time dependence of the length of the coloured zone of the paper strip in the detection of nitrogen. Upper curve, 10-μg semicarbazide sample on Silufol; lower curve, blank.

The sensitivity of the detection of nitrogen could be further increased, but this is not desirable because the blank values are rather high.

A pyrolysis temperature of 700° was selected, as was found to be sufficient for the substances studied. The flow-rate of hydrogen that serves as the hydrogenation medium and the carrier gas was adjusted to 0.35 l/h, which was found to be optimal for hydrogenation, for rinsing the reaction products from the tube and for detection. With volatile substances, the flow-rate must first be decreased and then adjusted to the above value.

REFERENCES

1 J. L. Lassaigne, *Justus Liebigs Ann. Chem.*, 48 (1843) 367.
2 G. Keinz and F. Schöller, *Mikrochim. Acta*, (1954) 327.
3 W. Huber and H. Fricke, *Chromatographia*, 3 (1970) 121.
4 A. Spěvák, V. Kratochvíl and M. Večeřa, *Collect. Czech. Chem. Commun.*, 26 (1961) 887.
5 J. B. Niederl and J. A. Sozzi, *Mikrochim. Acta*, (1957) 496.
6 F. Feigl and J. R. Amaral, *Anal. Chem.*, 30 (1958) 1148.
7 A. Sá, C. N. Carducci and P. Luis, *Mikrochim. Acta*, (1968) 53.
8 U. Bohnstedt, *Z. Anal. Chem.*, 163 (1958) 415.
9 K. Miyahara, *Microchem. J.*, 19 (1974) 416.
10 K. Miyahara, *Microchem. J.*, 19 (1974) 423.
11 K. Miyahara, *Microchem. J.*, 19 (1974) 429.
12 K. Miyahara, *Microchem. J.*, 19 (1974) 453.
13 G. de Groot, P. A. Greve and R. A. A. Maes, *Anal. Chim. Acta*, 79 (1975) 279.
14 A. A. Abramyan, A. S. Tevosyan and R. A. Megroyan, *Zh. Anal. Khim.*, 30 (1975) 817.
15 C. N. Carducci, A. Sá and P. Luis, *Mikrochim. Acta*, (1967) 172.
16 Ya. D. Zelvenskii, A. N. Gruzintseva and S. Yu. Gerchikova, *Zavod. Lab.*, 21 (1955) 277.
17 P. Luis, C. N. Carducci and A. Sá, *Mikrochim. Acta*, (1968) 1229.
18 O. Huber, H. Kolb and J. Weigl, *Z. Anal. Chem.*, 227 (1967) 420.
19 L. Barcza and P. Czuczy, *Mikrochim. Acta*, (1963), 293.
20 T. Meisel, A. Németh and L. Erdey, *Mikrochim. Acta*, (1961) 874.
21 J. Patrick and F. Schneider, *Mikrochim. Acta*, (1960) 970.
22 W. Noddack and I. Noddack, *J. Prakt. Chem.*, 5 (1957) 274.
23 W. Kristen, *Mikrochemie*, 35 (1950) 174.
24 F. Feigl and C. Stark, *Anal. Chem.*, 27 (1955) 1838.
25 G. Widmark, *Acta Chem. Scand.*, 8 (1954) 246.
26 G. Widmark, *Acta Chem. Scand.*, 7 (1953) 1395.
27 I. Irimescu and E. Chirnoagă, *Z. Anal. Chem.*, 128 (1948) 71.
28 G. Kainz, *Österreichische Chem.-Ztg.*, 58 (1957) 8.

Journal of Chromatography, 148 (1978) 175–181

CHROM. 10,460

LIQUID CHROMATOGRAPHY OF HYDROCARBONS ON POROUS POLY-(ETHYLENE GLYCOL) METHACRYLATE (SPHERON P-300)*

MILAN MINÁRIK and RADKO KOMERS

Institute of Chemical Process Fundamentals, Czechoslovak Academy of Sciences, 165 02 Prague 6 (Czechoslovakia)

and

JIŘÍ ČOUPEK

Chemical Research Department, Laboratory Instruments Works, 162 03 Prague 6 (Czechoslovakia)

SUMMARY

The chromatographic behaviour of saturated, unsaturated and aromatic hydrocarbons on a macroporous bead copolymer of 2-hydroxyethyl methacrylate and ethylene dimethacrylate, with *n*-heptane as the mobile phase was studied, concentrating on the effect of the structure of the solute on its retention. The behaviour of conjugated unsaturated and aromatic hydrocarbons is in agreement with the theory of liquid–liquid chromatography; it is concluded that the chromatographic properties of the above system are better interpreted by using the separation mechanism of liquid–liquid chromatography than that of liquid–solid chromatography.

INTRODUCTION

Synthetic polymeric phases are applied in liquid chromatography not only as gel phases and ion exchangers, but also as sorbents. The phases most widely used in this respect have so far been chemically bonded phases, the matrix of which is formed by siloxane polymers[1]. At the same time, however, the number of applications of polymeric packings in reversed-phase liquid chromatography (RPLC) has also increased, and only in normal-phase liquid chromatography (NPLC) has the use of polymeric packings remained somewhat stagnant.

The separation mechanism and the theory of the retention of the solute in adsorption liquid chromatography (LSC) on inorganic adsorbents have been examined by Snyder[2] in sufficient detail. The thermodynamic theory of the retention of the solute in liquid–liquid chromatography (LLC)[3] and in RPLC[4] has been worked out. There are different views about the mechanism of separation in sorption liquid chromatography on polymeric phases, including chemically bonded phases; systematic investigations of this problem and other practical information concerning the properties of polymeric materials have not yet provided a sufficient basis for a de-

* Part of the Thesis of M. Minárik, Czechoslovak Academy of Sciences, Prague, 1975.

tailed description of the behaviour of these phases over the whole range of their uses[5–8].

With bonded phases that possess the "brush" structure, the view that is almost unanimously accepted is that the separation mechanism consist in the adsorption of the solute molecules on the surface of a modified adsorbent[8–12]. The adsorption mechanism has even been used to interpret the separation of polycyclic aromatic hydrocarbons on 1,2,3-tris(2-cyanoethoxy)propane coated on silica gel[13]. On the other hand, the mechanism of separation on polymeric bonded phases is explained both by adsorption[7,11,12,14–19] and by partition[7,12,14,15,19–25] in RPLC, and similarly by adsorption[11,12,14,15] and by partition[12,14–17,22] in NPLC.

Most practical data on the chromatographic behaviour of porous polymeric packings relates to gel chromatography, in which sorption is regarded as a side-effect; for this reason, these results are inadequate for a complete description of the separation mechanism in sorption liquid chromatography on such packings. In spite of this, however, the above effect is very frequently attributed to adsorption[26–34], while partition[35,36] or both effects[37–39] are only rarely taken into account. Finally, it should also be pointed out that the results of work aimed directly at the sorption properties of porous polymeric packings in liquid chromatography are not uniform as regards the problem of the nature of the separation mechanism[40–49]. The behaviour of these packings is interpreted in terms of both LSC[42–49] and LLC[40–42]. It should be added, however, that the study of sorption chromatography on synthetic polymeric packings outside gel chromatography is almost exclusively restricted to styrene–divinylbenzene copolymers in RPLC[40–48].

In this paper, the chromatographic behaviour of hydrocarbons on a macroporous copolymer of 2-hydroxyethyl methacrylate and ethylene dimethacrylate (Spheron P-300) in *n*-heptane is described, and relationships between the retention and structure of the solute and the separation mechanism of the system are discussed.

EXPERIMENTAL

Chemicals

All compounds were pure commercial samples and were used without further purification.

Liquid chromatography

The retention volumes were measured with a liquid chromatograph (120 × 0.8 cm column) and with an R 401 differential refractometer (Waters) as detector. The samples were injected as 1–5% solutions in *n*-heptane in volumes of 0.2 ml and characterized by the retention volume, V_R, in siphon counts (1 count = 1.81 ml). The adjusted retention volumes, V_R', were calculated from the retention volumes by subtracting the dead column volume V_0; $V_R' = V_R - V_0$ ($V_0 = V_R$ for squalane). The column was packed with Spheron P-300 (Lachema, Brno, Czechoslovakia), exclusion limit $3 \cdot 10^5$, grain size 40–63 μm. The flow-rate of the mobile phase (*n*-heptane) was 1 ml/min.

RESULTS AND DISCUSSION

Table I gives the adjusted retention volumes of hydrocarbons that do not contain delocalized π-electrons. The retention volumes are so low that it is difficult to determine the character of this quantity as a function of some of the molecular parameters of the solute. A qualitative estimate of the order of elution indicates that retention is slightly reduced with increasing molecular weight, without any visible effect of branching of the hydrocarbon chain on this tendency. In addition, the retention is increased by the presence of the double bond and by the cyclic structure of the molecule of the solute.

TABLE I

ADJUSTED RETENTION VOLUMES OF LINEAR AND CYCLIC ALKANES AND LINEAR ALKENES ON SPHERON P-300 IN *n*-HEPTANE

Compound	*No. of carbon atoms*	V'_R	*Compound*	*No. of carbon atoms*	V'_R
Neohexane	6	1.7	*tert.*-Butylcyclohexane	10	1.7
n-Hexane	6	1.4	Cyclopentane	5	1.4
n-Octane	8	0.7	Cyclohexane	6	1.4
n-Decane	10	0.5	Decalin	10	1.1
2,2,4,6,6-Pentamethylheptane	12	0.5	Pentylcyclohexane	11	1.1
n-Dodecane	12	0.5	*tert.*-Pentylcyclohexane	11	1.0
n-Tetradecane	14	0.4	Tricyclohexylmethane	19	0.9
n-Pentadecane	15	0.4	1-Heptene	7	1.1
n-Tridecane	13	0.2	3-Heptene	7	1.1
n-Eicosane	20	0.2	1-Nonene	9	1.1
Squalane	30	0.0	1-Decene	10	0.9
Cycloheptane	7	2.0	1-Dodecene	12	0.8
Isopropylcyclohexane	9	1.9	1-Hexadecene	16	0.5

Table II gives the adjusted retention volumes of hydrocarbons that contain conjugated double bonds. If we call a certain type of the conjugated system a "functional group", then the values of the adjusted retention volumes of dienes, alkylbenzenes and alkylnaphthalenes form parallel straight lines for the individual functional groups in graphs of log V'_R *versus* the number of carbon atoms in the molecule (Fig. 1). If parallel straight lines are plotted through the points corresponding to the other compounds in Table II, the dependence obtained can be related to the empirical formula of the compound C_nH_{2n-z}. A similar type of dependence was obtained by Pierotti *et al.*[50] and Deal *et al.*[51] for the extraction equilibria of hydrocarbons in systems of *n*-heptane with several polar solvents bearing a hydroxyl group, and by Stevenson[52] in the LLC of alkylbenzenes in the system Carbowax 600–2,2,4-trimethylpentane. Such a correlation (Fig. 1) can, in terms of LLC, be regarded as the additivity of free energies[50,51,53,54]:

$$\Delta G_i^E = n_i \Delta G^E(C) + (m_i - 1)\Delta G^E(X) + p_i \Delta G^E(Y) \quad (1)$$

where ΔG_i^E is a change in the excess free energy of the solute during sorption, n_i, m_i and p_i denote the number of carbon atoms, the number of double bonds in conjuga-

TABLE II

ADJUSTED RETENTION VOLUMES OF UNSATURATED CONJUGATED HYDROCARBONS ON SPHERON P-300 IN *n*-HEPTANE

n (carbon number) and *z* are values determined by the empirical formula of compound C_nH_{2n-z}.

No.	*Compound*	V'_R	*n*	*z*	*No.*	*Compound*	V_R	*n*	*z*
1	1,3-Butadiene	4.5	4	2	17	*p*-Cymene	4.3	10	6
2	1,3-Pentadiene	3.6	5	2	18	*sec.*-Butylbenzene	4.4	10	6
3	2-Methylbutadiene	3.5	5	2	19	Hexamethylbenzene	3.1	12	6
4	2,3-Dimethylbutadiene	3.0	6	2	20	*p*-Di-*tert.*-butylbenzene	1.9	14	6
5	1,3-Cyclooctadiene	3.1	8	4	21	Styrene	12.7	8	8
6	Benzene	9.4	6	6	22	Ethylstyrene	7.8	10	8
7	Toluene	7.9	7	6	23	Tetralin	7.0	10	8
8	Cycloheptatriene	7.8	7	6	24	Divinylbenzene	14.4	10	10
9	Ethylbenzene	6.4	8	6	25	Naphthalene	21.5	10	12
10	*o*-Xylene	6.9	8	6	26	1-Methylnaphthalene	16.3	11	12
11	*m*-Xylene	5.7	8	6	27	2-Methylnaphthalene	16.0	11	12
12	*p*-Xylene	5.4	8	6	28	2-Ethylnaphthalene	13.1	12	12
13	Cumene	5.5	9	6	29	2,3-Dimethylnaphthalene	14.5	12	12
14	1,2,3-Trimethylbenzene	6.4	9	6	30	Diphenyl	23.5	12	14
15	1,2,4-Trimethylbenzene	5.5	9	6	31	Anthracene	42.6	14	18
16	Mesitylene	4.5	9	6	32	Phenanthrene	43.8	14	18

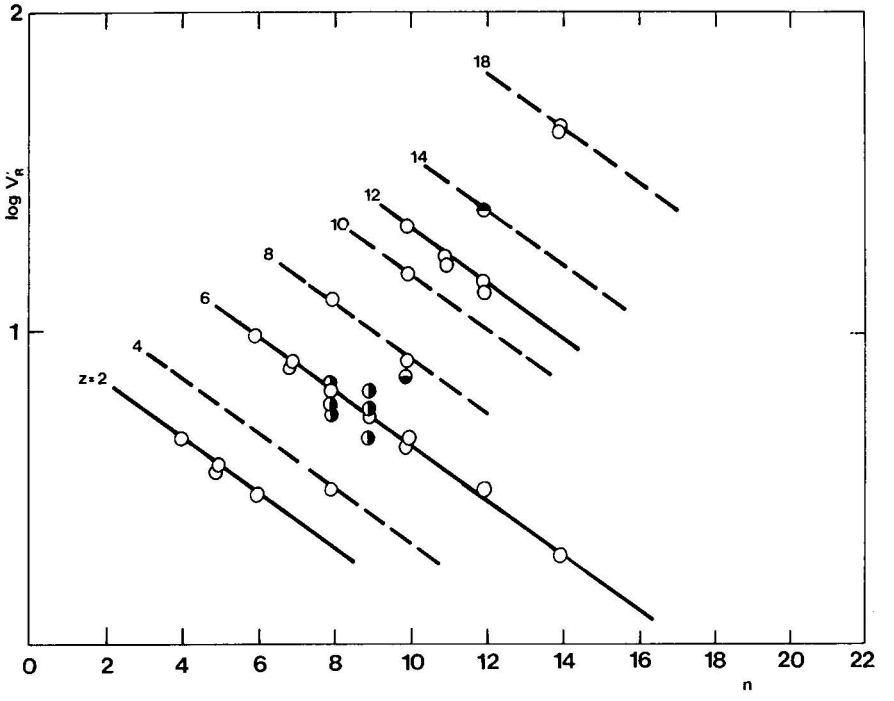

Fig. 1. Dependence of adjusted retention volumes (V'_R) of unsaturated hydrocarbons in Table II on the number of carbon atoms (*n*) for various *z* values of the empirical formula of compounds C_nH_{2n-z} on Spheron P-300 in *n*-heptane. Column, 120 × 0.8 cm; flow-rate of mobile phase, 1 ml/min. ◑, Isomeric di- and trimethylbenzenes; ◒, tetralin; ◓, diphenyl.

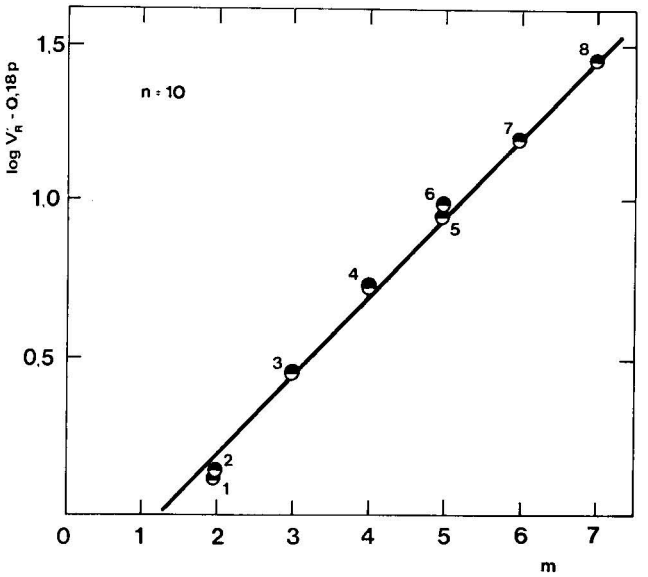

Fig. 2. Dependence of adjusted retention volumes (V'_R) on the number of double bonds (m) for individual functional groups (conjugated systems) at $n = 10$. Conditions as in Fig. 1. ◓, Calculated values from Fig. 1 for: 1 = dienes; 2 = cyclodienes; 3 = alkylbenzenes; 4 = alkylvinylbenzenes; 5 = divinylbenzene; 6 = alkylnaphthalenes; 7 = diphenyl; 8 = phenanthrene and anthracene.

tion and the number of rings in the molecule of solute i, respectively, and $\Delta G^E(C)$, $\Delta G^E(X)$ and $\Delta G^E(Y)$ are the unit energy increments of the carbon atom, the double bond and the ring of the solute, respectively. The linearity of eqn. 1, and thus the linear dependence of log V'_R on the individual quantities n, m and p, are shown in Fig. 2, along with Fig. 1; Fig. 2 (log V'_R *versus* m) represents the dependence of log V'_R of a hypothetical series of compounds with ten carbon atoms on the number of conjugated double bonds (m). The log V'_R values for the individual z were read off from Fig. 1 at $n = 10$ and corrected by the average value of log V'_R for each ring in the molecule. An interesting behaviour was observed with the diphenyl group, the V'_R of which satisfies the above correlation expressions, although the molecule of this compound is regarded as imperfectly planar[55], and consequently its π-electron system is not conjugated.

Assuming the existence of only non-specific (disperse) interactions between the solute and the mobile phase, the individual terms in eqn. 1 can be interpreted so that $\Delta G^E(X)$ represents an interaction of the delocalized π-electron pair of the solute with the hydroxyl groups of the stationary phase, and $\Delta G^E(C)$ expresses the negative interaction of the carbon atom of the solute with the stationary phase (identical with a decrease in the mutual interaction of the polar groups of the stationary phase due to the presence of the carbon atom of the solute in this phase). The term $\Delta G^E(Y)$ can be expressed in two ways: either by an increase in polarity, or by a decrease in the effective size of the solute molecule owing to the cyclic structure formation. The latter hypothesis seems more acceptable, and the different gel chromatographic behaviour of cyclic and linear hydrocarbons[56], similarly to differences in the linear activity coefficients of cyclic and linear hydrocarbons in polar solvents[51,57], support its plausibility.

Table III gives the adjusted retention volumes of aromatic hydrocarbons, which in the sense of the above definition are polyfunctional derivatives, because all of their delocalized π-electrons are not conjugated. In the coordinates log V'_R *versus* n, binuclear aromatic compounds roughly satisfy the straight line of the diphenyl group, while trinuclear compounds correspond to the straight line of anthracene in Fig. 1. At the same time, Table III shows the accuracy of such approximations.

TABLE III

RETENTION DATA OF INCOMPLETELY CONJUGATED POLYPHENYLIC COMPOUNDS ON SPHERON P-300 IN *n*-HEPTANE

$\Delta\log V'_R = (\log V'_R - \log V_R{}^{th})/\log V_R{}^{th}$ (see footnotes).

Compound	V_R	n	z	$\Delta\log V'_R$
Dibenzyl	21.5	14	14	0.1212*
4,1-Diphenylethylene	16.9	14	16	0.0353*
2,2-Diphenylpropane	9.8	15	14	−0.0990*
Cyclohexylidenediphenylmethane	5.0	19	18	−0.0750*
6,6-Diphenylfulvene	13.2	18	22	−0.1225**
Triphenylmethane	14.9	19	22	−0.0152**
Benzyl-*p*-diphenyl	17.1	19	22	0.0353**
1,1,1-Triphenylethane	9.9	20	22	−0.0984**
Triphenylethylene	16.0	20	24	0.0874**
1,2,2-Triphenylpropane	11.5	21	22	0.0473**

* $V'_R{}^{th}$ is the theoretical value of V'_R of the alkyl derivative of diphenyl with the same n as the tested compound.

** $V'_R{}^{th}$ is the theoretical value of V'_R of the alkyl derivative of anthracene with the same n as the tested compound.

The results presented in this work do not provide proof of the LLC separation mechanism of the chromatographic system, because the length of the aliphatic chains of the tested compounds was not sufficient to justify an assumption of the linear decrease of retention in the case of long alkyl chains also[4], typical of the LLC mechanism. On the other hand, it was shown that the separation mechanism of the above system exhibited characteristic features of LLC, such as a constant effect upon retention produced by each alkyl carbon atom and by each delocalized π-electron pair of the solute, as well as a considerable insensitivity of retention with respect to the other structural changes in the molecule of the solute. It would be difficult to interpret these properties by the LSC mechanism, in which, with the above system, one would expect a considerably smaller and less regular effect of the alkyl substitution on the retention of the compounds tested[58].

REFERENCES

1 R. E. Majors and M. J. Hopper, *J. Chromatogr. Sci.*, 12 (1974) 767.
2 L. R. Snyder, *Principles of Adsorption Chromatography*, Marcel Dekker, New York, 1968.
3 D. C. Locke and D. E. Martire, *Anal. Chem.*, 39 (1967) 921.
4 D. C. Locke, *J. Chromatogr. Sci.*, 12 (1974) 433.
5 K. Karch, I. Sebestian and I. Halász, *J. Chromatogr.*, 122 (1976) 3.
6 H. Colin, C. Eon and G. Guiochon, *J. Chromatogr.*, 122 (1976) 223.
7 J. A. Schmit, R. A. Henry, R. C. Williams and J. F. Dieckman, *J. Chromatogr. Sci.*, 9 (1971) 645.

8 V. Řehák and E. Smolková, *Chromatographia*, 9 (1976) 219.
9 J. J. Kirkland, in J. J. Kirkland (Editor), *Modern Practice of Liquid Chromatography*, Wiley-Interscience, New York, 1971, Ch. 5.
10 D. C. Locke, *J. Chromatogr. Sci.*, 11 (1973) 120.
11 K. J. Bombaugh, in J. J. Kirkland (Editor), *Modern Practice of Liquid Chromatography*, Wiley-Interscience, New York, 1971, Ch. 10.
12 J. J. Kirkland, *J. Chromatogr. Sci.*, 9 (1971) 206.
13 R. Vespalec, *J. Chromatogr.*, 118 (1976) 47.
14 E. J. Kikta, Jr., and E. Grushka, *Anal. Chem.*, 48 (1976) 1098.
15 R. P. W. Scott, *Contemporary Liquid Chromatography*, Wiley-Interscience, New York, 1976.
16 A. Pryde, *J. Chromatogr. Sci.*, 12 (1974) 486.
17 M. J. Telepchak, *Chromatographia*, 6 (1973) 234.
18 K. Karch, I. Sebestian, I. Halász and H. Engelhardt, *J. Chromatogr.*, 122 (1976) 171.
19 R. E. Majors, *Analusis*, 3 (1975) 549.
20 J. H. Knox and A. Pryde, *J. Chromatogr.*, 112 (1975) 171.
21 P. J. Twitchett and A. C. Moffat, *J. Chromatogr.*, 111 (1975) 149.
22 S. H. Chang, K. M. Gooding and F. E. Regnier, *J. Chromatogr.*, 120 (1976) 321.
23 R. C. Williams, in E. Grushka (Editor), *Bonded Stationary Phases in Chromatography*, Ann Arbor Sci. Publ., Ann Arbor, Mich., 1974, Ch. 3.
24 J. N. Seiber, *J. Chromatogr.*, 94 (1974) 151.
25 R. M. Carlson, R. E. Carlson and H. L. Kopperman, *J. Chromatogr.*, 107 (1975) 219.
26 K. W. Williams, *Lab. Pract.*, 21 (1972) 667.
27 J. L. Mulder and F. A. Buytenhuys, *J. Chromatogr.*, 51 (1970) 459.
28 L. Lonsky, *Allg. Prakt. Chem.*, 23 (1972) 213.
29 L. Fričová, *Chem. Listy*, 68 (1974) 613.
30 D. D. Bly, *Science*, 168 (1970) 527.
31 P. Flodin, *Anal. Chim. Acta*, 38 (1967) 89.
32 C. Wasternack, *Pharmazie*, 27 (1972) 67.
33 D. J. Harmon, in K. H. Altgelt and L. Segal (Editors), *Gel Permeation Chromatography*, Marcel Dekker, New York, 1971, p. 13.
34 D. M. W. Anderson, I. C. M. Dea and A. Hendrie, *Talanta*, 18 (1971) 365.
35 J. Lecourtier, R. Audebert and C. Quivoron, *J. Chromatogr.*, 121 (1976) 173.
36 C. J. W. Brooks and R. A. B. Keates, *J. Chromatogr.*, 44 (1969) 509.
37 H. Determann, *Gel Chromatography*, Springer, New York, 1968.
38 E. P. Otocka, *Accounts Chem. Res.*, 6 (1973) 348.
39 M. Popl, V. Dolanský and J. Čoupek, *J. Chromatogr.*, 130 (1977) 195.
40 G. Muto and A. Nakae, *Chem. Lett.*, 6 (1974) 549.
41 A. Nakae and G. Muto, *J. Chromatogr.*, 120 (1976) 47.
42 T. Hidekuni and S. Setsuya, *J. Chromatogr.*, 108 (1975) 354.
43 T. Hidekuni and S. Setsuya, *J. Chromatogr. Sci.*, 12 (1974) 507.
44 R. L. Gustafson, R. L. Albright, J. Heisler, J. A. Lirio and O. T. Reid, Jr., *Ind. Eng. Chem., Prod. Res. Develop.*, 7 (1968) 107.
45 M. W. Scoggins, *Anal. Chem.*, 44 (1972) 1285.
46 M. D. Grieser and D. J. Pietrzyk, *Anal. Chem.*, 45 (1973) 1348.
47 C. H. Chu and D. J. Pietrzyk, *Anal. Chem.*, 46 (1974) 330.
48 L. L. Zaika, *J. Chromatogr.*, 49 (1970) 222.
49 V. Martinů and J. Janák, *J. Chromatogr.*, 65 (1972) 477.
50 G. J. Pierotti, C. H. Deal and E. L. Derr, *Ind. Eng. Chem.*, 51 (1959) 95.
51 C. H. Deal, E. L. Derr and M. N. Papadopoulos, *Ind. Eng. Chem., Fundam.*, 1 (1962) 17.
52 R. Stevenson, *J. Chromatogr. Sci.*, 9 (1971) 257.
53 J. Novák, J. Růžičková, S. Wičar and J. Janák, *Anal. Chem.*, 45 (1973) 1365.
54 G. M. Wilson and C. H. Deal, *Ind. Eng. Chem., Fundam.*, 1 (1962) 20.
55 G. H. Schenk, G. L. Sullivan and P. A. Fryer, *J. Chromatogr.*, 89 (1974) 49.
56 M. Minárik, J. Čoupek and R. Komers, *Collect. Czech. Chem. Commun.*, in press.
57 P. Alessi and I. Kikic, *Gazz. Chim. Ital.*, 104 (1974) 739.
58 L. R. Snyder, in J. J. Kirkland (Editor), *Modern Practice of Liquid Chromatography*, Wiley-Interscience, New York, 1971, Ch. 6.

Journal of Chromatography, 148 (1978) 183–187

CHROM. 10,416

GEL PERMEATION CHROMATOGRAPHY OF STEREOISOMERS: MODEL COMPOUNDS OF POLY(VINYL CHLORIDE)

S. POKORNÝ, R. LUKÁŠ, J. JANČA and M. KOLÍNSKÝ

Institute of Macromolecular Chemistry, Czechoslovak Academy of Sciences, 162 06 Prague 6 (Czechoslovakia)

SUMMARY

The possibility of separating stereoisomers of 2,4-dichloropentane and 2,4,6-trichloroheptane by means of gel permeation chromatography on columns packed with S-Gel 832 was investigated using a recycling technique with minimal zone spreading. The results are discussed from the viewpoint of the assumed sizes of the molecules and with respect to a possible interaction of dissolved compounds with the eluent used. The results may not only help to elucidate some aspects of the separation process, but also to find suitable conditions for preparative fractionation of the above compounds employed as models of the PVC chain.

INTRODUCTION

Stereoisomers of 2,4-dichloropentane and 2,4,6-trichloroheptane are employed as model compounds in studying the structure of poly(vinyl chloride)[1–3]. With 2,4-dichloropentane, the analytical and preparative separation of stereoisomers was carried out by fractional distillation on a high-efficiency column[4] and by gas chromatography[2]. With 2,4,6-trichloroheptane, the distillation method was unsuccessful[4], while gas chromatography with a selective stationary phase (Benton 34)[5,6] yielded pure stereoisomers, which were identified and investigated by IR and NMR spectroscopy[2,7,8].

The separation of stereoisomers of 2,4-diphenylpentane and 2,4,6-triphenylheptane (model compounds of polystyrene) by gel permeation chromatography (GPC) with recycling has been described by Lesec *et al.*[9]. Columns packed with Poragel 60 Å and diisopropyl ether as eluent were used in this instance, and the separation was interpreted on the basis of different hydrodynamic volumes of the individual stereoisomers. In another paper by the same group[10], the separation of diastereoisomers of acetal alcohols was compared under similar conditions in diisopropyl ether and tetrahydrofuran (THF). A considerably poorer separation in THF was explained by interactions of the individual diastereoisomers with the eluent.

An interaction of molecules of various polarities with a polar eluent in GPC has been reported by Čoupek *et al.*[11] with appropriate model compounds (carboranes). Isomeric carboranes possess an identical rigid molecular structure, but differ greatly in

their dipole moments. In the separation of these compounds in THF, the order of elution followed exactly the decreasing dipole moment. When the chromatographic behaviour of carboranes was investigated in benzene, the separation was much poorer and the order of elution was reversed. This inversion could not be interpreted as unequivocally as the preceding instance, owing to the possibly greater part played by interactions between the solute and the gel.

In this work, we investigated the GPC separation of stereoisomers of 2,4-dichloropentane and 2,4,6-trichloroheptane, using THF as eluent on columns packed with the styrene–divinylbenzene copolymer S-Gel 832.

EXPERIMENTAL

Model compounds

Acetylacetone was used in the synthesis of 2,4-dichloropentane (2,4-DCP)[4]. The stereoisomeric mixture of 2,4-DCP contained 51.3% of the *iso*-form and 48.7% of the *syndio*-form (by analogy with syndiotactic and isotactic polymer chains, the *meso*-form of 2,4-DCP is called the *iso*-form and the DL-form is called the *syndio*-form). The mixture was analysed by means of gas chromatography using a packing of 10% of Benton B-34 + 10% of Apiezon L on Celite (60–80 mesh), with an 1800 × 1.9 mm column. Preparative gas chromatography with an F-21 (Perkin-Elmer, Überlingen, G.F.R.) apparatus packed as indicated above permitted the separation of the two stereoisomers of 2,4-DCP. The fraction referred to below as the *iso*-form of 2,4-DCP contained 99.7% of the *iso*-form and 0.3% of the *syndio*-form, while the fraction denoted as the *syndio*-form contained 99.2% of the *syndio*-form and 0.8% of the *iso*-form. Table I shows some of the physical properties of the stereoisomers of 2,4-DCP. The dipole moments of the *iso*- and *syndio*-forms of 2,4-DCP were measured with a Dipolmeter DM 01 apparatus (WTW, Weilheim, G.F.R.) in *n*-hexane and were 4.7 and 4.4 D, respectively.

2,4,6-Trichloroheptane (2,4,6-TCH) was prepared by a multistage synthesis from ethyl acetoacetate[6]. The stereoisomeric mixture contained 26.0% of the *iso*-

TABLE I

PHYSICAL PROPERTIES OF STEREOISOMERS OF 2,4-DICHLOROPENTANE AND 2,4,6-TRICHLOROHEPTANE

Compound	*Boiling point (°C/KPa)*	n_D^{20}*	*Conformation***	*Dipole moment (D)*	
				calc.	*measured*
2,4-Dichloropentane					
reaction mixture	142–147/101	1.4409	–	–	–
iso-form	40/1.6	1.4423	TG′	–	4.7
syndio-form	36/1.6	1.4390	TT	–	4.4
2,4,6-Trichloroheptane					
reaction mixture	102.5–104.5/2	1.4699	–		–
iso-form	102.5/2	1.4722	TGTG	2.20	–
hetero-form	103.5/2	1.4704	TTTG	2.21	2.68
syndio-form	104.5/2	1.4686	TTTT	4.10	4.07

* For 2,4-DCP *cf.* ref. 12, for 2,4,6-TCH *cf.* ref. 6.

** For 2,4-DCP *cf.* ref. 2, for 2,4,6-TCH *cf.* ref. 3.

form, 51.3% of the *hetero*-form and 22.7% of the *syndio*-form (analysis by gas chromatography, similar to 2,4-DCP). Some physical properties of the stereoisomers are given in Table I.

Methods

The GPC equipment consisted of a membrane pump, a loop injection system of volume 0.350 ml, stainless-steel columns (1200 × 8 mm) packed with the S-Gel 832 (Institute of Macromolecular Chemistry of the Czechoslovak Academy of Sciences, Prague, Czechoslovakia) with an exclusion limit of *ca.* 1000 units of molecular weight, an R 4 differential refractometer (Waters Assoc., Milford, Mass., U.S.A.), and an elution volume-meter with a photoelectric detector and siphon (2.7 ml). The signal from the detector together with the elution volume were recorded with a line recorder. The flow-rate of the eluent (THF) was *ca.* 30 ml/h.

Preliminary analyses of pure stereoisomers of 2,4-DCP were performed by a GPC procedure using a system of five columns. The separation of the mixtures was carried out using the recycling techniques described by Duvdevani *et al.*[13], which allows minimum zone spreading to be preserved, because the eluate does not pass through the pump before the repeated injection into the system of columns. A simple scheme of the arrangement is shown in Fig. 1. In the first position of the six-port valve A (solid line), the eluent passes from the pump (or from the injection device) through the measuring cell of the detector D into the first system of columns B, and from there through the reference cell of the detector into the second system of columns C. On passing through the columns C, the zone of compounds being separated would leave the separation system. If, however, after all of the compounds under investigation have passed through the detection cell E the six-port valve A is switched over to the second position (denoted by a dashed line), the zone of the compounds being sepa-

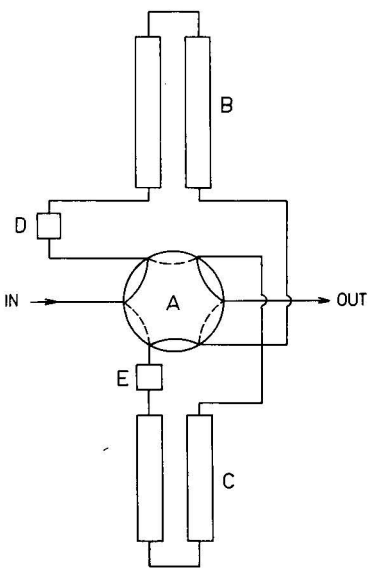

Fig. 1. Scheme of the GPC apparatus adapted for recycling. A, six-port valve; B and C, systems of columns; D and E, measuring and reference cell of detector, respectively.

rated will not leave the system, but will pass through the columns C into the detection cell D and the columns B. This procedure is repeated for a desired number of cycles. The advantages of this system are the minimal zone spreading and the possibility of detection after each passage through the system of columns. In our work, two columns packed with S-Gel 832 were used in either of the systems of columns (B,C).

RESULTS AND DISCUSSION

The analysis of pure stereoisomers of 2,4-DCP by GPC on five columns revealed a small difference in the elution volumes between the *syndio*-form (85.0 counts) and the *iso*-form (83.5 counts). This difference is insufficient for separation and the mixture of stereoisomers was therefore analysed by using the recycling techniques described above. A mixture consisting of 56.6% (w/w) of the *syndio*-form and 43.4% (w/w) of the *iso*-form was used. Fig. 2 shows the separation process, depending on the number of cycles. It can be seen that in order to achieve a baseline separation of both stereoisomers, 16 cycles are necessary, *i.e.*, passage through 32 columns. After these 16 cycles the zone of separated stereoisomers leaves the columns in a volume of 35 ml (the volume injected was 0.35 ml). Further, the quantitative ratio of the two peaks demonstrates that the *iso*-form leaves the columns first, in agreement with the test measurement of the two stereoisomers on the system of five columns. Consequently, in this arrangement the *iso*-form appears to be larger in molecular size than the *syndio*-form. This fact may be due to (a) different sizes of the molecules of the conformational structures TG′ or TT of the two stereoisomers, or (b) different interactions with the polar eluent (THF) caused by a difference in the dipole moments of the two stereoisomers.

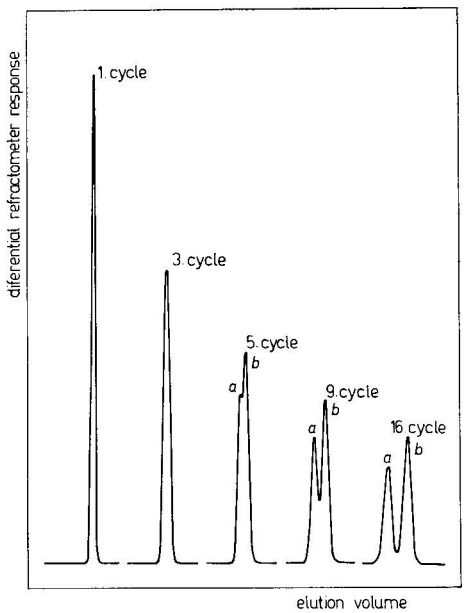

Fig. 2. Separation of stereoisomers of 2,4-dichloropentane: a, *iso*-form; b, *syndio*-form.

In constructing models of the two stereoisomers, the TG′ structure of the *iso*-form appears to be bulkier than the *syndio*-form, but the difference in sizes is minimal; moreover, this difference may play a major role only in a non-polar eluent. If a polar solvent (THF in our work) is used in the separation, the influence should probably be assigned to the different interactions of the solvent with the two stereoisomers on the basis of different polarities. The experimental result is in agreement with such an assumption, because the *iso*-form, the dipole moment of which (4.7 D) is higher than that of the *syndio*-form (4.4 D), leaves the column first (Table I).

The separation of stereoisomers of 2,4,6-TCH using the separation system described above was unsuccessful, even with an increased number of cycles (22). A further increase in the number of cycles was useless, because a chromatographic zone is dispersed in a volume of solvent equal to the volume of one system of columns.

The finding that the separation of stereoisomers of 2,4,6-TCH was unsuccessful even with a very efficient system using the recycling techniques may be explained by the unfavourable effect of two counteracting influences, namely the size of the individual stereoisomers and their polarity. While the size increases in the order *syndio*-form (TTTT) < *hetero*-form (TTTG) < *iso*-form (TGTG), the increase in the dipole moments, which may be a measure of the interaction of THF with the dissolved compound, follows the opposite order: *iso*-form (2.20D) < *hetero*-form (2.68 D) < *syndio*-form (4.07 D).

It follows from the above that while in the separation of stereoisomers of 2,4-DCP the use of a polar eluent (THF) has a favourable effect, in the separation of stereoisomers of 2,4,6-TCH it will probably be necessary to employ a less polar eluent, in which the difference in the sizes of molecules of the individual stereoisomers could play a favourable role without the unfavourable effect of solvation.

The search for suitable conditions for a successful analytical or preparative separation of stereoisomers of 2,4,6-TCH is the subject of further study.

ACKNOWLEDGEMENTS

The authors thank Dr. V. Halaška for measurements of the dipole moments of the stereoisomers of 2,4-DCP, and Mrs. E. Plachetková for analyses of the mixtures by gas chromatography.

REFERENCES

1 D. Doskočilová, J. Štokr, B. Schneider, H. Pivcová, M. Kolínský, J. Petránek and D. Lím, *Symposium on Macromolecular Chemistry, Prague 1965*, Preprint P5; *J. Polym. Sci., Part C*, 16 (1967) 215.
2 T. Schimanouchi and M. Tasumi, *Spectrochim. Acta*, 17 (1961) 755.
3 T. Schimanouchi, M. Tasumi and Y. Abe, *Makromol. Chem.*, 86 (1965) 43.
4 D. Lím and M. Kolínský, *J. Polym. Sci.*, 53 (1961) 173.
5 J. Petránek, M. Kolínský and D. Lím, *Nature (London)*, 207 (1965) 1290.
6 D. Lím, M. Kolínský, J. Štokr and J. Petránek, *J. Polym. Sci., Part B*, 4 (1966) 577.
7 D. Doskočilová and B. Schneider, *Collect. Czech. Chem. Commun.*, 29 (1964) 2290.
8 D. Lím, M. Kolínský, J. Štokr and J. Petránek, *J. Polym. Sci., Polym. Lett. Ed.*, 4 (1966) 577.
9 J. Lesec, B. Jasse and C. Quivoron, *C.R. Acad. Sci., Paris.* 278 (1974) 1433.
10 J. Lesec, F. Lafuma and C. Quivoron, *J. Chromatogr. Sci.*, 12 (1974) 683.
11 J. Čoupek, S. Pokorný, V. Gregor and V. Jehlička, *J. Chromatogr.*, 88 (1974) 323.
12 J. G. Pritchard and R. L. Vollmer, *J. Org. Chem.*, 28 (1963) 1545.
13 F. Davdevani, J. A. Biesenberger and M. Tan, *J. Polym. Sci., Part B*, 9 (1971) 429.

Journal of Chromatography, 148 (1978) 189–193

CHROM. 10,462

ANALYSIS OF NATURAL GAS BY GAS CHROMATOGRAPHY

JAROSLAV KUBÁT and JIŘÍ MACÁK
Department of Gas and Coke, Institute of Chemical Technology, Prague 6 (Czechoslovakia)
JIŘÍ MIZERA
Transgas, Prague (Czechoslovakia)
and
JAROMÍR ZACHOVAL
Department of Polymers, Institute of Chemical Technology, Prague 6 (Czechoslovakia)

SUMMARY

A method for the analysis of natural gas that is suitable for use in routine control analyses has been developed. A thermal conductivity detector is used for the determination of $N_2 + O_2$, CO_2 and C_1–C_2 hydrocarbons and a flame-ionization detector for other components, with programming of the column temperature. By concentrating C_6 and higher hydrocarbons in a short column section that can be disconnected during the analysis, a rapid and accurate analysis can be carried out by back-flushing. The integrator can be used to calculate real density and real calorific values simultaneously.

INTRODUCTION

To measure an amount of natural gas, especially in industrial situations, it is necessary to determine correctly all of the components that are used to express significant qualitative criteria, *i.e.*, true calorific values and true density.

Isothermal gas chromatography with a single column makes it possible to obtain only partial information on the total composition, this being dependent on the temperature and column length. Substantial improvements can be achieved by using temperature programming and detection with a thermal conductivity (TCD) and flame-ionization detector (FID) simultaneously[1]. Even in this instance a portion of heavier components remains adsorbed on the column packing. The problem of the total analysis of natural gas is dealt with in ASTM Standard D 1945, which prescribes the determination of nitrogen, carbon dioxide and C_1–C_5 hydrocarbons as individual peaks, and C_6 and higher hydrocarbons as a sum from back-flushing. As an example, ASTM D 1945 describes three methods by Purcell and Gilson[2]. Two of the methods concern isothermal analysis with back-flushing while the third uses temperature programming and back-flushing. All of the methods use a TCD. HP 5830 has been used to analyse natural gas[3], in a system of three columns packed with Porapak Q,

30% DC 200 on Chromosorb W and molecular sieve 5A, with thermal conductivity detection. The procedure is fully automatic.

In this paper, an automatic method for the analysis of natural gas is described that is suitable for use in routine control analysis.

EXPERIMENTAL AND RESULTS

Apparatus

A Packard Model 419 gas chromatograph, equipped with a temperature-programmed column, TCD, dual FID, three eight-way-, two-position "Kuhnke" valves controlled either manually or pneumatically, W + W 10-mV recorder and a Spectra-Physics Autolab System I integrator for integration of the peak areas were used. The procedure consists in the separation of natural gas components on a column packed with Porapak R. The column is divided into two sections, which can be connected according to scheme I, II or III (Fig. 1). The first short section serves to concentrate the C_6 and higher hydrocarbon fractions, so that these fractions can be determined by back-flushing. The detection of oxygen + nitrogen, carbon dioxide and C_1–C_2 hydrocarbons is performed with the TCD, while the other hydrocarbons are detected with the FID, the two detectors being arranged in a series.

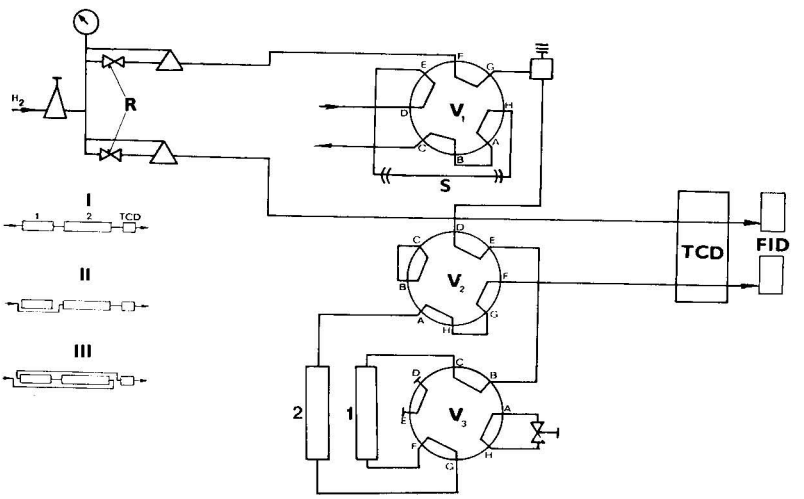

Fig. 1. Flow diagram of apparatus. R = Flow controllers; V_1 = sample valve; S = sample loop; V_2 = back-flush valve; V_3 = switch valve; 1 = column packed with Porapak R (1 m × 2 mm I.D.); 2 = column packed with Porapak R (3 m × 2 mm I.D.). I–III, connection schemes.

Chromatographic separation conditions

The dimensions of the analysis section of the column were: 1 m + 3 m × 2 mm I.D. and those of the reference section were 4 m × 2 mm I.D. The packing was Porapak R (80–100 mesh). The carrier gas (hydrogen) flow-rate was 20 ml in the analysis and reference sections, with an added gas (nitrogen) flow-rate of 15 ml/min and an air flow-rate of 300 ml/min. The TCD temperature was 150° with a detector current of 200 mA and the FID temperature was also 150°. The column temperature

was maintained isothermally at 30° for 1 min, then programmed from 30 to 180° at 15°/min, the final temperature being maintained for 9 min, followed by a cooling period of 10 min. The gas sample size was 0.25 ml and the recorder was operated at 10 mV.

Procedure

A sample of gas is introduced into the chromatograph through the eight-way valve V_1 (Fig. 1), equipped with a sample loop S of volume 0.25 ml. The Autolab System I is set to the "Run" mode and the pre-adjusted temperature programme is

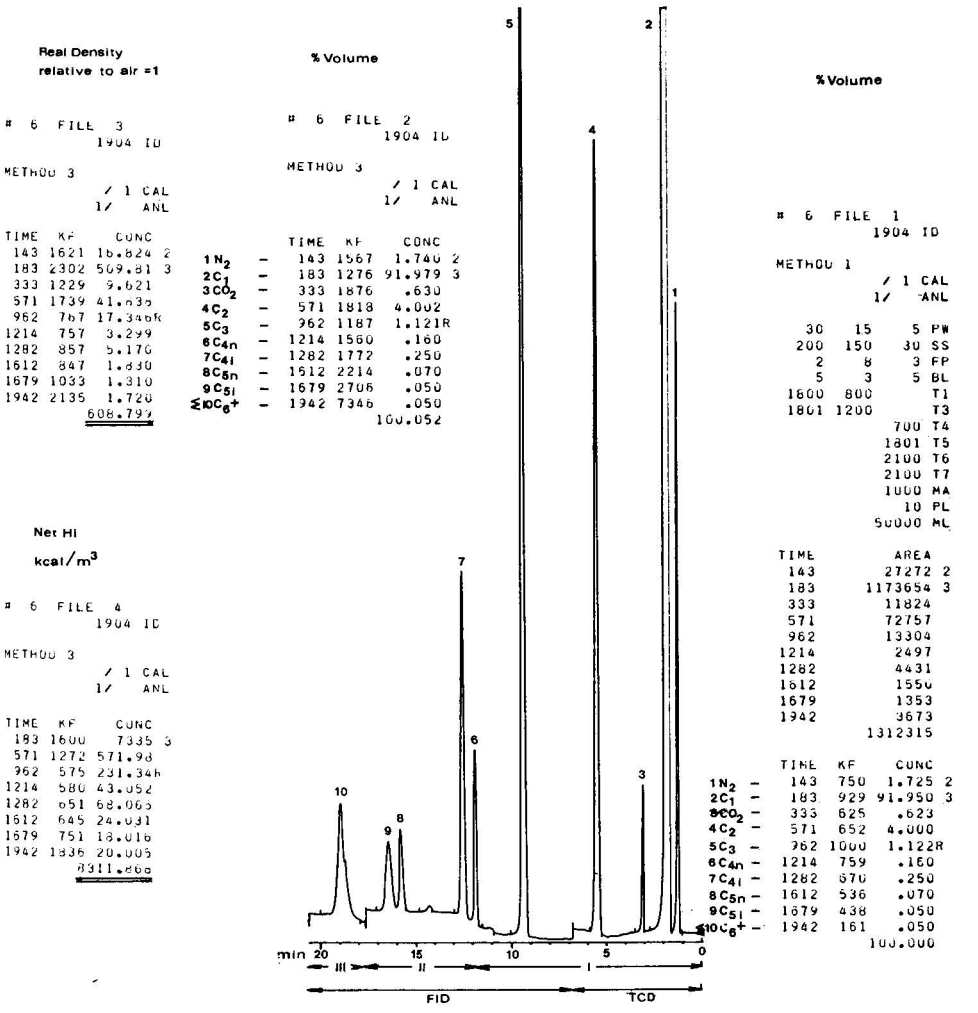

Fig. 2. Chromatogram of a natural gas sample. Peaks: 1 = air; 2 = methane; 3 = carbon dioxide; 4 = ethane; 5 = propane; 6 = isobutane; 7 = *n*-butane; 8 = isopentane; 9 = *n*-pentane; 10 = hexanes and heavier. In File 1 the gas composition is calculated by Method 1 (internal normalization). In File 2 the gas composition is calculated by Method 3 (external standard). In File 3, the real density is calculated by Method 3; the result is read by equating the scale factor 10^{-3} to 0.609. In File 4, the net caloric value (Net HI) is calculated by Method 3 to be 8311.9 kcal/m^3.

set simultaneously. The two column sections are connected in series at the start and the integrator accepts the signal from the TCD. After the elution of ethane (7 min) the integrator is switched to the FID signal. As soon as *n*-pentane has been eluted from the short column section (12 min), this section is disconnected via the valve V_3 so as to store C_6 and higher hydrocarbon fractions; this procedure makes it possible to eliminate the need to resolve C_6 and higher hydrocarbon fractions and to speed up the analysis. When the elution of *n*-pentane from the second column section is completed (18 min), the two column sections are connected again (V_3) and back-flushed (V_2). The integration is performed after the analysis is completed and the columns are cooled simultaneously. The results are shown in Fig. 2.

Quantitative determinations were performed with a standard mixture purchased from Messer-Griesheim (Duisburg, G.F.R.). The calculation of concentrations from peak areas is possible either by internal normalization or the external standard method (Methods 1 and 3, in Autolab System I language).

The calibration consists in correlating the concentrations of the components of a standard mixture with the relating peak areas that are marked by their retention times, the integrator being set in the "Calibration" mode. The Autolab System I uses these data to calculate the corresponding KF (calibration values), depending on the method selected. These KF values are used to calculate results for the sample being analysed, the "Analysis" mode being used. To calculate the results, Method 1 was chosen, the advantages of which are that the results are corrected to the contents of all components and they are independent of the exact amount injected. The advantage of Method 3, in which the concentrations are calculated by comparing the peak areas of the sample and the standards, can be used in the analysis of components of low concentration.

Method 3 can be used to calculate the characteristic constants real density (RD) or real calorific value (RCV). In this instance it is possible to add the real densities and real calorific values of the pure components to the corresponding peak areas and to calculate new KF values that can be used to calculate RD and RCV of samples. The Autolab System I makes it possible to store different calculation data in four independent memory files. The results obtained by Method 1 can be compared with the results obtained by Method 3 (Fig. 2). Method 1 was stored in File 1, Method 3 in File 2, the data to calculate RD in File 3 and those to calculate RCV in File 4.

DISCUSSION

The combination of a Packard Model 419 gas chromatograph with an Autolab System I integrator proved to be especially useful, and the method has the following advantages:

(1) It complies with ASTM Standard D 1945.

(2) The automatic switching over of the integrator from the TCD to the FID permits the accurate determination of all components.

(3) The storage of the higher hydrocarbons in the short column section concentrates them to a single sharp peak, which makes the integration easier and more exact.

(4) The pressure pulses due to switching over the valves, observable with the

TCD, and the irregularity of the baseline with temperature programming, are eliminated by using the FID.

(5) By using the Autolab System I it is possible to calculate the exact composition of natural gas and the real density and real calorific values simultaneously during the analysis, and thus to eliminate the need for expensive equipment for their determination.

REFERENCES

1 J. S. Stufkens and H. J. Bogaard, *Anal. Chem.*, 47 (1975) 383.
2 J. E. Purcell and C. P. Gilson, *Chromatogr. Newsl.*, 1, No. 2 (1972) 45.
3 L. E. Green, *Hewlett Packard Technical Paper*, No. 57 (1974).

Journal of Chromatography, 148 (1978) 195–201

CHROM. 10,404

REVERSED-PHASE LIQUID–LIQUID CHROMATOGRAPHY OF AROMATICS ON MACROPOROUS POLYSTYRENE GEL

M. POPL, V. DOLANSKÝ and J. FÄHNRICH

Department of Analytical Chemistry, Institute of Chemical Technology, Suchbátarova 1905, 16628 Prague 6 (Czechoslovakia)

SUMMARY

Retention data of polar substituted benzenes and naphthalenes were measured using reversed-phase liquid–liquid chromatography on macroporous polystyrene gel with methanol–water and acetonitrile–water as the eluents. The results of the chromatographic measurements are expressed in terms of retention indices (I). Considerable differences in the behaviour of the individual solutes were found in the two eluents. A method is suggested for predicting the retention indices of polysubstituted solutes as the sum of increments ($\Delta \log I$) from the monosubstituted compounds. To verify the liquid–liquid partition mechanism controlling this chromatographic separation, the partition coefficients of several compounds were measured for the model system toluene–aqueous methanol.

INTRODUCTION

In previous work[1], the behaviour of aromatic hydrocarbons on a macroporous polystyrene gel was studied using a mixture of methanol, diethyl ether and water as the eluent. This paper extends the gel characteristics to aromatic solutes with polar functional groups and shows how the elution behaviour of these substances is affected by the choice of the eluent. The reversed-phase partition chromatographic mechanism has been proposed[1] as the governing principle for separations on the materials studied. Nakae and Muto[2] have interpreted the chromatographic properties of a styrene–divinylbenzene copolymer and the temperature dependence of retention volumes in terms of the same mechanism. In an attempt to verify this mechanism, the extraction equilibria of selected compounds were measured in a model system consisting of toluene–aqueous methanol.

EXPERIMENTAL

A glass column (30 cm × 4 mm I.D.) packed with a crosslinked polystyrene gel in the form of spherical particles 25–32 μm in diameter and with an exclusion limit of molecular weight 40,000 (obtained using benzene as the eluent and a Waters polystyrene standard) was used. The dead volume of the column was measured as the elution volume of water. The column was packed with a gel suspension in metha-

nol; the pressure of eluent was maintained at 2.5–3.0 MPa and the packing was gradually added. Methanol–water and acetonitrile–water were employed as eluents, each at volume ratios of 7:3 and 3:2, the composition depending on the retention volumes of the solutes measured.

The eluent was delivered by a ISCO Dialagrad, Model 384, pulseless pump. The pressure was *ca.* 3.0 MPa at a flow-rate of 40 ml/h. The detector was a Waters Assoc. differential UV monitor with a cell of dead volume 8 μl and an optical path length of 1 cm, operating at a constant wavelength of 254 nm.

The extraction equilibria were studied in a separating funnel provided with a thermostating jacket. The sample was dissolved in methanol–water (4:1) to give a total volume of 30 ml, the mixture was transferred to the funnel and then 30 ml of toluene were added. To approximate infinite dilution conditions, a concentration of 1 g of sample per litre of methanol was used. The mixture was shaken vigorously and allowed to equilibrate for 2 h; samples of both phases were then removed and measured on a Unicam SP 800B UV spectrophotometer. The phase samples and the original methanolic solution were diluted so that the solvent composition was identical. In addition to methanol, the pure phases corresponding to the equilibrium composition of the two layers in the absence of the sample were used for the dilution. In this way, even substances whose UV spectra depend strongly on the solvent composition could be evaluated accurately.

RESULTS AND DISCUSSION

The results of the chromatographic experiments are expressed in terms of retention indices (I) (ref. 3). For benzene, naphthalene and phenanthrene, the log I values were defined as 1, 2 and 3, respectively. The retention index of a solute with $\log I > 1$ is calculated according to the equation

$$\log I = \log I_n + \frac{\log R_x - \log R_n}{\log R_{n+1} - \log R_n} \tag{1}$$

where R is the corrected elution volume and subscripts n, $n+1$ and x correspond to the lower and higher standards and to the solute measured, respectively.

For solutes with $\log I < 1$ the benzene–naphthalene interval must be extrapolated:

$$\log I = 1 - \frac{\log R_B - \log R_x}{\log R_N - \log R_B} \tag{2}$$

where subscripts B and N refer to benzene and naphthalene, respectively.

TABLE I

CORRECTED RETENTION VOLUMES, V', AND CAPACITY FACTORS, k', OF BENZENE AND NAPHTHALENE

Compound	*Log I*	*CH_3OH–H_2O*				*CH_3CN–H_2O*			
		3:2		*7:3*		*3:2*		*7:3*	
		V' (ml)	*k'*	*V' (ml)*	*k'*	*V' (ml)*	*k'*	*V' (ml)*	*k'*
Benzene	1	9.8	4.8	6.4	3.1	9.2	4.5	4.5	2.2
Naphthalene	2	31.2	15.2	20.2	9.9	21.4	10.4	9.9	4.8

The elution volumes and capacity factors for the standards are given in Table I. The capacity factors of all of the substances vary considerably according to the content of water in the mobile phase, whereas the retention indices are virtually independent of this ratio. The use of a mobile phase with a higher water content permitted more precise measurements of the retention indices for solutes with low

TABLE II

RETENTION INDICES (LOG *I*) FOR SUBSTITUTED BENZENES AND ESTABLISHED DEVIATIONS (*D*)

$D = \log I_{meas} - \log I_{calc}$, where $\log I_{calc}$ has been calculated as the sum of substituent contributions given in Table IV.

Compound	*Mobile phase*			
	CH_3OH–H_2O		CH_3CN–H_2O	
	$\log I_{meas}$	*D*	$\log I_{meas}$	*D*
Benzene	1.00	—	1.00	—
Phenol	0.51	−0.12	0.07	−0.09
Thiophenol	0.52	—	0.29	—
Nitrobenzene	1.29	0.01	0.87	−0.03
Chlorobenzene	1.32	—	1.42	—
Bromobenzene	1.46	−0.03	1.60	−0.05
Iodobenzene	1.73	—	1.89	—
Benzoic acid	0.57	0.42	−0.26	−0.31
Benzaldehyde	0.75	—	0.43	—
Methyl benzoate	0.60	—	0.74	—
Benzonitrile	0.82	—	0.46	—
Aniline	0.55	—	0.37	—
N,N-Dimethylaniline	1.46	—	−0.69	—
p-Dibromobenzene	1.93	−0.05	2.35	0.05
1,3,5-Tribromobenzene	2.56	0.09	2.92	−0.03
o-Cresol	0.79	−0.06	0.38	−0.11
2,6-Xylenol	1.03	−0.05	0.72	−0.10
o-Nitrotoluene	1.48	−0.02	1.23	0.00
p-Nitrotoluene	1.47	−0.03	1.19	−0.04
1-Fluoro-2,4-dinitrobenzene	1.79	—	0.92	—
1-Chloro-2,4-dinitrobenzene	1.93	0.05	1.40	0.18
m-Nitrophenol	1.33	0.42	0.32	0.26
2-Chloro-4-nitrophenol	1.16	−0.44	0.52	−0.80
Picric acid	1.54	0.07	0.71	0.85
Resorcinol	0.12	−0.14	−0.71	−0.03
Hydroquinone	0.01	−0.25	−1.10	−0.42
Pyrogallol	−0.04	0.15	−0.84	0.68
p-Toluenesulphonic acid	0.60	0.08	−0.88	0.08
p-Xylenesulphonic acid	0.66	−0.08	−0.72	−0.09
p-Hydroxybenzoic acid	−0.07	0.15	−0.73	0.06
3,5-Dinitrobenzoic acid	0.13	−0.58	0.09	0.24
o-Aminobenzoic acid	0.67	0.97	−0.09	0.67
o-Aminophenol	0.23	0.05	−1.33	−0.86
p-Aminophenol	−0.13	−0.31	−1.29	−0.82
o-Nitroaniline	1.33	0.50	0.80	0.53
m-Nitroaniline	1.25	0.42	0.66	0.39
p-Nitroaniline	1.07	0.24	0.49	0.22
2,4-Toluenediamine	0.09	−0.23	−1.66	−1.73
p-toluidine	0.53	−0.24	−1.46	−2.16

TABLE III

RETENTION INDICES (LOG *I*) FOR SUBSTITUTED NAPHTHALENES

Compound	*Mobile phase*	
	CH_3OH–H_2O	CH_3CN–H_2O
α-Naphthol	1.65	1.06
β-Naphthol	1.65	0.88
α-Naphthylamine	1.80	0.68
β-Naphthylamine	1.65	—
α-Chloronaphthalene	2.32	2.47
α-Bromonaphthalene	2.51	2.67
α-Nitronaphthalene	2.34	1.85
α-Naphthoic acid	0.10	—

retentions. The reproducibility of log *I* with change in the composition of the mobile phase is approximately ± 0.05; for solutes with small values of log *I* (below 0.5), the reproducibility is lower (about ± 0.2). This error is caused mainly by the inaccuracy in the determination of very short retention times.

The measured retention indices are given in Tables II and III. Considerable differences in the behaviour of the individual solutes in the aqueous methanol and aqueous acetonitrile mobile phases can be seen. The halobenzenes shows similar affinities towards both eluents and the individual members can easily be separated (Fig. 1). Other substances exhibit larger or smaller differences, so that the selectivity can be affected to a considerable extent by the choice of the eluent. For example, benzoic acid, benzaldehyde and methyl benzoate cannot be separated in aqueous methanol, whereas aqueous acetonitrile gives good results (Fig. 2). Similar conclusions were drawn by Locke[4] for reversed-phase partition chromatography when interactions in the non-polar stationary phase are weak and the separation properties of the system depend exclusively on the eluent composition or the solubility of the solute in the mobile phase.

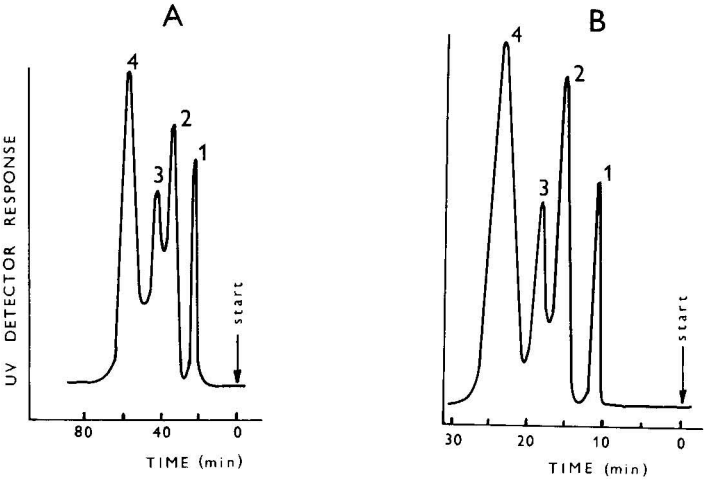

Fig. 1. Separation of halobenzenes: 1 = benzene; 2 = chlorobenzene; 3 = bromobenzene; 4 = iodobenzene. Eluent: (a) methanol–water (7:3), 20 ml/h; (b) acetonitrile–water (3:2) 40 ml/h.

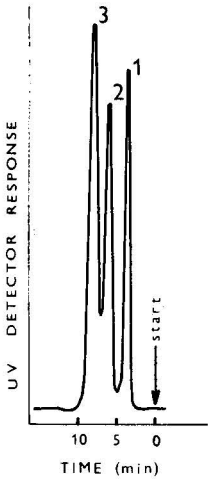

Fig. 2. Separation of benzenes with carboxylic substituents: 1 = benzoic acid; 2 = benzaldehyde; 3 = methyl benzoate. Eluent: acetonitrile–water (3:2), 40 ml/h.

A method has been developed for the characterization of the individual substituents, permitting the calculation of log I as the sum of Δ log I increments from the individual substituents (Table IV). These contributions predict the retention index with deviations (D) given in Table II. In this way, substances substituted with a methyl group, halogens, some phenols and nitro compounds can readily be characterized. The application of the contributions is limited in the case of intramolecular substituents interaction. Rather large deviations were found for nitrophenols, polyphenols and solutes with carboxylic groups using aqueous acetonitrile as the eluent. The poorest results were obtained with amino compounds. There is no explanation

TABLE IV

CONTRIBUTIONS (ΔLOG I) FOR VARIOUS FUNCTIONAL GROUPS IN SUBSTITUTED BENZENES

Functional group	*Mobile phase*	
	CH_3OH–H_2O	*CH_3CN–H_2O*
CH_3	0.22	0.33
F	0.23	0.12
Cl	0.32	0.42
Br	0.49	0.65
I	0.73	0.89
NO_2	0.28	−0.10
OH	−0.37	−0.84
SH	−0.48	−0.71
CHO	−0.25	−0.57
$COOCH_3$	−0.40	−0.26
C≡N	−0.18	−0.54
SO_3H	−0.70	−2.29
COOH	−0.85	−0.95
$N(CH_3)_2$	0.46	−1.70
NH_2	−0.45	−0.63

TABLE V

VALUES OF SOLUTE PARTITION COEFFICIENT, k^{25}, FOR TOLUENE/METHANOL-WATER (4:1) AT 25°

Compound	*Log* k^{25}	*Compound*	*Log* k^{25}
Phenol	−0.47	1-Fluoro-2,4-dinitrobenzene	0.76
Nitrobenzene	0.72	1-Chloro-2,4-dinitrobenzene	0.83
Benzoic acid	−0.30	*p*-Hydroxybenzoic acid	−1.78
Aniline	−0.28	2,4-Toluenediamine	−0.90
N,N-Dimethylaniline	0.87	Naphthalene	1.06

for the large difference between the retention indices of aminobenzene and *p*-toluidine with the aqueous acetonitrile as the eluent.

The chromatographic behaviour of substituted naphthalenes (Table III) is similar to that of benzenes. For halo-, nitro- and hydroxynaphthalenes and methanol–water as the eluent, the contributions found for the substituted benzenes can be employed with good precision. It seems that there are differences in the elution volumes depending on the position of substitution, which were not observed for alkyl substituents[1].

The results of the extraction equilibrium experiments are summarized in Table V, in which the partition coefficients (log k^{25}), i.e., equilibrium concentration of the solute in the toluene phase to that in the methanolic phase at 25° are given. In Fig. 3, the linear dependence of log I on log k^{25} is shown for aqueous methanol as the eluent:

$$\log I = 0.780 \log k^{25} + 0.972$$

(correlation coefficient $r = 0.951$). Although the correlation coefficient is not high, this dependence demonstrates a relationship between the elution behaviour and the distribution coefficient in model liquid phases. As the extraction system approximates

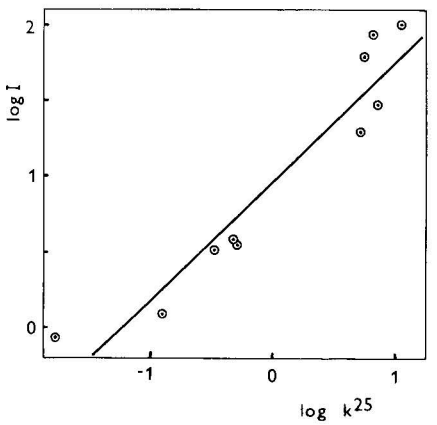

Fig. 3. Dependence of retention index, I, on solute partition coefficient, k^{25}, for toluene/methanol–water (4:1) at 25°.

the character of the gel matrix only roughly, this correlation can be considered to indicate the probability of the partition mechanism controlling the chromatographic system studied.

REFERENCES

1 M. Popl, V. Dolanský and J. Čoupek, *J. Chromatogr.*, 130 (1977) 195.
2 A. Nakae and G. Muto, *J. Chromatogr.*, 120 (1976) 47.
3 M. Popl, V. Dolanský and J. Mostecký, *J. Chromatogr.*, 91 (1974) 649.
4 D. C. Locke, *J. Chromatogr. Sci.*, 12 (1974) 433.

Journal of Chromatography, 148 (1978) 203–210

CHROM. 10,405

INVESTIGATION OF THE COMPOSITION OF COAL-TAR PHENOLS AND XYLENOLS BY CAPILLARY CHROMATOGRAPHY

P. BURYAN and J. MACÁK
Institute of Chemical Technology, 16628 Prague 6 (Czechoslovakia)
and
V. M. NABIVACH
Institute of Chemical Technology, 320640 Dniepropetrovsk 5 (U.S.S.R.)

SUMMARY

Gas chromatographic analyses of technical coal-tar phenol products, dehydrated phenols, tricresol, dicresol and xylenols were carried out in an open-tubular column, 50 m long, containing tri-(2,4-xylenyl)phosphate at 130°. More than 40 phenol derivatives were identified in the dehydrated phenols and xylenols.

INTRODUCTION

One of the sources of phenol and its derivatives for the chemical industry is the coke industry, in which coal is processed on a large scale by the method of high-temperature coking process. The waste and coal tar resulting from this process serve as a source of coal-tar phenols; by rectification of phenols different phenolic products (phenol, cresols, fractions of dicresol, tricresol and xylenol) are obtained.

The increasing application of phenol derivatives has placed increased demands on the quality and quantitative composition of phenolic products, which may vary with the consumer,

The investigation of the composition of phenol mixtures resulting from coking is complicated by the presence of a considerable amount of components with similar boiling points, differing by only 1–2°. Coal-tar phenols contain about 50 components boiling within the range 200–260° [1]. The problems of the analysis of the composition of mixtures of phenolic products and of the pure constituents have been solved successfully by means of gas–liquid chromatography[2–8].

Comparative data show that packed columns, in spite of their wide use for the analysis of technical products, do not provide the complete separation of all of the isomers of methyl-, ethyl- and dimethylphenols. Thus, in the analysis of coal-tar phenols, even with the application of selective stationary phases such as tri(2,4-xylenyl) phosphate and dimethyl phthalate, some derivatives of phenol such as 2-ethylphenol and 2,3-dimethylphenol, 3-ethylphenol and 2,3-dimethylphenol, 3-ethylphenol and 3,5-dimethylphenol, and other pairs, remain unseparated [2,3,9–12]. Consequently, the data on the qualitative and quantitative compositions of phenol fractions obtained

using packed columns are not exhaustive and in most instances provide information only about the main components present in the fractions. Capillary columns do not suffer from most of the drawbacks mentioned above. The high efficiency of capillary columns permits the separation of all similar boiling homologues of phenol within a short period.

EXPERIMENTAL

As the stationary liquid phase, tri(2,4-xylenyl) phosphate (TXP), which shows a high selectivity with respect to phenols, was used[13–16]. The methods of preparation of the capillary column and the coating of the liquid phase have been described previously[17]. For the identification and quantitative determination of some phenol derivatives, the peaks of which overlap in the capillary column (I), the main fractions were also analysed in a packed column (II) containing Apiezon L. The column parameters and the conditions of analyses are given in Table I.

TABLE I

CONDITIONS OF ANALYSIS IN COLUMNS I AND II

Parameter	*Column I*	*Column II*
Apparatus	Chrom-41	Chrom-41
Column material	Stainless steel	Glass
Column length and diameter (m × mm)	50 × 0.25	4.4 × 3
Stationary phase	95% TXP + 5% H_3PO_4	20% Apiezon L + 0.5% Carbowax 6000
Solid support	–	Chromaton N (AW-HMDS), 0.1–0.125 mm
Detector	Flame ionization	Flame ionization
Carrier gas (nitrogen) pressure (kPa)	152	230
Column temperature (°C)	130	160, 180
Injection port temperature (°C)	260	–
Scale sensitivity (mV)	20	1000
Sample size (μl)	0.1–0.15	0.5

RESULTS AND DISCUSSION

The chromatograms of some industrial fractions of coal-tar phenols produced by a phenol plant are shown in Figs. 1–4. The identification has been carried out by using Kováts retention indices[17] and by the method of addition of pure standards.

A comparison of the chromatograms obtained in columns I and II made it possible to establish that, with the exception of C_6–C_8 phenols, the following derivatives of phenol are present in the dehydrated phenol fraction: 2,4,6-, 2,3,6-, 2,4,5-, 2,3,5-, 2,3,4- and 3,4,5-trimethylphenols, 6-ethyl-2-methylphenol, 2-,3- and 4- isopropylphenols, 2-isopropyl-6-methylphenol, 2-ethyl-4-methylphenol, 4-ethyl-2-methylphenol, 5-ethyl-3-methylphenol, 2-ethyl-5-methylphenol, 3-ethyl-6-methylphenol, 4-ethyl-3-methylphenol 2-, 3- and 4-*n*-propylphenols, 2-isobutylphenol, 2-*sec*.-butylphenol, 2-methyl-4-*n*-propylphenol, 3-methyl-6-*n*-propylphenol, 2,4-diethylphenol, 2,3,5,6- and 2,3,4,6-tetramethylphenols and 4-indanol. A comparison of the data

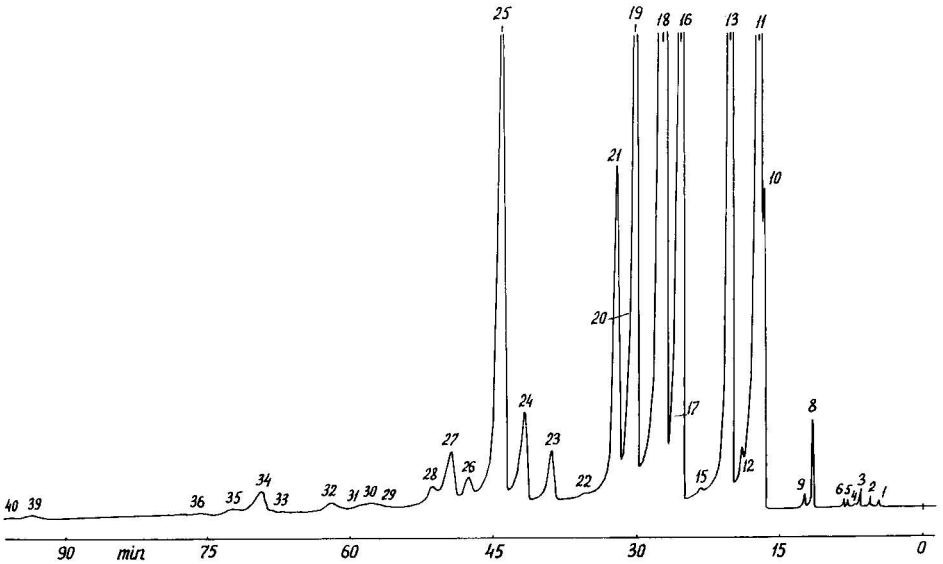

Fig. 1. Chromatogram of dehydrated phenol fraction; the interpretation of the peaks is given in Tables II and III.

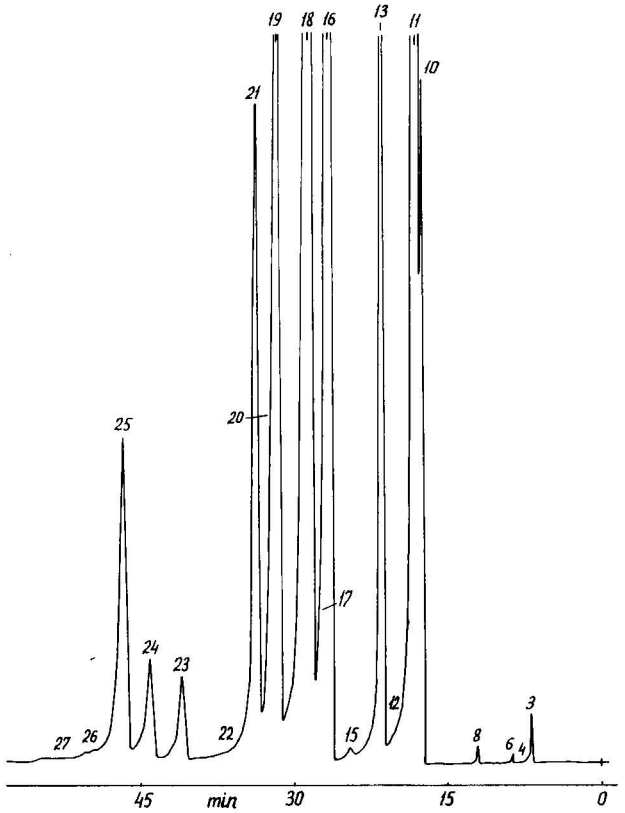

Fig. 2. Chromatogram of technical tricresol.

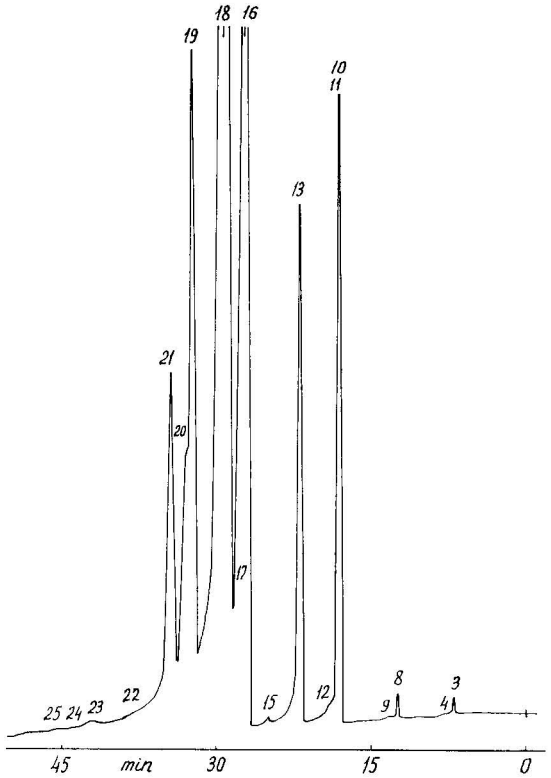

Fig. 3. Chromatogram of technical dicresol.

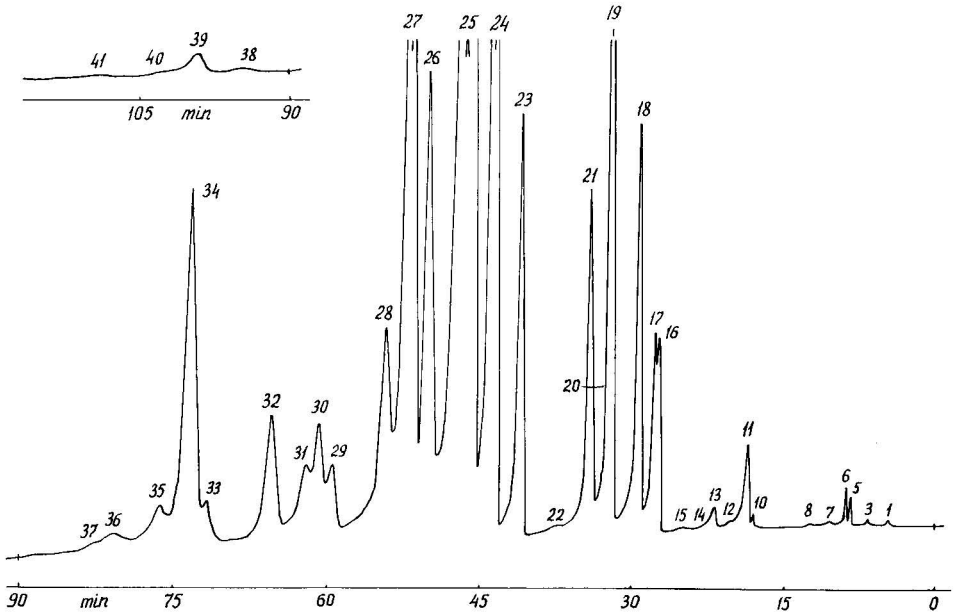

Fig. 4. Chromatogram of narrow xylenol fraction.

TABLE II

BOILING POINTS AND RELATIVE RETENTION TIMES OF PHENOL PRODUCTS IN COLUMN I

Number of peak on chromatograms	*Component*	*Boiling point (°C)*	*Relative retention time**
1–9	Unidentified	—	—
10	2,6-Dimethylphenol	200.6	0.96
11	Phenol	182.0	1.00
12	Unidentified	—	1.12
13	2-Methylphenol	191.0	1.21
14	Unidentified	—	1.25
15	6-Ethyl-2-methylphenol	213.0	1.41
16	4-Methylphenol	201.9	1.57
17	2,4,6-Trimethylphenol	220.6	1.61
18	3-Methylphenol	202.2	1.68
19	2-Isopropyl-6-methylphenol +	228–230	1.80
	2,4-dimethylphenol	211.3	1.87
20	2-Ethylphenol	204.5	1.91
21	2,5-Dimethylphenol	211.5	2.00
22	2,3,6-Trimethylphenol	234.0	2.08
23	2,3-Dimethylphenol	217.1	2.43
24	2-Isopropylphenol +	214.4	2.62
	4-ethylphenol	218.0	2.63
25	3,5-Dimethylphenol +	221.7	2.79
	2-ethyl-4-methylphenol +	222.3	2.79
	3-ethylphenol	217.0	2.82
26	4-Ethyl-2-methylphenol +	227.0	2.99
	2-*n*-propylphenol	221.0	3.02
27	2-Ethyl-5-methylphenol +	224.2	3.09
	3,4-dimethylphenol +	226.9	3.12
	3-ethyl-6-methylphenol	227.7	3.14
28	Unidentified	—	3.29
29	2,3,5,6-Tetramethylphenol +	248.0	3.56
	4-isopropylphenol	229.1	3.58
30	2,4,5-Trimethylphenol +	235.2	3.63
	2-isobutylphenol	228.3	3.63
31	2,3,4,6-Tetramethylphenol +	250.0	3.68
	3-isopropylphenol	228.0	3.68
32	2,3,5-Trimethylphenol +	235.3	3.94
	2-*sec.*-butylphenol	228.0	3.95
33	2,4-Diethylphenol	229.0	4.32
34	4-*n*-Propylphenol +	234.5	4.48
	5-ethyl-3-methylphenol	235.9	4.52
35	3-*n*-Propylphenol +	233.5–234.5	4.63
	2,3,4-trimethylphenol	234.5–237.0	4.74
36	2-Methyl-4-*n*-propylphenol +	240.0–242.6	4.80
	4-ethyl-3-methylphenol +	229.0	4.92
	3-methyl-6-*n*-propylphenol	235.0	4.92
37	2,5-Diethylphenol	242.5	5.13
38	5-Methyl-4-indanol +	250.0	5.71
	4-isobutylphenol +	243.9	5.79
	4-*sec.*-butylphenol	242.1	5.86
39	4-Indanol	247.0	6.07
40	3,4,5-Trimethylphenol	251.9	6.39
41	Unidentified	—	6.89

* Phenol = 1.00.

obtained with the results of analyses of analogous fractions published elsewhere[7,8,10,11,18–22] indicates that most of the above phenols have been identified here for the first time.

The high selectivity of TXP, the comparatively low temperature of the column 1 and also a low concentration did not permit some components to be identified, as their peaks showed too much tailing. This identification was achieved by increasing the size of the sample of the phenol fraction (4 μl) in the column at 180°, when several peaks were observed, including 5-indanol.

Peaks 1–9 and 12 (Figs. 1 and 4) remained unidentified, and are probably high-boiling hydrocarbons. Peak 28 also remained unidentified, and is probably 2-ethyl-3-methylphenol (according to the relationship between the logarithm of the relative retention times of phenols and the number of hydrocarbon atoms in the molecule).

During the analysis of xylenol fractions in column 1, in addition to the above compounds, 2,5-dimethylphenol, 5-methyl-4-indanol, 4-isobutylphenol and 4-*sec.*-butylphenol were identified. With an increase in the sample size to 4 μl in column II at 160°, the presence of 3-*n*-butylphenol, 3,4-diethylphenol, 2-ethyl-4,5-dimethylphenol and 6-methyl-4-indanol in xylenol fractions was established.

Quantitative calculations were carried out using the method of internal normalization without introducing the correction factor[7,23]. The areas of the peaks were determined with the aid of a 1-Tl digital proportional computer (Laboratorní přístroje, Prague, Czechoslovakia). The results of the analyses are given in Tables II and III.

Comparative calculations of the content of some components of fractions of dehydrated phenols obtained in both columns showed that the amounts of 2,4,6-trimethylphenol and 2-isopropyl-6-methylphenol giving overlapping peaks in column 1 with those of 4-methyl- and 2,4-dimethylphenol are small, not exceeding 0.25 and 0.20%, respectively. Approximately the same amount of ethylmethylphenols, the peaks of which overlap with the peaks of some dimethyl- and *n*-propylphenols, is contained in this fraction.

In column 1, the isomers of ethylphenol, except 3-ethylphenol, are separated from the corresponding dimethylphenols. However, the peak of 4-ethylphenol overlaps with that of 2-isopropylphenol. Calculations on the chromatograms obtained from column II showed that the total content of 3- and 4-ethylphenols in the phenol fraction does not exceed 1.5%. Hence, the total amount of isomers of ethylphenol in the dehydrated phenol fraction is 2.0–2.1%. Calculations on the chromatograms obtained

TABLE III

QUANTITATIVE RESULTS OF ANALYSES OF PHENOL PRODUCTS IN COLUMN I

Number of peak on chromatograms	*Component*	*Mean wt. (%)*				
		Dehydrated phenol	*Tricresol*	*Dicresol*	*Technical xylenol*	*Narrow xylenol fraction*
1–9	Unidentified	0.46	0.32	0.26	0.23	0.20
10	2,6-Dimethylphenol	0.83	1.30	2.70	0.10	0.05
11	Phenol	34.60	25.90		0.33	0.35
12	Unidentified	0.16	— *	—	0.03	0.04

TABLE III *(continued)*

Number of peak on chromatograms	*Component*	*Mean wt. (%)*				
		Dehydrated phenol	*Tricresol*	*Dicresol*	*Technical xylenol*	*Narrow xylenol fraction*
13	2-Methylphenol	11.80	4.65	2.60	0.20	0.08
14	Unidentified	—	—	—	0.01	0.01
15	6-Ethyl-2-methylphenol	0.10	0.04	0.03	0.07	0.03
16	4-Methylphenol	11.95	18.98	26.34	3.25	0.72
17	2,4,6-Trimethylphenol				1.02	0.75
18	3-Methylphenol	22.52	31.35	55.25	7.41	1.95
19	2-Isopropyl-6-methylphenol + 2,4-dimethylphenol	5.45	7.86	6.80	—	—
		—	—	—	10.50	4.21
20	2-Ethylphenol	0.61	1.07	1.50	—	—
21	2,5-Dimethylphenol	2.74	4.21	4.39	4.80	1.70
22	2,3,6-Trimethylphenol	0.17	0.09	—*	0.07	0.05
23	2,3-Dimethylphenol	0.48	0.74	0.13	3.10	2.70
24	2-Isopropylphenol + 4-ethylphenol	0.86	0.90	—	9.30	9.61
25	3,5-Dimethylphenol + 2-ethyl-4-methylphenol + 3-ethylphenol	5.70	2.42	—*	40.86	52.70
26	4-Ethyl-2-methylphenol + 2-*n*-propylphenol	0.20	0.17	—	3.01	3.75
27	2-Ethyl-5-methylphenol + 3,4-dimethylphenol + 3-ethyl-6-methylphenol	0.62	—*	—	8.30	11.22
28	Unidentified	0.15	—	—	1.75	1.89
29	2,3,5,6-Tetramethylphenol + 4-isopropylphenol	0.02	—	—	0.46	0.48
30	2,4,5-Trimethylphenol + 2-isobutylphenol	0.05	—	—	0.78	1.00
31	2,3,4,6-Tetramethylphenol + 3-isopropylphenol	0.04	—	—	0.48	0.49
32	2,3,5-Trimethylphenol + 2-*sec.*-butylphenol	0.07	—	—	0.87	1.02
33	2,4-Diethylphenol	—	—	—	0.17	0.21
34	4-*n*-Propylphenol + 5-ethyl-3-methylphenol	0.28	—	—	2.30	4.10
35	3-*n*-Propylphenol + 2,3,4-trimethylphenol	0.04	—	—	0.21	0.20
36	2-Methyl-4-*n*-propylphenol + 4-ethyl-3-methylphenol + 3-methyl-6-*n*-propylphenol	0.03	—	—	0.07	0.12
37	2,5-Diethylphenol	—	—	—	0.03	0.05
38	5-Methyl-4-indanol + 4-isobutylphenol + 4-*sec.*-butylphenol	—	—	—	0.01	0.02
39	4-Indanol	0.07	—	—	0.28	0.31
40	3,4,5-Trimethylphenol	—*	—	—	—*	—*
41	Unidentified	—	—	—	—	—*

* This component was not determined.

with an increased sample size permitted the determination of the approximate contents of 5-indanol and 3,4,5-trimethylphenol, the amount of which in phenol and xylenol fractions varies in the range 0.1–0.3%.

CONCLUSION

Qualitative and quantitative analyses of technical fractions of dehydrated phenols, tricresol, dicresol and xylenols in a capillary column 50 m long, containing tri(2,4-xylenol) phosphate as the stationary liquid phase, have been carried out. In this column, in the phenol and xylenol fractions, apart the main homologues of C_6–C_8 phenols, the isomers of trimethyl-, tetramethyl-, ethylmethyl-, diethyl- and propylphenols, 4- and 5-indanols and their homologues were identified.

The times required for the analysis of the dehydrated phenols and xylenols, tricresol and dicresol were 100–110, 50 and 40 min, respectively.

REFERENCES

1 J. Macák and P. Buryan, *Chem. Listy*, 69 (1975) 457.
2 V. M. Nabivach and V. I. Dal, *Gazovaya Khromatografiya Koksokhimicheskikh Produktov*, Tekhica, Kiev, 1967, p. 145.
3 K. Dietzsch, *Chem. Tech. (Leipzig)*, 19 (1967) 146.
4 H. Pichler, P. Hennenberger and G. Schwarz, *Brennst. Chem.*, 49 (1968) 175.
5 H. Pichler and P. Hennenberger, *Brennst. Chem.*, 50 (1969) 341.
6 H. Pichler, W. Ripperger and G. Schwarz, *Erdöl Kohle*, 23 (1970) 91.
7 I. S. Borovskaya and R. I. Sidorov, *Khim. Tverd. Topl.*, No. 6 (1972) 134.
8 L. I. Mariich and Zh. K. Lenkevich, *Khim. Tverd. Topl.*, No. 6 (1973) 95.
9 G. D. Kharlampovich, V. V. Moskovskikh and V. F. Kollegov, *Koks Khim.*, No. 4 (1967) 40.
10 M. E. Nejmark, I. E. Kogan, M. M. Bragilevskaya and O. A. Argujeva, *Koks Khim.*, No. 7 (1967) 42.
11 N. A. Kudryavtseva, A. I. Tarasov and N. I. Lulova, in *Gazovaya Khromatografiya*, Vol. 8, NIITEKhIM, Moscow, 1968, p. 71.
12 O. Mlejnek, *Chem. Zvesti*, 22 (1968) 591.
13 V. T. Brooks, *Chem. Ind. (London)*, 42 (1959) 1317.
14 E. R. Adlard and G. W. Roberts, *J. Inst. Petrol.*, (1965) 376.
15 C. Landault and G. Guiochon, *Anal. Chem.*, 39 (1967) 713.
16 J. Hrivňák and J. Macák, *Anal. Chem.*, 43 (1971) 1039.
17 J. Macák, P. Buryan and J. Hrivňák, *J. Chromatogr.*, 89 (1974) 309.
18 C. Karr, P. A. Estep and L. L. Hirst, *Anal. Chem.*, 32 (1960) 463.
19 L. I. Mariich, O. A. Agurjeva and I. A. Tselenskaya, *Koks Khim.*, No. 1 (1970) 29.
20 G. A. Markus, *Koks Khim.*, No. 4 (1972) 32.
21 Ju. K. Babina and N. A. Garjkavaya, *Khim. Prom.*, (1974) 345.
22 G. A. Markus, *Koks Khim.*, No. 9 (1975) 43.
23 W. A. Dietz, *J. Chromatogr. Sci.*, 10 (1972) 423.

Journal of Chromatography, 148 (1978) 211–218

CHROM. 10,505

GAS CHROMATOGRAPHIC DETERMINATION OF SULPHUR COMPOUNDS IN GASES USING A SINGLE-FLAME THERMIONIC DETECTOR

J. NOVOTNÝ and A. MÜLLER
Fuel Research Institute, Prague 9-Běchovice (Czechoslovakia)

SUMMARY

For both qualitative and quantitative determinations of individual sulphur compounds in technical gases from coal treatment, gas chromatography can be used. In order to separate these compounds, a column packed with Porapak Q, operating at 120° and using nitrogen as carrier gas, was employed. Under these conditions nearly a 100% separation of hydrogen sulphide and carbonyl sulphide was attained, which is essential in analysing gases from coal gasification.

To detect sulphur compounds in technical gases, a selective thermionic detector with a pressed caesium chloride tip was used with regard to a high content of further components in gases (carbon monoxide, carbon dioxide and hydrocarbons) and trace amounts of sulphur substances, except hydrogen sulphide.

The analysis of technical gases from pressure gasification of brown coals revealed that, in addition to a known amount of hydrogen sulphide, they contain mainly methyl mercaptan, carbonyl sulphide and trace amounts of carbon disulphide. Contrary to expectation, neither higher concentrations of carbonyl sulphide and carbon disulphide nor trace amounts of higher organic sulphur compounds [C_2H_5SH, $(CH_3)_2S_2$, etc.] were found.

INTRODUCTION

In view of the general problem of atmospheric pollution, a better knowledge of the contents of sulphur compounds in technical gases obtained from the pressure gasification of brown coals in the production of town gas is desirable. During this process, the sulphur contained in coal is transferred to the pressure gas, from which it is subsequently removed.

Sulphur in raw pressure gas occurs mainly as hydrogen sulphide (*ca.* 92–95%), the remainder being organic sulphur compounds, including CS_2, COS, CH_3SH, $(CH_3)_2S$, C_2H_5SH, $(C_2H_5)_2S$, $(CH_3)_2S_2$ and $(C_2H_5)_2S_2$. In pressure gas plants, these substances are removed from the gas by washing with methanol at low temperatures and under pressure. During this process (Rectisol process), gases rich in carbon dioxide, hydrogen sulphide and the above sulphur compounds are formed.

For the final treatment of these gases, either by combustion or by their conversion into other sulphur compounds (H_2SO_4), the formation and reactions of sulphur compounds during the production and purification of pressure gas should be known.

The considerable volatility of most of these compounds permits us to use gas chromatography for their determination. Contrary to the methods used up to now, based on oxidation or reduction of organic sulphur compounds, gas chromatographic determinations can be carried out without their separation from a considerable excess of hydrogen sulphide. Moreover, they can be separated into individual components.

For separating organic sulphur compounds several types of polar liquid phases have been recommended[1–7]. According to our experience, most of these phases are not suitable for such a purpose even if capillary columns are used, owing to the low separating capacity of these columns for hydrogen sulphide and carbonyl sulphide. As Hachenberg[8,9] claims, Porapak Q is suitable for the separation of these two compounds. In applying the gas chromatographic analysis of sulphur compounds to the analysis of technical gases, a high efficiency of separation of mixtures of these two compounds in the presence of a considerable excess of hydrogen sulphide is necessary.

In addition to sulphur components, some other compounds in gases are also eluted, mainly carbon monoxide, carbon dioxide, hydrogen, methane and hydrocarbons. Currently used detectors, such as thermal conductivity (TCD) and flame-ionization detectors (FID), are also very sensitive to these substances. Hence the most important consideration in the analysis of sulphur compounds in the presence of these other substances is the use of highly sensitive and selective detectors such as the flame photometric detector (FPD) and the thermionic detector (TID).

We carried out a number of tests using the TID. In comparison with the sophisticated construction of the FPD, the advantage of the TID is that any FID can be converted into a TID according to Dressler and Janák[10].

EXPERIMENTAL

Apparatus

A Chrom 4 chromatograph with a 2.5 m × 3.0 mm I.D. column packed with Porapak Q (60–80 mesh) was employed. Other chromatographic conditions are given in Table I.

TABLE I

CONDITIONS FOR SEPARATION OF HYDROGEN SULPHIDE, CARBONYL SULPHIDE AND ORGANIC SULPHUR COMPOUNDS

Condition	*Value*
Column temperature	116–120°
Overpressure of carrier gas (nitrogen)	0.133 MPa
Hydrogen flow-rate	26–31 ml/min
Air flow-rate	500 ml/min
Sensitivity	1:5000
Chart speed	10 mm/min
Background current	$3.8 \cdot 10^{-8}$ A
Alkali metal salt	CsCl (pressed)

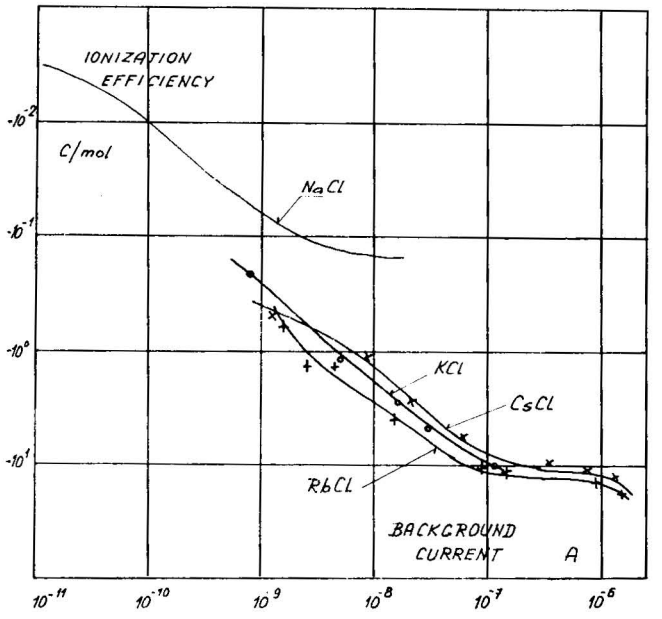

Fig. 1. Diagram of ionization efficiency of TID for hydrogen sulphide *versus* background current for various alkali metal chlorides.

Materials and methods

In order to obtain preliminary qualitative results, pure carbonyl sulphide, methyl mercaptan and nitrogen were used for the preparation of standard mixtures. The standard mixtures of gases were prepared in glass pipettes under a pressure of 0.356 MPa without using a sealing liquid, because it is always absorbing one of the components of the mixture and also sampling for chromatographic purposes by means of a syringe is easier.

The dependence of the ionization efficiency on the intensity of the background current according to Dressler and Janák[11] was determined, and indicated that with the mixture nitrogen–1 % (v/v) hydrogen sulphide the intensity of the negative response

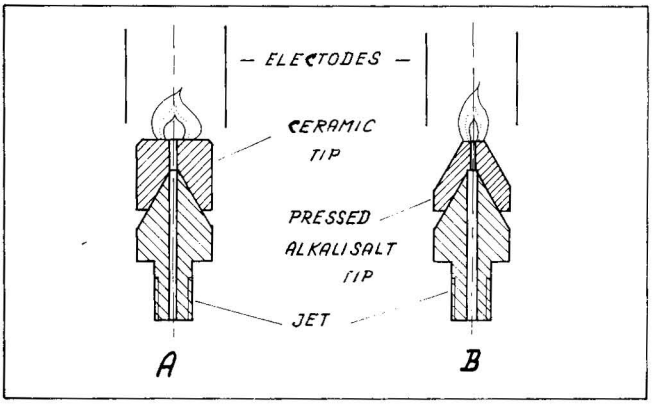

Fig. 2. Tips of TID: (A) ceramic tip; (B) pressed alkali metal salt tip.

increases according to the type of alkali metal chloride used in the order Na<K<Cs<Rb (Fig. 1). Caesium chloride and rubidium chloride provided the highest negative response, while the former gave more reproducible results. Instead of a ceramic tip filled with saturated solution of an alkali metal salt, a tip pressed from an alkali metal salt with a hole drilled in it[10] was used. The latter type of tip is durable and its response is only slightly dependent on the time when the detector is used. According to our experience, the response shape, especially with hydrogen sulphide, is dependent only on the shape of the upper surface of the tip. A flat, straight shape leads to tailing (Fig. 2A), whereas with a conical top on the tip (Fig. 2B) waves of hydrogen sulphide, carbonyl sulphide and methyl mercaptan are formed without tailing.

RESULTS AND DISCUSSION

Technical gases were sampled, using glass pipettes working under an overpressure of about 0.1 MPa, from operating streams in accordance with the recommended practice for manipulating such gases, and injected into the chromatograph with a syringe. The chromatograms obtained are shown in Figs. 3–6.

By comparing the peak areas of carbonyl sulphide and methyl mercaptan from the technical sample with those from the standard mixture by means of a calibration graph, the concentrations of these compounds in the technical gases were calculated (Table II). The following technical gases from a pressure gas plant were analysed:

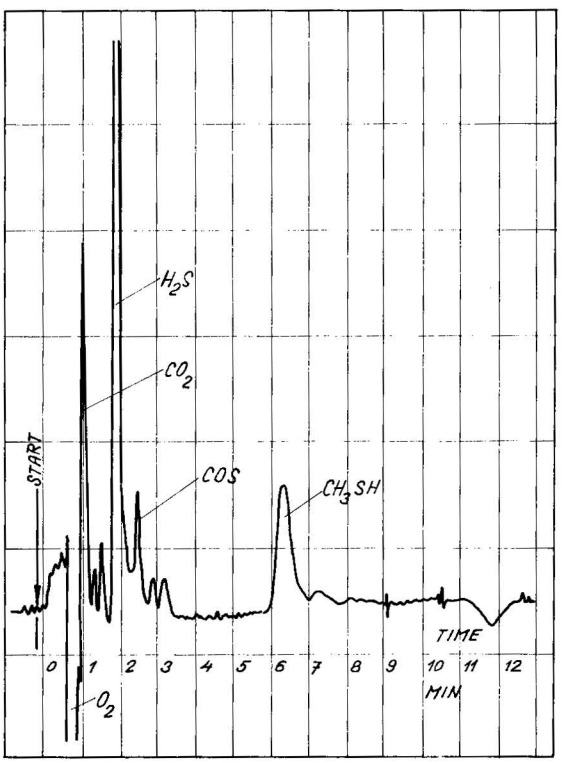

Fig. 3. Chromatogram of raw gas. Injection of 1 ml of gas (0.103 MPa; 20°). Conditions as in Table I.

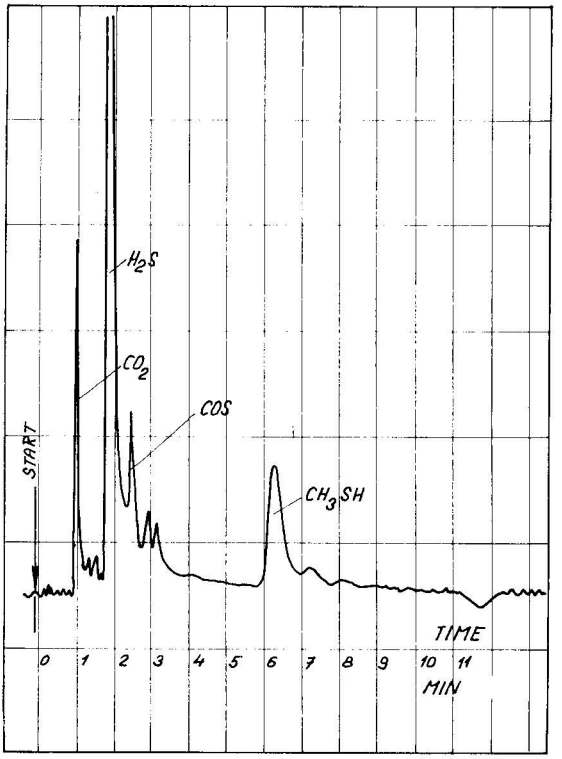

Fig. 4. Chromatogram of waste gas. Injection of 0.2 ml. Conditions as in Fig. 3 and Table I.

raw gas, after being cooled to 20–25°, entering the Rectisol, waste gas from the regeneration of methanol, hydrogen sulphide rich gas and clean gas leaving the Rectisol and supplied to the gas network.

The chromatograms in Figs. 3–6 and the results in Table II show that the content of methyl mercaptan in all of the technical gases was higher than that of carbonyl sulphide, which is contrary to the results obtained by other workers who analysed gases from coal treatment using other processes. For example, Koch and Paul[12] found that of the organic sulphur contained in gas from low-temperature carbonization of

TABLE II

CONTENTS OF ORGANIC SULPHUR COMPOUNDS AND HYDROGEN SULPHIDE IN TECHNICAL GASES FROM A PRESSURE GAS PLANT

*Technical gas sample**	*Gas (mg/Nm³)*		
	H_2S	COS	CH_3SH
Raw gas	5200	173	300
Waste gas	24,570	275	1523
Hydrogen sulphide rich gas	206,300	2460	14,532
Clean gas	59	10.5	—**

* See text for descriptions.
** Not detectable.

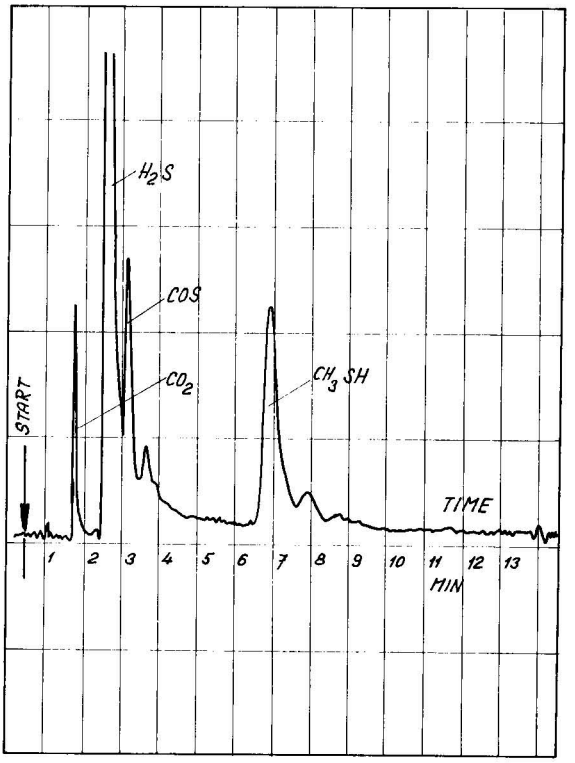

Fig. 5. Chromatogram of hydrogen sulphide rich gas. Injection of 0.05 ml. Conditions as in Fig. 3 and Table I.

brown coal, 34% (v/v) is in the form of carbonyl sulphide and 13% (v/v) in the form of methyl mercaptan.

A higher content of methyl mercaptan in raw gas is probably due to the process of coal gasification under pressure, which results in the greater formation of methane from carbon at the expense of carbon monoxide.

The waste gas and hydrogen sulphide rich gas displayed, in agreement with the gas purification process, high contents of carbonyl sulphide and methyl mercaptan (Figs. 4 and 5). As a result of the high efficiency of the purification process (Rectisol), the amount of carbonyl sulphide in clean gas, as shown in Fig. 6, was near to the detection limit and its content could not be determined by our method.

In all instances a satisfactory separation of hydrogen sulphide and carbonyl sulphide, which is particularly important in analysing waste gas and hydrogen sulphide rich gas, was attained.

Other sulphur organic compounds with higher boiling points, which would be eluted after methyl mercaptan, could not be detected in the raw gas. By increasing the sensitivity, but at the expense of reproducibility (strong noise), trace amounts of carbon disulphide (*ca.* 1 mg/m^3) were found. The retention time of this compound, under the conditions given in Table I, was 18 min.

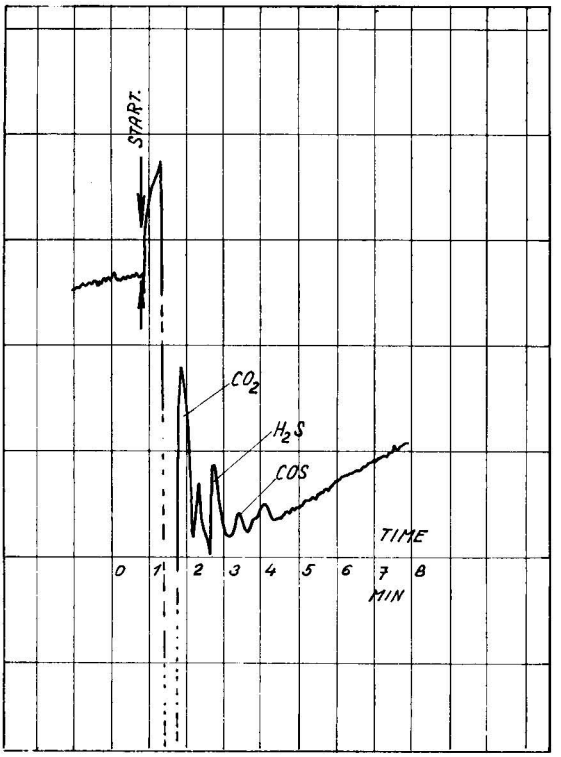

Fig. 6. Chromatogram of clean gas. Injection of 2.0 ml. Conditions as in Fig. 3 and Table I.

CONCLUSIONS

By using a TID, small amounts of organic sulphur compounds in the presence of a considerable excess of other gaseous components to which a TID shows low sensitivity can be determined with both high sensitivity and selectivity. The separation of hydrogen sulphide, also present in the excess, and to which the TID is sensitive, is made possible by using Porapak Q.

For converting an FID into a TID, caesium chloride pressed into a tip with a conical top was found to be suitable.

Contrary to previous measurements by other methods, the organic sulphur compounds in technical gases from pressure gas plants were found to be represented mainly by methyl mercaptan and by a minor amount of carbonyl sulphide.

REFERENCES

1 J. A. Schols, *Anal. Chem.*, 33 (1961) 359.
2 V. J. Farrugio and C. L. Jarreau, *Anal. Chem.*, 34 (1962) 271.
3 W. L. Thorusberry, *Anal. Chem.*, 43 (1971) 452.
4 K. R. Stewens, *Anal. Chem.*, 43 (1971) 837.
5 B. A. Schafer, *Anal. Chem.*, 42 (1970) 440.
6 R. Patrick, T. Schrodt and R. Kermore, *J. Chromatogr. Sci.*, 9 (1971) 381.
7 E. R. Adlard, L. F. Creaser and P. H. D. Mathews, *Anal. Chem.*, 44 (1972) 64.

8 H. Hachenberg, *Industrial Gas Chromatographic Trace Analysis*, Heyden, London, New York, Rheine, 1973, p. 168.
9 H. Hachenberg, *Brennst.-Chem.*, 49 (1968) 242.
10 M. Dressler and J. Janák, *Collect. Czech. Chem. Commun.*, 33 (1968) 3960.
11 M. Dressler and J. Janák, *Collect. Czech. Chem. Commun.*, 33 (1968) 3970.
12 K. Koch and B. Paul, *Brennst.-Chem.*, 8 (1963) 231.

Journal of Chromatography, 148 (1978) 219–222

CHROM. 10,406

GAS CHROMATOGRAPHIC DETERMINATION OF SMALL AMOUNTS OF FORMIC ACID IN MIXTURES CONTAINING PHENOL, ACETONE AND AROMATIC HYDROCARBONS

W. CZERWIŃSKI and A. STĘPIEŃ

Analytical Department, Institute of Industrial Chemistry, 01-793 Warszawa (Poland)

SUMMARY

A method for determining small amounts of formic acid in mixtures from the synthesis of phenol from cumene, in particular those obtained after the decomposition of cumene hydroperoxide, is described. The determination consists in extraction of formic acid as the sodium salt, acidification and esterification to methyl formate followed by gas–liquid chromatography with an internal standard.

INTRODUCTION

Formic acid is formed in small amounts as one of the side-products in the synthesis of phenol and acetone by cleavage of cumene hydroperoxide[1]. It appears in the so-called decomposition mixtures obtained by the action of sulphuric acid on cumene hydroperoxide, in crude phenol, distillation residues of phenol, in phenolate solutions and other mixtures from phenol production. The presence of formic acid in these intermediates is undesirable as it is corrosive towards apparatus made of stainless steel containing chromium[2] and nickel[3].

Because of the variety of substances present in the decomposition mixtures and the small content of formic acid, a gas chromatographic method was sought.

Formic acid has been determined in different mixtures by gas–liquid chromatography both directly and after the formation of derivatives. The direct determination of formic acid in addition to other acids has been carried out by employing an argon detector[4] or a thermalconductivity detector using a column containing a microporous polymer[5] (such as Porapak Q) or a column containing a fluoronated polymer coated with polyethylene glycol and azelaic acid[6] or a porous polymer coated with stearic acid[7]. It is generally considered that formic acid gives no response in a flame-ionization detector, as has been confirmed by recent work[8]. However, the possibility of determining formic acid by using this type of detector has been reported[9]. During the determination of formic acid by gas chromatography, thermal decomposition occurs[10], giving carbon monoxide, carbon dioxide, hydrogen and water if the injector or column temperature is above 150°, which might cause too low results. It is also possible to determine formic acid as carbon monoxide[11].

A number of papers have described methods involving the formation of deriva-

tives. Formic acid has been determined in aqueous solution by gas chromatography of formanilide[12] or of benzyl formate[13]. Free formic acid, acetic acid or their salts in cigarette smoke have been determined as methyl esters[14] formed by esterification with methanol containing dry hydrogen chloride followed by gas chromatographic separation on a polyethylene glycol column. Trimethylsilyl esters have also been used as derivatives in the determination of formic acid[15].

The purpose of this paper is to describe a combination of extraction and concentration of formic acid, preparation of the methyl ester and gas chromatography, which permits the determination of formic acid in the required range of 0.01–0.1 % in mixtures containing phenol, acetone, aromatic hydrocarbons and other compounds formed in the decomposition of cumene hydroperixide.

EXPERIMENTAL

Apparatus

A Giede Model GCHF 18.3 gas chromatograph with a flame-ionization detector was used. Argon was employed as the carrier gas, and electrolytic hydrogen from an Elhygen hydrogen generator and compressed air as auxiliary gases. A 3 m × 4 mm O.D. stainless-steel column packed with 10 % Carbowax 20M on 60–80 mesh Chromosorb W AW was used.

Reagents

The following reagents, mainly of reagent grade, were used in the determination: benzene, diethyl ether, methanol (dehydrated), sodium hydrogen carbonate, hydrochloric acid (sp. gr. 1.19), sulphuric acid (90 %), 0.2 *N* sodium hydroxide solution, formic acid (99 %) and ammonium chloride.

Anhydrous methanol–hydrogen chloride solution. The solution was prepared by bubbling through methanol (final drying with molecular sieve 4A) hydrogen chloride evolved from concentrated hydrochloric acid with 10 % ammonium chloride to which 90 % sulphuric acid was added dropwise. The operation was carried out in laboratory glass apparatus commonly used for this type of evolution of gases and their drying and absorption in liquids. Addition of ammonium chloride to hydrochloric acid[16] was used to prevent the formation of chlorine. Before entering the methanol, the gas stream was passed through a wash bottle containing sulphuric acid and a tower loosely packed with anhydrous calcium chloride. The concentration of the methanolic solution of hydrogen chloride should be about 2 *N* (checked by titration with 0.2 *N* sodium hydroxide solution). It was prepared in a volume sufficient for a number of analyses.

To this solution diethyl ether was carefully added, preferably by weighing in an ampoule to obtain an approximately 0.3 % solution. The solution was stored in a tightly stoppered flask in a cool place. The chromatogram of this solution obtained under the conditions of analysis described below should show only the peaks of diethyl ether and methanol after the initial peak of hydrogen chloride.

Procedure

Extraction and methylation. A 50-ml volume of the sample of the decomposition mixture was measured into a 250-ml separating funnel and 150 ml of benzene

were added with mixing. A 0.2-g amount of sodium hydrogen varbonate and 2 ml of distilled water were added and the mixture was shaken vigorously for about 3 min. After the layers had separated, the lower layer was carefully transfered into a 25-ml flask with a ground-glass joint. The benzene layer was washed with two 2-ml portions of water and the washings were combined with the solutions in the flask.

Water was evaporated from the solution by heating on a water-bath and aspirating the vapour from above the liquid by placing in the neck of the flask a glass tube connected to a water pump. Then 2 ml of methanol were added and evaporation was continued to dryness. The flask containing the residue (sodium formate, salts of other acids and excess of sodium hydrogen carbonate) was connected with a reflux condenser and 10.0 ml of the solution for methylation were introduced through the condenser. The contents of the flask were then mixed for 1 h using a magnetic stirrer. After removing the condenser, the flask was closed with a ground-glass stopper.

Gas chromatographic analysis. The conditions of separation were as follows: oven temperature, 50°; injector and detector temperature, 60°: carrier gas (argon) flow-rate at the outlet, 20 ml/min; hydrogen flow-rate, 20 ml/min; air flow-rate, *ca.* 200 ml/min; chart speed, 1 cm/min; amplifier range, × 10 at 10^9 of input resistance.

The size of the sample of the solution after esterification injected into the chromatograph was 3 μl. The following peaks were obtained on the chromatograms: hydrogen chloride, diethyl ether, methyl formate, methyl acetate (if acetic acid was present in the sample) and methanol (above the chart scale). The areas of the methyl formate and diethyl ether (internal standard) peaks were measured and their ratio calculated. The amount of formic acid in the sample taken was then read from the calibration graph.

Preparation of calibration graph. A standard solution consisting of 0.2 *N* formic acid in benzene was prepared; 2.0 ml of the solution were measured into a 250-ml separating funnel and benzene was added to a volume of 200 ml. Then 0.2 g of sodium hydrogen carbonate was added and the procedure as for the sample was followed as far as the production of the chromatogram. The areas of the methyl formate and diethyl ether peaks were measured, and the ratio was calculated.

Similar chromatograms were prepared using 0.5, 1.0, 3.0 and 5.0 ml of the 0.2 *N* formic acid solution in benzene and the ratios of the peak areas were calculated, and plotted against the amount of formic acid in milligrams in each volume of standard solution. A calibration graph was prepared for each methylation solution.

RESULTS AND DISCUSSION

Preliminary tests, carried out in order to determine formic acid in the samples directly with the use of a thermalconductivity detector, did not give satisfactory results. For this purpose a Porapak Q column was used at 160° and at an injector temperature 200° necessary for flash evaporation of the sample. The recovery of formic acid was much too low because of possible decomposition. Large acetone and water peaks made it difficult to achieve an acceptable resolution. It was evident that it was necessary to separate the formic acid and other acids from the bulk of the other compounds, mainly acetone and phenol. This was accomplished by extraction with sodium hydrogen carbonate solution from a benzene solution of the sample. The recovery of formic acid in the whole procedure, including esterification, was complete within the limits of

experimental error. This was established by an independent gas chromatographic determination of methyl formate in solution after methylation and comparison with the starting concentration of formic acid in the benzene solution.

The calibration graph was linear in the range required for control analysis (0.005–0.1 % of formic acid). The relative standard deviation of the results in this range was 10–5 %, respectively.

It was also possible to determine the acetic acid content, either from the methyl acetate peak using a suitable calibration graph for acetic acid or from the ratio of both ester peaks by employing a theoretical correction factor. In addition to the analysis of decomposition mixture obtained from cumene hydroperixode, the method has also been used to determine formic acid in crude phenols and distillation residues.

REFERENCES

1 J. Janda, J. Strečko and M. Masný, *Ropa Uhlie*, 8 (1966) 264.
2 S. Kazutaka, M. Todashi and Y. Naoki, *Boshoku Gijutsu*, 22 (1973) 10.
3 Ivo Pollo and S. Anioł, *Zesz. Nauk. Politech. Śląsk., Chem.*, 60 (1972) 87.
4 T. C. Grey and B. J. Stevens, *Anal. Chem.*, 38 (1966) 724.
5 J. D. Burger, *J. Gas Chromatogr.*, 6 (1968) 177.
6 Z. B. Klapishevskaya, Yu. S. Kuklin and V. D. Timofeyev, *Zavod. Lab.*, 41 (1975) 282.
7 A. F. Shushumow, N. N. Gudovicheva and M. K. Shchennikova, *Zavod. Lab.*, 40 (1974) 150.
8 B. A. Schaefer, *J. Chromatogr. Sci.*, 13 (1975) 86.
9 W. R. White and J. A. Leenheer, *J. Chromatogr. Sci.*, 13 (1975) 386.
10 L. Eek and M. T. Galceran, *Quim. Ind. (Madrid)*, 19 (1973) 466.
11 J. Angerer, *J. Clin. Chem. Clin. Biochem.*, 14 (1976) 73.
12 E. O. Umeh, *J. Chromatogr.*, 51 (1970) 139.
13 P. O. Bethge and K. Lindström, *Analyst (London)*, 99 (1974) 137.
14 E. T. Oakley, L. Weissbecker and F. E. Resnik, *Anal. Chem.*, 37 (1965) 380.
15 S. Masayoshi, H. Fumia and O. Yutaka, *Nippon Nogei Kagaku Kaishi*, 47 (1973) 321.
16 A. D. Mamedova and V. G. Kuliyeva, *Zavod. Lab.*, 33 (1967) 1406.

Journal of Chromatography, 148 (1978) 223–228

CHROM. 10,411

GAS CHROMATOGRAPHIC SEPARATION OF NAPHTHALENE AND BIPHENYL HOMOLOGUES ON CAPILLARY COLUMNS

K. TESAŘÍK

Institute of Analytical Chemistry of the Czechoslovak Academy of Sciences, 662 28 Brno (Czechoslovakia)

J. FRYČKA

Research Institute of Coke Chemistry, Urx'es Works, N.E., 757 27 Valašské Meziříčí (Czechoslovakia)

and

S. GHYCZY

Pliva, Pharmaceutical and Chemical Works, 41 000 Zagreb (Yugoslavia)

SUMMARY

Experimental conditions were investigated that would permit an optimal separation of methyl-, ethyl- and dimethylnaphthalenes, biphenyl, diphenylmethane, methylbiphenyls and acenaphthene to be obtained. Retention times were determined on efficient capillary columns prepared with the following stationary phases: SP 400, Reoplex 400, Amine 220, *p,p'*-azoxyphenetole, Bentone 34 mixed with didecyl phthalate and Ucon LB 550 X mixed with tris(cyanoethoxy)propane, and on a composite capillary column consisting of the last two columns, *i.e.*, Bentone 34 and didecyl phthalate plus Ucon LB 550 X and tris(cyanoethoxy)propane. The complete separation of all of the naphthalenes was obtained only on the last-mentioned composite column.

INTRODUCTION

The gas chromatographic separation of alkylnaphthalenes up to C_{12}, sometimes together with accompanying hydrocarbons, has been widely studied[1–17], but no procedure that permits the separation of all of the dimethylnaphthalenes on a single column from a single injection has been described however. The components that were not separated on a chromatographic column were identified by means of either spectral analysis[6,8] or analyses performed on two different columns[8–10].

The retention data published for the hydrocarbons in the present study were measured on conventional stationary phases of varying polarities[1,2,4–6,8,12,15], on adsorbents of both the first and second class according to Kiselev's classification[3,7,10,14,16] and on liquid crystals[9,11,13,17] in packed columns in most instances. Capillary columns[4,5,8,12,15] were used only with some of the conventional stationary phases (such as Apiezon L, DC 550, polyphenyl ether, polyethylene glycol adipate and Ucon 50 HB 2000). Even on capillary columns. the pairs of 2,6- and 2,7-dimethyl-

naphthalenes, 1,6- and 1,3-dimethylnaphthalenes and 1,4- and 2,3-dimethylnaphthalenes remained mostly unseparated. Adsorbents that showed steric effects[3,7,9–11,13,14,16,17] shifted the peaks of some of the unseparated pairs so that they could have been separated, but other pairs of peaks then appeared that were not separated. The above factors led to the assumption that a suitable combination of stationary phases together with a sufficient separation efficiency would make the complete separation of all of the dimethylnaphthalenes possible.

EXPERIMENTAL

Capillaries of soft (weak) glass with I.D. 0.25–0.28 mm were etched in the gaseous phase[18] and then coated by the dynamic method with a solution of the stationary phase of a suitable concentration. A 2% solution of phthalate and 2% Bentone 34 in benzene were used for the preparation of a mixed stationary phase. This mixture was agitated for several hours together with glass beads until a perfect dispersion was obtained[19] and the glass capillary was then coated with this dispersion. The capillary columns with conventional stationary phases, such as SP 400 silicone phase, Reoplex 400 polyester, Amine 220, a mixed phase containing Ucon LB 550 X and tris(cyanoethoxy)propane (85:15), and liquid crystals[20] of *p,p'*-azoxyphenetole, were prepared in the usual way. The characteristics of these columns are listed in Table I.

The measurements of the retention data were carried out in Fractovap Model C and Model 2100 instruments (Carlo Erba, Milan, Italy), equipped with flame-ionization detectors. The operating temperatures varied between 117° and 172°. A relatively high operating temperature, 172°, was used with the mixed phase of Bentone 34 and didecyl phthalate owing to its high capacity for all of the compounds chromatographed. With *p,p'*-azoxyphenetole the operating temperature of 141° was determined by the temperature range of the nematic interface.

Nitrogen was used as the carrier gas. Individual homologues of naphthalene and biphenyl were injected as solutions in cyclohexane.

RESULTS AND DISCUSSION

Retention times were determined for naphthalene, both of the methylnaphthalenes, ethylnaphthalenes and dimethylnaphthalenes on all of the capillary columns listed in Table I. The relative retention data (Table II) were calculated from retention times determined relative to that of naphthalene.

From the relative retention data, it can be seen that the same sequence is obtained for 1-methylnaphthalene and 2-methylnaphthalene on all of the stationary phases studied except *p,p'*-azoxyphenetole. The same applies to 1-ethylnaphthalene and 2-ethylnaphthalene. It is characteristic of these isomers that their separation numbers (according to Purnell), *S*, converge to 90,000 on all of the stationary phases studied, but on the columns packed with Bentone 34 and *p,p'*-azoxyphenetole they acquire substantially smaller values (*ca.* 8000).

The complete separation of all of the dimethylnaphthalenes was not obtained on any of the capillary columns. The pairs of 2,6- and 2,7-dimethylnaphthalenes, 1,3-, 1,6- and 1,7-dimethylnaphthalenes, and 1,4, 2,3- and 1,5-dimethylnaphthalenes, can

TABLE I

CHARACTERISTICS OF THE COLUMNS USED

Column No.	*Column length (m)*	*Stationary phase*	*No. of theoretical plates*	*Capacity ratio (for naphthalene)*
1	36	SP-400	160,000	2.6
2	62	Reoplex 400	174,000	4.1
3	23	Amine 220	68,000	2.6
4	44	Ucon + TCEP*	100,000	3.45
5	21	*p,p'*-azoxyphenetole	10,000	2.2
6	20	Bentone 34 + didecyl phthalate	54,000	3.8
7	64	composite columns 4 + 6	140,000	4.2

* TCEP = tris(cyanoethoxy)propane.

be separated only with difficulty on columns packed with the conventional stationary phases SP 400, Reoplex 400 and Amine 220. The separation of 2,6- and 2,7-dimethylnaphthalenes with a relative volatility of 1.015 and of 1,4- and 2,3-dimethyl naphthalenes is also difficult on the mixed phase containing Ucon LB 550 X plus tris(cyanoethoxy)propane. 1,5- and 1,6-dimethylnaphthalenes remain unseparated on the column coated with *p,p'*-azoxyohenetole; 1,3-, 1,4-, 1,2- and 1,5-dimethylnaphthalenes can be separated with difficulty on the mixed phase of Bentone 34 plus didecyl phthalate.

Combinations of the conventional stationary phases used in the capillary columns prepared, which might be effected by simple connection of capillary columns of appropriate lengths, did not lead to a substantial improvement in the separation of

TABLE II

RELATIVE RETENTION DATA FOR NAPHTHALENE HYDROCARBONS

Compound	*Column No.**						
	1	*2*	*3*	*4*	*5*	*6*	*7*
	Operating temperature (°C)						
	117	*120*	*127*	*128*	*141.5*	*172*	*140*
Naphthalene	1.00	1.00	1.00	1.00	1.00	1.00	1.00
2-Methylnaphthalene	1.87	1.60	1.81	1.81	2.01	1.65	1.81
1-Methylnaphthalene	2.04	1.86	2.03	2.31	1.95	1.79	2.01
2-Ethylnaphthalene	3.17	2.39	2.95	2.92	2.70	2.40	2.85
1-Ethylnaphthalene	3.25	2.53	3.01	2.99	2.40	2.46	2.91
2,6-Dimethylnaphthalene	3.40	2.57	3.23	3.19	4.30	2.60	3.24
2,7-Dimethylnaphthalene	3.46	2.56	3.23	3.24	3.88	2.73	3.30
1,7-Dimethylnaphthalene	3.77	2.90	3.63	3.43	3.41	3.10	3.65
1,3-Dimethylnaphthalene	3.72	3.03	3.63	3.70	3.70	3.20	3.78
1,6-Dimethylnaphthalene	3.79	3.06	3.68	3.50	4.00	2.99	3.60
1,4-Dimethylnaphthalene	4.13	3.42	4.02	4.02	3.90	3.21	4.00
2,3-Dimethylnaphthalene	4.15	3.50	4.08	4.09	4.56	3.46	4.32
1,5-Dimethylnaphthalene	4.18	3.52	4.13	—	4.01	3.23	4.11
1,2-Dimethylnaphthalene	4.50	3.90	4.45	4.38	4.66	3.22	4.20
1,8-Dimethylnaphthalene	5.00	4.70	5.23	5.03	4.86	3.56	4.68

* As in Table I.

dimethylnaphthalenes as all of the compounds involved behaved almost identically on all of these stationary phases.

Graphical investigations of combinations of the conventional phases and *p,p'*-azoxyphenetole showed that the assumed possibility of separating all of the alkylnaphthalenes is valid and that the relative volatilities for the pairs of dimethylnaphthalenes, which were the most difficult to separate, are 1.010–1.018. A more favourable value (1.020) was found only in for the connection of *p,p'*-azoxyphenetole with Reoplex 400 in the ratio 1:1.

Combinations of the conventional phases with the column containing Bentone 34 plus didecyl phthalate showed the same relative volatilities and also varied between 1.010 and 1.019. The highest value was again obtained for a combination containing 40% of Reoplex 400.

In contrast, the combination of *p,p'*-azoxyphenetole with the mixed phase of Bentone 34 plus didecyl phthalate gave only limited possibilities of separating 1,4- and 1,3-dimethylnaphthalenes with a relative volatility of 1.010.

The combination of capillary columns with the mixed phases of Ucon LB 550 X plus tris(cyanoethoxy)propane and Bentone 34 plus didecyl phthalate gave the possibility of separating all of the dimethylnaphthalenes (Table II). The pair of 1,6- and 1,7-dimethylnaphthalenes with a relative volatility of 1.014 remained separable only with difficulty.

Using this combination of stationary phases for the analyses of alkylnaphthalene fractions in practice, the samples will contain, in addition to naphthalene homologues, also other aromatic hydrocarbons[1,5,8,12,15]. Therefore the retention times of biphenyl, diphenylmethane, three monomethylbiphenyls, acenaphthene and acenaphthylene were also determined. Their relative retention data are listed in Table III, and a comparison with the values in Table II shows that more exacting demands on the separation system will be necessary for the separation of biphenyl and 2-ethylnaphthalene ($S = 36{,}000$) only. The pairs of 1,8-dimethylnaphthalene and 3-methylbiphenyl, with relative retention times 4.67 and 4.68, and acenaphthene and 4-methylbiphenyl with values of 4.84 and 4.88, remained virtually unseparable. With tar fractions the problem is made simpler by the absence of 1,8-dimethylnaphthalene[5,8,21]. An example of a chromatogram obtained in practice is shown in Fig. 1.

TABLE III

RELATIVE RETENTION DATA FOR BIPHENYL DERIVATIVES, ACENAPHTHENE AND ACENAPHTHYLENE

Column No. 7 (see Table I) under the conditions described in Table II.

Compound	*Relative retention time**
2-Methylbiphenyl	2.19
Biphenyl	2.76
Diphenylmethane	3.13
3-Methylbiphenyl	4.67
4-Methylbiphenyl	4.88
Acenaphthene	4.84
Acenaphthylene	5.61

* Naphthalene = 1.00.

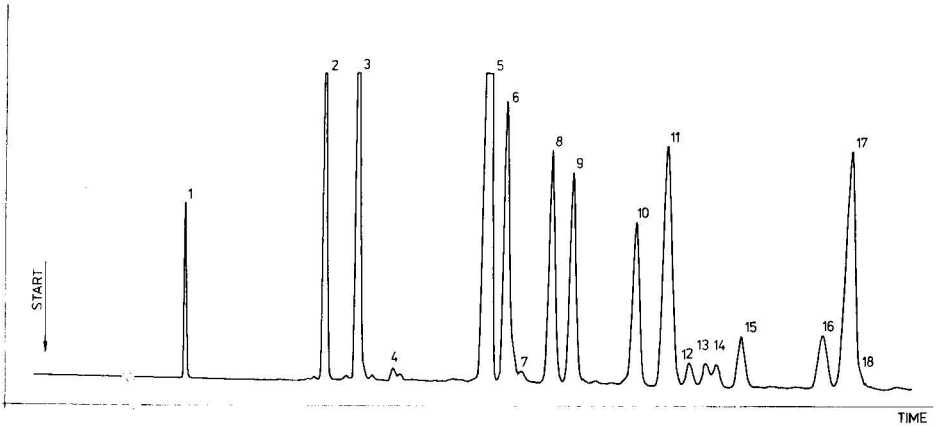

Fig. 1. Chromatogram of alkylnaphthalene fraction from coal tar. The column was coated with Bentone 34 and didecyl phthalate (50 : 50) and connected to column packed with Ucon LB 550 X and tris(cyanoethoxy)propane (85 : 15). Peaks: 1 = naphthalene; 2 = 2-methylnaphthalene; 3 = 1-methylnaphthalene; 4 = 2-methylbiphenyl; 5 = biphenyl; 6 = 2-ethylnaphthalene; 7 = 1-ethylnaphthalene; 8 = 2,6-dimethylnaphthalene; 9 = 2,7-dimethylnaphthalene; 10 = (1,6-dimethylnaphthalene), 1,7-dimethylnaphthalene; 11 = 1,3-dimethylnaphthalene; 12 = 1,4-dimethylnaphthalene; 13 = 1,5-dimethylnaphthalene; 14 = 1,2-dimethylnaphthalene; 15 = 2,3-dimethylnaphthalene; 16 = 3-methylbiphenyl (+ 1,8-dimethylnaphthalene); 17 = acenaphthene; 18 = 4-methylbiphenyl.

CONCLUSION

A separation system of capillary columns consisting of combinations of a conventional stationary phase [Reoplex 400 or a mixed phase containing Ucon LB 550 X plus tris(cyanoethoxy)propane] and a modified adsorbent (Bentone 34) or liquid crystals (*p,p'*-azoxyphenetole) permits the methyl-, ethyl- and dimethylnaphthalenes and most of the accompanying hydrocarbons to be separated.

ACKNOWLEDGEMENTS

The authors' thanks are due to Carlo Erba for the kind loan of a Fractovap Model 2100 instrument, Merck (Darmstadt, G.F.R.), Associate Professor H. Kelker (Hoechst, Frankfurt/M, G.F.R.) for providing *p,p'*-azoxyphenetole, Dr. H. D. Sauerland (Rütgerswerke, Duisburg-Meiderich, G.F.R.) and Dr. M. van der Stricht (Labofina, Brussels, Belgium), for some naphthalene homologues and Ing. J. Kříž (University of Chemical Technology, Prague) for some methylbiphenyls.

REFERENCES

1 T. C. L. Chang and C. Karr, *Anal. Chim. Acta*, 24 (1961) 343.
2 R. V. King, F. A. Fabrizio and A. R. Donall, in N. Brenner, J. Callen and M. Weiss (Editors), *Gas Chromatography*, Academic Press, New York, 1962, p. 149.
3 M. van der Stricht and J. van Rysselberge, *J. Gas Chromatogr.*, 1 (1963) 29.
4 J. Q. Walker and D. L. Ahlberg, *Anal. Chem.*, 35 (1963) 2028.
5 F. J. Kabot and L. S. Ettre, *Anal. Chem.*, 36 (1964) 250.

6 K. M. Vaysberg, I. I. Shabalin, Z. A. Kruglov, M. A. Shmeleva and L. P. Petrova, *Khim. Tekhnol. Topl. Masel*, No. 9 (1965) 53.
7 H. D. Sauerland and M. Zander, *Erdöl-Kohle-Erdgas-Petrochem.*, 19 (1966) 502.
8 J. Mostecký, M. Popl and J. Kříž, *Anal. Chem.*, 42 (1970) 1132.
9 M. S. Vigdergauz and R. V. Vigalok, *Neftekhimiya*, 11 (1971) 141.
10 K. M. Vaysberg, V. G. Gizitdinova, E. A. Kruglov and Z. P. Pechernikova, *Gazov. Khromatogr.*, No. 15 (1971) 30.
11 H. D. Sauerland and M. Zander, *Erdöl-Kohle-Erdgas-Petrochem.*, 25 (1972) 526.
12 L. I. Mariich and Z. K. Lenkevich, *Koks Khim.*, No. 7 (1973) 32.
13 G. Chiavari and M. Pastorelli, *Chromatographia*, 7 (1974) 30.
14 M. F. Gannord, C. Vidal-Madjar and G. J. Guiochon, *J. Chromatogr. Sci.*, 12 (1974) 839.
15 L. Soják and L. Barnoky, *Ropa Uhlie*, 16 (1974) 654.
16 J. Fryčka, *Chromatographia*, 8 (1975) 413.
17 S. Wasik and S. Chesler, *J. Chromatogr.*, 122 (1976) 451.
18 K. Tesařík and M. Novotný, in H. G. Struppe (Editor), *Gas Chromatographie 1968*, Akademie Verlag, Berlin, 1968, p. 575.
19 K. Nesvadba, J. Matěna, L. Odstrčil and M. Slavík, *Chem. Prům.*, 16 (1966) 392.
20 G. Kraus, K. Seifert and H. Schubert, *J. Chromatogr.*, 100 (1974) 101.
21 K. F. Lang and I. Eigen, *Fortschr. Chem. Forsch.*, 8 (1967) 91.

Journal of Chromatography, 148 (1978) 229–235

CHROM. 10,461

GAS CHROMATOGRAPHIC ANALYSIS OF CHLORINATED ETHANES

LUDĚK ŽILKA and MIROSLAV MATUCHA

Institute for Research, Production and Application of Radioisotopes, Přístavní 24, 17004 Prague 7 (Czechoslovakia)

SUMMARY

The separation of the products from the chlorination of ethane by temperature-programmed gas chromatography on a packed column was studied. The gas chromatographic behaviour of all nine possible components (from ethyl chloride to hexachloroethane) was characterized by the retention indices on the following stationary phases: OV-101, Halocarbon K-352, SE-30, OV-17, methyl phenyl silicone oil MFSD-5, SP-2340 and β,β'-oxydipropionitrile.

Quantitative analysis was accomplished with a flame-ionization detector, for which the correction factors of the chlorinated ethanes were determined.

INTRODUCTION

Chlorinated hydrocarbons are important as solvents, raw materials and intermediates for organic synthesis and in special applications (*e.g.*, as insecticides).

In general, the products of chlorination consist of several chlorinated hydrocarbons and often include positional isomers; other compounds such as hydrogen chloride and chlorine are usually removed before analysis. So far as we know, the gas chromatography of all nine possible chloroethanes has not been investigated. The most complete study was the work of Balandina and Subbotin[1], who described the separation of eight chloroethanes (*i.e.*, except hexachloroethane) on tricresyl phosphate. Six chloroethanes were separated on SE-30 by Hinshaw[2], higher chlorinated ethanes (from tri- to hexachloroethane) by Solomons and Ratcliffe[3] and less chlorinated ethanes by Mamedov *et al.*[4] and Kosorotov and Kolesničenko[5].

Various combinations of chloroethanes have been separated on a number of stationary phases: non- or weakly polar squalane[6,7], paraffin oil[8–13], Apiezon L[5,8,14], Halocarbon[15] and silicone oils or elastomers[2–4,7,11,16–21], polar alkyl phthalates[4,13,16,17,19–22], aryl phosphates[1,4,8,21,23–25], Carbowax 4000 and 20M[8,14], polyethylene glycol adipate[1,7,23], β,β'-oxydipropionitrile (β,β'-ODPN)[4,26] and Porapak-Q[27].

The most frequently used detectors in the chromatography of chloroethanes are the thermal conductivity detector (TCD)[1–5,7,8,11,13,16–19,21,25,27], and the flame-ionization detector (FID)[3,6,14,15,23,24,26]. The advantages of the gas density balance (GDB) were confirmed even for these compounds[15] (predictable response, non-specificity, linearity and sufficient sensitivity). A combination of an FID with a

thermionic detector (TID), which is more specific for chlorinated compounds, was also used for chloroalkanes[14]. The detection of chlorinated compounds by means of an electron-capture detector (ECD) is well known. Combinations of different types of detectors are to be preferred as additional information is provided. The different responses depend on the physico-chemical properties which are exploited for the detection, *e.g.*, an increasing number of chlorine atoms in a molecule causes an increase in the response of the TCD, GDB and ECD and a decrease in that of the FID.

From the published data, the following problems emerge: the overlapping of the peaks of 1,1,1-trichloroethane and 1,2-dichloroethane on non-polar stationary phases, and of 1,1-dichloroethane and 1,1,1-trichloroethane on polar phases. This paper presents the results of the gas chromatography of all nine chloroethanes on seven various stationary phases. Owing to the large differences in the volatilities of these compounds, temperature-programmed gas chromatography was employed. Detection was accomplished with an FID.

EXPERIMENTAL

A Packard Model 7409 gas chromatograph equipped with a double FID and a temperature programmer was used. Glass columns (2 m × 3 mm I.D.) were used with the following column packings:

(1) 5% MFSD-5 (VÚOS, Rybitví, Czechoslovakia) on Supelcoport (80–100 mesh) (Supelco, Bellefonte, Pa., U.S.A.);

(2) 5% Halocarbon K-352 (Supelco) on Supelcoport (80–100 mesh);

(3) 3% OV-17 (Serva, Heidelberg, G.F.R.) on Chromosorb W HP (100–120 mesh) (Serva);

(4) 5% OV-101 (Serva) on Supelcoport (80–100 mesh);

(5) 5% SP-2340 (Supelco) on Supelcoport (80–100 mesh);

(6) 3% SE-30 (Becker, Delft, The Netherlands) on Chromaton N-AW-DMCS (100–120 mesh) (Lachema, Brno, Czechoslovakia);

(7) 5% β,β'-ODPN (Becker) on Supelcoport (80–100 mesh);

(8) 10% Squalane (Becker) on Chromaton N-AW-DMCS (80–100 mesh).

The following chemicals were employed: ethyl chloride (Synthesia, Kolín, Czechoslovakia), 1,1-dichloroethane (Spolana, Neratovice, Czechoslovakia), 1,1,1-trichloroethane (Dow Chem., Midland, Mich., U.S.A.), 1,2-dichloroethane (Spolana), 1,1,2-trichloroethane (Spolana), pentachloroethane (Spolana), 1,1,2,2-tetrachloroethane (Chemie, Apolda, G.D.R.), 1,1,1,2-tetrachloroethane (ÚVVVR, Prague, Czechoslovakia), hexachloroethane (ÚVVVR) and C_6–C_{17} *n*-alkanes (VŠCHT, Prague, Czechoslovakia).

The chromatographic behaviour of the chloroethanes was characterized by their relative retention temperatures (*RRT*) (relative to *n*-octane). Several rates of temperature increase were examined and 8°/min was found to be optimal. The initial temperature was usually 40°, except for the Halocarbon K-352 column (50°) and the β,β'-ODPN column (30° and a rate of 5°/min). The carrier gas (argon) flow-rate was 30 ml/min except for the β,β'-ODPN column (50 ml/min). The retention index, I_r, for chloroethane (x) was found by interpolation from

$$I_r = n + 100 \cdot \frac{RT_x - RT_n}{RT_{n+1} - RT_n}$$

where the retention temperatures, RT, of n and $n + 1$ alkanes and chloroethane, x, are $RT_n < RT_x < RT_{n+1}$.

Correction factors, F_i, were calculated from the expression

$$F_i = \frac{G_x A_{STD}}{G_{STD} A_x}$$

where G_x and G_{STD} are the amount of chloroethane and of n-octane used as the internal standard, respectively, and A_x and A_{STD} are the peak areas of chloroethane and the internal standard, respectively. Peak areas were measured by triangulation with a high chart speed. In all instances, the chromatograms were recorded at the same sensitivity in order to eliminate any errors due to the attenuator switching.

RESULTS AND DISCUSSION

The chromatographic behaviour of all nine possible products of ethane chlorination (from ethyl chloride to hexachloroethane) was studied on the following stationary phases, with different polarities: OV-101, SE-30, K-352, OV-17, MFSD-5, SP-2340 and β,β'-ODPN. The retention temperatures and relative retention temperatures on the various stationary phases are given in Table I. The differences in the retention characteristics of the chloroethanes on these stationary phases depend mainly on the volatility and polarity of the chloroethane molecule, as well as on the polarity of the stationary phase. The differences in the gas chromatographic behaviour of the individual compounds on the stationary phases investigated are, however, more apparent from their retention indices given in Table II. The retention indices of chloroethanes are generally higher on a polar than for a non-polar stationary phase. From the retention indices shown it follows that the weak polar stationary phases (polysiloxanes) of the OV-17 type are the most suitable for the separation of the chloroethanes, which is demonstrated in Fig. 1.

If a correlation between the retention data and certain physical parameters is

TABLE I

RETENTION TEMPERATURES (RT) AND RELATIVE RETENTION TEMPERATURES (RRT) OF CHLOROETHANES ON VARIOUS STATIONARY PHASES

Compound	*K-352*		*SE-30*		*OV-101*		*OV-17*		*MFSD-5*		*SP-2340*	
	RT (°C)	*RRT*	*RT* (°C)	*RRT*	*RT* (°C)	*RRT*	*RT* (°C)	*RRT*	*RT* (°C)	*RRT*	*RT* (°C)	*RRT*
Ethyl chloride	65.0	0.63	45.0	0.65	53.0	0.89	54.0	0.69	56.0	0.64	56.0	0.83
1,1-Dichloroethane	72.0	0.70	47.7	0.68	54.3	0.92	61.7	0.79	67.0	0.77	74.3	1.10
1,1,1-Trichloroethane	78.7	0.77	52.0	0.75	55.3	0.93	67.0	0.86	74.0	0.85	74.3	1.10
1,2-Dichloroethane	78.7	0.77	52.0	0.75	55.3	0.93	72.3	0.92	80.0	0.92	97.7	1.44
1,1,2-Trichloroethane	94.0	0.92	62.7	0.91	59.0	0.99	94.0	1.20	102.0	1.17	123.0	1.82
n-Octane	102.7	1.00	69.0	1.00	59.3	1.00	78.3	1.00	87.0	1.00	67.7	1.00
1,1,1,2-Tetrachloroethane	107.8	1.05	73.1	1.06	63.5	1.07	105.7	1.35	115.3	1.33	121.2	1.79
1,1,2,2-Tetrachloroethane	117.0	1.14	82.0	1.19	67.0	1.13	121.7	1.55	131.0	1.51	154.0	2.27
Pentachloroethane	131.7	1.28	94.0	1.36	75.5	1.27	130.3	1.66	141.0	1.62	142.0	2.10
Hexachloroethane	153.0	1.49	110.4	1.60	83.0	1.40	145.6	1.86	150.7	1.73	140.1	2.07

TABLE II

BOILING POINTS (b.p.), CORRECTION FACTORS (F_i) AND RETENTION INDICES OF CHLOROETHANES

Compound	*b.p. (°C)*	F_i	*Retention index*						
			SE-30	*OV-101*	*K-352*	*OV-17*	*SP-2340*	*MFSD-5*	*β,β-ODPN*
Ethyl chloride	13.1	—	—	—	—	—	—	—	—
1,1-Dichloroethane	57.0	3.51	—	600.0	—	658.8	879.5	650.0	842.9
1,1,1-Trichloroethane	74.0	4.46	628.6	660.0	631.6	715.0	879.5	733.3	828.6
1,2-Dichloroethane	84.0	3.23	628.6	660.0	631.6	754.9	1077.6	753.3	1042.9
1,1,2-Trichloroethane	113.0	4.18	747.5	790.0	745.6	898.1	1275.6	888.2	—
n-Octane	125.5	1.00	800.0	800.0	800.0	800.0	800.0	800.0	800.0
1,1,1,2-Tetrachloroethane	129.5	—	827.2	870.0	829.5	959.4	1261.0	959.5	—
1,1,2,2-Tetrachloroethane	146.0	5.58	888.4	922.1	882.7	1051.1	1535.4	1047.4	—
Pentachloroethane	162.0	5.62	963.2	1025.0	965.0	1100.0	1429.2	1100.0	—
Hexachloroethane	186.0	—	1057.8	1100.0	1088.2	1176.5	1412.4	1230.6	—

established, it could facilitate the identification of unknown substances. An approximately linear correlation between the retention index for non-polar or slightly polar stationary phases and the boiling point is shown in Fig. 2. The increments of the retention indices of 1,1,1-trichloro-, penta- and hexachloroethanes decrease with increasing polarity of the stationary phase, contrary to 1,2-dichloro-, 1,1,2-trichloro- and 1,1,2,2-tetrachloroethane, for which the retention index increases.

In contrast to non-polar and weakly polar stationary phases, the plotted points

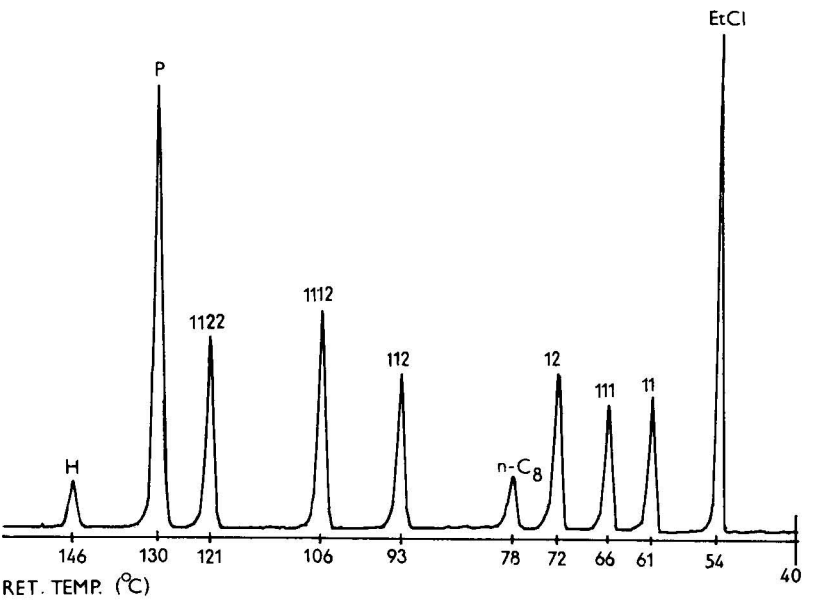

Fig. 1. Temperature programmed gas chromatography of chloroethanes on an OV-17 column. EtCl = ethyl chloride; 11 = 1,1-dichloroethane; 111 = 1,1,1-trichloroethane; 12 = 1,2-dichloroethane; *n*-C_8 = n-octane (internal standard); 112 = 1,1,2-trichloroethane; 1112 = 1,1,1,2-tetrachloroethane; 1122 = 1,1,2,2-tetrachloroethane; P = pentachloroethane; H = hexachloroethane.

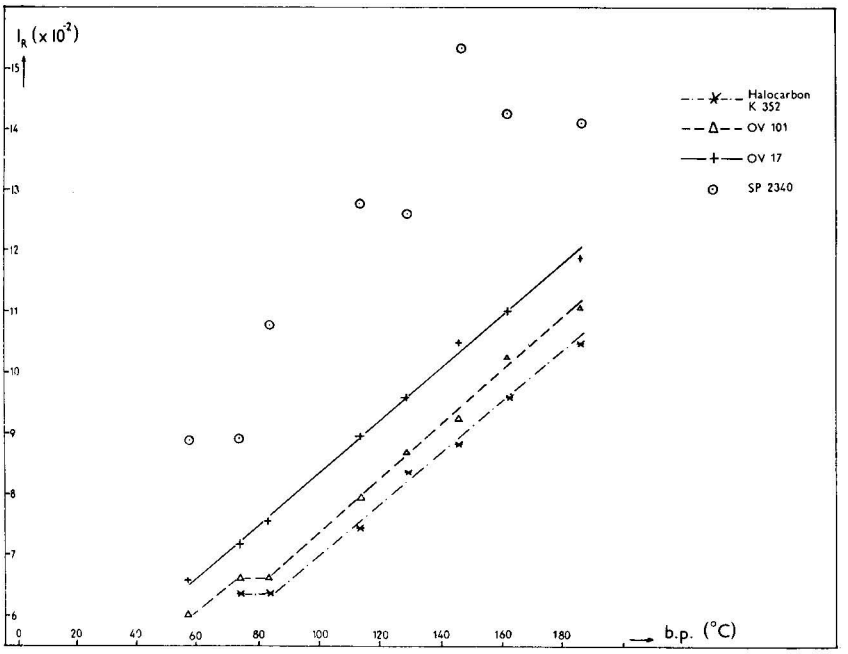

Fig. 2. Correlation between the retention index measured with columns of different polarity and the boiling point of chloroethanes (1,1-dichloroethane–hexachloroethane).

deviate from a linear correlation for the strongly polar SP-2340 phase. On the non-polar Halocarbon K-352, OV-101 and SE-30, the retention of 1,1-dichloroethane is less than that of 1,2-dichloroethane and 1,1,1-trichloroethane, for which retention times are equal. On the other hand, on the polar stationary phase SP-2340 1,1-dichloroethane and 1,1,1-trichloroethane are not separated and have lower retentions than 1,2-dichloroethane. Finally, on the strongly polar β,β'-ODPN the retention of 1,1,1-trichloroethane is lower than that of 1,1- and 1,2-dichloroethanes (Table II). Similar behaviour of the chloroethanes on polar stationary phases was reported by Urone *et al.*[8], Mamedov *et al.*[4] and Baladina and Subbotin[1] and on non-polar stationary phases by Urone *et al.*[8] and Kosorotov and Kolesničenko[5].

In a similar manner to the Rohrschneider characterization of stationary phases, the influence of the polarity of the stationary phase on the retention indices of chloroethanes was investigated. To compare the polarities, the increase in the retention index of 1,1,2,2-tetrachloroethane obtained with any polar stationary phase in comparison with that obtained with a non-polar stationary phase (Squalane) is given as follows[7]:

$$\Delta I_{R(CHCl_2CHCl_2)} = I_{R(CHCl_2CHCl_2)}\ (\text{polar}) - I_{R(CHCl_2CHCl_2)}\ (\text{non-polar})$$

Then the value of $\Delta I_{R(CHCl_2CHCl_2)}$ obtained with a given stationary phase is presumed to indicate its polarity. The influence of the polarity of the stationary phase on the retention index is demonstrated in Fig. 3. As the retention indices on a new stationary phase can be predicted by measuring the retention index of 1,1,2,2-tetrachloroethane

on a particular stationary phase, the relationship illustrated in Fig. 3 appears to be very useful for the selection of new stationary phases and for identification purposes. It is evident that this relationship is not a simple function of one molecular property, and the influences of molecular weight, volatility, the polarity and polarizability of the molecule and steric effects must be taken into account.

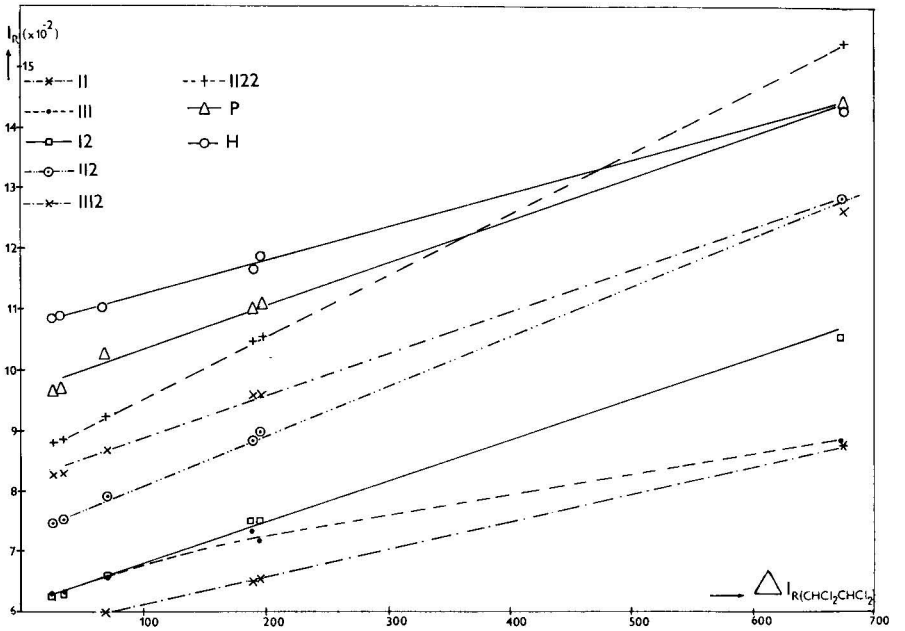

Fig. 3. Influence of the polarity of the stationary phase [measured as $\Delta I_{R(CHCl_2CHCl_2)}$] on the retention index of chloroethanes (1,1-dichloroethane–hexachloroethane).

The selection of a stationary phase is also restricted by the lower and upper temperature limits. For instance, EGSS-X could not be used for lower chloroethanes because of its lower temperature limit of 90°; on the other hand, β,β'-ODPN, the upper temperature limit of which is 70°, is not suitable for more highly chlorinated ethanes.

The correction factors for chloroethanes are given in Table II. As expected, the FID response decreases as the degree of chlorination increases. The correction factor for an FID is a complicated function of the operating conditions (carrier gas, hydrogen and air flow-rates and temperature), which must therefore be maintained constant in all analyses.

CONCLUSIONS

Temperature-programmed gas chromatography on weakly polar stationary phases of the OV-17 type is convenient for the analysis of chlorinated ethanes, for which a linear correlation between retention index and boiling point was found. The results obtained on stationary phases of different polarity could possibly be used for

identification purposes. The chromatographic behaviour of chloroethanes is influenced by several factors (molecular weight, volatility, polarity and polarizibility of the molecule). For quantitative analysis an FID can be used, the response of which decreases with increasing degree of chlorination.

REFERENCES

1 L. A. Balandina and A. I. Subbotin, *Zavod. Lab.*, 34 (1968) 154.
2 L. D. Hinshaw, *J. Gas Chromatogr.*, 8 (1966) 300.
3 D. A. Solomons and J. S. Ratcliffe, *J. Chromatogr.*, 76 (1973) 101.
4 M. A. Mamedov, T. P. Popova and N. S. Murzina, *Zh. Anal. Khim.*, 23 (1968) 1716.
5 V. I. Kosorotov and A. F. Kolesničenko, *Chim. Prum.*, 8 (1975) 571.
6 O. L. Hollis and W. V. Hayes, *Anal. Chem.*, 34 (1962) 1223.
7 R. Iwate, Y. Makide and T. Tomirage, *Bull. Chem. Soc. Jap.*, 47 (1974) 3071.
8 P. Urone, J. E. Smith and R. J. Katnik, *Anal. Chem.*, 34 (1962) 476.
9 R. R. Barefoot and J. E. Cural, *Chem. Can.*, 7 (1955) 45.
10 A. T. James and A. J. P. Martin, *Brit. Med. Bull.*, 10 (1954) 170.
11 G. W. Warren and L. J. Priestly, Jr., *Anal. Chem.*, 31 (1959) 1013.
12 I. A. German and N. Ciot, *Rev. Chim.*, 16 (1965) 382.
13 D. A. Vjachirov and L. E. Reschetnikova, *Zh. Prikl. Khim.*, 31 (1958) 802.
14 D. Jentzsch, *Z. Anal. Chem.*, 221 (1966) 377.
15 C. L. Guillemin, *J. Chromatogr. Sci.*, 7 (1969) 493.
16 J. H. Knox, *Chem. Ind. (London)*, 10 (1955) 1631.
17 T. E. Archer, A. Bevenue and G. Zweig, *J. Chromatogr.*, 6 (1961) 457.
18 K. Malinowska, *Chem. Anal. (Warsaw)*, 9 (1964) 585.
19 J. B. Evans and J. E. Willard, *J. Amer. Chem. Soc.*, 78 (1956) 2908.
20 F. H. Pollard and C. J. Hardy, *Anal. Chim. Acta*, 16 (1957) 135.
21 G. F. Harrison, in D. H. Desty (Editor), *Vapour Phase Chromatography*, Butterworths, London, 1957, p. 333.
22 C. J. Hardy, *Analyst (London)*, 79 (1954) 726.
23 A. J. Lazaris, *Neftekhimiya*, 5 (1965) 166.
24 G. M. Sassu, F. Zilio-Grandi and A. Conté, *J. Chromatogr.*, 34 (1968) 394.
25 E. Gloesener, *J. Pharm. Belg.*, 11–12 (1961) 379.
26 J. Efer, D. Quaas and W. Spichale, *Chem. Tech. (Leipzig)*, 20 (1965) 44.
27 A. Forris and J. G. Lehman, *Separ. Sci.*, 4 (1969) 225.

Journal of Chromatography, 148 (1978) 237–245

CHROM. 10,407

RAPID CHROMATOGRAPHIC SEPARATION OF TECHNICAL ENZYMES ON SPHERON ION EXCHANGERS

O. MIKEŠ, P. ŠTROP and J. SEDLÁČKOVÁ

Institute of Organic Chemistry and Biochemistry, Czechoslovak Academy of Sciences, Prague (Czechoslovakia)

SUMMARY

New types of ion exchangers with a hydroxyalkyl methacrylate matrix (Spheron) that are suitable for the sorption and high-performance liquid chromatography of technical enzymes are described. Their use is illustrated by examples of the sorption and desorption of a microbial protease and by examples of the rapid, semi-preparative chromatography of technical enzymes (protease, glucose oxidase, pectinase).

INTRODUCTION

The rapid separation of technical enzymes by reversible sorption and modern high-performance liquid chromatography (HPLC) is important from the viewpoint of the development of industrial bioengineering. A necessary prerequisite of this development is the availability of suitable ion exchangers. The main requirements which these materials must fulfil are summarized in Table I.

Recently, we reported[1–3] on novel ion exchangers with a Spheron matrix, which have been employed successfully for the chromatography of biopolymers and their fragments, *i.e.*, proteins, peptides, amino acids, nucleic acids, oligonucleotides and nucleotides. We found later that the diethylaminoethyl derivative of Spheron is also suitable for the chromatography of sugars[4]. These Spheron ion exchangers, based on a hydroxyalkyl methacrylate matrix, conform to the requirements given in Table I. We have attempted to illustrate the possibilities of their application in the field of technical enzymes by an example of reversible adsorption of protease and by the chromatography of several other enzymes.

EXPERIMENTAL

Materials

The ion exchangers used are summarized in Table II. They were prepared in our laboratory from Spheron P-300, particle size 20–40 μm (Lachema, Brno, Czechoslovakia) on a small scale by methods described elsewhere[1–3]. Samples of the ion

TABLE I

REQUIRED CHARACTERISTICS OF ION EXCHANGERS FOR HIGH-PERFORMANCE LIQUID CHROMATOGRAPHY (HPLC) AND REVERSIBLE SORPTION OF TECHNICAL ENZYMES

Required characteristic	*Reason*
(1) *Macroporosity*, allowing penetration of enzymes into beads	In the case of *microporous resins* only the functional groups situated on the surface of beads are available for chromatography of enzymes
(2) A sufficiently *hydrophilic character*, which guarantees that the native conformation of the enzymes and thus their activity are retained	Many ion-exchange resins with a *hydrophobic* matrix denature enzymes
(3) *Resistance* of matrix to *enzymes* and to *microbes*	Culture liquids and technical enzymes often attack *polysaccharide matrices* of conventional ion exchangers
(4) *Rigidity of matrix*, which ensures resistance of particles to pressure	HPLC and manipulation during sorption of enzymes require *ion exchanger particles not deformable whose abrasion is minimal*
(5) *Spherical shape* and *appropriate size* of ion exchanger particles	Spherical particles give *best flow-rates*. HPLC needs fine particle size, technical application coarse size
(6) Possibility of *repeated use* without loss of capacity and *chemical resistance*	Regeneration of ion exchangers after separation of crude technical enzymes often calls for *solutions at extreme pH values* or for *organic solvents*
(7) *Minimal changes in volume* as result of changes in pH and ionic strength	Regeneration, cycling, equilibration and sorption of enzymes must be effected *in the same column* without a substantial bed change

TABLE II

ION EXCHANGERS USED

Designation	*Composition*	*Functional group*	*Capacity for small ions (mequiv./g)*
Cation exchangers			
CM-Spheron P 300	Carboxymethyl-Spheron	$-COOH$	2.0
S-Spheron P 300	Sulphonyl-Spheron	$-SO_3H$	1.0
Anion exchanger			
DEAE-Spheron P 300	Diethylaminoethyl-Spheron	$-N(C_2H_5)_2$	2.0

exchangers are commercially available*. The types of technical enzymes and their sources are shown in Table III.

Preparation of ion exchangers

Fresh, dry ion exchangers were suspended in water before use, the suspension

* Small batches of Spheron ion exchangers are prepared by Lachema, Brno, Czechoslovakia. The Spheron gels and their derivatives are distributed by Koch-Light Labs., Colnbrook, Great Britain.

TABLE III

TECHNICAL ENZYMES USED

Enzyme	*Characteristic*	*Source*
Proteolytic	Crude protease from *Aspergillus sojae*	Japan*
Glucose oxidase	Technical preparation of fungal origin (*Aspergillus niger*)	Boehringer, Mannheim, G.F.R.**
Pectolytic	Leozym, technical preparation of fungal origin (*Aspergillus niger*)	Product of Lihovary a Konservárny, Leopoldov, Czechoslovakia***

* Courtesy of Dr. J. Turková, of this Institute.
** Courtesy of Dr. J. Čoupek, Laboratorní přístroje, Prague.
*** Experimental sample, courtesy of Dr. L. Rexová, Institute of Chemistry, Slovak Academy of Sciences, Bratislava.

was deaerated *in vacuo* of a water aspirator and the resin was allowed to settle several times. All ion exchangers (volume always 10–11 ml) were stirred before and after use with 50 ml of the regenerating solution on a glass filter; the solution was aspirated off after 10 min. This procedure was repeated several times. The sequence of the regenerating solutions was as follows: 2 *M* sodium chloride solution, water, 2 *M* sodium hydroxide solution (with cation exchangers), water, 2 *M* hydrochloric acid, water; anion exchangers were washed first with the acid, then with water and lastly with the hydroxide. Ion exchangers in the H^+ or OH^- form were equilibrated with the first eluting buffer by an appropriate procedure[5].

Chromatography

The ion exchangers treated as described were packed into a jacketed column of the type used in amino acid analyzers; a 20 × 0.8 cm column was formed. The column was cooled with tap water. The enzyme was always dissolved in 0.2–0.4 ml of the first eluting buffer and the solution placed under a buffer layer on top of the column. The buffers were supplied from the gradient mixing device to the column by a two-piston proportional pump (Instrument Development Workshops, Czechoslovak Academy of Sciences, Prague, Czechoslovakia), operating with minimum pulses. The emergence of the effluent components was recorded at 285 and 254 nm by means of two through-flow cells connected in series. The absorbance was recorded in EZ 4 and TZ 21 S line recorders (Laboratorní přístroje, Prague, Czechoslovakia), simultaneously recording also the collection of fractions by a collector operated on a time principle. The pH of the fractions was measured with a compensating pH meter (Instrument Development Workshops) and the conductivity with a Type OK-102/1 conductivity meter (Radelkis, Budapest, Hungary).

Sorption and desorption

CM-Spheron (*ca.* 10 g) for the sorption was prepared as described above; subsequently the resin was placed on a glass filter (S_2, diameter 5 cm) where a *ca.* 2.5-cm column had formed; the latter was covered with a disc of filter-paper.

Technical protease (0.5 g) was dissolved in 200 ml of cold water, a small amount of sediment was centrifuged off and the pH of the solution was adjusted to 4.5 with 10% acetic acid. This solution was passed by gravity through the CM-

Spheron column at 4°; fractions of 20 ml were collected (*cf.*, Fig. 2). After the application of 200 ml of the supernatant, the glass filter was washed with 200 ml of equilibrating buffer; the components that were not sorbed were thus displaced. Subsequently, desorption was effected by elution of the ion exchanger with the desorption buffer; fractions of 10 ml were collected. All fractions were tested by measurement of the absorbance at 280 nm, conductivity, pH and proteolytic activity.

The active fractions desorbed were pooled (80 ml), frozen with stirring to a crushed ice form and mixed with 120 ml of cold acetone at −20°. The precipitate thus formed was centrifuged for 30 min at −10° and 1100 *g*. The sediment was freed from acetone at 4° *in vacuo* on a water aspirator.

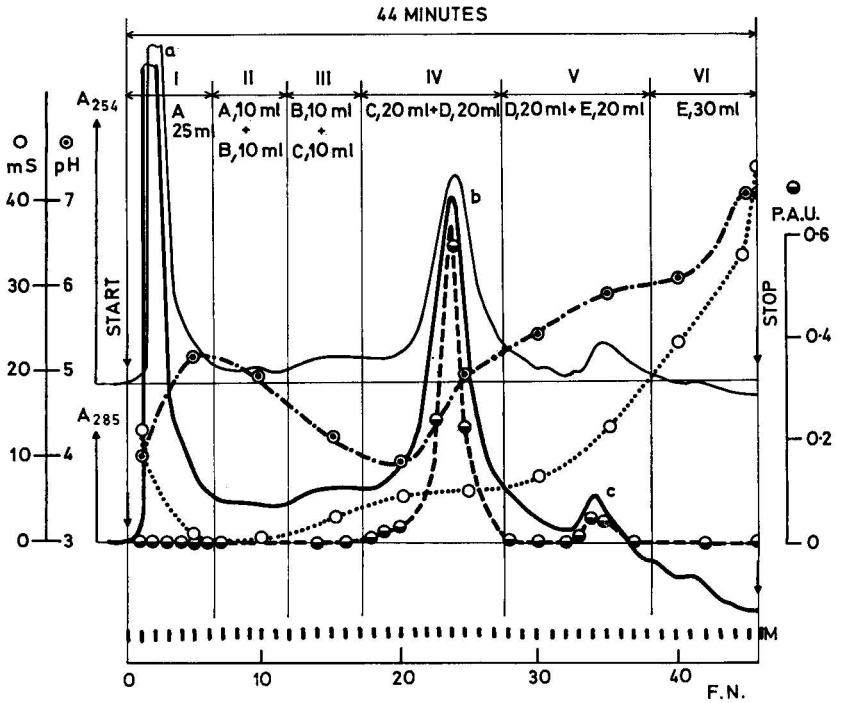

Fig. 1. Chromatography of crude protease on CM-Spheron. The ion exchanger was equilibrated with buffer A. Load: 20 mg of enzyme in 0.3 ml of the same buffer. I: buffer A without gradient. Subsequently linear gradients II (A + B), III (B + C), IV (C + D) and V (D + E) were applied. VI: buffer E without gradient. Flow-rate, 4.07 ml/min; fractions, 4.24 ml; temperature, 10°; counter pressure, 5–10 atm. Buffers: A, 0.005 *M* ammonia + formic acid, pH 4.5; B, 0.05 *M* ammonia + formic acid, pH 4.5; C, 0.25 *M* ammonia + acetic acid, pH 6.0; D, 0.5 *M* ammonia + acetic acid, pH 8.0; E, buffer D, 1.0 *M* in NaCl, pH 8.0. Full lines (———), record of effluent absorbance at 285 and 254 nm by two flow-through cells connected in series; chart speed, 5 mm/min. The broken line (– – –) shows proteolytic activity measured on 0.5-ml aliquots; the activity is given in absorbance units (280 nm) of trichloroacetic acid filtrate of digested haemoglobin (a proteolytic activity unit P.A.U. corresponds to absorbance 1.0). The position of the values was corrected to account for the retardation of fractions with respect to the record by a shift corresponding to the tubing volume + half the volume of the fraction. The fractions were also subjected to measurement of pH (–·–·–) and conductivity (.....), expressed in millisiemens (mS). a, Inactive substances; b, neutral proteinases; c, basic proteinases. M represents automatic marking of fraction collection. F.N. = Fraction number.

Determination of enzymatic activities

Aliquots taken from individual fractions were assayed by the following methods. Proteolytic activity was determined in terms of haemoglobin cleavage using a modification[6] of Anson's method[7]. The activity of glucose oxidase was determined manometrically according to oxygen uptake[8], and polygalacturonanase activity by the method of Somogyi[9], *i.e.*, by the determination of the increase in reducing saccharides after cleavage of pentagalacturonic acid.

RESULTS

The chromatography of the sample of microbial protease (Fig. 1) showed that

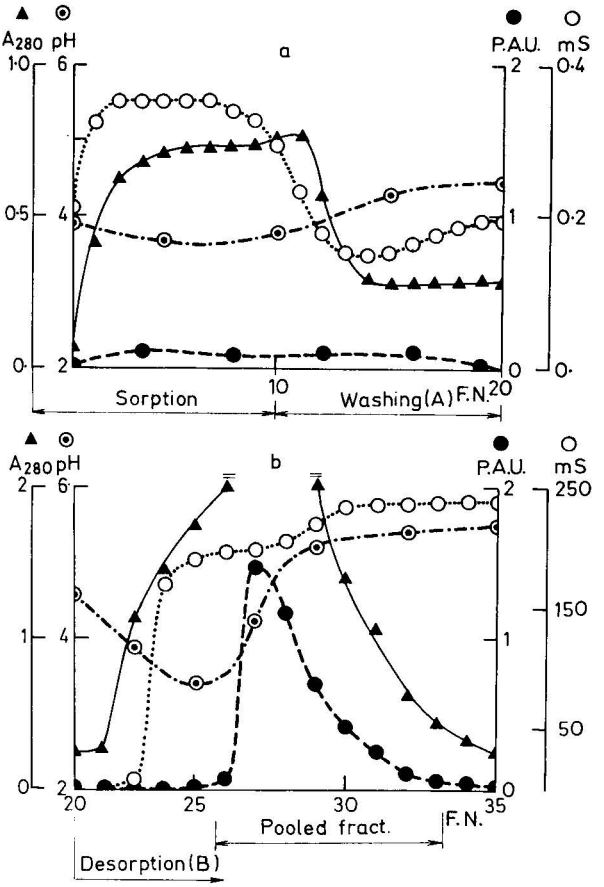

Fig. 2. Course of sorption (a) and desorption (b) of crude protease to CM-Spheron. (a) A solution of 0.5 g of the enzyme preparation in 200 ml of water, pH 4.5, was filtered by gravity through a 5 × 2.5 cm column of ion exchanger formed on a glass filter and equilibrated with buffer A. Fractions (20 ml) were collected at 3-min intervals. The ion exchanger was then washed with 200 ml of buffer A at the same rate. (b) Desorption was effected by washing with 150 ml of buffer B; 10-ml fractions were collected at 2-min intervals. The fractions were subjected to all measurements described in Fig. 1. Buffers: A, 0.005 *M* ammonia + formic acid, pH 4.5; B, 0.25 *M* ammonia + acetic acid, pH 6, 0.5 *M* in NaCl. The operation was carried out at 4°. F.N. = Fraction number; P.A.U. = proteolytic activity units.

proteolytic enzymes are reversibly sorbed to the carboxymethyl derivative of Spheron. This ion exchanger could therefore serve well for the technical sorption and desorption of these enzymes. To check this possibility, the experiment illustrated in Fig. 2 was carried out; the Büchner funnel was replaced with a glass filter. The product desorbed was precipitated with acetone in the cold and analysed by chromatography on DEAE-Spheron (Fig. 3). The solution applied was brown because of the pigments present in the protease; these pigments had adsorbed on the protease during the acetone precipitation. These pigments were eluted from the resin virtually in one band together with the main zone of the protease. The experiment showed that CM-Spheron can be used for reversible sorption of basic and neutral enzymes. It also illustrates the possibility of using this ion exchanger and also of DEAE-Spheron for the rapid, semi-preparative analysis of technical proteases.

The chromatography of technical glucose oxidase (Fig. 4) represents another example of use of DEAE-Spheron for similar purposes when more complicated mixtures are to be analyzed. The chromatography of the same enzyme preparation on the sulphonic acid derivative S-Spheron can be effected in 25 min, as reported earlier (without testing the activity of individual fractions; ref. 1, Fig. 8).

Leozym, a pectolytic technical enzyme, was analyzed chromatographically as

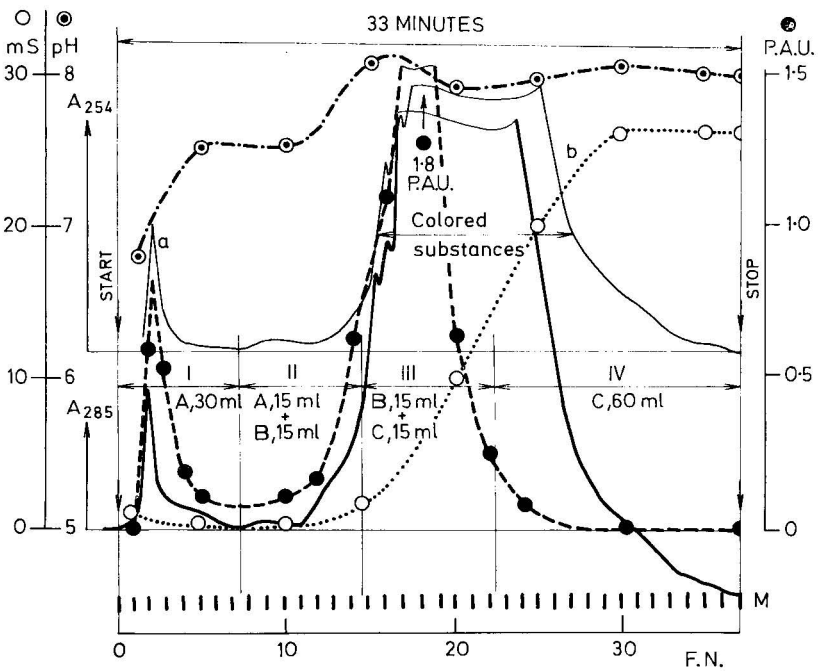

Fig. 3. Chromatogram of proteolytic enzyme desorbed from CM-Spheron (*cf.*, Fig. 2) on a column of DEAE-Spheron. The ion exchanger was equilibrated with buffer A. Load: about half of the sediment after acetone precipitation of desorbed protease, dissolved in 0.4 ml of buffer A. I: buffer A without gradient, followed by linear gradients II (A + B) and III (B + C). IV: buffer C without gradient. Flow-rate, 4.5 ml/min; 4.05-ml fractions; temperature, 10°; counter pressure, 5–10 atm; other parameters and tests of fractions as in Fig. 1. Buffers: A, 0.01 *M* acetic acid + sodium hydroxide, pH 6.8; B, 0.2 *M* acetic acid + sodium hydroxide, pH 6.6; C, buffer B, 1 *M* in NaCl, pH 6.5. F.N. = Fraction number; P.A.U. = proteolytic activity units. a = Basic, and b = neutral substances.

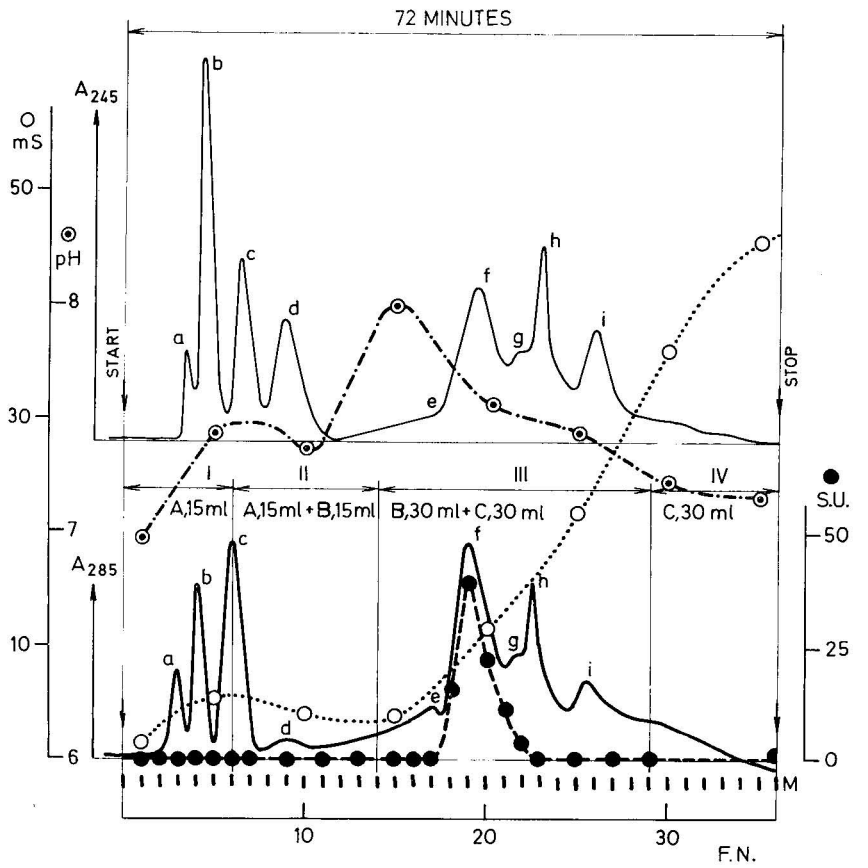

Fig. 4. Chromatography of technical glucose oxidase on DEAE-Spheron. Load: 15 mg of preparation in 0.2 ml of buffer A. The ion exchanger was equilibrated with buffer A. I. buffer A without gradient. Linear gradients II (A + B) and III (B + C). IV, buffer C without gradient. Flow-rate, 2 ml/min; 4-ml fractions; temperature, 14°; counter pressure, 3–7 atm; chart speed, 2 mm/min. Buffers: A, 0.01 *M* acetic acid + NaOH, pH 6.8; B, 0.3 *M* acetic acid + NaOH, pH 5.5; C, buffer B, 1 *M* in NaCl, pH 5.3. Broken line, glucose oxidase activity of effluent in Sarret units (S.U.; 1 S.U. corresponds to the consumption of 600 μl of oxygen at 30°) with correction of shift of values (see legend to Fig. 1 for explanation). The remaining testing of fractions and details of description are identical with those described in the legend to Fig. 1. Corresponding peaks in both parts of the chromatogram are designated by a–i. The UV spectrum of the chromophore of compound d differed significantly from the remaining ones. F.N. = Fraction number.

shown in Fig. 5 and a rapid and satisfactory separation of the main components was achieved.

DISCUSSION

The rate of separation, illustrated by the examples given in Figs. 1 and 3–5, does not represent the limit of applicability of Spheron ion exchangers. An up-to-date liquid chromatograph was not used in the experiments described above. The apparatus was built of readily available components not designed for HPLC and therefore better parameters could not be achieved. Likewise, the particle size of the resin,

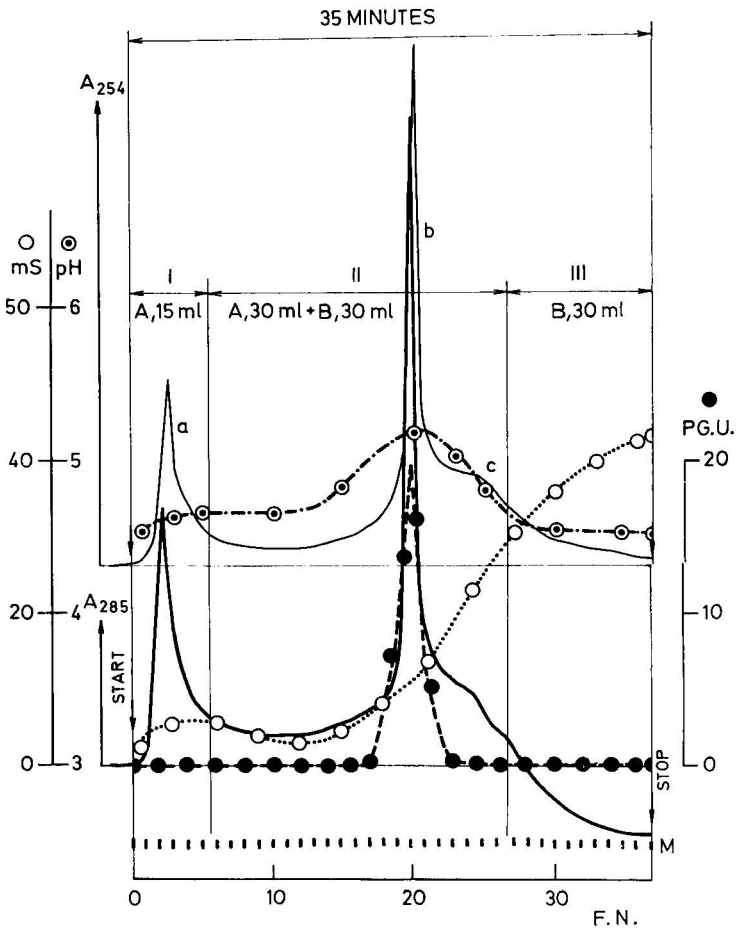

Fig. 5. Chromatogram of technical pectolytic enzyme on DEAE-Spheron. The ion exchanger was equilibrated with buffer A. Load: 25 mg in 0.3 ml of the same buffer. I: buffer A without gradient. II: linear gradient of buffer A + B. III: buffer B without gradient. Flow-rate, 3.0 ml/min; 2.84-ml fractions; temperature, 16°; counter pressure, 6–10 atm. Buffers: A, 0.3 *M* acetic acid + sodium hydroxide, pH 4.5; B, buffer A, 1 *M* in NaCl. Broken line: activity of polygalacturonase in units (PG.U.) μmole · min^{-1} · ml^{-1} × 10^3, corrected for the shift of fractions as described in the legend to Fig. 1. F.N. = Fraction number. a and c, Balast proteins; b, polygalacturonase.

20–40 μm, is not optimal for the chromatography of biopolymers. A smaller size of the beads of Spheron resins than are developed at present will permit shorter diffusion times and thus provide new possibilities for speeding up the chromatography of biopolymers to an extent comparable with the HPLC of other types of compounds.

An important factor in the use of Spheron ion exchangers in bioengineering and in the analysis of technical enzymes is that these resins are so hydrophilic that they do not denature the enzymes. They can therefore be widely applied not only in separation procedures based on sorption but also for the immobilization of enzymes in enzyme reactors. Their mechanical and chemical stability and the possibility of their repeated use without loss of their original properties make them very suitable

for this purpose. The synthetic matrix of these resins, moreover, is not digested by any enzyme and they are not likely to be attacked by microbial infection.

The experiment illustrated in Fig. 2 shows that these ion exchangers, even when used in the form of a low and wide bed of a glass filter, sorb very well; the course of the experiment is essentially that of chromatography, even though less perfect than in a column arrangement. The re-calculation of flow-rates used with Spheron ion exchangers during chromatography in our columns (*i.e.*, 8 ml/cm^2 · min) for columns used in laboratories operating on the kilogram scale and pilot plants gives values of tens of litres per minute and even higher. These values are of technical importance. The development of Spheron ion exchangers should therefore also be directed to materials suitable for this purpose.

ACKNOWLEDGEMENTS

The authors thank Dr. Ljuba Rexová-Benková for the determination of polygalacturonase activity, Dr. Lada Huderová-Svobodová for her help with the determination of glucose oxidase activity, and the colleagues mentioned in Table III for the samples of the enzymes.

REFERENCES

1 O. Mikeš, P. Štrop, J. Zbrožek and J. Čoupek, *J. Chromatogr.*, 119 (1976) 339.
2 O. Mikeš, P. Štrop and J. Čoupek, *J. Chromatogr.*, in press.
3 O. Mikeš, P. Štrop, J. Zbrožek and J. Čoupek, in preparation.
4 O. Mikeš, Z. Chytilová, J. Farkaš, P. Vrátný and P. Štrop, *Czechoslovak Federation Biochemical Meeting, Starý Smokovec (Czechoslovakia), May 4–6, 1977, Abstr. No. 8.14, Bull. Czech. Biochem. Soc.*, 5 (1977) 89.
5 O. Mikeš, in Z. Deyl, K. Macek and J. Janák (Editors), *Liquid Column Chromatography*, Elsevier, Amsterdam, 1975, p. 355.
6 J. Turková and O. Mikeš, *Collect. Czech. Chem. Commun.*, 36 (1971) 2739.
7 M. L. Anson, *J. Gen. Physiol.*, 22 (1938) 79.
8 A. Kleinzeller, *Manometrické Metody*, Stát. Zdravotnické Vydavatelství, Prague, 1954, pp. 10 and 21.
9 M. Somogyi, *J. Biol. Chem.*, 195 (1952) 19.

Journal of Chromatography, 148 (1978) 247–254

CHROM. 10,492

HIGH-PERFORMANCE LIQUID CHROMATOGRAPHY OF COMPOUNDS OBTAINED DURING THE PRODUCTION OF N-NITROSODIPHENYLAMINE

L. VODIČKA, J. KŘÍŽ and J. BURDA

Laboratory of Synthetic Fuels, Institute of Chemical Technology, Suchbátarova 5, 166 28 Prague 6 (Czechoslovakia)

and

P. NOVÁK

Department of Organic Technology, Institute of Chemical Technology, Suchbátarova 5, 166 28 Prague 6 (Czechoslovakia)

SUMMARY

The conditions for the high-performance liquid chromatographic separation of a mixture of compounds obtained during the production of N-nitrosodiphenylamine were established. Silica gel with 20-μm spherical particles was used as the stationary phase and *n*-pentane–methanol as the mobile phase. Elution data for diphenylamine, N-nitrosodiphenylamine, 4-nitrodiphenylamine, 4-nitrosodiphenylamine, aniline, carbazole and toluene were measured using *n*-pentane containing 2, 4 and 6% (w/w) of methanol. The eluate was monitored by means of a UV detector at 254 nm. A procedure for the determination of a low content (0.1–2%, w/w) of diphenylamine in N-nitrosodiphenylamine is described.

INTRODUCTION

N-nitrosodiphenylamine (N-NODFA) is an important diphenylamine (DFA) derivative with many uses, *e.g.*, as a stabilizer for certain types of explosives, as a polymerization catalyst and as a nitrosation agent in organic synthesis. N-NODFA is also an important intermediate in the production of rubber industry chemicals. It has not been found to be toxic[1], but it is suspected of being carcinogenic as are other nitrosamines[2].

In view of the above, the development of a suitable method for the determination of N-NODFA is desirable. Determinations of N-NODFA (and other nitroso compounds) using titration with chromium(II) chloride[3] and reduction with tin(II) chloride[4] with subsequent bromination have been described. There is also a semi-quantitative determination of N-NODFA by means of a "spot test"[5,6]. A photometric determination[7] is based on the formation of a coloured palladium–N-NODFA complex. Further, both N-NODFA and DFA can be determined by spectrophotometric methods[8], especially in the UV region[9], and by polarography[10,11]. However,

most spectral measurements, in both the UV[12,13] and IR[14–17] regions, were concerned with structural studies of N-NODFA and similar compounds[18–21].

Thin-layer chromatography (TLC) permits the simultaneous determination of DFA, N-NODFA and their derivatives, as well as of products of their decomposition[22–25].

High-performance liquid chromatography (HPLC) is a very useful method for the analysis of these compounds, which are characterized by a low thermal stability. The main advantages are the rapidity of the analysis and the possibility of determining also impurities present in low concentrations. The determination is not affected by the presence of other compounds of the same type, in contrast to chemical and photometric methods.

N-NODFA is obtained by a nitrosation of DFA following the scheme

$$C_6H_5 \cdot NH \cdot C_6H_5 + NaNO_2 + H_2SO_4 \rightarrow C_6H_5 \cdot N(NO) \cdot C_6H_5$$

DFA N-NODFA

The reaction is carried out in toluene. The aim of this work was to develop a method for the determination of small amounts of DFA in the presence of N-NODFA. In addition to these two compounds, it is necessary to separate chromatographically aniline and carbazole originating in technical diphenylamine, and 4-NODFA and 4-NO_2DFA as nitrosation by-products.

EXPERIMENTAL

Apparatus

A Varian 8500 liquid chromatograph (Varian, Palo Alto, Calif., U.S.A.) with a syringe pump was used. Sample injection was performed by the stop-flow technique, with a 5- or 10-μl syringe (Micromesure AG Hamilton, Bonaduz, Switzerland) directly into the column, using a septumless injection device. A fixed-wavelength (254 nm) UV detector (Varian) was employed and the chromatograph was operated at ambient temperature. Chromatograms were recorded on a Varian A25 dual-pen strip-chart recorder.

Columns

(1) A stainless-steel column (50 cm × 2 mm I.D.) manufactured in the Laboratory of Synthetic Fuels was packed by the tap–fill method with 20-μm spherical particles of Pragosil 20 silica gel. This material was manufactured in collaboration between the Nuclear Research Institute, Řež, and the Prague Institute of Chemical Technology.

(2) A stainless-steel column (25 cm × 2 mm I.D.) MicroPak SI 10 (Varian) was also used.

Materials

N-NODFA, DFA, 4-NODFA, 4-NO_2DFA and 4-toluidine were obtained from the Department of Organic Technology, Institute of Chemical Technology, Prague. Aniline and carbazole were obtained from commercial sources.

Mobile phase

n-Pentane (VEB Jenapharm-Laboratorchemie, Apolda, G.D.R.) and methanol (Lachema, Brno, Czechoslovakia) were dried over Nalsit A 4 activated molecular sieve, distilled in glass using a calcium chloride closure to prevent access of moisture and stored over activated molecular sieves.

Diethyl ether was dried over sodium, distilled and stored over molecular sieves. 2-Propanol (Lachema) of analytical-reagent grade was used without further treatment.

Qualitative analysis

Three test mixtures were prepared, as follows. (i) For observing the resolution (R_s) of the chromatographic peaks of DFA and N-NODFA, a solution of both standards in methanol was prepared with ratios resulting in approximately equal responses on the UV detector set at 254 nm. (ii) The second test mixture was used for estimating the feasibility of quantitative monitoring of both components, the ratio of their concentrations being 1:100. (iii) The third test mixture contained, in addition to N-NODFA and DFA, the following components: toluene (nitrosation medium), aniline and carbazole (impurities in DFA), and 4-NODFA and 4-NO_2DFA (nitrosation by-products).

Three mobile phases were tried: (A) *n*-pentane–2-propanol (99:1, w/w); (B) *n*-pentane–diethyl ether (50:50, w/w); (C) *n*-pentane–methanol. The proportion of methanol in system C was varied from 2 to 6% (w/w) at flow-rates from 10 to 120 ml/h, while evaluating (a) the possibility of separating all seven compounds, *i.e.*, toluene, N-NODFA, DFA, aniline, carbazole, 4-NO_2DFA and 4-NODFA, and (b) the possibility of separating N-NODFA and DFA with a resolution (R_s) sufficiently large for the quantitative determination of low contents (0.1–2%) of DFA in N-NODFA to be feasible.

Retention data were measured for the *n*-pentane–methanol system at methanol concentrations of 2, 4 and 6% (w/w) and with a flow-rate of 40 ml/h.

Quantitative analysis

Quantitative analyses were performed on a 50-cm stainless-steel column packed with Pragosil 20. *n*-Pentane containing 2% (w/w) of methanol was used as the mobile phase at a flow-rate of 20 ml/h. An external standard method was used and calibration graphs were constructed for N-NODFA and DFA. The contents of both components were determined from a single chromatogram obtained on a dual-pen strip-chart recorder. The input terminals of both channels were connected with each other and with the detector output. The voltages chosen for recording the N-NODFA and DFA peaks was 10 and 1 mV, respectively, at a UV detector sensitivity set at 0.08 absorbance unit full scale.

RESULTS AND DISCUSSION

A satisfactory separation of the compounds studied was not achieved with the eluents *n*-pentane–diethyl ether and *n*-pentane–2-propanol. On the other hand, the system *n*-pentane–methanol was found to give good separations of N-NODFA, DFA and the other compounds.

All of the compounds were separated on the column packed with Pragosil 20, the peaks being symmetrical. When the MicroPak SI 10 column was used, strong adsorption of aniline on the column occurred, making the detection of low contents of this compound impossible. There was also considerable tailing of all of the other compounds studied. Further work was therefore performed with the column packed with Pragosil 20. Fig. 1 shows a chromatogram of a test mixture on the MicroPak SI 10 column. All subsequent chromatograms were obtained on the Pragosil 20 column.

Table I gives the retention data measured at methanol concentrations of 2, 4 and 6% (w/w) and a flow-rate of 40 ml/h.

When using the mobile phase containing 2% (w/w) of methanol, the compounds are eluted in the following sequence: toluene, N-NODFA, DFA, aniline,

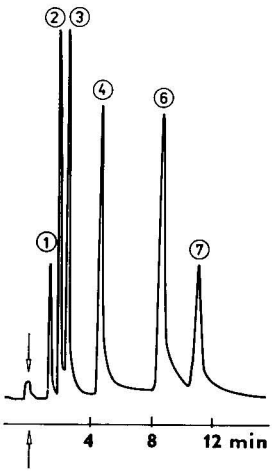

Fig. 1. Separation of a test mixture on MicroPak SI 10 column (25 cm × 2 mm I.D.). Mobile phase *n*-pentane–methanol (96:4, w/w); flow-rate, 30 ml/h; pressure, 3 MPa. Peaks: 1 = toluene; 2 = N-NODFA; 3 = DFA; 4 = carbazole; 6 = 4-NO_2DFA; 7 = 4-NODFA.

TABLE I

RETENTION VALUES

k' = capacity factor, calculated from the equation $k' = (t_R - t_0)/t_0$, where t_R (sec) is the sample retention time and t_0 (sec) is the hold-up time.

Compound	*Proportion of methanol in mobile phase*					
	2%		*4%*		*6%*	
	k'	t_R	k'	t_R	k'	t_R
Toluene	0.21	97	0.19	96	0.18	95
N-NODFA	1.8	222	1.7	215	1.6	208
DFA	2.5	280	2.3	264	2.1	248
Aniline	6.8	624	6.0	566	5.2	500
Carbazole	8.6	769	6.0	566	4.7	457
4-NO_2DFA	22.3	1873	13.0	1129	9.3	824
4-NODFA	26.8	2238	15.0	1288	10.5	925

carbazole, 4-NO_2DFA and 4-NODFA .The mobile phase containing 4% (w/w) of methanol does not separate aniline and carbazole, and with 6% (w/w) of methanol carbazole is eluted before aniline, the sequence of the other compounds remaining unchanged. Fig. 2 shows the behaviour of the retention times when the concentration of methanol in the mobile phase is changed, measured at two different flow-rates. Fig. 3 illustrates the separation of a test mixture at flow-rates of 20 and 120 ml/h.

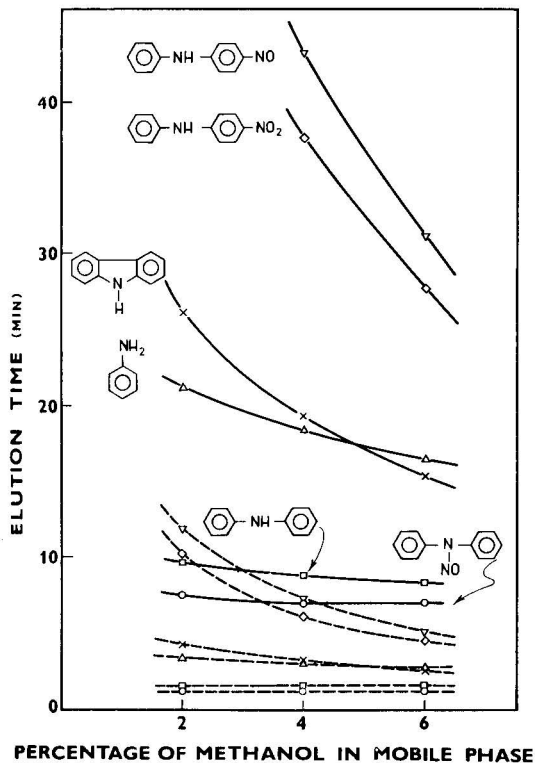

Fig. 2. Dependence of the elution time on the composition of the mobile phase, using a column (50 cm × 2 mm I.D.) packed with Pragosil (20 μm). Solid line, flow-rate 20 ml/h, pressure 1.5 MPa; broken line, flow-rate 120 ml/h, pressure 8 MPa.

The resolution (R_s) for N-NODFA and DFA is given in Table II for various concentrations of methanol in the mobile phase and for various flow-rates of the mobile phase. The R_s values presented are the averages of three measurements.

As the minor component (DFA) is eluted on the descending slope of the major component (N-NODFA), from the point of view of quantitative monitoring of DFA the resolution must be greater the smaller is the amount of this minor component that has to be determined. For concentrations of DFA in N-NODFA in the range of 0.1–2% the value of R_s should be about 3, which can be achieved by using a flow-rate of 10–20 ml/h and *n*-pentane containing 2% (w/w) of methanol as the mobile phase.

If some compounds with longer elution times are present (*e.g.*, 4-NO_2DFA or

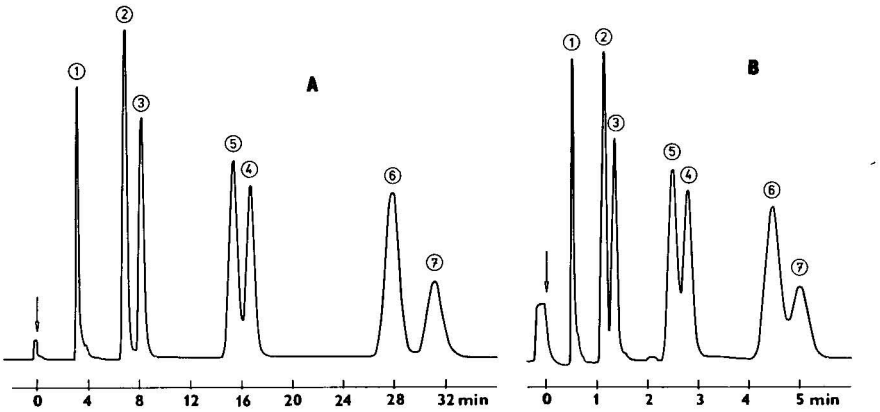

Fig. 3. Influence of flow-rate on separation, using a column (50 cm × 2 mm I.D.) packed with Pragosil (20 μm). Mobile phase, *n*-pentane–methanol (94:6, w/w). A, Flow-rate 20 ml/h, pressure 1.5 MPa; B, flow-rate 120 ml/h, pressure 8 MPa. Peaks: 1 = toluene; 2 = N-NODFA; 3 = DFA; 4 = carbazole; 5 = aniline; 6 = 4-NO_2DFA; 7 = 4-NODFA.

TABLE II

RESOLUTION (R_s) FOR N-NODFA AND DFA

R_s calculated from the relationship

$$R_s = \frac{2(t_D - t_N)}{W_N + W_D}$$

where t_N = elution time for N-NODFA; t_D = elution time for DFA; W_N = peak width of N-NODFA, measured at the base; W_D = peak width of DFA, measured at the base.

Proportion of methanol in mobile phase (%)	*Flow-rate of mobile phase (ml/h)*				
	10	*20*	*40*	*80*	*120*
2	3.3	2.7	2.6	1.9	1.6
4	2.4	2.4	2.2	1.7	1.4
6	2.3	1.7	1.7	1.3	1.1

4-NODFA), the time of analysis is longer under these conditions. If the determination of all compounds by a single analysis is required, isocratic conditions and a programmed flow-rate can be used. Fig. 4 shows a chromatogram obtained by using a programmed flow-rate. The slope of the programmed flow-rate was recorded simultaneously together with the chromatogram on dual-pen strip-chart recorder.

Fig. 5 illustrates the analysis of a sample containing a small amount of DFA in addition to N-NODFA. A dual-pen strip-chart recorder with different sensitivities in the two channels was used in this instance.

The determination of DFA in addition to N-NODFA using *p*-toluidine as an internal standard was unsuccessful. Some samples prepared from technical N-NODFA changed their composition very rapidly after addition of *p*-toluidine, as a result of a reaction between N-NODFA and *p*-toluidine.

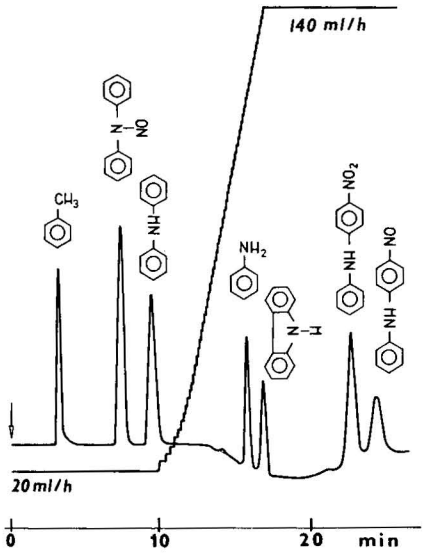

Fig. 4. Chromatogram of test mixture illustrating the use of flow-rate programming. Mobile phase, *n*-pentane–methanol (98:2, w/w). Flow-rate: from 20 to 140 ml/h. The column (50 cm × 2 mm I.D.) was packed with Pragosil (20 μm).

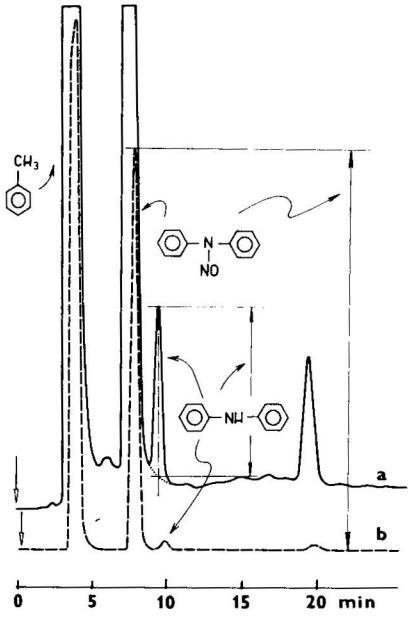

Fig. 5. Analysis of a sample containing a small amount of DFA in addition to N-NODFA. A dual-pen strip-chart recorder with different sensitivities (1 and 10 mV) on the two channels was used. The column (50 cm × 2 mm I.D.) was packed with Pragosil (20 μm).

REFERENCES

1 N. A. Zhilova and A. A. Kasparov, *Toksikol. Nov. Prom. Khim. Veshchestv*, (1968) 157.
2 V. Šicho and J. Káš, *Prům. Potravin*, 25 (1974) 16.
3 N. H. Furman and R. S. Bottei, *Anal. Chem.*, 29 (1957) 121.
4 K. V. Ryan, *Sci. Proc. Roy. Dublin Soc.*, 19 (1928) 85.
5 F. Feigl and N. C. Costa, *Anal. Chem.*, 28 (1956) 1311.
6 F. Feigl and W. Anger, *Z. Anal. Chem.*, 182 (1961) 13.
7 A. I. Ivankova, I. D. Vvedenskaya and D. F. Shcherbov, *Issled. Tsvet. Fluorestsent. Reakts. Opred. Blagorod. Metal*, 31 (1969).
8 W. Selig, *U.S. At. Energy Comm. Monograph Series*, UCRL-6903 (1962) 13 pp.; *C. A.*, 57 (1962) 11861 d.
9 W. A. Schroeder, P. E. Wilcox, K. N. Trueblood and A. O. Dedder, *Anal. Chem.*, 23 (1951) 1740.
10 R. B. Martin and M. O. Tashcjian, *J. Phys. Chem.*, 60 (1956) 1028.
11 H. Lund, *Acta Chem. Scand.*, 11 (1957) 990.
12 K. Tabli and S. Nagakura, *Bull. Chem. Soc. Jap.*, 38 (1965) 965.
13 A. E. Luckij, *Zh. Obshch. Khim.*, 30 (1960) 3782.
14 E. J. Beljajev, L. G. Soboleva, K. P. Sedyč and Z. F. Burjogina, *Fiz. Khim. Tekhnol.*, (1969) 227.
15 J. C. Earl, R. J. W. Le Fèvre, A. G. Pulford and A. Walsh, *J. Chem. Soc.*, (1951) 2207.
16 R. L. Williams, R. J. Pace and G. J. Jeacocke, *Spectrochim. Acta*, 20 (1964) 225.
17 F. Pristera, *Anal. Chem.*, 25 (1953) 844.
18 A. Alm, *Explosivstoffe*, 17 (1969) 156.
19 Y. Matsunaga, *Bull. Chem. Soc. Jap.*, 29 (1956) 969.
20 S. P. Maštakova, N. S. Fumina and Z. A. Gribov, *Zh. Anal. Khim.*, 29 (1971) 430.
21 M. Piskorz and T. Urbański, *Bull. Acad. Polon., Ser. Sci. Chim.*, 11 (1963) 607.
22 J. Hansson and A. Alm, *J. Chromatogr.*, 9 (1962) 385.
23 R. Prensmann, *Z. Anal. Chem.*, 202 (1964) 187.
24 K. S. Yasuda, *J. Chromatogr.*, 14 (1964) 65.
25 K. Yasuda, *Bunseki Kagaku (Jap. Anal.)*, 17 (1968) 732.

Journal of Chromatography, 148 (1978) 255–263

CHROM. 10,415

ION-PAIR ADSORPTION CHROMATOGRAPHY OF BASIC DRUGS USING STRAIGHT-PHASE SYSTEMS ON SILICA GEL THIN LAYERS

ROKUS A. DE ZEEUW, FRANC J. W. VAN MANSVELT and JAN E. GREVING

Department of Toxicology, Laboratory for Pharmaceutical and Analytical Chemistry, State University, Groningen (The Netherlands)

SUMMARY

A general approach to the ion-pair adsorption chromatography of basic drugs on silica gel thin layers is described. Under acidic or neutral conditions, basic drugs will migrate as uncharged ion pairs if a suitable inorganic counter ion such as Br^- or Cl^- is present in sufficient amounts. The latter can be achieved by dissolving halide salts in the developing solvent, or by impregnating the sorbent with halide salts prior to development. The ion-pair chromatographic systems tested are compared with systems in which the drugs migrate in their basic form and the results suggest that the use of ion-pair systems has great potential as a general screening technique for basic drugs when carried out in combination with a general basic development system.

INTRODUCTION

Basic drugs play a major role in medicine and pharmacy. Their extensive use as therapeutic agents, their toxicity and their potential addictive properties make their detection and identification highly important. Thin-layer chromatography (TLC) has been shown to be a useful technique for this purpose, but the large number of basic drugs in use, together with the fact that in some sub-classes structural differences between the individual components are minimal, has resulted in the publication of numerous TLC systems[1–6]. In most of these systems the drugs are assumed to migrate in their unionized, basic form*; silica gel and alumina are the sorbents of choice and the differences between the various systems are found in the composition of the developing solvent. However, few systematic attempts seem to have been made to investigate whether the TLC of basic drugs can also be performed under conditions in which the drug molecules are not present in their basic form.

We recently described the ion-pair adsorption chromatography of quaternary ammonium compounds on silica gel thin layers[7], in which quaternary cations migrated as uncharged ion pairs, based on the reaction

$$Q^+ + X^- \rightleftarrows QX$$

* Such systems will be referred to as basic systems.

As this approach seemed to be applicable to other organic components if they can be converted into a stable, ionized form, we have investigated if basic drugs (primary, secondary and tertiary amines) can be chromatographed according to the same principle, namely

$$BH^+ + X^- \rightleftarrows BHX$$

As this equation indicates, the basic drugs should be present in their protonated form (BH^+) to give ion pairs with a suitable counter ion (X^-). The latter may be the case in chromatography under acidic conditions.

The work presented here describes our first experiences with a selection of basic drugs and their ion-pair chromatographic behaviour is compared with that in basic systems.

EXPERIMENTAL

Chemicals

Basic drugs were obtained as salts from commercial suppliers or were gifts, and were used as received. The free bases were obtained by extraction from aqueous alkaline media (pH 12 for amphetamines, pH 9.5 for the remaining drugs) with chloroform, yielding free base concentrations of approximately 1 mg/ml in chloroform.

All other chemicals and solvents were of analytical grade and were obtained from E. Merck (Darmstadt, G.F.R.).

Thin-layer chromatography

Plates were 20 × 20 cm pre-coated silica gel 60-F_{254} plates (Merck), or were hand-made using the same sorbent with a layer thickness of 0.25 mm.

Chromatography under acidic conditions was achieved by means of a 0.1 *M* phosphate buffer (pH 2). Pre-coated plates were immersed in about 200 ml of buffer solution for 15 sec, blotted and dried. For hand-made plates, the buffer was used in preparing the spreading slurry.

The inorganic counter ions tested were acetate, sulphate, nitrate, chloride, bromide, iodide and perchlorate. They were applied as their potassium, sodium or lithium salts and added to the chromatographic system in one of the following modes:

(a) by using an aqueous solution of the desired counter ion in the spreading procedure of hand-made plates; this aqueous solution may also be the phosphate buffer as described above;

(b) by dipping pre-coated plates in a methanolic solution of the desired counter ion;

(c) by dissolving the counter ion in the developing solvent, provided that the latter is able to dissolve the required amount (this is usually the case with solvents containing large percentages of methanol).

The concentrations of the counter ions tested ranged from 0.025 to 0.5 *M*.

After all of the spreading or dipping procedures, the plates were dried for 30 min at 105° in an oven with a fan, except for those containing iodide and perchlorate, which were dried overnight at ambient temperature in order to avoid oxidation to

iodine and to reduce explosion risks, respectively. The dried plates were stored in a desiccator until required for use.

Spotting was effected with the aid of Microcaps (Drummond, Broomall, Pa., U.S.A.). Volumes of 1 or 5 μl were spotted, 2 cm from the bottom edge of the plate and at least 0.5 cm apart.

Development was carried out in 24 × 22 × 5 cm tanks to a height of 10 cm over the starting points in unsaturated chambers[8]. The solvent systems used were chloroform–methanol (90:10), chloroform–methanol (90:10) on 0.1 *M* sodium hydroxide-impregnated plates[9], methanol, methanol on 0.1 *M* sodium hydroxide-impregnated plates[10] and methanol–25% ammonia (100:1.5).

Detection was carried out under UV light of 254 nm and/or by spraying with an appropriate reagent, such as acidified iodoplatinate, Dragendorff or ninhydrin reagent[5].

RESULTS AND DISCUSSION

Excellent ion-pair chromatography could be obtained with chloride, bromide, iodide or perchlorate as counter ions, provided that the counter ion concentration applied to the system was at least 0.1 *M*. The ion pairs thus formed had good stability, did not decompose on silica gel and had adequate mobility in the solvent systems used. Compact spots were obtained with counter ion concentrations of 0.1 *M* and above. At lower concentrations, tailing of the spots occurred. With higher counter ion concentrations (0.2–0.5 *M*), the R_F values of the individual components had a tendency to increase slightly.

Other inorganic counter ions, such as sulphate and nitrate, did not give adequate ion pairs as their use resulted in a markedly reduced migration, if any, of the basic drugs, usually accompanied by pronounced tailing. Organic acids, such as acetic acid, toluenesulphonic acid, bromothymol blue and bromocresol purple, were also tested as counter ions, dissolved in the developing solvents, but were also unsatisfactory. This may be due to lack of ionization of the organic acids under acidic conditions, so that ion pairs with the basic drugs cannot be formed, or to interactions of the organic acids with the sorbent.

As the use of iodide and perchlorate had practical disadvantages because of iodine formation and explosion risks, bromide and chloride systems were selected for general use and were compared with a series of basic development systems. The systems studied are summarized in Table I. The use of phosphate as acidic buffer resulted in no migration of the components investigated with the chloroform–methanol system; with methanol as solvent most of the components again remained at the starting point, but some components tended to migrate slightly as streaks. The absence of migration can be explained by the fact that the protonated bases formed under the acidic conditions are strongly bound to the sorbent. When the buffer was omitted, as was done in systems E and M, all substances migrated, as indicated in Table II. If the methanolic system E is compared with system D, it can be seen that the addition of OH^- had hardly any influence on the R_F values, nor on the separation sequence. If system M is compared with system L, it can be seen that the addition of OH^- to the chloroform–methanol system resulted in an increase in most R_F values, possibly owing to an increase in polarity, but again the separation sequence remained essential-

TABLE I

ION-PAIR AND BASIC TLC SYSTEMS STUDIED

System	*Silica gel prepared or dipped in*	*Solvent*
A	Aqueous phosphate buffer (pH 2)	Methanol
B	No special treatment	Br^- in methanol
C	No special treatment	Cl^- in methanol
D	0.1 *M* NaOH in methanol	Methanol
E	No special treatment	Methanol
F	No special treatment	Methanol–ammonia (100:1.5)
G	Aqueous phosphate buffer (pH 2)	Chloroform–methanol (90:10)
H	Aqueous phosphate buffer (pH 2), followed by Br^- in methanol	Chloroform–methanol (90:10)
I	Br^- in methanol	Chloroform–methanol (90:10)
K	Cl^- in methanol	Chloroform–methanol (90:10)
L	0.1 *M* NaOH in methanol	Chloroform–methanol (90:10)
M	No special treatment	Chloroform–methanol (90:10)

ly the same. Therefore, it can be assumed that under the "neutral" conditions of systems E and M the drugs migrate in their basic form, despite the absence of a strongly basic component in the sorbent or in the solvent.

This observation is of special importance for the chloroform–methanol (90:10) system. This system, applied to sodium hydroxide-impregnated silica gel, has

TABLE II

$R_F \times 100$ VALUES OF BASIC DRUGS IN ION-PAIR AND BASIC TLC SYSTEMS

Concentrations of the counter ions or hydroxides in the spreading slurry or in the solvent were 0.1 *M*.

Drug	*System**									
	B	*C*	*D*	*E*	*F*	*H*	*I*	*K*	*L*	*M*
Oxycodone	44	39	35	32	76	25	34	34	68	51
Ethylmorphine	37	30	28	27	59	29	40	30	35	32
Codeine	30	30	24	27	57	21	34	25	32	32
Morphine	25	24	22	24	55	06	16	09	32	31
Quinine	59	55	34	36	74	22	55	41	23	16
Cocaine	55	47	41	44	89	23	24	30	74	52
Aminophenazone	75	74	75	74	89	37	59	60	65	61
Phenazone	74	73	73	73	86	51	50	52	59	55
Amphetamine	67	65	28	24	61	36	27	29	34	20
Methylamphetamine	64	59	19	17	51	42	31	31	27	14
Ephedrine	67	61	19	18	50	35	23	24	08	07
Amitriptyline	48	41	28	34	77	56	39	38	58	40
Nortriptyline	68	65	11	15	49	56	39	36	37	20
Imipramine	44	36	24	29	72	61	45	39	55	40
Desipramine	62	56	11	12	41	61	46	39	30	18
Yohimbine	79	77	73	73	93	30	29	31	65	52
Dextromoramide	82	82	82	80	93	69	69	70	94	80

* See Table I for descriptions. Systems B and C are ion-pair systems using methanol as solvent; systems D, E and F are "basic" systems using methanol as solvent. Systems H, I and K are ion-pair systems using chloroform–methanol (90:10) as solvent; systems L and M are "basic" systems using chloroform–methanol (90:10) as solvent.

been recommended by Moffat and Clare[11] as one of the best thin-layer systems for basic drugs, based on its discriminating power, but the need to use impregnated plates has been regarded a time-consuming disadvantage. With the above evidence, indicating that no impregnation is needed, it can be expected that chloroform–methanol (90:10) will gain further prominence as a general system for basic drugs[12]. As already indicated[11], this chloroform–methanol system has a much better discriminating power than methanol–ammonia (100:1.5), which was confirmed in our work by comparing the spread of the components in either system L or M with that in system F. On the other hand, it should be noted that the addition of 1.5% of ammonia to methanol (F) results in a marked increase in all R_F values compared with methanol alone (E) or methanol on sodium hydroxide-impregnated plates (D). This is also represented graphically in Figs. 1 and 2. As this increase can hardly be explained by an increase in polarity alone, the reason for this phenomenon remains unknown.

When a suitable counter ion, such as Br^-, was added to the pH 2-buffered chloroform–methanol system, all substances migrated as compact spots and yielded the R_F values given in Table II, system H. The protonated bases can now form relatively stable ion pairs which migrate as such. When Br^- was added to the pH 2-buffered methanol system, again migration of all substances was observed, but as the solvent had a tendency to wash out the buffer the spot shapes became irregular and showed tailing.

When trying to find the optimal pH of the buffer system and to avoid the wash-out effect, we then observed that the use of the buffer is not essential for ion-pair chromatography: The mere presence of a suitable amount of Br^- in the system, either in the sorbent layer or in the solvent, is sufficient. This is reflected in systems I (Br^- in the sorbent) and B (Br^- in the solvent). If the R_F values in system I (chloroform–methanol plus Br^-) are compared with those in system M (chloroform–methanol), it can be seen that ion-pair chromatography gives distinctly different patterns from those obtained in basic systems. The same applies to the methanol systems B (ion pair) and E (basic).

Excellent ion-pair chromatography was also obtained with Cl^- as counter ion, as can be seen from the R_F values in systems C and K. Although the R_F values in the Cl^- systems tended to be similar to those in the Br^- systems, there were some marked differences, such as a decrease in the R_F values of ethylmorphine, codeine, morphine and quinine in system K compared with system I. A decrease in the R_F values of cocaine, ephedrine, amitriptyline and imipramine is also noticeable.

Some of the separation patterns are depicted graphically in Figs. 1 and 2 for the methanol systems and in Figs. 3 and 4 for the chloroform–methanol systems. Fig. 1 shows the R_F patterns of a variety of basic drugs. It can be seen that some drugs show little or no difference in R_F values between ion-pair and basic development systems (dextromoramide, yohimbine and morphine), whereas others, such as ephedrine and quinine, show substantial changes in R_F values when going from ion-pair systems (B and C) to basic systems (D and E). The latter effect is also observed with other ephedrine-like substances, such as amphetamine and methylamphetamine, but these have been omitted from the figures for simplicity.

Another class of components that shows considerable changes in R_F values when changing from ion-pair to basic systems is that of the tricyclic antidepressants, as illustrated in Fig. 2. All four components show relatively high R_F values in the ion-

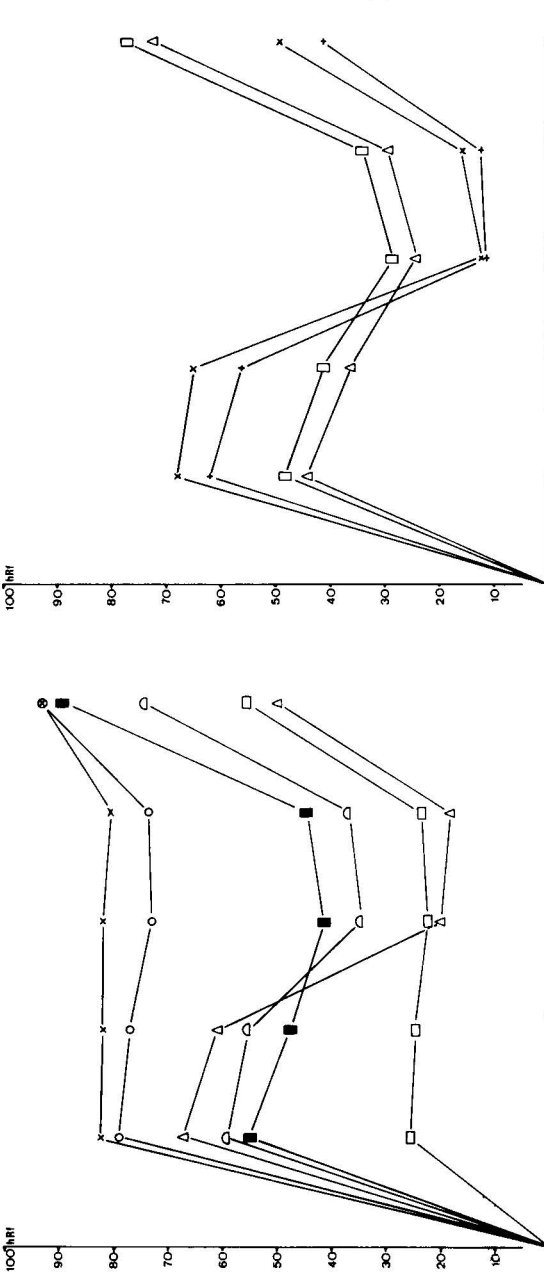

Fig. 1. R_F values of some basic drugs in ion-pair TLC systems and in basic TLC systems using methanol as solvent. See Table I for description of systems A–F. ×, Dextromoramide; ○, yohimbine; ■, cocaine; ◘, quinine; □, morphine; △, ephedrine.

Fig. 2. R_F patterns of some tricyclic antidepressants in ion-pair TLC systems and in basic TLC systems using methanol as solvent. See Table I for description of systems A–F. □, Amitriptyline; △, imipramine; ×, nortriptyline; +, desipramine.

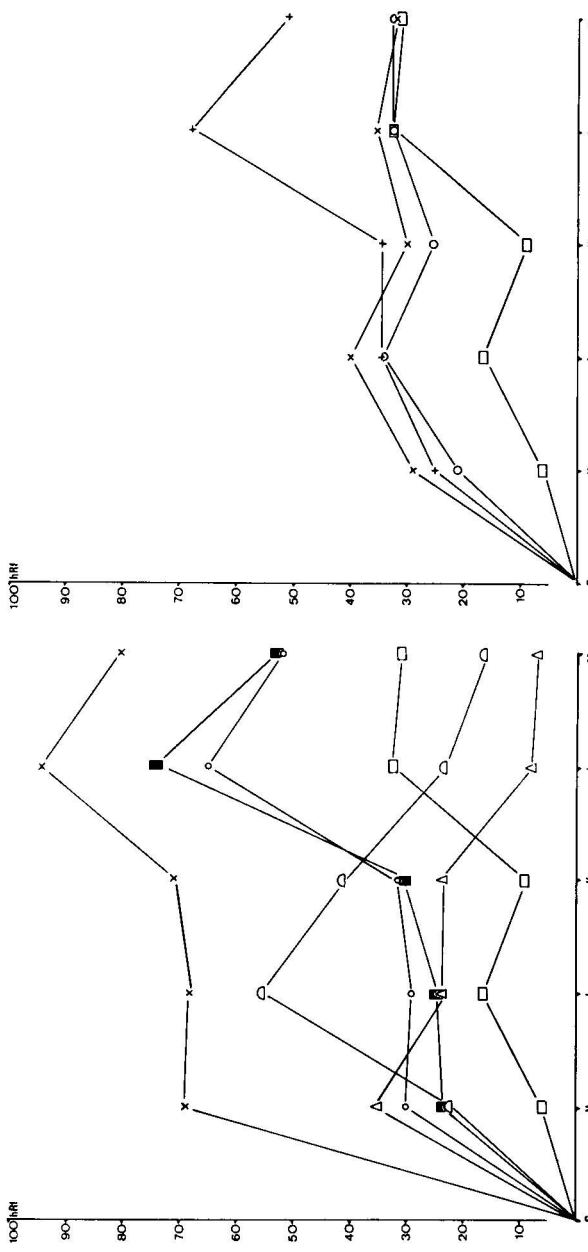

Fig. 3. R_F patterns of some basic drugs in ion-pair TLC systems and in basic TLC systems using chloroform–methanol (90:10) as solvent. See Table I for description of systems G–M. ×, Dextromoramide; ■, cocaine; ○, yohimbine; □, morphine; ◘, quinine; △, ephedrine.

Fig. 4. R_F patterns of some opiates in ion-pair TLC systems and in basic TLC systems using chloroform–methanol (90:10) as solvent. See Table I for description of systems G–M. +, Oxycodone; ×, ethylmorphine; ○, codeine; □, morphine.

pair systems B and C, with the secondary amines nortriptyline and desipramine running higher than their corresponding tertiary derivatives. In the basic systems D and E, all components have lower R_F values, which is much more pronounced for the secondary than for the tertiary amines. However, this results in a reversal of the separation sequence, with the tertiary amines now running ahead of the secondary amines.

Fig. 3 shows the R_F values of the same substances as in Fig. 1, but in the chloroform–methanol system. Again, marked differences can be observed when changing from ion-pair systems (H, I and K) to basic systems (L and M). However, it should be noted that there are substantial differences between the ion-pair systems as such, indicating that the choice of counter ion can play a role (compare I and K), as well as the pH (compare H and I). Apparently, these factors are more pronounced in the chloroform–methanol systems than with methanol alone. Structurally related substances may show identical patterns, as can be seen with the opiates and the amphetamines, but aminophenazone and phenazone display a different behaviour. In all methanol systems and in the basic chloroform–methanol systems L and M, these two drugs run closely together, with aminophenazone having slightly higher R_F values. The separation becomes slightly better in the ion-pair systems I and K, and is reasonable in system H, albeit that in the latter system the separation sequence is reversed, with phenazone now running faster. Within the group of tricyclic antidepressants another interesting phenomenon can be noted. In the ion-pair systems H, I and K, amitriptyline and nortriptyline run together, as do imipramine and desipramine, so that the migration rate is determined by changes in the tricyclic ring structure. However, in the basic systems L and M, the two tertiary amines amitriptyline and imipramine run together despite the differences in their ring structures, whereas the secondary amines nortriptyline and desipramine have much lower R_F values, indicating that the secondary amine function has a predominant effect on the migration in basic systems.

Fig. 4 depicts the separation behaviour of the four opiates studied. The ion-pair systems give good separations between morphine and codeine. The separation of ethylmorphine and codeine, which differ by only one methylene group, is best in system H, provided that oxycodone is absent. The latter compound can be tested for easily in the basic system L or M.

Development times for the ion-pair systems were of the same order as those for the basic systems, namely 30–45 min. The spot shapes and sizes as well as the reproducibility were also comparable to those in the basic systems. Detection can be carried out under UV light (not recommended for phosphate-containing plates) or with the usual detection reagents.

CONCLUSION

The straight-phase ion-pair adsorption systems presented here are rapid, simple and rather insensitive to small changes in temperature and relative humitidy, and therefore seem to be more advantageous than reversed-phase ion-pair partition systems, which require carefully standardized conditions[13–16]. Moreover, the ion-pair adsorption systems are able to utilize the high separation selectivity of the silica gel sorbent.

The major advantage of ion-pair adsorption chromatography is that the separation is based on different physico-chemical principles compared with separa-

tions in basic systems, thus providing a new and independent parameter for the identification of a particular drug. Therefore, the use of ion-pair adsorption systems can be recommended as additional general screening techniques, especially in combination with the already existing basic systems[11]. Ion-pair systems may also offer increased possibilities in specific separation problems in which basic systems do not provide adequate resolution.

Further investigations to evaluate the further potential of this technique are being carried out.

ACKNOWLEDGEMENTS

We thank P. E. W. van der Laan for valuable assistance and Ciba-Geigy, Basle, Switzerland, for gifts of amitriptyline, nortriptyline, imipramine and desipramine.

REFERENCES

1 K. Macek, I. M. Hais, J. Kopecký and J. Gasparič (Editors), *Bibliography of Paper and Thin-Layer Chromatography, 1961–1965*, Elsevier, Amsterdam, 1968.
2 K. Macek, I. M. Hais, J. Kopecký, J. Gasparič, V. Rábek and J. Churáček (Editors), *Bibliography of Paper and Thin-Layer Chromatography, 1966–1969*, Elsevier, Amsterdam, 1972.
3 K. Macek, I. M. Hais, J. Kopecký, V. Schwarz, J. Gasparič and J. Churáček (Editors), *Bibliography of Paper and Thin-Layer Chromatography, 1970–1973*, Elsevier, Amsterdam, 1976.
4 I. Sunshine (Editor), *Handbook of Analytical Toxicology*, CRC Press, Cleveland, Ohio, 1969.
5 E. G. C. Clarke (Editor), *Isolation and Identification of Drugs*, Pharmaceutical Press, London, 1969.
6 G. Zweig and J. Sherma (Editors), *Handbook of Chromatography*, Vol. 1, CRC Press, Cleveland, Ohio, 1972.
7 R. A. de Zeeuw, P. E. W. van der Laan, J. E. Greving and F. J. W. van Mansvelt, *Anal. Lett.*, 9 (1976) 831.
8 R. A. de Zeeuw, *Anal. Chem.*, 40 (1968) 915.
9 G. F. Phillips and J. Gardiner, *J. Pharm. Pharmacol.*, 21 (1969) 793.
10 W. W. Fike, *Anal. Chem.*, 38 (1966) 1967.
11 A. C. Moffat and B. Clare, *J. Pharm. Pharmacol.*, 26 (1974) 665.
12 M. L. Bastos, G. E. Kananen, R. M. Young, J. R. Montforte and I. Sunshine, *Clin. Chem.*, 16 (1970) 931.
13 K. Gröningsson and G. Schill, *Acta Pharm. Suecica*, 7 (1969) 447.
14 K. Gröningsson, *Acta Pharm. Suecica*, 8 (1970) 635.
15 K. Gröningsson and M. Weimers, *Acta Pharm. Suecica*, 12 (1975) 65.
16 K. Gröningsson, H. Westerlind and R. Modin, *Acta Pharm. Suecica*, 12 (1975) 97.

Journal of Chromatography, 148 (1978) 265–268

CHROM. 10,408

DETERMINATION OF CARBON MONOXIDE CONCENTRATIONS IN AIR BY GAS CHROMATOGRAPHY USING AN ARGON IONIZATION DETECTOR

PETER POPP and GUDRUN OPPERMANN

Academy of Sciences of the German Democratic Republic, Central Institute for Isotope and Radiation Research, Leipzig (G.D.R.)

SUMMARY

A simple gas chromatographic method using an argon detector and a simple enrichment technique permits the determination of carbon monoxide concentrations in air within the range 0.3–300 ppm. Results from measurements at a Leipzig street crossing over a period of about 28 h are given.

INTRODUCTION

Automobile exhaust gases are among the most important sources of atmospheric pollution in towns. Of the toxic compounds emitted by automobiles, carbon monoxide and hydrocarbons are particularly important owing to their high concentrations.

Whereas the gas chromatographic analysis of hydrocarbons in air is relatively simple because of the high sensitivity of the flame-ionization detector[1], the detection of inorganic gases, especially carbon monoxide, is more difficult. Although the helium detector is extremely sensitive to carbon monoxide[2], its application is limited because of its insufficient reliability.

This paper describes a simple gas chromatographic method using an argon detector and a simple enrichment technique for the determination of carbon monoxide concentrations in air.

EXPERIMENTAL

A Chromatron GCHF 18.3 gas chromatograph equipped with an argon detector, developed at the Central Institute for Isotope and Radiation Research, Leipzig[3], was used for the measurements.

The air samples were collected using glass sampling bulbs. Gas samples were injected with gas-tight syringes. The lower detection limit of the argon detector for carbon monoxide was 3 ppm when the size of the air sample was 25 ml.

In order to determine smaller carbon monoxide concentrations, the air samples from the glass bulbs were led into a pre-column by means of a stream of

neon, cooled at liquid nitrogen temperature and filled with molecular sieve 5A. The pre-column (stainless steel, 12 cm × 4 mm I.D.) was fixed on the gas sampling valve of the gas chromatograph instead of the sample loop.

At the desired time, the pre-column was heated and at the same time the sample was led into the carrier gas by means of the gas sampling valve. The neon flow-rate and the time, in which the neon streams through the column, were chosen so that the air was flushed out of the cooled loop, but the retention time of carbon monoxide was so long that at the time of the injection it had not reached the end of the pre-column. The chromatographic column consisted of a glass tubing (1 m × 3 mm I.D.) filled with molecular sieve 5A. With this procedure, it was possible to enrich carbon monoxide concentrations from air samples up to 250 ml.

RESULTS AND DISCUSSION

Air samples were collected at a Leipzig street crossing and carbon monoxide concentrations were determined in samples taken over a period of about 28 h. During the busy periods, the carbon monoxide concentrations reached levels of over 20 ppm

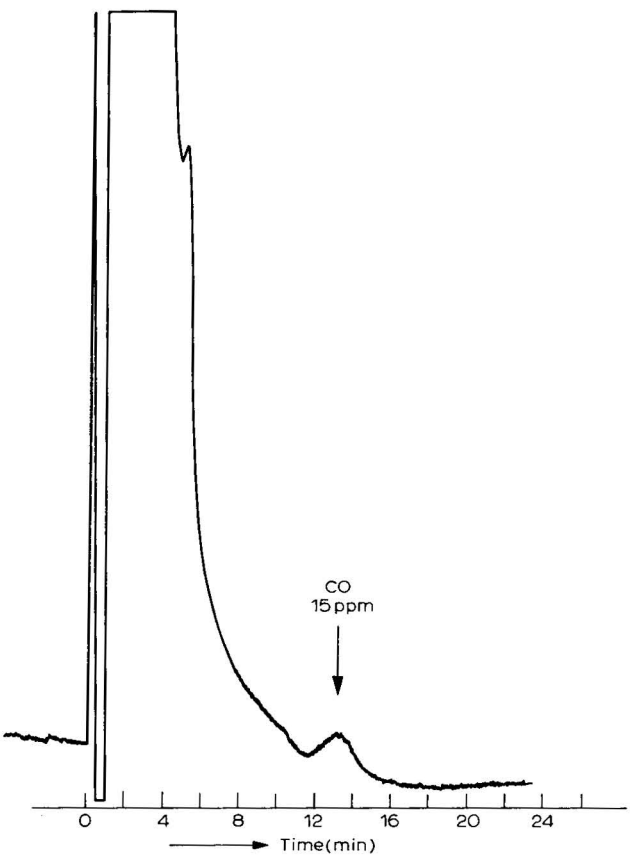

Fig. 1. Analysis of air at a street crossing: temperature, 28°; argon flow-rate, 30 ml/min; air sample size, 25 ml.

and it was possible to determine the concentrations by means of injections with gas-tight syringes. A chromatogram of an injection of 25 ml of air containing 15 ppm of carbon monoxide is shown in Fig. 1.

During the night the carbon monoxide concentrations decreased to a minimum of 0.5 ppm. Because the lower detection limit of the argon detector was 3 ppm (with a 25-ml air sample injected), the carbon monoxide concentration was determined by using the enrichment procedure described above. The volume of the air sample carried with the neon stream into the pre-column was calculated by using the equation for exponential dilution:

$$C = C_0 e^{-Qt/V}$$

where C = concentration of air at time t, C_0 = initial concentration, Q = dilution neon flow-rate and V = volume of the glass bulb. It was possible to determine carbon monoxide concentrations down to 0.3 ppm (enriched from a 250-ml air sample) by this means. A chromatogram obtained in such a way is shown in Fig. 2. The air

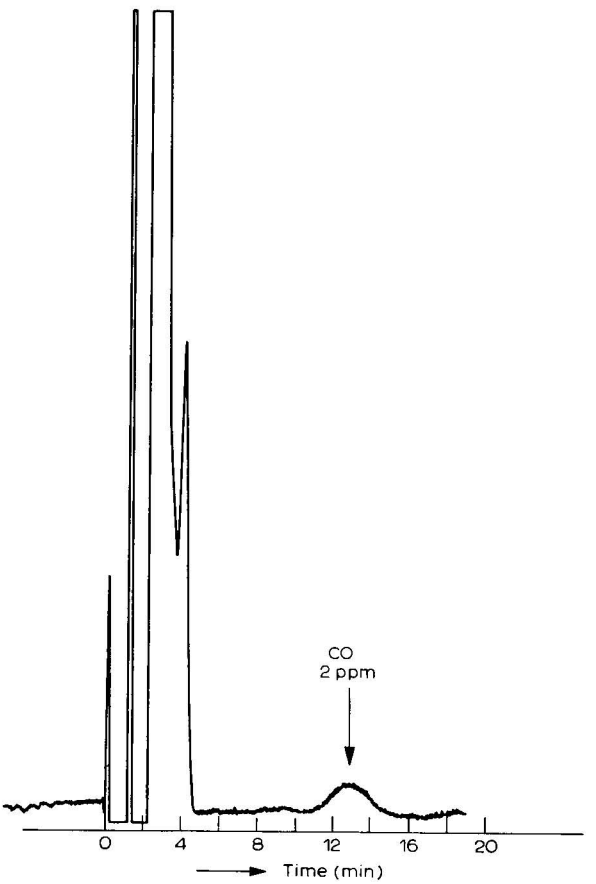

Fig. 2. Analysis of air at a street crossing: temperature, 28°; argon flow-rate, 30 ml/min; sample size, 1.5 ml of neon and air containing carbon monoxide from 200 ml of air.

volume, calculated according to the exponential law, was 200 ml. The carbon monoxide peak corresponded to a concentration of 2 ppm.

The change in carbon monoxide concentration over a period of about 28 h, depending on the density of traffic, is shown in Fig. 3. The carbon monoxide concentration and the density of traffic increase and decrease in parallel, but shifted with respect to time, both minimal and maximal carbon monoxide concentrations being reached 2–3 h later than the corresponding minimal and maximal densities of traffic. Maximal concentrations up to 21 ppm of carbon monoxide were obtained with 2000 cars/h and minimal concentrations down to 0.5 ppm with 50–100 cars/h.

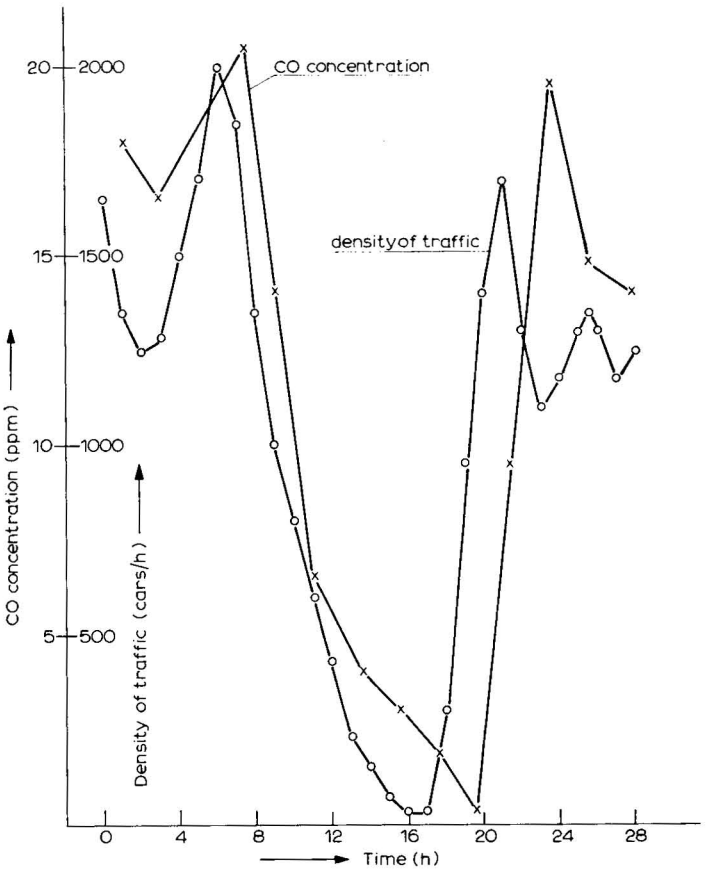

Fig. 3. Carbon monoxide concentration at a street crossing depending on the density of traffic.

REFERENCES

1 J. A. Giannovario, R. L. Grob and P. W. Rulon, *J. Chromatogr.*, 121 (1976) 285.
2 F. Bruner, P. Ciccioli and R. Rastelli, *J. Chromatogr.*, 77 (1973) 125.
3 P. Popp and G. Oppermann, *Chem. Tech. (Leipzig)*, 28 (1976) 95.

Journal of Chromatography, 148 (1978) 269–272

CHROM. 10,471

GAS CHROMATOGRAPHIC IDENTIFICATION OF SOME INDOOR AIR POLLUTANTS USING CORRELATION EQUATIONS

M. MUCHTAROVA
Centre of Hygiene, Sofia (Bulgaria)
and
N. DIMOV
Chemical-Pharmaceutical Institute, Sofia (Bulgaria)

SUMMARY

A calculation method for the identification of indoor air pollutants analysed by gas chromatography is described. It is based on correlation between the retention and the molecular properties of a substance. The equation

$$r_{1,2}^{calc} = A + B \cdot t_b^r + C/V_{mol}^r$$

where t_b^r is the relative boiling point, V_{mol}^r the relative molecular volume and A, B and C are constants gives values of the relative retention, $r_{1,2}^{calc}$, that differ from the experimental values by only ± 0.02 unit.

INTRODUCTION

The gas chromatographic (GC) identification of indoor air pollutants could be difficult and time consuming, because of the great variety of pollutants present. The certainity of their identification when only retention data are used could be increased by comparing the values with those obtained by some calculation method. The application of several calculation methods[1–5] to indoor air analyses showed, however, unacceptable discrepancies between the calculated and experimental retention values. The method[6] employing the vapour pressure (p^0) and molecular volume (V_{mol}) of the substances of interest is relatively reliable but it is difficult to obtain p^0.

In this work, the correlation between relative retention ($r_{1,2}$) and relative boiling point (t_b^r) and any relative molecular property of the compound was studied as a possible solution of this problem. Freshly painted surfaces produce an air pollutant mixture of solvents and diluents, such as aromatic hydrocarbons, aliphatic alcohols and acetates. Mixtures containing representatives of these classes were used in this study.

All investigations were based on the assumption that there exists a linear correlation of the type

$$r_{1,2} = A + B \cdot t_b^r + C \cdot MP + D \qquad (1)$$

where MP is any molecular property, D is the difference between the calculated and experimental relative retentions and A, B and C are constants. The value of D is the criterion to be used in selecting a suitable molecular property and we aimed at arriving at a D value equal to or less than 0.02 unit.

EXPERIMENTAL

The compounds chosen for the investigation and their properties are listed in Table I.

TABLE I

PROPERTIES OF AROMATIC HYDROCARBONS, ALIPHATIC ALCOHOLS AND ACETATES USED IN THE CORRELATION ANALYSIS

Compound	t_b (°C)	*Mol. wt.*	*Specific gravity*	V_{mol}
Benzene	80.1	78.0	0.879	88.7
Toluene	110.8	92.1	0.866	106.1
Ethylbenzene	136.2	106.2	0.867	122.5
p- and *m*-xylene	138.5	106.2	0.862	123.0
o-Xylene	144.4	106.2	0.880	120.6
Ethanol	78.3	46.1	0.789	58.4
Isobutanol	108.0	74.0	0.803	92.0
sec.-Butanol	100.0	74.0	0.806	92.0
n-Butanol	117.5	74.0	0.810	91.5
Isopentanol	132.0	88.1	0.812	108.6
Ethyl acetate	77.1	88.1	0.901	97.8
Isobutyl acetate	118.0	116.2	0.875	134.3
n-Butyl acetate	126.1	136.2	0.881	131.7
Isoamyl acetate	142.0	130.2	0.876	149.7

We studied one apolar phase, Apiezon L (ApL), a phase of moderate polarity, benzyldiphenyl (BDP), and a polar phase, polyethylene glycol 20M (PEG 20M). In addition, Chromosorb 101 was included, as it is very useful in the separation of alcohols and other polar compounds. The columns used had different lengths, the support was Chromosorb W, at least two amounts of each stationary phase were studied and the temperature was varied within $\pm 20°$ of the optimal. For every column length, amount of stationary phase and temperature, at least three values of the retention time were measured. The dead volume was determined before and after every analysis. An amount of 0.2 μl of mixtures containing only one class of substance and a standard was injected. A Pye Unicam Series 104 chromatograph with a flame-ionization detector with sensitivity 100 and 5000 was used. *o*-Xylene was chosen as the standard as it gives an individual peak in the separations examined with the columns used.

RESULTS AND DISCUSSION

The solution of a correlation matrix showed that the best correlation between $r_{1,2}$ and the substance property existed when t_b^r and $1/V_{mol}^r$ were used:

$$r_{1,2} = A + B \cdot t_b^r + C/V_{mol}^r + D \qquad (2)$$

TABLE II

VALUES OF CONSTANTS IN EQN. 2

Stationary phase	*Aromatic hydrocarbons*			*Aliphatic alcohols*			*Acetates*		
	Constants	*Difference between* $r_{1,2}^{calc}$ *and* $r_{1,2}^{exp}$		*Constants*	*Difference between* $r_{1,2}^{calc}$ *and* $r_{1,2}^{exp}$		*Constants*	*Difference between* $r_{1,2}^{calc}$ *and* $r_{1,2}^{exp}$	
		Average	*Maximum*		*Average*	*Maximum*		*Average*	*Maximum*
ApL	$A = -8.95$ $B = 5.71_5$ $C = 4.42$	0.02	0.03	$A = -1.05$ $B = 1.23$ $C = 0.36_5$	0.01	0.02	$A = -0.67$ $B = 0.84_5$ $C = 0.14_5$	0.02	0.03
BDP	$A = -8.77$ $B = 5.49_5$ $C = 4.35_5$	0.01	0.02	$A = 0.59$ $B = 0.83$ $C = 0.11$	0.03	0.04	$A = -1.65_5$ $B = 1.82_5$ $C = 0.64_5$	0.02	0.03
PEG 20M	$A = -6.14_5$ $B = 4.09$ $C = 3.05$	0.00	0.01	$A = -1.55$ $B = 1.72$ $C = 0.64$	0.01	0.02	$A = -1.97_5$ $B = 2.78$ $C = 0.32_5$	0.03	0.04
Chromosorb 101	$A = -5.74$ $B = 3.96$ $C = 2.85$	0.00	0.01	$A = -0.88$ $B = 1.38$ $C = 0.22_5$	0.02	0.03	$A = -0.34_5$ $B = 0.74_5$ $C = 0.00$	0.02	0.03

The solution of eqn. 2 for the aromatic hydrocarbons, aliphatic alcohols and acetates for the stationary phases examined gave values of the constants A, B and C shown in Table II). It can be seen that the average difference between $r_{1,2}^{calc}$ and $r_{1,2}^{exp}$ was about 0.02 unit or less, the greatest difference being 0.04 unit. The accuracy achieved permits the identification of very closely situated peaks.

As a practical illustration, air from inside a furniture plant was examined. From the nature of the plant, we would have expected as pollutants toluene, *m*- and *p*-xylene, ethanol, isobutanol and *n*- and isobutyl acetate. GC analysis on Chromosorb 101 at 200° showed, however, more peaks on the chromatogram (Table III). As all of the unknown peaks occurred before that of toluene, if there were any aromatic hydrocarbons present it could have been only benzene. The $r_{1,2}^{calc}$ value for benzene is 0.30 unit, which corresponds to $r_{1,2}^{exp}$ of peak X_3. Hence peak X_3 was identified as benzene. The next peaks could be either alcohols or ethyl acetate. The $r_{1,2}^{calc}$ values for the possible compounds are as follows: ethyl acetate, 0.14, *n*-butanol, 0.26 and isobutanol, 0.17. It is evident that peak X_1 belongs to *sec.*-butanol, while peak X_2 seems to be *n*-butanol.

TABLE III

EXPERIMENTAL AND CALCULATED RELATIVE RETENTIONS FOR POLLUTANTS IN A REAL INDOOR AIR

Retention time, t_R (sec)	$r_{1,2}^{exp}$	$r_{1,2}^{calc}$	*Pollutant*
63	0.07	0.06	Ethanol
103	0.17	(0.17)	X_1 (*sec.*-butanol)
113	0.20	0.21	Isobutanol
128	0.23	(0.26)	X_2 (*n*-butanol)
153	0.30	(0.30)	X_3 (benzene)
196	0.41	0.44	Isobut-l acetate
235	0.51	0.51	Toluene
365	0.85	0.84	*p*- + *m*-x-lene
426	1.00	1.00	*o*-X-lene (standard)

In more complicated instances, the use of the method of Dimov and Schopov[6] allows such changes in the temperature of analysis to be made that lead to reliable identification. In more common instances, however, the method proposed above provides a sufficiently accurate identification in a very easy and convenient way.

REFERENCES

1 J. Takács, C. Szita and G. Tarján, *J. Chromatogr.*, 56 (1971) 1.
2 V. G. Berezkin and V. S. Kruglikova, *Izv. Akad. Nauk SSSR, Ser. Khim.*, (1964) 1505.
3 A. A. Nartinov and N. S. Vigdergauz, *Neftekhimiya*, 10 (1970) 763.
4 G. Schomburg, *Chromatographia*, 4 (1971) 286.
5 J. Bonastre and P. Grenier, *Bull. Soc. Chim. Fr.*, 118 (1968) 1292.
6 N. Dimov and D. Schopov, *J. Chromatogr.*, 44 (1969) 170.

Journal of Chromatography, 148 (1978) 273–281

CHROM. 10,409

GAS CHROMATOGRAPHIC, SPECTROPHOTOMETRIC AND ELECTROCHEMICAL BEHAVIOUR OF SUBSTITUTED *s*-TRIAZINES

V. PACÁKOVÁ and I. NĚMEC

Department of Analytical Chemistry, Charles University, Albertov 2030, 12840 Prague 2 (Czechoslovakia)

SUMMARY

The behaviour of 18 *s*-triazine herbicides was studied gas chromatographically, spectrophotometrically and electrochemically. The retention indices were measured on three stationary phases, Carbowax 20M, Versamid 900 and an SE-30 + Reoplex 400 mixed phase, and the effect of the substituents in the 2-, 4- and 6-positions on the retention data is discussed. The differences in the retention indices on two phases, ΔI, were correlated with the basicities and the dipole moments of the substances studied. The UV spectra of the *s*-triazines were measured in methanol. A study of the anodic electrochemical behaviour of these substances was carried out in anhydrous acetonitrile. The $E_{1/2}$ values obtained indicated that the substances strongly resisted oxidation and the results are discussed together with the gas chromatographic and spectrophotometric data in relation to the structures of the *s*-triazines.

INTRODUCTION

s-Triazines are widely used as herbicides in agriculture and industry. They affect primarily the roots of plants and destroy most weeds. Some of these substances, in addition to being important herbicides, exhibit fungicidal properties or are used as pharmaceuticals.

The *s*-triazine herbicides were first synthesized by Geigy, by substituting 1,3,5-triazine (*s*-triazine) in the 2-, 4- and 6-positions. The *s*-triazine character is determined by the substituent in the 2-position, generally chlorine (the commercial name ends with -azine), methoxy (ending -tone) and thiomethyl (ending -tryne). The 4- and 6-positions are usually substituted with various aminoalkyl groups.

The herbicidal effect of *s*-triazines depends on the nature of the substituent in the 2-position and on the number of carbon atoms in the aminoalkyl groups in the 4- and 6- positions; the effectiveness decreases with an increase in the number of carbon atoms. The selective effects of these substances can be varied by replacing Cl with OCH_3 or SCH_3.

The *s*-triazines have been analyzed spectrophotometrically in the visible and UV regions and by paper (PC) and thin-layer chromatography (TLC)[1]. The spectral methods are sufficiently sensitive but are lacking in separation possibilities. PC and

TLC permit separations, but yield only semi-quantitative results. The shortcomings of the above methods are overcome by using gas chromatography (GC), which can be used both for the determination of the purity of the preparations[2,3] and for the analysis of residues[3–11]. Polar stationary phases, possibly combined with non-polar phases, are most often employed for separations of *s*-triazines. The support must be inert, because of the polar character of the *s*-triazines. Triazines can be detected with a flame-ionization detector, as well with specific detectors, *e.g.*, coulometric[4,6], flame-photometric[4,12], Coulson electrolytic conductance[4,6,8–10,13,14] and thermionic[13] detectors.

In view of the importance of these substances, studies of their properties and the development of sensitive methods for their determination are required. Most papers published so far have been concerned with applications and deal with the determination of one or several components in soil, water or grain. A systematic study of the basic properties of *s*-triazine herbicides is lacking, and was attempted in this work, in which the GC, spectrophotometric and electrochemical behaviour of variously substituted *s*-triazines was studied.

EXPERIMENTAL

Methods

GC measurements were carried out isothermally on a Hewlett-Packard 5700 A instrument with a flame-ionization detector. Metal columns (140 cm × 3 mm I.D.) were used. The temperatures of the column were 195° and 215° and those of the injection block and the detector were 230° and 210°, respectively. Nitrogen was used as the carrier gas at a flow-rate of 40 ml/min. The columns were packed with 3% (w/w) Carbowax 20M on Chromosorb W (silanized, 60–80 mesh), 5% Versamid 900 on Chromosorb W (60–80 mesh) and a mixed phase of 5% SE-30 + 2% Reoplex 400 on Chromaton N-AW (60–80 mesh).

Spectrophotometric measurements were performed on a Unicam SP-800 instrument with 1-cm quartz cuvettes in absolute methanol at 20°, at concentrations of 10^{-6}–10^{-4} *M*.

Electrochemical measurements were carried out in a 0.1 *M* sodium perchlorate solution in anhydrous acetonitrile using a platinum rotating disk indicator and saturated calomel reference electrodes (S.C.E.). A detailed description of the apparatus and the measurements has been given elsewhere[15].

Materials

All test *s*-triazines were products of Geigy, Basle, Switserland. The substances were purified by multiple recrystallization from methanol and then their purity was checked by determination of the melting points, elemental analysis and GC.

Methanol (spectrally pure, Lachema, Brno, Czechoslovakia) was purified by the procedure described by Smisko and Dawson[16]. Acetonitrile (p.a. grade, Merck, Darmstadt, G.F.R.) was purified by the procedure described earlier[15]. The *n*-alkanes used in the calculation of the retention indices were obtained from the Applied Science Labs., State College, Pa., U.S.A.

SE-30 and Carbowax 20M were products from Carlo Erba, Milan, Italy,

Reoplex 400 and Versamid 900 were obtained from Hewlett-Packard, Avondale, Pa., U.S.A., Chromaton N-AW (60–80 mesh) was supplied by Lachema and Chromosorb W (silanized, 60–80 mesh) by Carlo Erba.

RESULTS AND DISCUSSION

Gas chromatographic behaviour

Carbowax 20M, Versamid 900 and Reoplex 400 + SE-30 were selected as stationary phases for the study of the effect of the structures of *s*-triazines on their GC behaviour. McReynolds indices for these phases (see Table I) indicated that Carbowax 20M will most strongly retain acidic substances (nitropropane). Reoplex 400 + SE-30 and Versamid 900 retain acidic and basic substances aproximately equally. The non-selective character of these phases was also verified by the linear dependence of $\log p_o$ (p_o = saturated vapour pressure) on the retention indices (Fig. 1).

TABLE I

McREYNOLDS CONSTANTS

Stationary phase	$\Sigma\Delta I^*$	*Benzene*	*Butanol*	*2-Pentanone*	*Nitropropane*	*Pyridine*	*2-Methylpentanol*	*Iodobenzene*
SE-30 + Reoplex 400 (5:2)	940	115	214	160	230	221	196	93
Versamid 900	969	108	309	137	208	207	222	110
Carbowax 20M	2308	322	536	368	572	510	387	282

* $\Sigma\Delta I = \Delta I_{\text{benzene}} + \Delta I_{\text{butanol}} + \Delta I_{\text{2-pentanone}} + \Delta I_{\text{nitropropane}} + \Delta I_{\text{pyridine}}$

The retention indices of the *s*-triazines were measured at 195° and 215° on the three stationary phases[17] and the results are given in Table II. An example of the separation of a mixture of *s*-triazines on Carbowax 20M is shown in Fig. 2.

All of the stationary phases tested are suitable for the separation of *s*-triazines. Compared with Carbowax 20M, the retention indices on Versamid 900 and Reoplex 400 + SE-30 are 300–400 and 600–700 units lower, respectively, so that lower experimental temperatures can be used.

The retention data for the *s*-triazines depend primarily on the nature of the substituent in the 2-position. Methoxy-*s*-triazines are eluted first, then chloro derivatives and finally thiomethyl-*s*-triazines.

In the series of chloro-*s*-triazines, the order of retention depends chiefly on the spatial shielding of the –NH groups in the 4- and 6-positions by alkyl groups and on their number. The lowest retention index on Versamid 900 is exhibited by chlorazine [2-chloro-4,6-bis(diethylamino)-*s*-triazine] (the value, 2021, was calculated from the data given by Henkel and Ebing[18]), which contains only *tert.*-amino groups. It is followed by trietazine, propazine, terbutylazine, atrazine and simazine. The *tert.*-butyl group gives rise to greater spatial shielding than the isopropyl group and the weakest shielding is caused by ethyl groups. For this reason simazine is eluted last. A similar dependence can also be observed in the series of methoxy- and thiomethyl-*s*-triazines.

The difference in the retention indices on Carbowax 20M and Reoplex 400 +

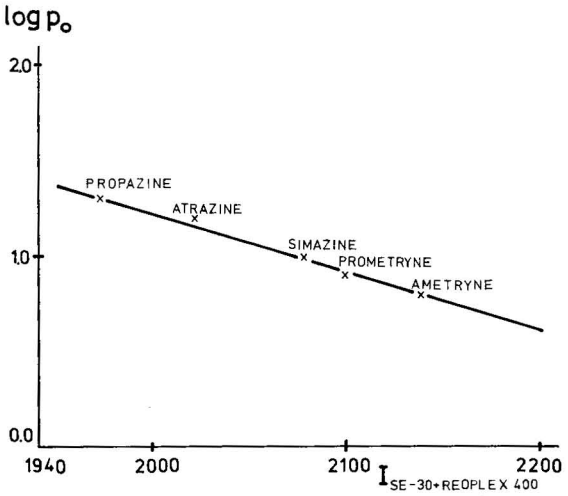

Fig. 1. Dependence of log p_o on retention indices of *s*-triazines.

SE-30, ΔI, depends on the nature of the substituent in the 2-position and also on the number and kind of alkyl groups bound to the amino groups in the 4- and 6-positions. *s*-Triazines have acid–base properties. In acidic media, the neutral form is converted into the protonated form. The dissociation constant is most strongly affected by the substituent in the 2-position. It follows from the comparison of the chemical properties that the basicity of these substances increases with substituents in the 2-position in

TABLE II

RETENTION INDICES OF 18 *s*-TRIAZINES ON THREE STATIONARY PHASES

Common name	*2-Substituent*	*4-Substituent*	*6-Substituent*	*Mol.wt.*	I_A*	I_B*	I_C*	ΔI_{A-C}	ΔI_{A-B}
—	Cl	NH_2	NHtBu	201.5	2336	—	1766	570	—
Ipazine	Cl	$N(Et)_2$	NHiPr	243.6	2461	2142	1907	554	319
—	Cl	NHtBu	NHtBu	257.8	2501	2185	1938	563	316
Trietazine	Cl	NHEt	$N(Et)_2$	229.7	2557	2196	1932	625	361
Propazine	Cl	NHiPr	NHiPr	229.7	2633	2262	1973	660	371
Terbutylazine	Cl	NHEt	NHtBu	229.7	2664	2288	1999	665	376
Atrazine	Cl	NHEt	NHiPr	215.7	2722	2318	2023	699	404
Simazine	Cl	NHEt	NHEt	201.5	2806	2375	2078	728	431
Prometone	OCH_3	NHiPr	NHiPr	225.3	2539	2199	1916	623	340
Terbutone	OCH_3	NHtBu	NHEt	225.3	2570	2205	1938	632	365
sec.-Bumetone	OCH_3	NHEt	NHsecBu	225.3	2676	2302	2015	662	374
Simetone	OCH_3	NHEt	NHEt	197.2	2680	2270	1990	690	410
Prometryne	SCH_3	NHiPr	NHiPr	241.3	2758	2378	2099	659	380
Terbutryne	SCH_3	NHEt	NHtBu	241.3	2793	2403	2122	671	390
Ametryne	SCH_3	NHEt	NHiPr	227.3	2837	2418	2139	698	419
Desmetryne	SCH_3	NHMe	NHiPr	213.3	2868	2452	2141	727	416
Simetryne	SCH_3	NHEt	NHEt	213.3	2915	2465	2185	730	450
Metoprotryne	SCH_3	NHiPr	$NH(CH_2)_3$-OMe	271.4	3202	2726	2457	745	476

* A = Carbowax 20M (215°); B = Versamid 900 (195°); C = SE-30 + Reoplex 400 (195)°.

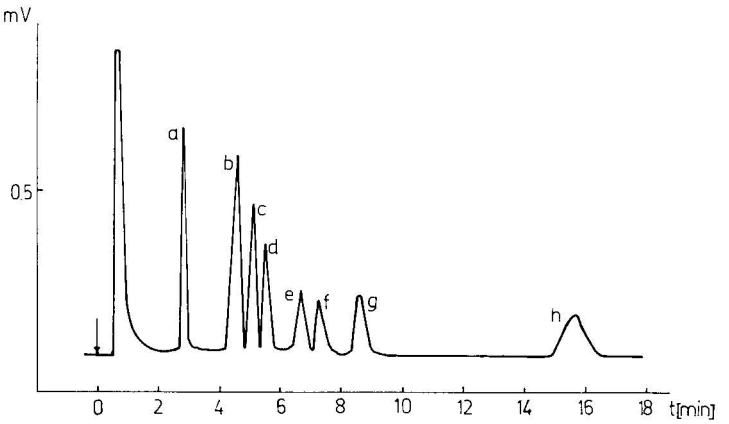

Fig. 2. Separation of *s*-triazines on Carbowax 20M at 215°. (a) 2-Chloro-4-amino-6-*tert.*-butylamino *s*-triazine; (b) 2-chloro-4,6-bis(*tert.*-butylamino)-*s*-triazine; (c) prometone; (d) terbutone; (e) propa zine; (f) terbutylazine; (g) atrazine; (h) simetryne.

the order Cl < SCH_3 < OCH_3 < OH. These properties are also reflected in the GC behaviour; the highest ΔI values were obtained for the weakest bases, *i.e.*, the strongest conjugated acids.

The properties of related *s*-triazines are compared in Table V, from which some other dependences can be derived. In the series of chlorotriazines (propazine, atrazine and simazine), the difference in retention indices on Carbowax 20M and Reoplex 400 + SE-30 is proportional to pK_B. The dipole moment also has an effect on the retention indices.

The dependence of the retention indices on the two stationary phases can be used for identification purposes. As can be seen in Fig. 3, the individual groups of *s*-triazines lie on different straight lines.

Spectrophotometric behaviour

Although the triazine herbicides are much more soluble in methanol than in water, no systematic study of their UV spectra in methanol has been carried out. Therefore, we measured the UV spectra of 18 commercial *s*-triazine herbicides, determining $\lambda_{max.}$ and the molar absorptivity, ε. These data are given in Table III.

In contrast to the spectra in aqueous solutions, where all *s*-triazines exhibit two absorption maxima[19], methoxy- and thiomethyl-*s*-triazines have only a single maximum between 219 and 230 nm, with $\varepsilon_1 \approx 10^4$. Chloro-*s*-triazines have one more maximum from 263 to 270 nm, with $\varepsilon_2 \approx 10^3$ (Table III).

The spectra of atrazine, atratone and ametryne are shown in Fig. 4; the spectra of the other chloro-, methoxy- and thiomethyl-*s*-triazines differ only in the maximum position and ε, but the character of the spectra remains the same.

As can be seen from Table III, the differences in the $\lambda_{max.}$ and ε values are small and cannot be used for characterization of these herbicides. Only chloro-*s*-triazines can be differentiated, on the basis of the occurrence of the second maximum.

Similar to the gas chromatographic data, replacement of H in the –NH groups

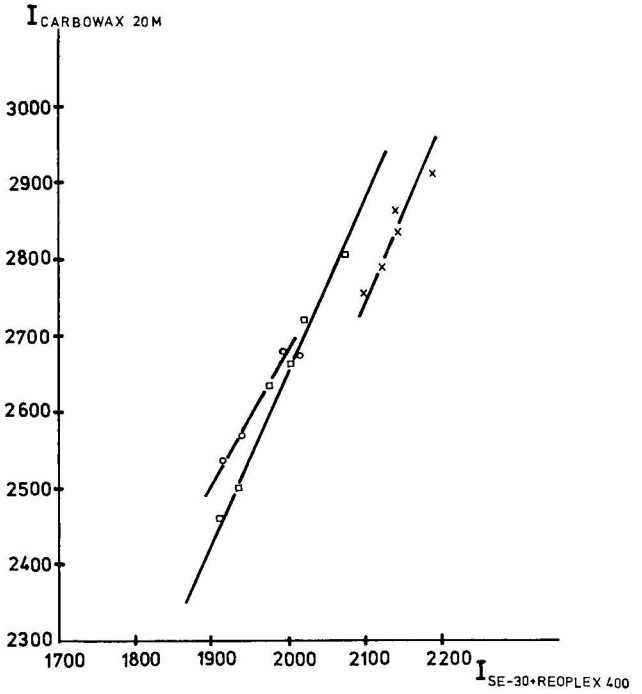

Fig. 3. Dependence of $I_{\text{Carbowax 20M}}$ on $I_{\text{SE-30+ Reoplex 400}}$ for chloro-*s*-triazines (□), methoxy-*s*-triazines (○) and thiomethyl-*s*-triazines (×).

TABLE III

ABSORPTION MAXIMA AND MOLAR ABSORPTIVITY OF 18 *s*-TRIAZINES

s-Triazine	λ_1 *(nm)*	ε_1* ($l \cdot mol^{-1} \cdot cm^{-1}$)	λ_2 *(nm)*	ε_2** ($l \cdot mol^{-1} \cdot cm^{-1}$)
2-Chloro-4-amino-6-*tert.*-butylamino-*s*-triazine	231	12000	Broad maximum	
2-Chloro-4,6-bis(*tert.*-butylamino)-*s*-triazine	223	36000	264	3300
Trietazine	227	44300	267	4300
Propazine	222	32000	268	3100
Terbutylazine	223	19500	263	1800
Atrazine	222	41000	263	3900
Simazine	222	36000	263	3100
Ipazine	227	43100	266	4300
Prometone	219	40200	—	—
Terbutone	219	33600	—	—
Simetone	222	38300	—	—
Prometryne	223	42000	—	—
Terbutryne	223	21200	—	—
Ametryne	222	40000	—	—
Desmetryne	221	33700	—	—
Simetryne	222	44400	—	—

* For the concentration range 10^{-6}–10^{-5} *M*.

** For the concentration range 10^{-5}–10^{-4} *M*.

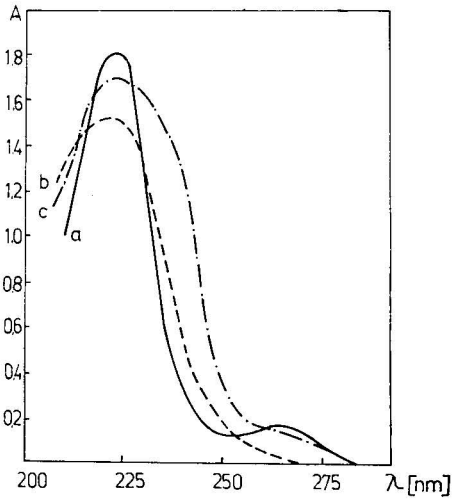

Fig. 4. Absorption spectra of atrazine (a), atratone (b) and ametryne (c) ($5 \cdot 10^{-5}$ *M* solution in methanol).

with alkyl groups affects the spectrophotometric properties of *s*-triazines. An increase in the number of alkyl groups leads to a bathochromic shift; this can be demonstrated by comparing the $\lambda_{max.}$ values of simazine and trietazine or atrazine and ipazine (see Table III). The lengths of the alkyl chains in the 4- and 6-positions do not substantially affect the $\lambda_{max.}$ values.

Electrochemical behaviour

Data on the electrochemical oxidation of *s*-triazines are lacking in the literature. As these substances are very resistant, studies were carried out in anhydrous acetonitrile, which permits electrochemical oxidations of such substances. Moreover, hydrolysis and other interfering effects do not occur in the anhydrous medium and consequently the results are easier to interpret in relation to the structure of the test substances.

The *s*-triazines yielded a single anodic wave on a platinum rotating disk electrode in a 0.1 *M* anhydrous acetonitrile solution of sodium perchlorate[20] (see Table IV).

It follows from Table IV that chloro-*s*-triazines have the highest $E_{1/2}$ values in the series of the chloro, methoxy and thiomethyl derivatives. The differences in the $E_{1/2}$ values for the methoxy and thiomethyl derivatives are small.

In the series of chloro-*s*-triazines, the $E_{1/2}$ values depend on the number of alkyl groups per amino group in the 4- and 6-positions, similar to the spectrophotometric and GC data. Replacement of hydrogen atoms with alkyl groups leads to a considerable decrease in $E_{1/2}$ (simazine with respect to trietazine, atrazine with respect to ipazine). On the other hand, the length of the alkyl group has no perceptible effect on the $E_{1/2}$ values.

As the *s*-triazine proper is not oxidized (see Table IV), the exocyclic amino groups in the 4- and 6-positions act as electron donors. The presence of an electro-

TABLE IV

ANODIC HALF-WAVE POTENTIALS ($E_{1/2}$) OF 17 *s*-TRIAZINES

s-Triazine	$E_{1/2}$ *(V vs. S.C.E.)*	*s-Triazine*	$E_{1/2}$ *(V vs. S.C.E.)*
s-Triazine	Not oxidized	Prometone	1.77
Ipazine	1.77	Terbutone	1.79
2-Chloro-4,6-bis(*tert.*-butylamino)-*s*-triazine	2.07	Simetone	1.79
Trietazine	1.77	Prometryne	1.83
Propazine	1.95	Terbutryne	1.78
Terbutylazine	2.01	Ametryne	1.77
Atrazine	2.02	Desmetryne	1.78
Simazine	1.97	Simetryne	1.79

negative atom (Cl) causes a decrease in the electron density on the nitrogen atom (the dipole moment increases, see Table V) and $E_{1/2}$ increases. Hence *s*-triazines derivatives with a methoxy or thiomethyl group in the 2-position and containing *tert.*-amino groups will be most readily oxidized in anhydrous acetonitrile, *i.e.*, will have the lowest $E_{1/2}$ values.

The $E_{1/2}$ values were correlated with the pK_B values obtained in an aqueous solution[21], and marked agreement was found; the substances with the highest pK_B, *i.e.*, the least basic substances, have the highest $E_{1/2}$ values.

A comparison of the experimental data and some literature values[21] for a series of similar *s*-triazines is given in Table V.

TABLE V

COMPARISON OF SOME CHARACTERISTICS OF SIMILAR *s*-TRIAZINES

s-Triazine	$I_{Carb.}$	ΔI	$E_{1/2}$	μ^* *(ref. 21)*	pK_a *(refs. 21, 22)*
Propazine	2633	660	1.95	4.52	1.85
Prometryne	2758	659	1.83	3.54	4.05
Prometone	2539	623	1.77	2.94	4.28
Atrazine	2722	699	2.02	4.63	1.68
Ametryne	2837	698	1.77	3.15	4.10
Simazine	2806	728	1.97	—	1.65
Simetryne	2915	730	1.79	—	4.04
Simetone	2680	690	1.79	—	4.17
Terbutylazine	2664	665	2.01	—	1.94
Terbutryne	2793	671	1.78	—	4.38
Terbutone	2570	632	1.79	—	4.46

*μ = Dipole moment in Debijes.

CONCLUSION

Individual *s*-triazines can be differentiated chiefly on the basis of the retention indices (Table V). The differences in the retention indices on two stationary phases with different polarities can serve for distinguishing methoxy- from thiomethyl- and

chloro-*s*-triazines, which do not differ significantly. On the other hand, chloro-derivatives can be differentiated from methoxy and thiomethyl derivatives on the basis of the $E_{1/2}$ values, similar to differentiation on the basis of the pK_B values. The differences between thiomethyl- and methoxy-*s*-triazines are small. Spectrophotometric data only permit the differentiation of chloro-*s*-triazines on the basis of the occurrence of the second absorption maximum. *s*-Triazines variously substituted in the 2-position differ in their dipole moments, but no general conclusions can be drawn because of the limited number of literature values available.

ACKNOWLEDGEMENT

We are obliged to Dr. E. Matisová of the Institute of Chemical Technology in Bratislava for kindly supplying us with 8 *s*-triazines.

REFERENCES

1 E. Behrens, *Residue Rev.*, 32 (1970) 355.
2 K. Stammbach, H. Kilcher, K. Friederick, M. Larsen and G. Székely, *Weed Res.*, 4 (1964) 61.
3 D. E. Otto, *J. Ass. Offic. Anal. Chem.*, 54 (1971) 1388.
4 K. Ramsteiner, W. D. Hörmann and D. O. Eberle, *J. Ass. Offic. Anal. Chem.*, 57 (1974) 192.
5 C. A. Benfield and E. D. Chilwell, *Analyst (London)*, 89 (1964) 475.
6 W. D. Hörmann, G. Formica, K. Ramsteiner and D. O. Eberle, *J. Ass. Offic. Anal. Chem.*, 55 (1972) 1031.
7 C. J. Harris, *Weed Res.*, 5 (1965) 275.
8 H. J. Young and A. Chu., *J. Agr. Food Chem.*, 21 (1973) 711.
9 W. E. Westlake, A. Westlake and F. A. Gunther, *J. Agr. Food Chem.*, 18 (1970) 686.
10 J. F. Lawrence, *J. Agr. Food Chem.*, 22 (1974) 137.
11 M. A. Berezovský and G. N. Nemova, *Agrokhimiya*, (1973) 12.
12 M. C. Bowman and M. Beroza, *J. Ass. Offic. Anal. Chem.*, 53 (1970) 499.
13 R. Greenhalgh and W. P. Cochrane, *J. Chromatogr.*, 70 (1972) 37.
14 W. P. Cochrane, B. P. Wilson and R. Greenhalgh, *J. Chromatogr.*, 75 (1973) 207.
15 Z. Samec and I. Němec, *J. Electroanal. Chem.*, 31 (1971) 161.
16 J. Smisko and L. R. Dawson, *J. Phys. Chem.*, 59 (1955) 84.
17 H. Augustová, *Thesis*, Charles University, Prague, 1976.
18 H. G. Henkel and W. J. Ebing, *J. Gas Chromatogr.*, 2 (1964) 215.
19 T. M. Ward and J. B. Weber, *Spectrochim. Acta*, 25A (1969) 1167.
20 P. Artner, *Thesis*, Charles University, Prague, 1976; P. Artner and I. Němec, in preparation.
21 J. B. Weber, *Residue Rev.*, 32 (1970) 93.
22 E. Smolková, Jr., in preperation.

Journal of Chromatography, 148 (1978) 283–291

CHROM. 10,410

A POSSIBILITY OF MODELLING THE *IN VIVO* ACCUMULATION OF COMPOUNDS BY CHROMATOGRAPHY

Z. DEYL, M. ADAM, J. MUSILOVÁ and K. MACEK

Physiological Institute, Czechoslovak Academy of Sciences, Prague, and Research Institute for Rheumatic Diseases, Prague (Czechoslovakia)

SUMMARY

A method for studying the interactions of proteins with various compounds by a chromatographic procedure has been developed. In principle, the protein being tested is used as the packing in a column on which tested solutes are applied and eluted with appropriate buffer systems. As exemplified for collagen, the method is capable of detecting small alterations of the protein structure and may be applicable to environmental problems.

INTRODUCTION

In a living body, numerous interactions take place between solid biopolymers and both low- and high-molecular-weight solutes. The modelling of these interactions with adequate interpretation is not easy and methods using one of the components involved in the interaction as a column packing or chromatographic support can be made use of[1–3]. A better understanding of such interactions may help to interpret some poorly understood physiological and pathophysiological situations and to elucidate the effects of the accumulation of pollutants in organisms.

Of course, such modelling imposes various demands on the solid phase that are comparable to the demands commonly made on column packings, *e.g.*, the mechanical properties, swelling properties, grain size and shape must be within reasonable limits comparable to those used for chromatographic supports and packings[4].

To our knowledge, only collagen, the main fibrillar protein of the connective tissue, has been used up to now to demonstrate these types of interactions[1–3,5]. The rationale of a collagen-based model is based on the fact that the interactions of collagen with other molecular species may alter the amounts of nutrients reaching most of the cells in an animal's body, with obvious biological consequences.

In the present study, we have tried to obtain evidence that the alterations which occur under in vivo conditions are analogous to chemical modifications and that models of this type are justified for studying interactions and accumulatory effects in vivo. Numerous models of this type can be selected with regard to the effect

of hazardous compounds. The influence of ageing upon the capability of collagen to bind different compounds was used as a representative model.

EXPERIMENTAL

Preparation of cartilage collagen

Bovine nasal septal cartilage from animals of different ages (foetal, newborn, 1-year-old adult and over 10-years-old) from a local slaughterhouse was kept frozen at −20°. The material was sliced into small pieces and subjected to a series of cxtractions[1]. To 10 g of the starting material 300 ml of water and 600 ml of ethanol were added. The mixture was left overnight and was then centrifuged for 30 min at 50,000 rpm. The resulting sediment was subjected to the same procedure and, after the second centrifugation, the sediment was suspended stepwise in water, absolute ethanol and diethyl ether (300 ml of each). In each step the suspension was allowed to stand overnight and centrifuged before adding the next solvent. Finally, 300 ml of 8 *M* urea which was 1.0 *M* with respect to sodium chloride were added, the mixture was allowed to stand overnight and then centrifuged and the procedure was repeated three or four times. The resulting sediment was washed with distilled water and freeze-dried. This material was homogenized in small portions in liquid nitrogen and the fraction of between 50 and 100 mesh was used for packing the chromatographic column. A light micrograph of a cluster of collagen particles from a column that had been operated for several runs is shown in Fig. 1.

Characterization of crude collagen used for column packing

Pronase was used for the proteolytic cleavage of collagen[6] in order to solubilize the material for further characterization. Briefly, after purification by ultrafiltration, sterilized 0.01 % pronase solution in 0.1 *M* calcium acetate solution (pH 7.18) was mixed with the cartilage sample to make the collagen to enzyme ratio 100:1. The reaction mixture was incubated at 20° for 40 h. Enzyme-treated samples were centrifuged (at 4° and 9000 rpm for 30 min) and the insoluble residue was extracted stepwise with sodium chloride–phospahte buffer (pH 7.4, ionic strength $I = 0.5$) and citrate buffer (pH 3.7). The extraction procedure was as described for skin collagen[6].

Proteoglycan complexes that were released by pronase digestion from the collagen preparation were separated from the collagen solution by DEAE-cellulose chromatography as described by Miller[7].

Additional analyses were carried out according to Bitter and Muir[8] (hyaluronic acid), Stegeman[9] (hydroxyproline), Blumenkranz and Asboe-Hansen[10] (uronic acids), Boas[11] (hexosamine) and Lowry *et al.*[12] (protein content).

Chromatographic separation

This was performed on a 20 × 1 cm stainless-steel column packed by pouring in the collagen suspension. As soon as the first portion (5 ml) had settled, pressure was introduced using a double-piston pump operated at 30 atm. Before operation, the column was equilibrated with 0.01 *M* sodium citrate buffer (pH 3.4). Samples were applied as aqueous solutions (3000 mg, dry weight); excess of the sample (overloaded column) was washed out with 0.01 *M* sodium citrate buffer (pH 3.4). Adsorbed material was eluted with a pH gradient ranging from 3.4 to 7.3 (0.01 *M* sodium citrate

Fig. 1. Light micrograph of a cluster of collagen fibres. This material served as the column packing for six runs. Note the presence of cells (fibroblasts). Magnification 300×.

buffer) followed with a linear sodium chloride gradient (0–1.0 *M*) at pH 7.3 (0.01 *M* sodium citrate buffer). The amount of glycosaminoglycans and proteoglycans was determined by measuring the hexuronic acid concentration of the eluate (4-ml fractions were collected at a flow-rate of 1 ml/min). With γ-globulin the UV absorbance at 280 nm was considered to be indicative of the eluate concentration, while the absorbance at 440 nm was applied with actinomycin C and absorbance at 250 nm with penicillin G. All measurements were carried out on a Unicam SP-700 spectrophotometer.

Substances tested

Chondroitin 6-sulphate, hyaluronic acid and γ-globulin were obtained from Miles Laboratories (Elkhardt, Ind., U.S.A.) and penicillin G and actinomycin C from Serva (Heidelberg, G.F.R.) Skin proteoglycans were prepared by the method of Miller[7].

RESULTS AND DISCUSSION

The properties of collagen packings differ depending on the age of the animal from which the material was prepared. With advancing age of the animal, the material became more resistant towards proteolytic cleavage, *i.e.*, more reactive groups were involved in crosslinks (Table I). Although the preparation procedure removed most of the non-collagenous material, a certain amount of proteoglycans remained bound to collagen (Table II).

TABLE I

THE EXTRACTIBILITY OF COLLAGEN FROM DIFFERENT SOURCES BY PRONASE
40 h, 20°, pronase to collagen ratio 1:100 (w/w).

Type of preparation (animal)	*Collagen (mg per 100 mg of total collagen)*			
	Pronase extract	*0.45 M NaCl extract after pronase digestion*	*Citrate extract after pronase extraction*	*Total*
Calf	39.263	9.052	5.694	54.009
1-year-old cow	27.557	16.838	6.284	49.076
>10-years-old cow	16.818	5.763	2.962	25.543

TABLE II

PROTEOGLYCANS BOUND TO COLLAGEN PACKINGS AND RELEASED BY PRONASE DIGESTION
Conditions as in Table I.

Type of preparation (animal)	*Total protein (mg per 100 mg of collagen)*	*Uronic acids (mg per 100 mg of collagen)*	*Hexosamine (mg per 100 mg of collagen)*
Calf	1.8	0.30	0.1
1-year-old cow	7.5	1.32	1.1
>10-years-old cow	5.6	0.98	0.4

If the column packing is prepared from foetal collagen and chondroitin 6-sulphate is used as the solute, then all material is eluted from the column at pH 7.3 and a salt concentration of 0.25 *M*. If the column packing is prepared from a newborn individual, a small portion of the material loaded appears as a fast-moving peak. With increasing age, the binding capacity of the slowly moving peak decreases and the amount of material eluted in the fast-moving peak increases. This fast-moving peak is usually not very sharp and its maximum appears at about pH 6–7. In column packings obtained from animals aged more than 10 years most of chondroitin 6-sulphate is eluted in the fast-moving peak (Fig. 2).

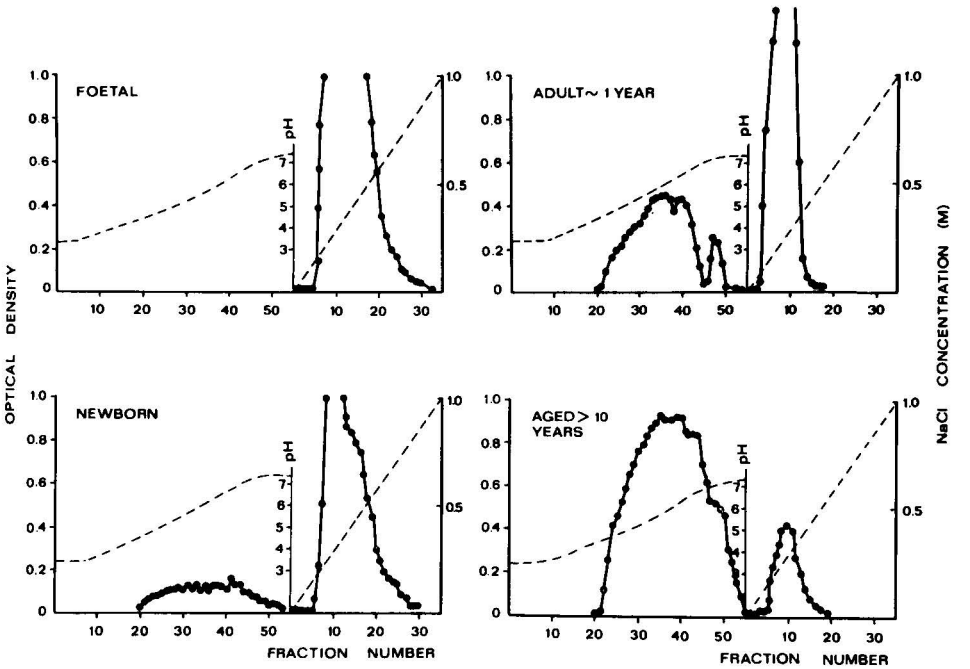

Fig. 2. Chromatographic profile of chondroitin 6-sulphate on collagen. Column packing prepared from animals of different ages (650 mg, dry weight); amount applied, 3000 mg as hexuronic acid. Chondroitin 6-sulphate was applied to the column equilibrated with 0.01 *M* sodium citrate buffer (pH 3.4) and eluted with a pH gradient as indicated (broken line in the right-hand side of each figure). Subsequently (left-hand side of each figure) a linear sodium chloride gradient (0–1.0 *M*) was introduced (also indicated by broken line).

Analogous ontogenetic relations are also observed when γ-globulin, hyaluronic acid or proteoglycans are used as the solutes (Figs. 3, 4 and 5). Also, peptides that are foreign to the organism, such as actinomycin C and penicillin, behave as indicated in Figs. 6 and 7. The relative proportions of the slow- and fast-moving peaks differ in the individual solutes. With hyaluronic acid, the slow-moving peak is small. If the column packing is prepared from aged animals, the retention volume of the fast-moving peak is shifted to lower values and the maximum appears at about pH 5.

The results obtained have to be judged from the viewpoint that collagen, when used as a column packing, behaves as an amphoteric ion exchanger. Therefore, it may

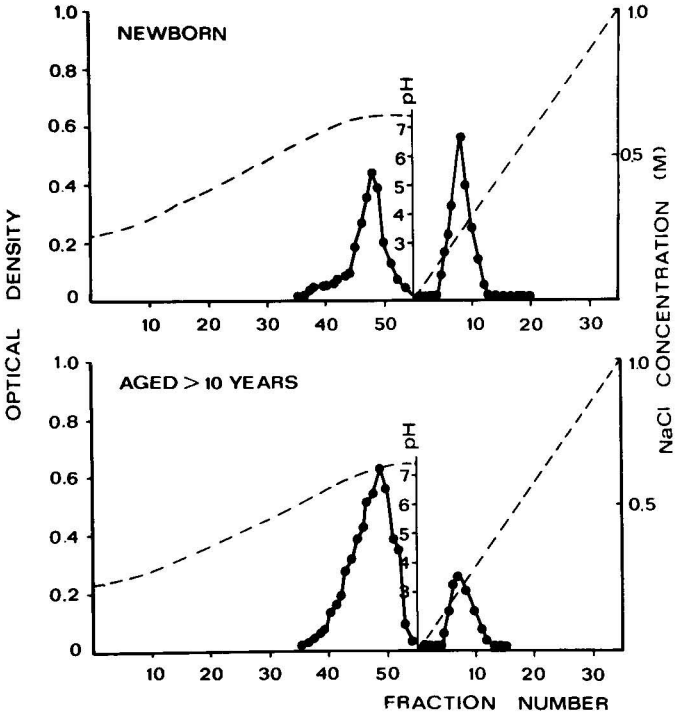

Fig. 3. Chromatographic profile of γ-globulin on collagen. Column packing prepared from animals of different ages. Separation conditions as in Fig. 1.

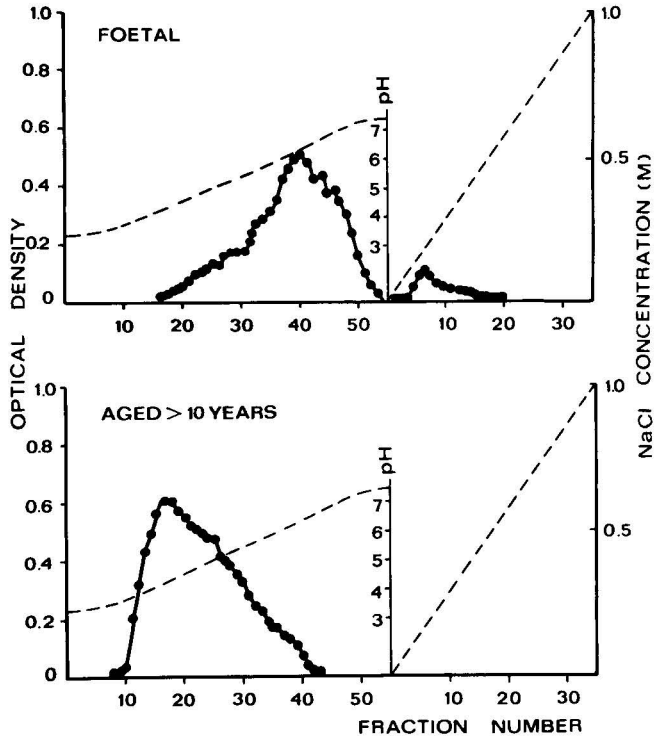

Fig. 4. Chromatographic profile of hyaluronic acid on collagen. Packing prepared from animals of different ages. Separation conditions as in Fig. 1.

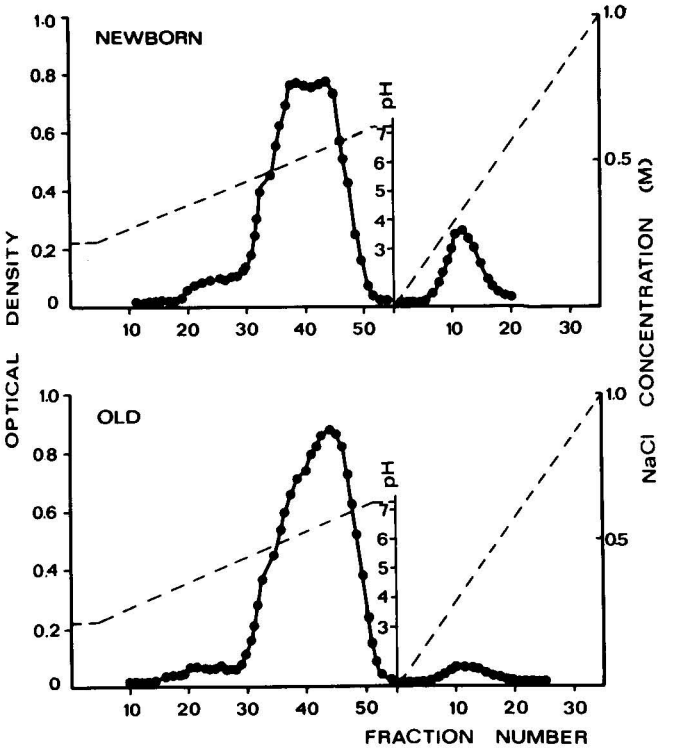

Fig. 5. Chromatographic profile of proteoglycans on collagen. Column packing prepared from newborn and old (>10 years) animals. Separation conditions as in Fig. 1.

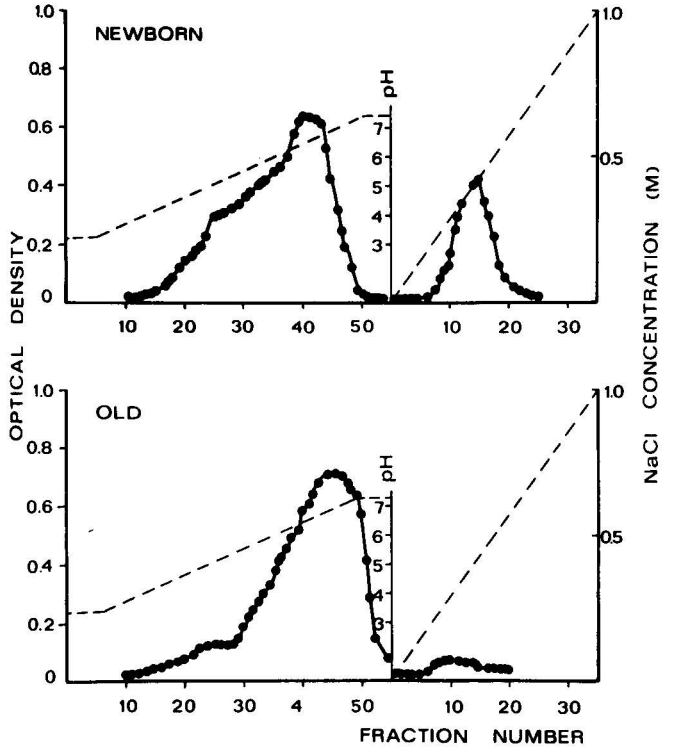

Fig. 6. Chromatographic profile of actinomycin C on collagen. Column packing prepared from newborn and old (>10 years) animals. Separation conditions as in Fig. 1.

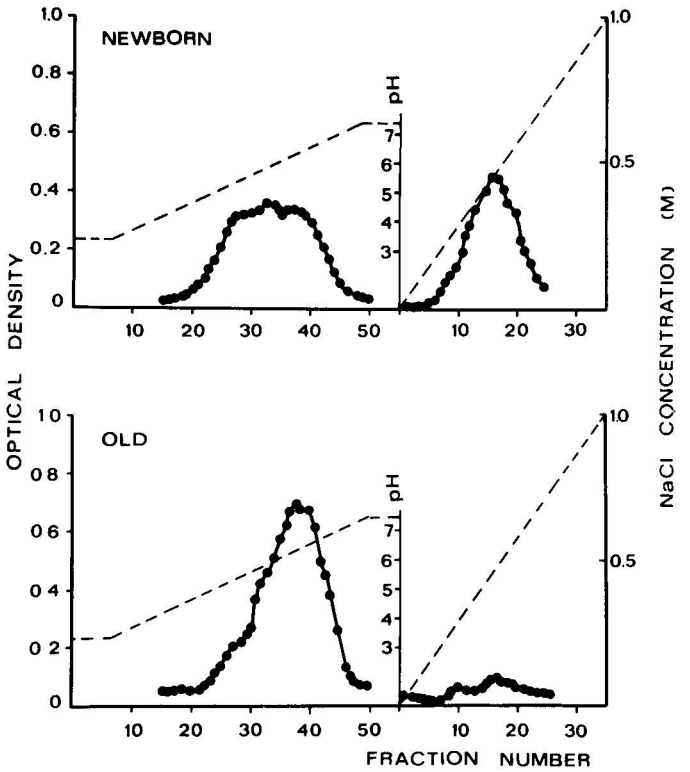

Fig. 7. Chromatographic profile of penicillin G on collagen. Column packing prepared from newborn and old (>10 years) animals. Separation conditions as in Fig. 1.

happen that the variation in the dissociation of the amphoteric counter ions allowing selective desorption may be compensated for by variations in the charge of the functional groups of the exchanger, which increase the sorption, and *vice versa*.

When glutaraldehyde-crosslinked collagen gels were used[3,5], the elution patterns of chondroitin 6-sulphate varied considerably with ionic strength and pH. This result indicates that ionic interactions are involved in this type of chromatography, as in conventional gel chromatography this type of interaction would not be expected. The influence of ionic strength is greater than that of pH. The effect of ionic strength seems to be eliminated at $I = 0.4$. Hanada and Anan[2] state that "it should be pointed out that the physiological ionic strength and pH are in a range where small changes in the environment seem to exert a great influence on the interaction". Also, chromatographic investigations of the collagen–glycosaminoglycan interaction give superior results to those obtained on this interaction in an electric field, where the interpretation of the results may be ambiguous. The same statement can be made for the antibiotics tested.

The fact that the compounds tested are eluted from the column in two discrete peaks indicates the existence of two different ways of binding these solutes to the collagenous matrix. At acidic pH values the column packing should behave as a weak cation exchanger and basic groups in amino acid side-chains should be dissociated.

It has been shown by other workers that some of these side-chains,namely those of lysine, are converted into crosslinks of the Schiff base type, which would result in a decreased binding capacity if the number of residues reacted is sufficiently large (for a review, see ref. 13). If the number of residues reacted is small than there should be no difference in the chromatographic profiles. In our experiments, however, the peak that occurs during the pH gradient elution is increased when the packing is prepared from older animals, which indicates that the occurrence of lysine-derived crosslinks is not decisive for the binding capacity of the column at acidic pH values. There are two other possibilities that could explain the altered behaviour of the column: (a) crosslinks introduced into the structure cause conformational changes and perhaps changes in the assembly of individual protein molecules into fibres, thus making other regions available for the tested solutes and; (b) the collagenous component present binds different amounts of non-collagenous components, mainly proteoglycans, with the same result as in the first instance. Our results indicate that both mechanisms participate in the age-dependent changes of the collagenous matrix.

The method of studying *in vivo* interactions of different compounds with proteins and perhaps with other naturally occurring compounds appears to be widely applicable. The ability of the method to indicate small changes in structure appears to be adequate, as demonstrated in the case of the ageing collagen structure and its capability to bind different high- and low-molecular-weight compounds.

REFERENCES

1 A. Wasteson and B. Öbrink, *Biochim. Biophys. Acta*, 170 (1968) 201.
2 E. Hanada and F. K. Anan, *J. Biochem. (Tokyo)*, 74 (1973) 505.
3 M. Németh-Csóka, *Ergeb. Exp. Med.*, 20 (1973) 149.
4 J. Janák, J. Čoupek, M. Krejčí, O. Mikeš and J. Turková, in Z. Deyl, K. Macek and J. Janák (Editors), *Liquid Column Chromatography*, Elsevier, Amsterdam, 1975, p. 169.
5 E. Hanada and F. K. Anan, *Bull. Tokyo Med. Dental Univ.*, 21 (1974) 107.
6 M. Adam, P. Fietzek and K. Kühn, *Eur. J. Biochem.*, 3 (1968) 411.
7 E. J. Miller, *Biochemistry*, 10 (1971) 1652.
8 T. Bitter and H. Muir, *Anal. Biochem.*, 4 (1962) 330.
9 H. Stegeman, *Hoppe Seyler's Z. Physiol. Chem.*, 311 (1958) 41.
10 N. Blumenkranz and G. Asboe-Hansen, *Anal. Biochem.*, 54 (1973) 484.
11 N. F. Boas, *J. Biol. Chem.*, 204 (1953) 553.
12 O. H. Lowry, N. J. Rosenborough, A. L. Farr and R. J. Randall, *J. Biol. Chem.*, 193 (1951) 265.
13 S. P. Robins, in D. A. Hall (Editor), *Methodology of Connective Tissue Research*, Joynson-Bruvvers Ltd., Oxford, 1976, p. 37.

Journal of Chromatography, 148 (1978) 293–297

CHROM. 10,413

AFFINITY CHROMATOGRAPHY OF PROTEASES ON HYDROXYALKYL METHACRYLATE GELS WITH COVALENTLY ATTACHED INHIBITORS

J. TURKOVÁ

Department of Protein Chemistry, Institute of Organic Chemistry and Biochemistry, Czechoslovak Academy of Sciences, 166 10 Prague (Czechoslovakia)

and

A. SEIFERTOVÁ

Development Laboratory, Léčiva, 190 00 Prague (Czechoslovakia)

SUMMARY

The efficient isolation of trypsin and chymotrypsin from a crude pancreatic extract was achieved by affinity chromatography on specific adsorbents prepared by coupling of both naturally occurring protease inhibitors and also synthetic low-molecular-weight protease inhibitors to hydroxyalkyl methacrylate gels. Specific sorbents prepared with synthetic inhibitors are stable and are suitable for the isolation of chymotrypsin and trypsin even on a large scale.

INTRODUCTION

The last few years have witnessed great progress in the simple isolation of numerous biologically active substances, especially enzymes, owing to the introduction of affinity chromatography. This method makes use of the property of these substances to form stable, specific and reversible complexes such as, *e.g.*, complexes of enzymes with their inhibitors, substrates or effectors, antibodies with antigens and lectins with polysaccharides. The efficient isolation of trypsin and chymotrypsin from a crude pancreatic extract on specific adsorbents prepared by the coupling of protease inhibitors to hydroxyalkyl methacrylate gels may serve as an example.

The gels used were developed and prepared by Čoupek *et al.*[1] at the Institute of Macromolecular Chemistry of the Czechoslovak Academy of Sciences and their structure is shown in Fig. 1. The copolymerization of hydroxyalkyl methacrylate with alkylene dimethacrylates gives rise to heavily crosslinked microparticles of a xerogel, which subsequently aggregate and yield macroporous structures of spheroids. Because of this structure, the gels have some chemical properties in common with the most commonly used support, agarose. Thus, *e.g.*, the hydroxyl groups of the gel can be activated with cyanogen bromide[2], in a similar manner to the hydroxyl groups of agarose. Amino acids, peptides and proteins can be bound to the activated gels through their amino groups. At the same time, however, the gels resemble, because of their macroreticular structure, inorganic supports. They do not change in volume with

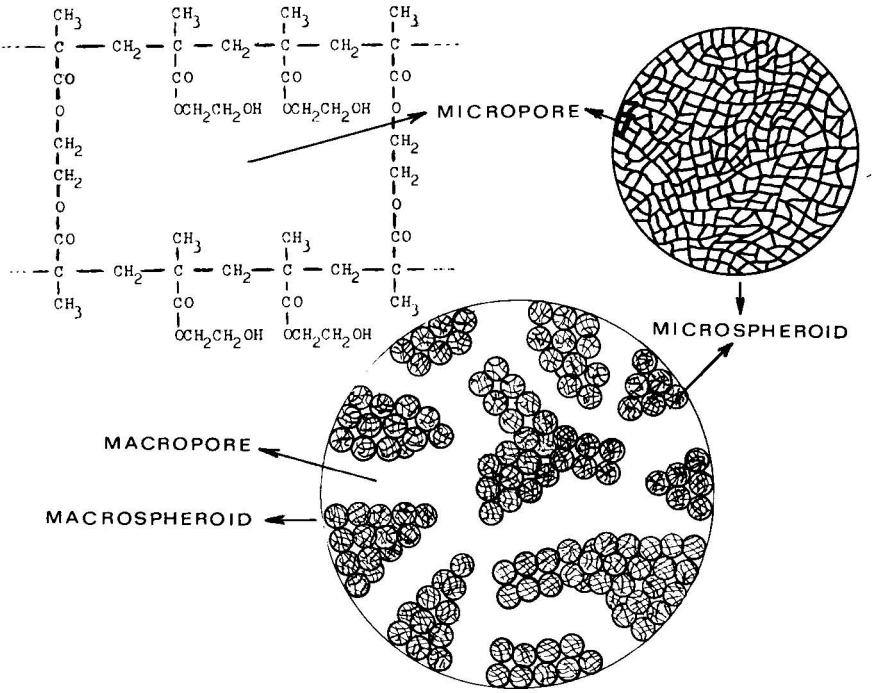

Fig. 1. Structure of hydroxyalkyl methacrylate gels (Spheron).

changes in pH or after the addition of organic solvents, and they are not attacked by microorganisms and show excellent flow properties because of their rigidity. These properties permit the use of the gels in large-scale operations.

EXPERIMENTAL

Materials

The hydroxyalkyl methacrylate gels (Spheron 300) of particle size 100–200 μm were prepared by the method described earlier[1], as well as Spheron with attached hexamethylenediamine (NH_2-Spheron)[2,3] and N-benzyloxycarbonylglycyl-D-phenylalanine-NH_2-Spheron (Z-Gly-D-Phe-NH_2-Spheron)[4]. Aminobenzamidine was attached to NH_2-Spheron by use of soluble carbodiimide according to Hixson and Nishikawa[5]. Ovomucoid and antilysine were coupled to cyanogen bromide-activated Spheron[2]. Ovomucoid was purchased from Koch-Light (Colnbrook, Great Britain) and antilysine (polyvalent lung trypsin inhibitor) was purchased from Léčiva (Prague, Czechoslovakia).

Chromatography of crude pancreatic extract on ovomucoid-Spheron

A sample of active pancreatic extract (100 ml) was placed on a column (10 × 2 cm) which was subsequently eluted with an aqueous solution of ammonium formate (0.05 *M* formic acid adjusted to pH 8.0 with 5% aqueous ammonia). The course of the chromatography is shown in Fig. 2(I).

Chromatography of fraction (a), eluted from an ovomucoid-Spheron column [cf., Fig. 2(I)], on a column of antilysine-Spheron

The fraction of material not adsorbed (180 ml) was placed directly on the antilysine-Spheron column (10 × 2 cm). The course of the chromatography is shown in Fig. 2(II).

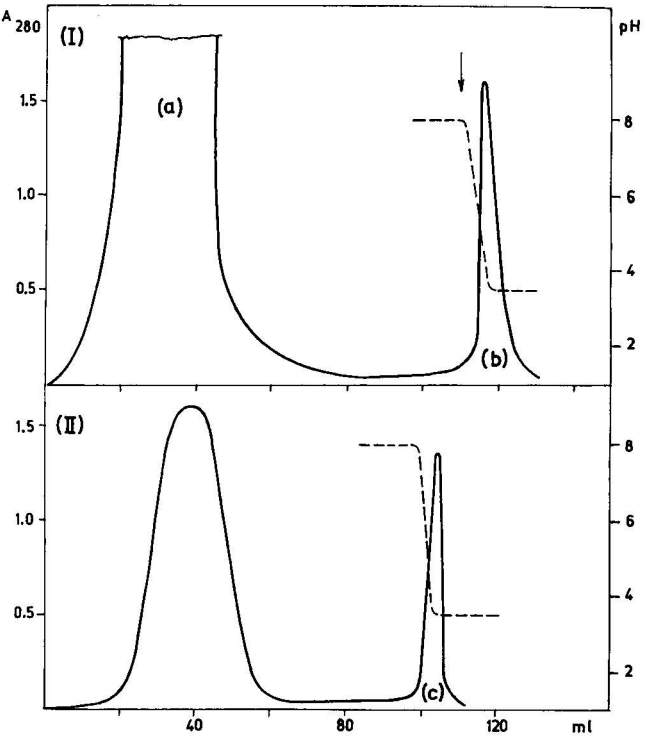

Fig. 2. Chromatography of crude pancreatic extract on ovomucoid-Spheron (I) and antilysine-Spheron (II). (I) A sample of active pancreatic extract (100 ml) was placed on a column of ovomucoid-Spheron (10 × 2 cm), which was subsequently eluted with an aqueous solution of ammonium formate (0.05 *M* formic acid adjusted to pH 8.0 with 5% aqueous ammonia). Fractions (6 ml) were collected at 20-min intervals. The arrow designates the change in pH from 8.0 to 3.5 (0.1 *M* formic acid adjusted to pH 3.5 with ammonia). (II) The fraction (a) of material not adsorbed (180 ml) was placed directly on the antilysine-Spheron column (10 × 2 cm). The course of the chromatography was analogous to that described for (I). (a) Contaminants and chymotrypsin; (b) trypsin; (c) chymotrypsin; ———, absorbance at 280 nm; – – –, pH.

Chromatography of crude pancreatic extract on N-benzyloxycarbonylglycyl-D-phenylalanine-NH_2-Spheron

A sample of active pancreatic extract (100 ml) was applied to the column (6.0 × 1.5 cm). The course of the chromatography is shown in Fig. 3(I).

Chromatography of fraction A, filtered through a column of N-benzyloxycarbonylglycyl-D-phenylalanine [cf., Fig. 3(I)], on a column of NH_2-benzamidine-NH_2-Spheron (25 × 1 cm)

The course of chromatography is shown in Fig. 3(II).

RESULTS AND DISCUSSION

To isolate chymotrypsin and trypsin from a crude pancreatic extract we used first specific adsorbents prepared by coupling naturally occurring, high-molecular-weight protease inhibitors to Spheron 300 activated with cyanogen bromide. Fig. 2(I) shows the isolation of trypsin on Spheron P 300 with attached ovomucoid. The capacity of the column was 1.5 mg of trypsin per millilitre of gel. Because volatile buffers were used for desorption, the enzyme fraction after lyophilization yielded a trypsin preparation containing less than 5% of salts, thus conforming to standards of commercial preparations. The activity of the trypsin preparation obtained was 31.3 units/g, assayed with lysine ethyl ester as substrate. This activity is considerably higher than the activity prescribed by the standard for commercial preparations.

The fraction of the material not adsorbed to ovomucoid-Spheron was directly applied to Spheron with attached antilysine [Fig. 2(II)]. Chymotrypsin was then specifically adsorbed to this polyvalent protease inhibitor at an alkaline pH. The capacity of the column was 1.4 mg of chymotrypsin per millilitre of gel. The fraction of desorbed chymotrypsin afforded, after lyophilization, a preparation with less than 5% of salts. Its activity, 46.5 units/g, determined with tyrosine ethyl ester as substrate, was again higher than that required by standards.

The activity of ovomucoid-Spheron dropped to 20% after ten runs. Regeneration by washing with 4 *M* urea restored the original capacity of the specific adsorbent to 90%, yet after four runs a considerable decrease in the capacity was again observed. The capacity of antilysine-Spheron decreased to 23% after ten runs. Washing of the adsorbent with 4 *M* urea regenerated 94% of the original capacity, yet a rapid decrease was observed after repeated use of the regenerated adsorbent. Because of the low stability and high cost of naturally occurring protein inhibitors, we focused our attention on the use of specific adsorbents prepared from low-molecular-weight synthetic inhibitors.

NH_2-Spheron was prepared by coupling of hexamethylenediamine to cyanogen bromide-activated Spheron P 300. Subsequently, N-benzyloxycarbonylglycyl-D-phenylalanine or aminobenzamidine were attached to NH_2-Spheron. Fig. 3(I) shows the affinity chromatography of a crude pancreatic extract on Z-Gly-D-Phe-NH_2-Spheron. The capacity of the column was 1.35 mg of enzyme per millilitre of gel. The activity of the lyophilized preparation obtained was 49.5 units/g, determined with tyrosine ethyl ester as substrate.

The material emerging in the first peak was applied to a column of NH_2-benzamidine-NH_2-Spheron [Fig. 3(II)]. The capacity of the column was 1.3 mg per millilitre of gel. The activity of the lyophilized preparation was 33 units/g, determined with lysine ethyl ester.

The data presented here show that identical results were obtained with specific adsorbents prepared both with naturally occurring protease inhibitors and with low-molecular-weight synthetic inhibitors. Unlike the naturally occurring inhibitors, which undergo denaturation because of their protein character and thus irreversibly lose their activity, the synthetic low-molecular-weight inhibitors are completely stable. The capacity of specific adsorbents prepared with these inhibitors can be regenerated almost infinitely, *e.g.*, by washing with 6 *M* guanidine hydrochloride. Synthetic low-molecular-weight inhibitors coupled to both chemically and mechanically stable

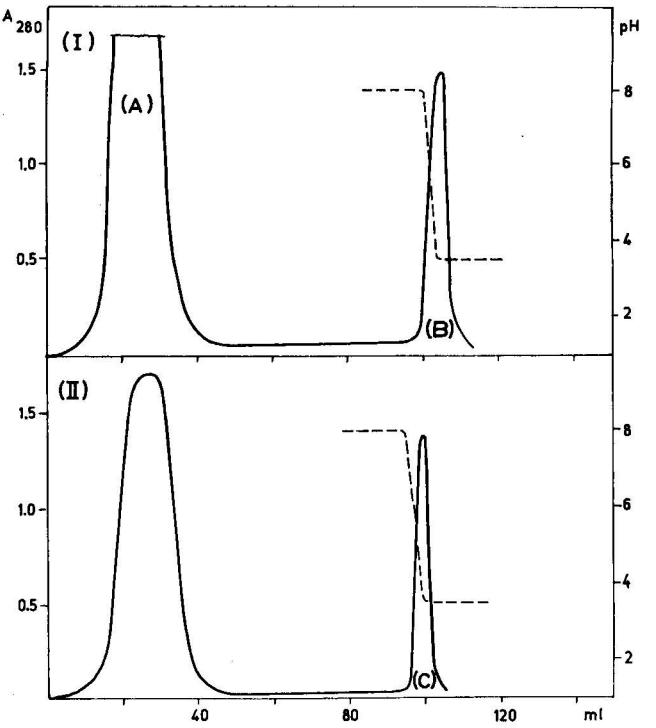

Fig. 3. Chromatography of crude pancreatic extract on N-benzyloxycarbonylglycyl-D-phenylalanine-NH_2-Spheron (I) and NH_2-benzamidine-NH_2-Spheron (II). (I) A sample of active pancreatic extract (100 ml) was applied to the column of N-benzyloxycarbonylglycyl-D-phenylalanine-NH_2-Spheron (6.0 × 1.5 cm). The course of the chromatography was identical with that shown in Fig. 2. (II) Fraction (A), filtered through a column of N-benzyloxycarbonylglycyl-D-phenylalanine, was placed directly on a column of NH_2-benzamidine-NH_2-Spheron (25 × 1 cm). The course of chromatography is identical with that shown in Fig. 2. (A) Contaminants and trypsin; (B) chymotrypsin; (C) trypsin; ———, absorbance at 280 nm; – – –, pH.

hydroxyalkyl methacrylate gels therefore represent specific sorbents suitable for the isolation of enzymes even on a large scale.

REFERENCES

1 J. Čoupek, M. Křiváková and S. Pokorný, *J. Polym. Sci., Polym. Symp.*, 42 (1973) 182.
2 J. Turková, O. Hubálková, M. Křivákový and J. Čoupek, *Biochim. Biophys. Acta*, 322 (1973) 1.
3 J. Turková, O. Valentová and J. Čoupek, *Biochim. Biophys. Acta*, 420 (1976) 309.
4 J. Turková, K. Bláha, O. Valentová, J. Čoupek and A. Seifertová, *Biochim. Biophys. Acta*, 427 (1976) 586.
5 H. F. Hixson, Jr., and A. H. Nishikawa, *Arch. Biochem. Biophys.*, 154 (1973) 501.

Liquid Chromatography Detectors

by R. P. W. SCOTT, *Chemical Research Dept., Hoffmann-La Roche, Nutley, N.J.*

JOURNAL OF CHROMATOGRAPHY LIBRARY - Volume 11

The rapid development of liquid chromatography over the past decade has been due to the introduction of highly sensitive linear liquid chromatography detectors. This book provides a comprehensive treatment of the function and optimal working conditions of liquid chromatography detectors. Divided into four parts, the book gives detailed descriptions of the general characteristics of liquid chromatography, bulk property, and solute property detectors, as well as their use in liquid chromatography. The necessary detector specifications are defined which will permit a rational comparison of the performance of one detector with that of another.

CONTENTS: Introduction. **Parts: 1. General Characteristics of Liquid Chromatography Detectors.** History, function and classification of detectors. Performance criteria of LC detectors. Detector characteristics that affect column performance. Summary of detector criteria. Ancillary equipment. **2. Bulk Property Detectors.** General characteristics of bulk property detectors. The refractive index detector. The dielectric constant detector. The electrical conductivity detector. Additional bulk property detecting systems. **3. Solute Property Detectors.** Principles of detection. The ultraviolet absorption detector. The fluorometric detector. The polarographic detector. The heat of adsorption detector. The spray impact detector. The radioactivity detector. The electron capture detector. Transport detectors. **4. The Use of Detectors in Liquid Chromatography.** The selection of the appropriate detector. Quantitative and qualitative analysis. Practical hints on detector operation. Special detector techniques. Spectroscopic detectors. **Subject Index.**

1977 x + 248 pp. US $34.50/Dfl. 84.00
ISBN 0-444-41580-7

ELSEVIER

P.O. Box 211, Amsterdam
The Netherlands

52 Vanderbilt Ave
New York, N.Y. 10017

The Dutch guilder price is definitive. US $ prices are subject to exchange rate fluctuations.

7056

Gas Chromatography of Polymers

by **V.G. BEREZKIN, V.R. ALISHOYEV** and **I.B. NEMIROVSKAYA,** Institute of Petrochemical Synthesis, Academy of Sciences of the U.S.S.R., Moscow.

JOURNAL OF CHROMATOGRAPHY LIBRARY, Vol. 10

1977. xiii+225 pages. US $41.25/Dfl. 103.00.
ISBN 0-444-41514-9

This book is devoted to the strategy of application of GC in polymer chemistry and discusses, in detail, the use of GC in research work and the polymeric compounds industry. It is the second, revised and enlarged edition of the original version published in the U.S.S.R. in 1972.
The following principal applications are covered: analysis of monomers and solvents, determination of the contents of volatile substances in polymers, study of polymer formation processes, investigation into types of disintegration of high-molecular-weight compounds, polymer analysis by reaction and pyrolytic chromatography, and study of polymers and their reactivity with the aid of inverse chromatography.
This work will be of value to research institutions, industrial enterprises and senior students engaged in the fields of polymer or analytical chemistry and GC.

CONTENTS: Basic principles of gas chromatography. GC methods for the analysis of monomers and solvents. The study of polymer formation reactions. Determination of volatile compounds in polymer systems. Study of the kinetics and mechanisms of chemical transformations of polymers at elevated temperatures. Reaction GC of polymers. Pyrolysis GC. Inverse GC. Conclusion.

ELSEVIER SCIENTIFIC PUBLISHING COMPANY
P.O.Box 211, Amsterdam,
The Netherlands

Distributor in the U.S.A. and Canada:
ELSEVIER NORTH-HOLLAND, INC.,
52 Vanderbilt Ave., New York., N.Y. 10017

The Dutch guilder price is definitive.
US $ prices are subject to exchange rate fluctuations.

2086 E

Instrumental Liquid Chromatography

A practical manual on high-performance liquid chromatographic methods

by **N.A. PARRIS**

JOURNAL OF CHROMATOGRAPHY LIBRARY, Vol. 5.

1976 x+329 pages. US $38.50/Dfl. 100.00
ISBN 0-444-41427-4

Available texts on liquid chromatography have tended to emphasize the developments in the theoretical understanding of the technique and methodology or to list numerous applications, complete with experimental details. The present work is intended to bridge the gap between these two treatments by providing, with the minimum of theory, a practical guide to the use of the technique for the development of separations. The material is based largely on practical experience and high-lights details which may have important operational value for laboratory workers. Information regarding the usefulness of available equipment and column packings is given, together with chapters devoted to the methodology of each separation method. Applications of liquid chromatography are described with reference to the potential of the technique for qualitative, quantitative and trace analysis as well as for preparative applications. Numerous applications from the literature are tabulated and cross-referenced to sections concerned with the optimisation procedures of the particular methods. In addition, many of the figures have been drawn from hitherto unpublished work. Although written primarily for workers currently involved with the application or the development of liquid chromatographic methods, the book will also be of value to those who seek to establish whether methods for their particular interests have been reported or seem feasible.

ELSEVIER SCIENTIFIC PUBLISHING COMPANY
P.O.Box 211, Amsterdam,
The Netherlands

Distributor in the U.S.A. and Canada:
ELSEVIER/NORTH-HOLLAND INC.,
52 Vanderbilt Ave., New York., N.Y. 10017

The Dutch guilder price is definitive.
US $ prices are subject to exchange rate fluctuations.

1933 E

Chemical Derivatization in Liquid Chromatography

by J.F. LAWRENCE *and* R.W. FREI

JOURNAL OF CHROMATOGRAPHY LIBRARY, Vol. 7

1976 viii + 214 pages
US $34.50/Dfl. 90.00
ISBN 0-444-41429-0

This book is intended for all investigators concerned with the use of physical separation techniques for solving complex analytical problems. It is the first publication to provide a comprehensive account of modern derivatization in liquid chromatography with special emphasis on the practical aspects. Many examples are given in sufficient detail to permit the worker to reproduce a method without resorting to the original literature. Thus, the book will be particularly useful on the bench top of the laboratory, as well as in practically-oriented courses.

CONTENTS: INTRODUCTION: Pre-separation techniques. Post-separation techniques. BACKGROUND: Chromatographic principles. Spectrometry. Direct measurements from solid surfaces. Further reading. INSTRUMENTATION: TLC equipment. HPLC equipment. Further reading. APPLICATIONS: UV-visible derivatization. Fluorimetric derivatization. Radiochemical derivatization. Derivatization and mass spectrometry. Subject index.

ELSEVIER SCIENTIFIC PUBLISHING COMPANY
P.O.Box 211, Amsterdam,
The Netherlands

Distributor in the U.S.A. and Canada:
ELSEVIER/NORTH-HOLLAND INC.,
52 Vanderbilt Ave., New York., N.Y. 10017

The Dutch guilder price is definitive.
US $ prices are subject to exchange rate fluctuations.

1938 E

GENERAL INFORMATION

(A leaflet *Instructions to Authors* can be obtained by application to the publisher.)

Types of Contributions. The following types of papers are published in the *Journal of Chromatography* and the section on *Biomedical Applications*: Regular research papers (full-length papers), short communications and notes. Short communications are preliminary announcements of important new developments and will, whenever possible, be published with maximum speed. Notes are usually descriptions of short investigations and reflect the same quality of research as full-length papers, but should preferably not exceed four printed pages. For reviews, see page 2 of cover under Submission of Papers.

Manuscripts. Manuscripts should be typed in double spacing on consecutively numbered pages of uniform size. The manuscript should be preceded by a sheet of manuscript paper carrying the title of the paper and the name and full postal address of the person to whom the proofs are to be sent. Authors of papers in French or German are requested to supply an English translation of the title of the paper. As a rule, papers should be divided into sections, headed by a caption (e.g., Summary, Introduction, Experimental, Results, Discussion, etc.). All illustrations, photographs, tables, etc. should be on separate sheets.

Title. The title of the paper should be concise and informative. Since titles are widely used in information retrieval systems, care should be taken to include the key words. The title should be followed by the authors' full names, academic or professional affiliations, and the address of the laboratory where the work was carried out. If the present address of an author is different from that mentioned, it should be given in a footnote. Acknowledgements of financial support are *not* to be made in a footnote to the title or name of the author, but should be included in the Acknowledgements at the end of the paper.

Summary. Full-length papers and review articles should have a summary of 50–100 words which clearly and briefly indicates what is new, different and significant. In the case of French or German articles an additional summary in English, headed by an English translation of the title, should also be provided. (Short communications and Notes are published without a summary.)

Illustrations. The figures should be submitted in a form suitable for reproduction, drawn in Indian ink on drawing or tracing paper. One original and two photocopies are required. Attention should be given to any lettering (which should be kept to a minimum) and to spacing on axes of graphs in order to ensure that numbers etc. remain legible after reduction. Axes of a graph should be clearly labelled. The figures should preferably be of such a size that the same degree of reduction can be applied to all of them. Photographs should have good contrast and intensity. Sharp, glossy photographs are required to obtain good halftones. References to the illustrations should be included in appropriate places in the text using arabic numerals. Each illustration should have a legend, all the *legends* being typed (with double spacing) together on a *separate sheet*. If structures are given in the text, the original drawings should be supplied. Coloured illustrations are reproduced at the authors' expense, the cost being determined by the number of pages and by the number of colours needed. The written permission of the author and publisher must be obtained for the use of any figure already published. Its source must be indicated in the legend.

References. References should be numbered in the order in which they are cited in the text, and listed in numerical sequence on a separate sheet at the end of the article. The numbers should appear in the text at the appropriate places in square brackets. In the reference list, periodicals [1], books [2], multi-author books [3] and proceedings [4] should be cited in accordance with the following examples:

1 A. T. James and A. J. P. Martin, *Biochem. J.*, 50 (1952) 679.
2 L. R. Snyder, *Principles of Adsorption Chromatography*, Marcel Dekker, New York, 1968, p. 201.
3 H. C. S. Wood and R. Wrigglesworth, in S. Coffey (Editor), *Rodd's Chemistry of Carbon Compounds, Vol. IV, Heterocyclic Compounds*, Part B, Elsevier, Amsterdam, Oxford, New York, 2nd ed., 1977, Ch. 11, p. 201.
4 E. C. Horning, J.-P. Thenot and M. G. Horning, in A. P. De Leenheer and R. R. Roncucci (Editors), *Proc. 1st Int. Symp. Quantitative Mass Spectrometry in Life Sciences, Ghent, June 16–18, 1976*, Elsevier, Amsterdam, Oxford, New York, 1977, p. 1.

Abbreviations for the titles of journals should follow the system used by *Chemical Abstracts*. Articles not yet published should be given as "in press", "submitted for publication", "in preparation" or "personal communication". The *Journal of Chromatography; Journal of Chromatography, Biomedical Applications* and *Chromatographic Reviews* should be cited as *J. Chromatogr.*

Proofs. One set of proofs will be sent to the author to be carefully checked for printer's errors. Corrections must be restricted to instances in which the proof is at variance with the manuscript. "Extra corrections" will be inserted at the author's expense.

Reprints. Fifty reprints of Full-length papers, Short communications and Notes will be supplied free of charge. Additional reprints can be ordered by the authors. An order form containing price quotations will be sent to the authors together with the proofs of their article.

News. News releases of new products and developments, and information leaflets of meetings should be addressed to: The Editor of the News Section, Journal of Chromatography/Journal of Chromatography, Biomedical Applications, Elsevier Scientific Publishing Company, P.O. Box 330, Amsterdam, The Netherlands.

Advertisements. Advertisement rates are available from the publisher on request. The Editors of the journal accept no responsibility for the contents of the advertisements.

BIBLIOGRAPHIES IN CHROMATOGRAPHY

BIBLIOGRAPHY OF LIQUID COLUMN CHROMATOGRAPHY 1971-1973

And Survey of Applications

edited by Z. DEYL, *Physiological Institute, Czecholslovak Academy of Science 5, Prague and* J. KOPECKÝ, *Institute of Hygiene and Epidemiology, Prague.*

Supplementary Volume No. 6, 1976
Published in conjunction with the Journal of Chromatography

1976. xx + 1136 pages.
US $103.70/Dfl. 259.00.
Paperback
Subscription Price:
US $57.50/Dfl. 150.00.
ISBN 0-444-41469-x

This book provides ready access to information on papers dealing with all types of liquid column chromatography from 1971 to 1973. Together with the other Bibliography supplements in the series it completes the survey on chromatographic and electromigration separation procedures.

Individual items are classified according to the chemical nature of the compounds separated, as in the Journal of Chromatography, so both sources can be used side by side. Short notices attached to most of the entries refer to the sorbent or ion-exchange material used.

The Biblicgraphy will serve workers in many different fields of science and technology by enabling them to find, in the shortest possible time, full details on the applications of the LC technique to a particular compound or group of compounds. It also provides information about current instrumentation and sorbents used. The bibliography contains an author index and an extensive list of 20,000 compounds chromatographed.

BIBLIOGRAPHY OF PAPER AND THIN-LAYER CHROMATOGRAPHY 1970-1973

And Survey of Applications

edited by K. MACEK, et al.

Supplementary Volume No. 5,

1976. xviii + 744 pages.
US $79.95/Dfl. 200.00.
Paperback
ISBN 0-444-41229-9

BIBLIOGRAPHY OF ELECTROPHORESIS 1968-1972

And Survey of Applications

edited by Z. DEYL, et al.

Supplementary Volume No. 4,

1975. xvi + 862 pages.
US $79.95/Dfl. 200.00.
Paperback.
ISBN 0-444-41225-5

BIBLIOGRAPHY OF COLUMN CHROMATOGRAPHY 1967-1970

And Survey of Applications

edited by Z. DEYL, et al.

Supplementary Volume No. 3,

1973. xix + 1067 pages.
US $71.95/Dfl. 180.00.
Paperback.
ISBN 0-444-41008-2

BIBLIOGRAPHY OF PAPER AND THIN-LAYER CHROMATOGRAPHY 1966-1969

And Survey of Applications

edited by K. MACEK, et al.

Supplementary Volume No. 2,

1972. xvi + 992 pages.
US $79.95/Dfl. 200.00.
ISBN 0-444-40953-X

BIBLIOGRAPHY OF PAPER AND THIN-LAYER CHROMATOGRAPHY 1961-1965

And Survey of Applications

Supplementary Volume No. 1,

1968. only available in microfilm
US $59.95/Dfl. 150.00.
ISBN 0-444-40676-x

ELSEVIER SCIENTIFIC PUBLISHING COMPANY

P.O. Box 211, Amsterdam, The Netherlands

Distributor in the U.S.A. and Canada:
ELSEVIER/NORTH-HOLLAND INC.,
52 Vanderbilt Avenue, New York, N.Y. 10017

The Dutch guilder price is definitive. US $ prices are subject to exchange rate fluctuations

1925 Ea